Distinguishing the Influence of Singular β-Catenin Functions in Development Using a Novel in Vivo Approach

---

Dissertation

zur

Erlangung der naturwissenschaftlichen Doktorwürde

(Dr. sc. nat.)

vorgelegt der

Mathematisch-naturwissenschaftlichen Fakultät

der

Universität Zürich

von

Max Hans-Peter Gay

von Zürich ZH

Promotionskomitee

Prof. Dr. Lukas Sommer (Vorsitz / Leitung der Dissertation)

Prof. Dr. Konrad Basler

Prof. Dr. Esther Stoeckli

Zürich, 2015

Table of Content

1. Summary

During the metazoan development a single fertilized ovum will prosper to develop a fully functional multicellular organism. This incredible process is due to the proliferation and differentiation of stem cells. These actions are regulated by signaling pathways of which a small number is evolutionary preserved throughout vertebrates and invertebrates alike. One of these is the canonical Wnt/β-catenin signaling pathway. It is not only involved in many processes throughout embryonic development, but plays a vital role in adult tissue homeostasis, cell renewal and regeneration. In the canonical Wnt cascade, β-catenin is the essential mediator for the transduction of the signal to the nucleus. In the nucleus β-catenin binds to T cell-specific transcription factors / Lymphoid enhancer-binding factor 1 (TCF/Lef) family members by physically displacing Groucho/ Transducin-like enhancer of split (TLE) repressors. This process either leads to the recruitment of co-transcription factors to TCF/Lef transactivators or it removes repressive TCF/Lefs from the chromatin. As the central, non-redundant component of the pathway, β-catenin is the bottleneck of canonical Wnt signaling. This trait has made β-catenin especially attractive as a target for genetic manipulation to elucidate the impact of canonical Wnt signaling in vivo. However, aside from its role in canonical Wnt signaling, β-catenin is also an important linking protein in the cadherin adhesion complex, in which it couples transmembrane cadherin to the actin bound α-catenin. This dual role of β-catenin in mediating Wnt signaling and cell-cell adhesion made it difficult to assign a specific phenotype obtained upon β-catenin gene (*Ctnnb1*) manipulation to either or both functions of β-catenin. The lab of Konrad Basler took it upon themselves to generate a novel mouse model to resolve this predicament. In this model *Ctnnb1* was modified to transcribe a mutated version of the β-catenin protein, which preserves adhesion and TCF/Lef binding, but lacks the capability to recruit co-transcription factors necessary for transcriptional activation. For the first part the intent of this thesis will be to validate the functionality of this model in the dorsal neural tube and in derivatives of the neural crest.

Neural crest stem cells (NCSCs) are a unique population of cells that originate from the neural tube and migrate throughout the developing embryo to give rise to a wide variety of cell types. Derivatives of NCSCs include sensory, autonomic and enteric neurons, glial cells of the peripheral nervous system (PNS), smooth muscle cells of the cardiac outflow tract, pigment cells in the skin, bone and cartilage of the head, the cornea and the primary vitreous of the eye. Canonical Wnt/β-catenin signaling has been shown to play multiple roles in neural crest development. First of which is the induction of the neural crest at the neural plate border. Additionally, NCSCs maintain an undifferentiated state when exposed to Wnt along with bone morphogenic protein (BMP). Moreover, Wnt/β-catenin signaling is involved in the generation of sensory neurons and melanocytes as well as contributing to the proper development of the

eyes and other cranial derivatives such as bone and cartilage. The second objective of this thesis will be to determine the influence of the single functions of β-catenin in NCSC derivatives, which rely on Wnt-signaling, in particular the sensory lineage and contributors to the eye.

The first publication of this thesis demonstrates that the mutated protein of β-catenin performs as anticipated. Mouse embryos solely expressing the mutated protein in the dorsal neural tube preserved epithelial integrity of the tissue as opposed to their counterparts lacking β-catenin entirely in the same structure. Moreover, in the corresponding tissue targets of TCF/Lef mediated transcription, as well as output of a Wnt reporter are lost in both types of mutant embryos.

In the second publication of this thesis I could distinguish singular processes of sensory neurogenesis in the developing dorsal root ganglia (DRG) that depend on individual functions of β-catenin, by comparing multiple mouse models to one another. Embryos deprived of β-catenin in their NCSCs virtually lost their sensory lineage, as proper progression of the cell cycle was perturbed in DRG progenitors. DRGs were present, but reduced in size in embryos expressing only the mutated β-catenin protein in DRG progenitors, as correct cell cycle progression was rescued at intermediate stages. Interestingly, NCSCs lacking α-catenin generated average size DRGs. Moreover, these α-catenin deprived embryos also displayed the regular expression of transcription factors regulating sensory neurogenesis, whereas both β-catenin mutants displayed these factors to different degrees. These findings could demonstrate that neither the coalescing of the DRG, proliferation of DRG progenitors, nor sensory neurogenesis are dependent on β-catenin to mediate adhesion, but rather on at least two different functions of β-catenin. The switch of these functions appears to be temporally regulated. One function is to induce TCF/Lef transcription. A further function of β-catenin, which is possibly rescued by the mutated protein since it preserves its TCF/Lef binding site, could be the de-repression of TCF repressed genes. This hypothesis is supported by the presence of repressive TCFs in DRG progenitors.

In the frame of the third part of my thesis the dependency of the different β-catenin functions was analyzed in NCSCs contributing to the eye (ocular NCSCs). Multiple structures of eye of both NCSC and non-NCSC origin displayed varying phenotypes between both β-catenin mutants and control animals. These comparison gives us reason to hypothesize that different derivatives of ocular NCSCs depend on β-catenin to perform either adhesion functions, induce TCF/Lef transactivation, or de-repress TCF/Lef repressed genes depending on the developing derivative.

2. Zusammenfassung

In der Entwicklung von Metazoen entsteht aus einer einzelnen befruchteten Eizelle ein völlig funktionsfähiger mehrzelliger Organismus. Dieser unglaubliche Prozess ereignet sich nur angesichts der Tatsache, dass Stammzellen sich vermehren und in verschiedene Zelltypen ausdifferenzieren. Diese Vorgänge werden von Signaltransduktionswegen gesteuert, von denen eine geringe Anzahl evolutionär zwischen Wirbel- und Wirbellosentieren erhalten ist. Einer von diesen evolutionär präservierten Transduktionswegen ist der kanonische Wnt Signalweg. Er ist nicht nur in mehrere Vorgänge während der Entwickelung involviert, sondern spielt auch in adultem Gewebe eine wichtige Rolle, bei der er Homöostase, Zellerneuerung und Regeneration im Gewebe reguliert. Das Protein β-Catenin ist der essenzielle Vermittler des kanonischen Wnt Signalweges, in dem er das Signal in den Zellkern weiterleitet. Im Zellkern bindet sich β-Catenin zu TCF/Lef Transkriptionsfaktoren und entfernt dabei die Transkriptionsrepressoren Groucho/TLE. Dieser Vorgang führt entweder dazu, dass repressive TCF/Lef vom Chromatin entfernt werden oder dass sich Co-Transkriptionsfaktoren binden und somit TCF/Lef transaktivieren. Als die einzige zentrale, unersetzbare Komponente ist β-Catenin das Nadelöhr des kanonischen Wnt Signalwegs. Diese Eigenschaft macht β-Catenin besonders attraktiv als Zielobjekt der genetischen Manipulation, die erlaubt, in vivo die Bedeutsamkeit des Wnt Signalweg zu erforschen. Abgesehen von seiner Rolle im Wnt Signalweg ist β-Catenin auch ein wichtiges Bindeglied des Cadherin Adhäsion Komplexes, in dem es Transmembrane Cadherin mit Aktin gebundenes α-Catenin verbindet. Diese doppelte Rollenverteilung machte es schwierig, Phänotypen, die durch Manipulation des β-Catenin Genes (*Ctnnb1*) erhalten wurden, einer bestimmten Funktion zuzuordnen. Um Forscher von diesem Dilemma zu erlösen, nahm es das Forschungslabor von Konrad Basler auf sich, ein neuartiges Mausmodel zu generieren. In diesem Model wurde *Ctnnb1* so verändert, dass das erworbene mutierte β-Catenin Protein weiterhin die Adhäsion aufrecht erhält und TCF/Lef bindet, aber nicht mehr die Fähigkeit hat, die Co-Transkriptionsfaktoren zu rekrutieren, die notwendig sind für die Aktivierung der Transkription. Im ersten Teil dieser Arbeit werde ich die Funktionalität dieses Models im dorsalen Neuralrohr und in den Derivaten der Neuralleiste validieren.

Neuralleisten-Stammzellen sind eine einzigartige Zellenpopulation, die aus dem Neuralrohr entstammen und durch den entwickelnden Embryo migrieren, um sich an verschiedenen Zielorten in unterschiedliche Zelltypen zu differenzieren. Die Derivaten von Neuralleisten-Stammzellen beinhalten sensorische, autonomische und enterische Neuronen, Gliazellen des peripheren Nervensystems, glatte Muskelzellen des Herzausflusstrakts, Pigmentzellen der Haut, Knochen und Knorpel des Schädels, wie auch die Cornea und primäre Glaskörper des Auges. Es wurde gezeigt, dass der kanonische Wnt/β-Catenin Signalweg mehrmals während

der Entwicklung von Neuralleisten-Stammzellen wichtig ist. Als erstes bestimmt es die Grenzen der Neuralplatte während der Neurulation und ausserdem bewahren Neuralleisten-Stammzellen einen undifferenzierten Zustand, wenn sie Wnt und BMP ausgesetzt sind. Im Weiteren ist der Wnt/β-catenin Signalweg sowohl wichtig für die Generation von sensorischen Neuronen und Pigmentzellen, als auch notwendig für die korrekte Entwicklung des Auges, wie auch weiteren Derivaten des Schädels, wie Knochen und Knorpel. Das zweite Ziel dieser Arbeit war es, die Bedeutsamkeit der einzelnen Funktionen von β-Catenin in Neuralleisten-Stammzellen Derivaten festzulegen, die abhängig sind vom Wnt Signalweg, vor allem die sensorische Zellen und die Zellen, die zur Entwicklung des Auges beitragen.

Die erste Publikation dieser Doktorarbeit zeigt, dass das mutierte β-Catenin sich so verhält wie erwartet. Mäusembryonen, die nur das mutierte Protein im dorsalen Neuralrohr exprimieren, bewahren die Integrität des Epitheliums des Gewebes im Gegensatz zu Embryonen, die gar kein β-Catenin in den gleichen Strukturen aufweisen. Darüber hinaus zeigen wir im gleichen Gewebe, dass die TCF/Lef Transkription gestört ist, durch das Fehlen von Proteinen, die der Transkription nachgeordnet sind.

In der zweiten Publikation meiner Arbeit konnte ich in der sensorischen Neurogenese der Spinalganglien einzelne Vorgänge nachweisen, die von unterschiedlichen Funktionen von β-Catenin abhängig sind. Dabei verglich ich mehrere verschiedene Mausmodelle miteinander. Embryonen ohne β-Catenin in ihren Neuralleisten-Stammzellen entwickelten keine Spinalganglien, da die Zellteilung der Vorläuferzellen gestört wurde. In den Mäusen mit dem mutierten β-Catenin waren hingegen Spinalganglien vorhanden, aber kleiner in der Grösse. Diese Tiere wiesen zwar in frühen Stadien die gleiche Störung im Zellzyklus auf, aber konnten zu späteren Zeitpunkten wieder Normalität erlangen. Interessanterweise blieben Spinalganglien in Mäuseembryonen ohne α-Catenin unverändert. Die Vorläuferzellen der Spinalganglien dieser Embryonen wiesen auch eine normale Expression von Transkriptionsfaktoren, die sensorische Neurogenese steuern, auf. Diese wurden jedoch unterschiedlich in den β-Catenin Mutanten exprimiert. Hiermit konnten wir demonstrieren, dass das Zusammenballen der Spinalganglien und die sensorische Neurogenese unabhängig sind von der Fähigkeit von β-Catenin Zell-Zell Adhäsion zu vermitteln. Darüber hinaus lässt es uns darauf schliessen, dass diese Prozesse von zwei unterschiedlichen Funktionen von β-Catenin gesteuert sind, die zeitverzögert reguliert werden. Die eine Funktion ist es TCF/Lef Transkription herbeizuführen. Die andere Funktion ist wahrscheinlich die De-Repression von Genen, die von repressiven TCF/Lef Transkriptionsfaktoren gebunden werden.

Im Rahmen des dritten Teils dieser Arbeit analysierten wir die verschiedenen Funktionen von β-Catenin in Neuralleisten-Stammzellen, die zu der Entwickelung des Auges beitragen. Mehrere Strukturen des Auges wiesen unterschiedliche Phänotypen zwischen den beiden β-

Catenin Mutanten auf, unabhängig davon, ob die Zellen von den Neuralleisten-Stammzellen abstammten oder nicht. Dieser Vergleich gab uns Grund anzunehmen, dass verschiedene Derivate der Neuralleisten-Stammzellen des Auges unterschiedlich abhängig von den drei vorhergenannten Funktionen von β-Catenin sind.

3. Introduction

3.1. Wnt-signaling

Wnt signaling is one of a handful of molecular cascades that play a crucial role throughout the lifespan of metazoans. It regulates key processes in development as well as adult tissue homeostasis. Deregulation of Wnt signaling is associated with various human diseases including cancer (Grigoryan et al., 2008; Huang and He, 2008; Moon et al., 2004).

3.1.1. Wnt

In mammals Wnt proteins are a family comprised of 19 members that are produced and secreted by a defined subset of cells. Wnts are glycosylated and lipid modified in the endoplasmic reticulum and transported to the Golgi apparatus. Subsequently, they are bound by the multipass transmembrane protein Wntless (Wls) and exocytosed from the cell (Banziger et al., 2006; Yu et al., 2014). Wls has been shown to be required for the secretion of virtually all Wnts (Najdi et al., 2012). Secreted Wnts initiate intracellular signal transduction by interacting with one of the 10 seven transmembrane receptors of the Frizzled (Fzd) family in addition to single pass transmembrane co-receptors. Particular intracellular signaling pathways are activated depending on which of the co-receptors forms the receptor complex with Fzd. Canonical Wnt is associated with the binding of the Wnt ligand to the Fzd and Lrp5/6 forming heterotrimeric complex, which result in an inactivation of the processes which lead to the degradation of the β-catenin protein and allow it to shuttle into the nucleus. Wnt induced cascades, which do not transmit their signaling via β-catenin are referred to as non-canonical pathways. These are compromised, among others, of the Wnt/planar cell polarity (PCP) and the Wnt-dependent/protein kinase C (PKC)-dependent pathways (Angers and Moon, 2009; van Amerongen et al., 2008).

3.1.2. Canonical Wnt/β-catenin signaling

In the absence of Wnt, cytosolic β-catenin levels are virtually non-existent as free floating β-catenin is rapidly phosphorylated targeting it for ubiquitinylation leading to subsequent degradation by the proteasome. Phosphorylation of β-catenin is regulated by the destruction complex composed of adenomatous polyposis coli gene product APC, Axin, glycogen synthase kinase 3 (GSK3), and casein kinase 1 (CK1). In canonical Wnt signaling, Wnts interaction with the Fzd Lrp5/6receptor leads to a phosphorylation of the Lrp5/6 intracellular domains, creating a binding site for Axin. The recruitment of Axin to the plasma membrane disrupts the destruction complex, relinquishing phosphorylation of β-catenin and leading to its accumulation in the cytosol. Consequently, β-catenin translocates into the nucleus and

interacts with TCF/Lef family members (hereafter referred to as TCFs) to regulate transcription of specific genes. In addition to conducting canonical Wnt-signaling β-catenin also is a central component of cell-cell cadherin mediated adhesion complex. Newly synthesized β-catenin can be immobilized by transmembrane cadherin proteins at adherens junctions. This process allows β-catenin to evade phosphorylation in the cytoplasm and subsequent degradation in the absence of Wnt. At adherens junctions β-catenin interacts with actin bound α-catenin, thereby indirectly modulating the actin cytoskeleton. The activity of protein kinases or the downregulation of cadherin actuate the release of β-catenin from the adherens junctions (Clevers, 2006; Port and Basler, 2010; Rogers et al., 2012; Valenta et al., 2012).

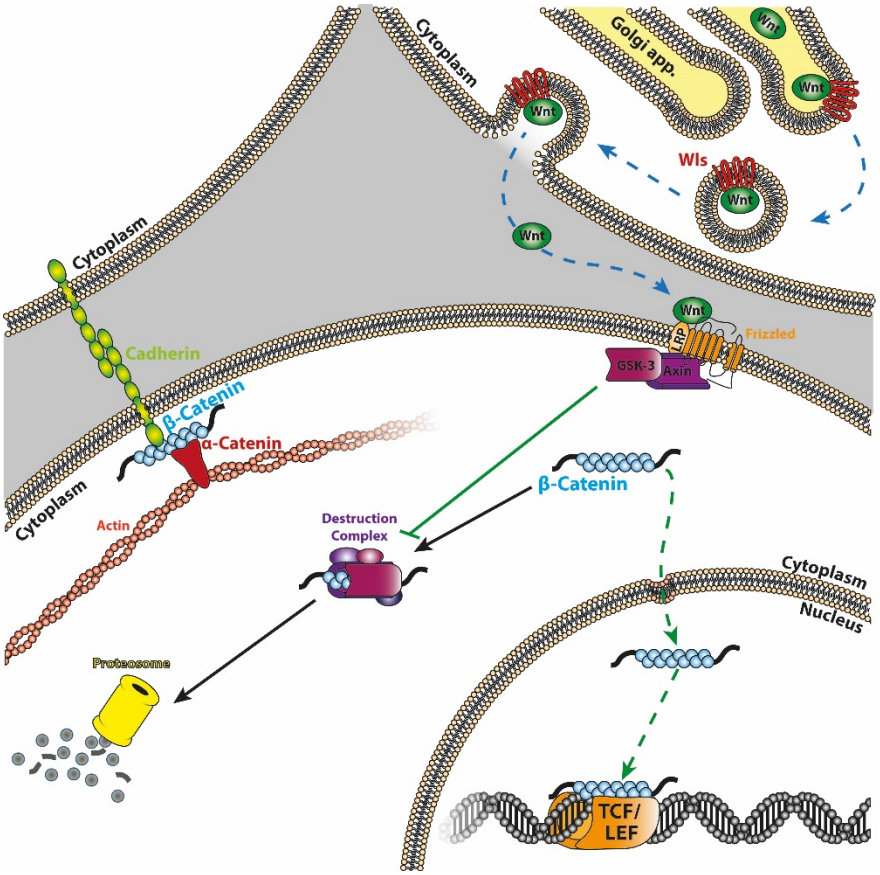

Figure 1 The canonical Wnt signaling pathway

*β-catenin conjugates adherens junctions by interlinking transmembrane cadherin with actin bound α-catenin. In the absence of Wnt, cytosolic β-catenin is phosphorylated by the destruction complex containing Axin and GSK3 (black arrow). Wnt secretion is induced when Wnts that have been lipid modified und transported to the golgi complex encounter Wls, which supports exocytosis of the bound Wnt (blue dotted arrows). Upon the binding of Wnt ligand to Frizzled and Lrp receptors, the disruption complex is disrupted, β-catenin accumulates in the cytosol, translocates to the nucleus and interacts with TCF/*Lef *transcription factors (green arrows). Unpublished schematic.*

In the absence of Wnt signaling, TCFs act as transcriptional repressors by forming a complex with transcriptional co-repressors of the Groucho/TLE family. Nuclear β-catenin binds to TCFs and physically displaces Groucho/TLE. Classically, this removal of the co-repressors converts TCFs into transcriptional activators. The bound β-catenin provides a platform for the recruitment of a multitude of transcriptional co-activators, which leads to initiation and propagation of transcription. Recently, however, a further consequence of β-catenin's binding to TCFs was discovered. Evidence has revealed, that some TCFs are more inclined to act as repressors than transcriptional activators. Studies indicate that TCF3 is inclined to act as a repressor, whereas Lef1 preferentially acts as an activator. Moreover, it was shown that TCF4 and TCF1 have the ability to fulfill both modes of action depending on the spatial and temporal context. The interaction of β-catenin with these repressive TCFs leads to the de-repression of the repressed target genes (Archbold et al., 2012; Chodaparambil et al., 2014; Lien et al., 2014; Nguyen et al., 2009; Shy et al., 2013; Valenta et al., 2012; Wray et al., 2011; Wu et al., 2009; Yi et al., 2011).

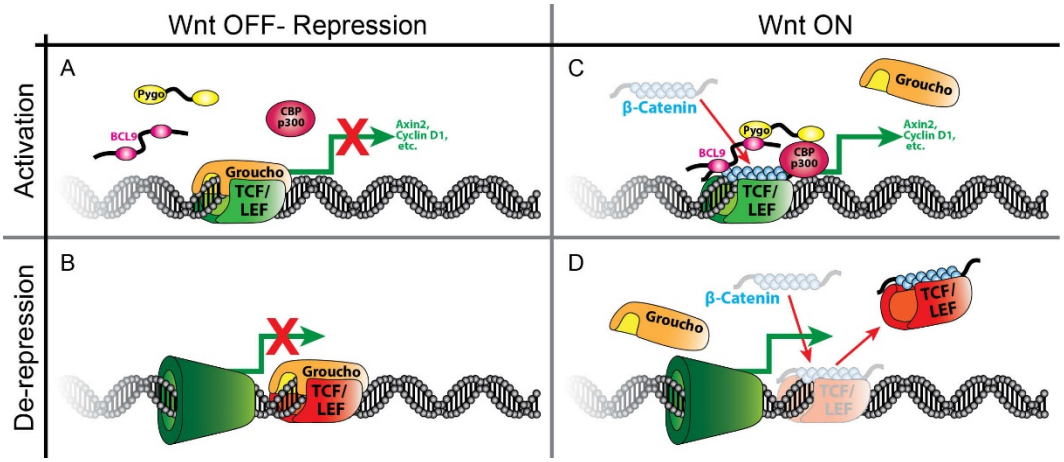

Figure 2 The TCF/β-catenin transcriptional switch

*(A, B) In a Wnt OFF situation, TCF/*Lef *transcription factors bound with Groucho co-repressors act as transcriptional repressors. In a Wnt ON situation, β-catenin physically removes co-repressors and either (C) transactivates TCF/*Lef *by providing an interacting platform for the multitude of transcriptional co-activators, or (D) promotes transcriptional de-repression. Unpublished schematic.*

3.1.3. β-catenin

The β-catenin protein plays a dual role in metazoan organisms. It is a central mediator of gene expression in the canonical Wnt-signaling pathway, in addition to being an important subunit in the cadherin-based cell-cell adhesion complex. The aptitude of β-catenin to perform both functions lies in its structural composition. The β-catenin protein is composed of 12 Armadillo repeats and is flanked by an amino-terminal domain (N-terminus) and a conserved helix-C next to a carboxy-terminal domain (C-terminus). The functionality of β-catenin is defined by the interacting molecules bound to its core region (Armadillo repeats R3-R9). The main interaction partners of β-catenin for adherence junctions (cadherin), the destruction complex (APC), and nuclear function (TCF/Lef) share overlapping binding sites, which inhibits them to bind simultaneously. The majority of the transcriptional co-activators bind to the C-terminus and have the potential to affect chromatin structure either by modifying histones or by controlling nucleosome arrangement, whereas other binding partners promote the association with the RNA polymerase II complex. Actin associated α-catenin binds to the N-terminus of β-catenin. This interaction links transmembrane cadherin to the actin cytoskeleton via β-catenin. Further N-terminus binding factors Pontin52 and B-cell CLL/lymphoma9 protein (BCL9) are presumably involved in chromatin remodeling that favors gene transcription. (Mosimann et al., 2009; Valenta et al., 2012; Xu and Kimelman, 2007)

β-catenin is the bottleneck of canonical Wnt signaling, as it is the central, non-redundant component of the pathway. This trait has made β-catenin especially attractive as a target for genetic manipulation to elucidate the impact of Wnt signaling in vivo. Most commonly these genetic manipulations were performed by conditionally knocking-out β-catenin. The dual role of β-catenin however made it difficult to collate a specific phenotype obtained upon β-catenin gene (*Ctnnb1*) manipulation to either or both functions of β-catenin. In the first publication of this thesis, we characterize a newly generated mouse model, in which a mutated form of the β-catenin protein preserves the capability to mediate adhesion, but lacks the functionality to transactivate TCF. Since its discovery more than 30 years ago, β-catenin has been identified as a multifaceted molecule. To this day, however, it is believed, that all its functions have still not been determined, which allows researchers only to fathom the complexity of how these different functions are coordinated. The generation and analysis of new genetic mouse lines, like the one we present, promises a great advancement in understanding these processes.

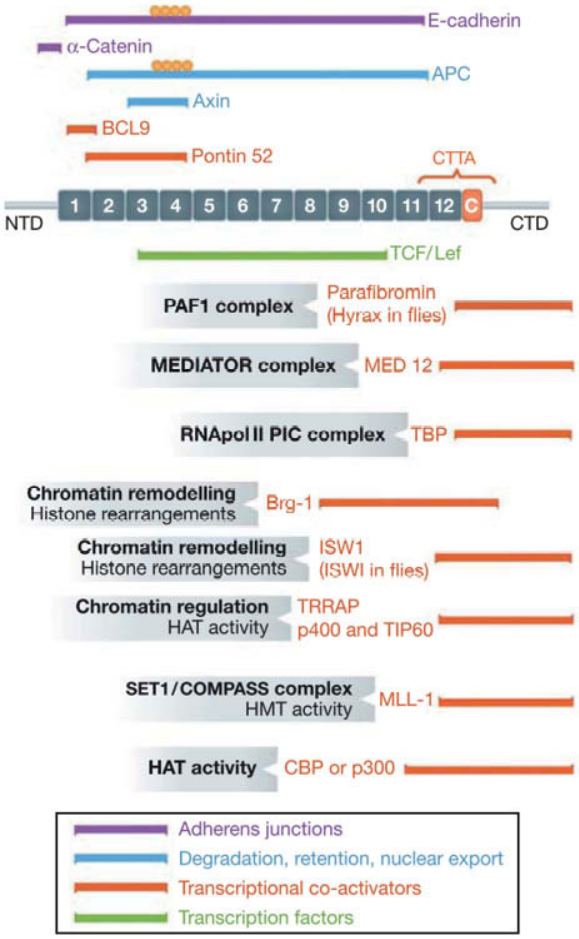

Figure 3 Binding sites of β-catenin interaction partners

The β-catenin protein consists of 12 Armadillo repeats (numbered boxes), flanked by an amino-terminal domain (NTD) and a carboxy-terminal domain (CTD). Between the last Armadillo repeat and the CTD is a conserved helix-C (C). Coloured bars show binding sites for β-catenin interaction partners. Colour code: purple, components of adherens junctions; blue, members of the β-catenin destruction complex; orange, transcriptional co-activators; green, transcription factors providing DNA binding. C-Terminal Transcriptional Activators (CTTA), the critical domain for their binding is marked by brackets. Little yellow circles indicate phosphorylation sites on either E-cadherin or APC that enhance the interactions. In the grey boxes, the function is indicated of the particular β-catenin interactor or of a complex, where this binding partner is a member. Adapted from Valenta et al., 2012.

APC, Adenoma Polyposis Coli; TCF/Lef, T-cell factor/Lymphoid enhancer factor; BCL9, B-cell lymphoma-9. Brg-1 is also known as SMARCA4, CBP as CREBBP. HAT, histone acetyl-transferase; HMT, histone methyltransferase; MLL, mixed lineage leukaemia; PAF-1, Polymerase-associated factor-1; PIC, Pre-Initiation complex; TBP, TATA-box binding protein; TRRAP, Transformation/transcription domain-as-sociated protein.

3.2. Neural crest cells

Neural crest cells (NCCs) are an extraordinary population of migratory cells unique to vertebrate development. During embryonic development NCCs originate from the dorsal region of the freshly formed neural tube. Consequent to their emigration from the dorsal neural tube by means of epithelial to mesenchymal transition (EMT), they migrate through the body along distinct pathways to respective target sites. Upon arrival NCCs differentiate into the diverse cell type specific to their newly acquired niche (Crane and Trainor, 2006; Le Douarin et al., 2008; Ruhrberg and Schwarz, 2010).

3.2.1. Regulatory steps from neural crest induction to migration

The processes of specification, EMT and migration of NCCs are controlled by molecular players such as extracellular growth factors and intracellular signaling molecules and transcription factors, which form a multimodule gene regulatory network (Sauka-Spengler and Bronner-Fraser, 2008).

NCCs originate at the neural plate border (prospective dorsal neural tube) around the time of neural tube closure. Signals from neural and non-neural ectoderm interact with those of the underlying mesoderm resulting in induction of NCCs. A complex signaling interaction due to exposure to bone morphogenic protein (BMP), fibroblast growth factors (FGF) and Wnts leads to an up regulation of a unique set of genes in the neural plate border region. These so-called border neural plate border specifier genes include Zic factors, Pax3/7, Msx1/2 and Dlx3/5. Their presence activates the expression of transcription factors such as Snail1, Snail2, AP-2, FoxD3, Sox9, c-Myc and Id in expected NCCs. All these changes in gene expression enable NCCs to undergo EMT and commence migration (Bronner, 2012; Prasad et al., 2012; Sauka-Spengler and Bronner-Fraser, 2008).

Since emigration of NCCs occurs subsequent to neural tube closure, it follows the same rostral-caudal gradient as neurulation. Upon delamination from the dorsal neural tube, NCCs express the transcription factor Sox10 and the low affinity neurotrophin receptor p75 (Paratore et al., 2001; Southard-Smith et al., 1998; Stemple and Anderson, 1992). Migration is guided along specific pathways until the target sites are reached. Interestingly, these distinct pathways are not promoted by defined routes, but restricted mainly by the mediation of repulsive signals, which inhibit NCCs from entering certain regions (Sauka-Spengler and Bronner-Fraser, 2008).

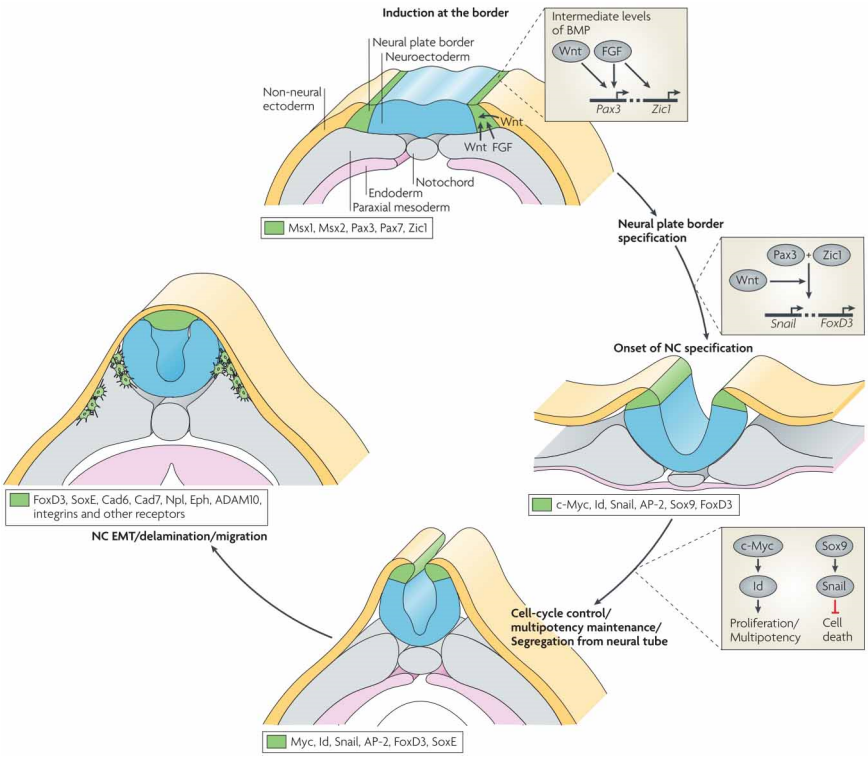

Figure 4 Regulatory steps in neural crest formation

A combination of Wnt-, FGF-, and BMP-signaling initiates the specification NCCs at the neural plate border. Expression of early NCC specifiers in nascent NCCs distinguishes them from the dorsal neuroepithelium and cues the progenitors of NCC to undergo EMT and delaminate from the dorsal neural tube. Upon emigration from the neural tube migrating NCCs express Sox10 and p75, which are a distinct set of genes marking NCCs. Adapted from Sauka-Spengler and Bronner-Fraser, 2008.

3.2.2. Neural crest populations

Generally NCCs are subdivided into four groups: cranial, vagal, cardiac and trunk. The division into different subpopulations depends on the rostro-caudal axial level from which NCCs delaminate.

Prior to their migration cranial NCCs emigrate from the fore-mid- and hindbrain regions of the neural tube. They give rise to the craniofacial skeleton and tissues of the eyes, ears, and nose. Additionally, they contribute to form the sensory neurons, glia, Schwann cells, smooth muscle and melanocytes of the head. Cranial NCCs that generate cranioalfacial structures first populate the pharyngeal apparatus, upon which they acquire mesenchymal fates. Pharyngeal arches are a transient structures, which upon their colonization of cranial NCCs are remodeled into terminal structures (Cordero et al., 2011; Trainor, 2005).

Vagal NCCs leave the neural tube at the level of somites 1-7 and give rise to the enteric nervous system (ENS). In mice vagal NCCs invade the anterior foregut at embryonic day (E) E9 and migrate in a rostral to caudal direction. They colonize the entire gut by E15.5 (Heanue and Pachnis, 2007).

The cardiac NCCs delaminate from neural tube levels of the post-otic hindbrain to somite 3 and migrate to the heart and pharyngeal arches 3, 4, and 6. They are committed to a smooth muscle lineage of the cardiac outflow tract and participate in its separation into aorta and pulmonary artery (Jiang et al., 2000; Sieber-Blum, 2004).

Trunk NCCs leave the neural tube from somite 7 to the most caudal region of the neural tube and migrate along two separate pathways. The ventral pathway leads NCCs between the somites to their destinations. Cells migrating along this pathway differentiate into neurons and glia cells of sympathetic (SG) and dorsal root ganglia (DRG) as well as Schwann cells of the peripheral nervous and chromaffin cells in adrenal glands. Trunk NCCs migrating along the dorsolateral pathway between the somites and the ectoderm become melanoblasts, which will give rise to the pigment cells of the skin (Crane and Trainor, 2006; Huber, 2006; Ruhrberg and Schwarz, 2010) .

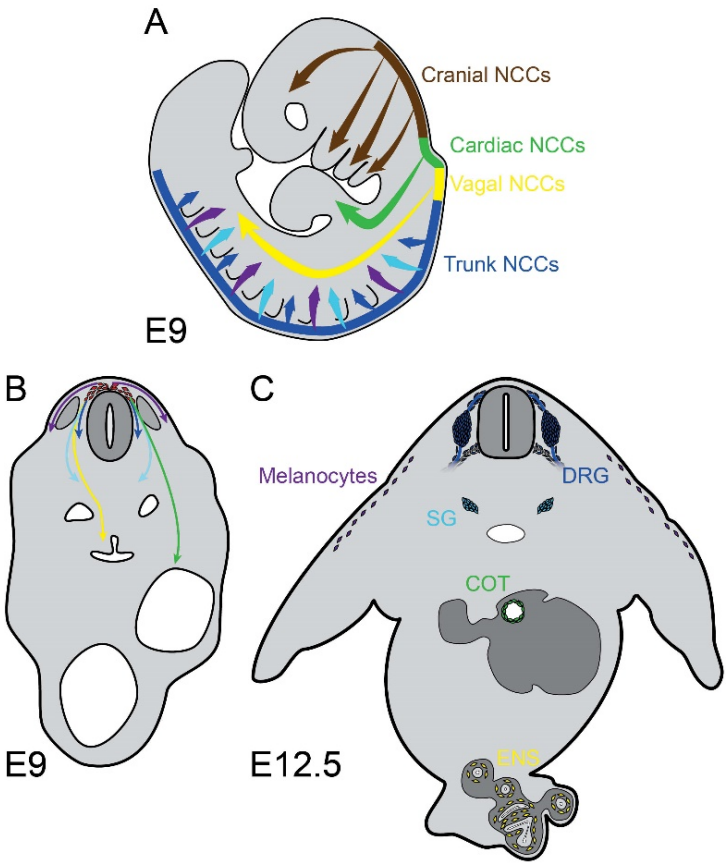

Figure 5 NCC subpopulations and migration paths

NCCs are divided into four subtypes depending on the rostral-caudal axis level, cranial (brown), cardiac (green), vagal (yellow) and trunk (blue) NCCs. (B) At E9 NCCs migrate along distinct pathways to their target niches. (C) At E12 NCCs have reached their destinations and differentiated into specific derivatives. Cranial NCCs emigrate to the pharyngeal arches (A brown arrows), acquire a mesenchymal fate and give rise to craniofacial tissues. The cardiac NCCs migrate to the heart (A, B green arrows) and commit to a smooth muscle lineage of the cardiac outflow tract (COT, C green). Vagal NCCs invade the anterior foregut, migrate in a rostral to caudal direction (A, B yellow arrows) and give rise to the enteric nervous system (ENS, C yellow). Trunk NCCs migrate along two separate pathways. The ventral pathway (A, B blue arrows) leads NCCs, which differentiate into neurons and glia cells of sympathetic (SG, C light blue) and dorsal root ganglia (DRG, C dark blue) between the somites. Trunk NCCs migrating along the dorsolateral pathway (A, B violet arrows) between the somites and the ectoderm become melanocytes (C violet). Unpublished schematic.

3.2.3. Neural crest stem cells (NCSCs)

Stem cell are defined as a cells possessing the potential to differentiate into multiple progeny as wells as the ability to self-renewal/proliferate. The fact NCCs can generate many different cell types would characterize them as multipotent stem cells. However, this argument has led to a long ongoing debate in the scientific community. The focus of discussion revolved around whether NCCs are a multipotent, multifated cell population, which restrict their fate gradually after emigration or whether they are a pool of heterogeneous, restricted progenitors prespecified in the neural tube.

The hypothesis for multipotent neural crest stem cells (NCSCs) was originally founded by the demonstration of individual cells from cultured isolated NCCs grown at clonal density to adopt several different fates (Baroffio et al., 1991; Sieber-Blum and Cohen, 1980; Stemple and Anderson, 1992). This hypothesis was bolstered by the labelling of numerous lineages upon in vivo dye injections into single neuroepithelial cells or emigrating NCCs (Bronner-Fraser and Fraser, 1989; Bronner-Fraser and Fraser, 1988). Furthermore, it could be shown that isolated NCCs are not only multipotent, but are also able to self-renew (Stemple and Anderson, 1992).

The main findings conflicting to these data were those from the laboratory of Kalcheim and colleagues. In their report Krispin et al. could correlate the position of NCCs in the tube to the time they would delaminate and to the fate they would adopt, by marking single neuroepithelial cells in chick neural tubes (Krispin et al., 2010). These experiments supported the pre-specification theory.

Recent work from our lab could settle this dispute for the trunk subpopulation of NCCs by in vivo quantitative clonal analyses of single lineage traced trunk NCCs in mice combined with definitive differentiation markers. It could be demonstrated that a vast majority of individual trunk NCCs are multipotent (Baggiolini et al., 2015).In this respect we will refer to NCCs from here on out as NCSCs (Bronner, 2015).

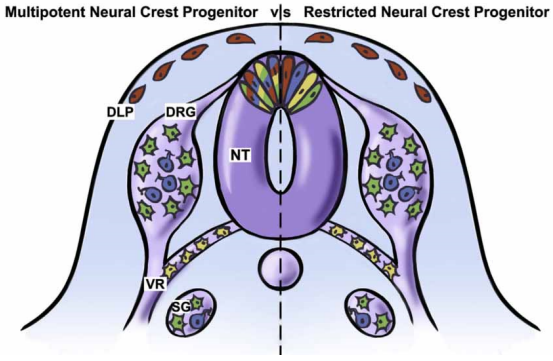

Figure 6 Multipotent vs restricted fate resume

NCCs contribute to diverse cells such as neurons (blue) and glia (green) of the DRG and SG; Schwann cells (yellow) of the ventral root (VR); and melanocytes (red) along the dorsolateral pathway (DLP). This capacity of NCCs was attributed to one of the two scenarios. Left: Premigratory NCCs in the dorsal neural tube (NT) are multipotent, migrate to diverse sites and differentiate into appropriate cell types in response to local environmental cues. Right: Unipotent premigratory NCCs may be a mixture of restricted precursors, which migrate to appropriate sites and differentiate according to their predetermined fates. Adapted from Bronner, 2015.

3.3. Wnt-β-catenin signaling in NCSC development

Neural crest development is dependent on Wnt signaling at multiple stages. As previously described, Wnt expression at the neural plate border instructs cells to assume a NCSC fate. Later, Wnt together with BMP growth factors induce lineage expansion by preserving the undifferentiated state of NCSCs (Kléber et al., 2005). Furthermore, Wnt signaling has been shown to be important in NCSC lineage decisions, in particular derivatives of the cranial and trunk populations, using conditional-knock-out models for β-catenin (Brault et al., 2001; Hari et al., 2002). However, the loss of cadherin mediated adhesion in these models was rarely attributed to specific phenotypes in these and other studies, which utilized conditional knock-out models of β-catenin in other tissues (Grigoryan et al., 2008). In the second and third part of this thesis we demonstrated the importance of separating the single functions of the β-catenin by comparing the development of sensory, respectively ocular, lineages derived from NCSCs in different mouse models.

3.3.1. Wnt/β-catenin function in the sensory lineage

The dorsal root ganglia (DRG) consists of sensory neurons and associated glia derived from the peripheral sensory lineages of trunk NCSC. In the DRG sensory subtypes are characterized by the expression of neurotrophin receptor kinases (Trk) A, B, or C. Neuronal subtype specification is classically thought to occur in sequential waves of neurogenesis driven by proneural transcription factors. The basic helix-loop-helix (bHLH) transcription factor neurogenin 2 (Neurog2) initiates a first wave of neurogenesis and is expressed in an early population of migratory NCSCs. It is continuously expressed throughout their migration until they reach the forming DRG, after which it is largely down regulated. Migratory cells expressing Neurog2 at high levels give rise to mechanoreceptive and proprioceptive neurons expressing TrkB and TrkC. A subpopulation of Neurog2-positive cells, which express weak levels of the protein give rise to TrkA expressing nociceptive neurons. A later wave of neurogenesis is formed by Sox10-positive DRG progenitors, of which a subgroup will express the bHLH transcription factor neurogenin 1 (Neurog1) post migration within the coalesced DRG. This Neurog1-mediated wave mainly gives rise to neurons expressing TrkA, but can partially contribute to the TrkB and TrkC population. Furthermore, both waves of DRG progenitors generate glia (Marmigère and Ernfors, 2007; Sommer et al., 1996).

The third and final wave of neurogenesis produce the boundary cap cells (BCCs). BCCs give rise to peripheral glia, which appear in small clusters at the surface of the spinal cord, at prospective motor exit points and dorsal root entry zones. A fraction of cells surrounding the dorsal root entry zone migrate into the formed DRG and generate a small population of TrkA-positive neurons (Maro et al., 2004).

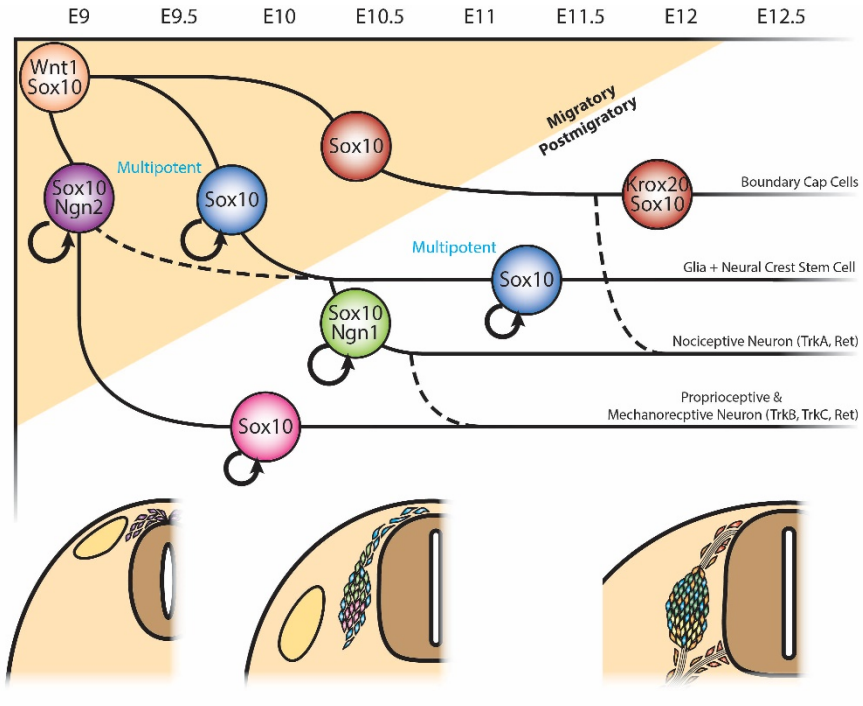

Figure 7 Genetic cascades of sensory neurogenesis

Distinct genetic cascades control the first two waves of sensory neurogenesis. The first wave of Sox10 expressing cells co-express Neuorg2. High levels of Neurog2 bias cells to commit to a proprioceptive or mechanoreceptive neuron fate. Cells expressing low or no level of Neurog2 remain uncommitted and obtain second wave potential (dashed line). Cells of the second wave of neurogenesis continuously express Sox10 throughout migration and in the DRG, where they continue to divide at a high rate. These cells start to express Neurog1, upon which they mainly produce nociceptive neurons, but also contribute in part to the proprioceptive and mechanoreceptive neurons (dashed line). The third wave arises from BCCs expressing Sox10 and Krox20 and contribute to the nociceptive neurons (dashed line). Simplified reproduction of schematic from Marmigère and Ernfors, 2007

A report from our laboratory demonstrated that the loss of β-catenin is also fatal for the development of the DRG (Hari et al., 2002). The phenotype acquired from this experiments was assigned to the different functions of β-catenin to the best of knowledge, but these hypotheses could never be completely validated. Considering that adhesion as well as signaling functions of β-catenin are important for DRG development made the sensory lineage an optimal candidate to discriminate the importance of the two functions using the novel β-catenin mouse model that preserves adhesion, but lacks TCF transcription. In the second publication of this thesis we reassessed the functions of β-catenin in development of the DRG by comparing the new mouse model with the most commonly used β-catenin knock-out model.

3.3.2. Wnt/β-catenin function in the ocular lineage

The vertebrate eye is a complex structure that is constructed during development from four general precursor sources: neural ectoderm, surface ectoderm, mesoderm and cranial NCSCs to which we refer to as ocular NCSCs. The eye originates from bilateral telencephalic optic grooves. The contact of these grooves with the surface ectoderm induces the formation of lens placodes, which invaginate to form the double layered optic cups. The outer layer evolves into the retinal pigment epithelium, and the inner layer will form the retina. As optic vesicles grow, their connections with forebrain are constricted to the optic stalk. A groove at the inferior aspect of the optic vesicle, referred to as the optic fissure, is the entry point of the hyaloid artery, which nourishes the optic cup and lens. The fissure will gradually fuse and allow the eye to inflate (Gage et al., 2005; Harada et al., 2007; Lamb et al., 2007).

During these processes ocular NCSCs, surround not only the outer part of the eye to form the sclera, extraocular muscle, corneal endothelium and stroma, but also migrate through the optic fissure into the optic cup. Ocular NCSCs in the developing eye give rise to the primary vitreous, the choroid vasculature and structures of the chamber angle, such as the trabecular meshwork. However, few mesoderm derived cells also contribute to these structures (Gage et al., 2005; Ittner et al., 2005).

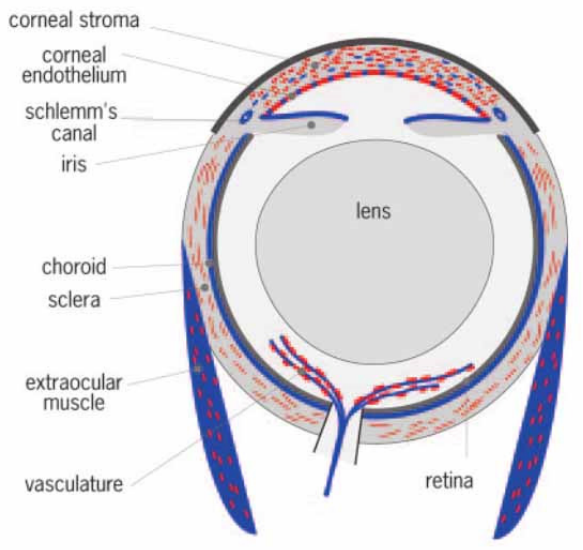

Figure 8 NCSCs and mesoderm fates in the mammalian eye

Cross-sectional diagrams summarizing contributions of neural crest (red) and mesoderm (blue) to mouse eyes. The sclera, extraocular muscle, corneal endothelium and stroma, the choroid vasculature, and structures of the chamber angle are mainly derived from ocular NCSCs with the addition of few mesoderm derived cells. Adapted from Gage et al., 2005.

Wnt signaling has been shown to play a major role at all stages of ocular development (Fuhrmann, 2008; Grigoryan et al., 2008). However, its role in ocular NCSCs has not been strongly pursued. Conditional loss of β-catenin in cranial NCSCs has been shown to not only lead to an absence of cranial bones and cartilage (Brault et al., 2001), but also influences the proper eye development. Loss of β-catenin in ocular NCSCs has been shown to inhibit the fusion of the optic cup as well as lead to an absence of the corneal endothelium and stroma at progressed stages of eye development (Zacharias and Gage, 2010). Late stage effects of the loss of β-catenin have not been reported to date. For this reason we found it intriguing to investigate functional roles of β-catenin in ocular NCSCs in eye development. The preliminary findings of this investigation make up the third part of this thesis and gave us reason to hypothesize that multiple functions of β-catenin are required in ocular NCSCs individually or simultaneously depending on the developing derivative.

3.3.3. Tools to investigate Wnt/β-catenin signaling and functions of β-catenin in NCSC development

Scientific research has greatly profited from the use of transgenic mouse models. One of which is the Cre/LoxP system. The Cre/LoxP system permits alteration of genes in specific tissue by targeting a distinct exon/gene and splicing it in only these tissues. An exon/gene, which is flanked by two loxP sites due to genetic manipulation, will be excised in the presence of a Cre-recombinase. The expression of the Cre enzyme is driven by a tissue specific promoter. NCSC specific Cre-lines were used in combination with multiple transgenic mouse lines to determine the importance of individual functions of β-catenin, as well as the relevance of autocrine Wnt secretion in the derivatives of NCSCs. Description of used mouse lines is elaborated in the **Material and method** chapter of this thesis.

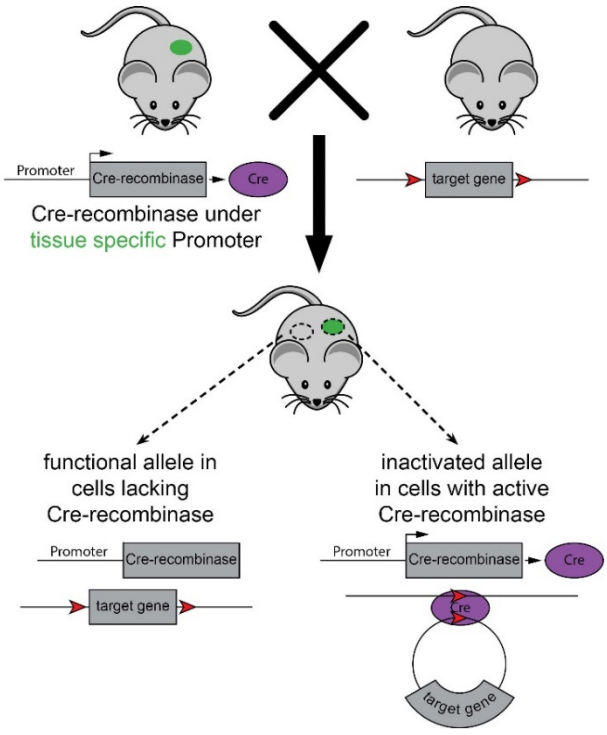

Figure 9 Tissue specific deletion using Cre/loxP system

Deletion of a gene flanked by two loxP sites is distinctively obtained in cells in which the tissue specific promoter is active. Unpublished schematic.

4. Materials and methods

4.1. Animals and genotyping

There are two main mouse lines used for gene specific recombination of NCSCs. The first is *Wnt1-Cre* in which Cre recombinase transcription is driven by the *Wnt1* promoter that is active in the dorsal neural tube at stages before neural crest delamination (Danielian et al., 1998; Hari et al., 2002; Hari et al., 2012; Jiang et al., 2000). The second is the *Sox10-Cre* in which Cre is first expressed in NCSCs only after their emigration from the neural tube (Hari et al., 2012; Matsuoka et al., 2005).

Two floxed mouse lines combined with the previously mentioned new mouse model for β-catenin were used to determine the functionality of β-catenin in NCSCs. In the first mouse line the exons 2-6 of *Ctnnb1* are flanked by loxP sites (*Ctnnb1*^{flox}), which when recombined lead to excision of the floxed exons, a frame shift mutation and production of a *Ctnnb1* null-allele (Brault et al., 2001). The second mouse model was an α-catenin ablation line in which the exon 2 of the α-catenin gene (*Ctnna1*) is floxed (*Ctnna1*^{flox}) generating an early frame shift and translation termination (Lien et al., 2006; Vasioukhin et al., 2001). The novel *Ctnnb1*^{dm} mouse line contains a single amino acid change in the first Armadillo repeat of β-catenin (D164A) as well as a truncation of the C-terminus. The generation and functionality of this model will be described in the first publication of this thesis.

To determine the importance of autocrine Wnt secretion in NCSCs we made use of a conditional allele of *Wls* mouse model generated by the lab of Prof. Konrad Basler. The targeting approach was to splice the first exon, which encodes the transcriptional start and the complete signal sequence. Excision of the floxed region therefore leads to a null-allele of *Wls*.

Lineage tracing was performed by crossing *ROSA26* reporter lines into our mouse models. In these reporter lines Cre-recombination removes a floxed “stop” sequence from in between the promoter of the ubiquitously expressed ROSA26 protein and a β-galactosidase, respectively enhanced green fluorescent protein (*EGFP*), allele (Mao et al., 2001; Soriano, 1999). Furthermore, we made use of the *BAT-gal* Wnt-reporter line in which β-galactosidase is expressed under the control of mulitmerized TCF/Lef-binding sites. This allowed us to observe the activity of TCF/Lef mediated transcription in single cells.

Name	Genetic	
Wnt1-Cre	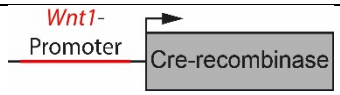	(Danielian et al., 1998)
Sox10-Cre	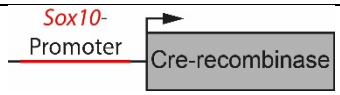	(Matsuoka et al., 2005)
Ctnnb1^{flox}	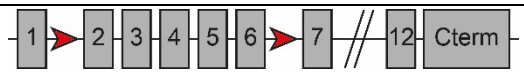	(Brault et al., 2001)
Ctnnb1^{dm}	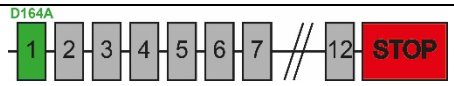	(Valenta et al., 2011)
Ctnna1^{flox}	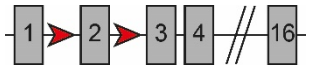	(Vasioukhin et al., 2001)
Wls^{flox}	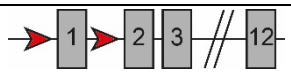	(Gay et al., in revision)
R26R (R26R$^{β\text{-}galactosidase}$)	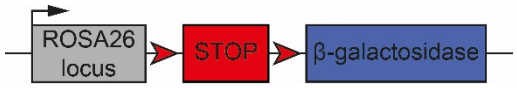	(Soriano, 1999)
EGFP (R26R^{GFP})	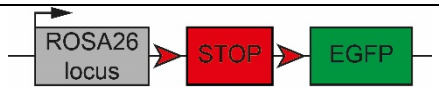	(Mao et al., 2001)
BAT-gal (Wnt Reporter)	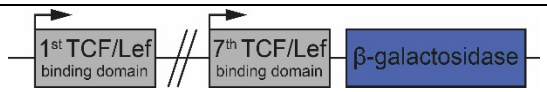	(Maretto et al., 2003)

Table 1 Transgenic mouse lines

Genotyping was performed by PCR on genomic DNA obtained from the amniotic sac of embryos or toe clippings from postnatal animals. The primers, concentrations and programs used are listed in Table 2.

Gene	Primers	Reagent concentrations	Program
Wnt1-Cre *Sox10-Cre* (447 bp)	Fwd Primer: 5'-atg ccc aag aag aag agg aag gt- 3' Rev Primer: 5'-gaa atc agt cgc ttc gaa cgc tag a-3'	**Quiagen** 16.78 H2O 2.5µl 10xPCR buffer 1.5 µl MgCl2 (25 mM) 0.5 µl dNTPs (10 mM) 0.25 µl Fwd Primer (20µM) 0.25 µl Rev Primer (20µM) 0.22 µl Taq polymerase 3 µl DNA	94°C 3 min 30x (94°C 1 min, 57°C 45sec 72°C 1 min) 72°C 5 min
Ctnnb1^{flox} (Wt: 221 bp; Flox: 324 bp)	Fwd Primer: 5'-aag gta gag tga tga aag ttg tt-3' Rev Primer: 5'-cac cat gtc ctc tgt cta ttc-3'	**Invitrogen** 13.85 H2O 2.5 µl 10xPCR buffer 1.8 µl MgCl2 (50 mM) 0.66 µl dNTPs (10 mM) 0.35 µl Fwd Primer (20µM) 0.35 µl Rev Primer (20µM) 0.22 µl Taq polymerase 2 µl Solution Q 3 µl DNA	94°C 2 min 40x (94°C 1 min, 59°C 45sec 72°C 1.5 min) 72°C 10 min
Ctnnb1^{dm} Nterm: (Wt: 475 bp; Mnt: 628bp) Cterm: (Wt: 349 bp; Mnt: 415 bp)	**N-terminal:** Fwd Primer: 5'-tcc ctg aga cgc tag atg-3' Rev Primer: 5'-gag tcc cag cag tac aac- 3' **C-terminal:** Fwd Primer: 5'-gtc cac acg tca tgc ttt ac-3' Rev Primer: 5'-tgg ctt gtc ctc aga cat tcg-3'	**Invitrogen** 15.12 µl H2O 2.5 µl 10xPCR buffer 0.75 µl MgCl2 (50 mM) 0.5 µl dNTPs (10 mM) 1 µl Fwd Primer (20µM) 1 µl Rev Primer (20µM) 0.13 µl Taq polymerase 4 µl DNA	94°C 2 min 30x (94°C 30 sec, 56°C 30sec 72°C 40 sec) 72°C 5 min
Ctnna1^{flox} (Wt: 100 bp; Flox: 350 bp)	Fwd Primer: 5'-cat ttc tgt cac ccc caa aaga cac-3' Rev Primer: 5'-gca aaa tga tcc agc gtc ctg gg-3'	**Quiagen** 16.86 H2O 3.6 µl 10xPCR buffer 2.88 µl MgCl2 (25 mM) 0.72 µl dNTPs (10 mM) 1.8 µl Fwd Primer (20µM) 1.8 µl Rev Primer (20µM) 0.18 µl Taq polymerase 3 µl DNA	94°C 2 min 35x (94°C 30 sec, 68°C 1 min 72°C 45 sec) 72°C 2 min

Table 2 Primers, concentrations and programs

Gene	Primers	Reagent concentrations	Program
Wls^{flox} (Wt: 267 bp; Flox: 353 bp)	Fwd Primer: 5'-ccc cct ttc cct ctc ggt tcc-3' Rev Primer: 5'-ggc ggc atg gaa gcc aag ggc-3'	**Qiagen** 17.5 H2O 2.5 µl 10xPCR buffer 0.75 µl MgCl2 (25 mM) 0.5 µl dNTPs (10 mM) 0.75 µl Fwd Primer (20µM) 0.75 µl Rev Primer (20µM) 0.25 µl Taq polymerase 2 µl DNA	94°C 3 min 33x (94°C 30 sec, 57°C 30 sec 72°C 1 min) 72°C 5 min
R26R (Wt: 500 bp; Mnt: 250 bp)	SoA Primer: 5'-aaa gtc gct ctg agt tgt tat-3' SoB Primer: 5'-gcg aag agt ttg tcc tca acc-3' SoC Primer: 5'-gga gcg gga gaa atg gat atg-3'	**Qiagen** 17.12 H2O 3 µl 10xPCR buffer 1.8 µl MgCl2 (25 mM) 0.66 µl dNTPs (10 mM) 0.4 µl SoA (20µM) 0.4 µl SoB (20µM) 0.4 µl SoC (20µM) 0.22 µl Taq polymerase 2 µl Solution Q 4 µl DNA	94°C 3 min 35x (94°C 45 sec, 54°C 45 sec 72°C 1 min) 72°C 5 min
EGFP (200 bp)	Fwd Primer: 5'-cgc acc atc ttc ctt caa gga cga c-3' Rev Primer: 5'-aac tcc agc agg acc atg tga tcg-3'	**Invitrogen** 17.22 H2O 2.5 µl 10xPCR buffer 0.9 µl MgCl2 (50 mM) 0.66 µl dNTPs (10 mM) 1.5 µl Fwd Primer (10µM) 1.5 µl Rev Primer (10µM) 0.25 µl Taq polymerase 2 µl Solution Q 3 µl DNA	94°C 2 min 35x (95°C 30 sek, 61°C 30sec 72°C 45 sec) 72°C 7 min
β-galactosidase (464 bp)	Fwd Primer: 5'-tcc caa cag ttg cgc agc ctg aat g-3' Rev Primer: 5'-ata tcc tga tct tcc aga taa ctg ccg-3'	**Qiagen** 20.15 H2O 3 µl 10xPCR buffer 1.8 µl MgCl2 (25 mM) 0.75 µl dNTPs (10 mM) 0.05 µl Fwd Primer (20µM) 0.05 µl Rev Primer (20µM) 0.2 µl Taq polymerase 4 µl DNA	94°C 2 min 40x (94°C 15 sec, 66°C 20 sec 72°C 45 sec) 72°C 10 min

Table 2 Primers, concentrations and programs

4.2. Immunohistochemistry, X-gal- and EdU-staining

After their isolation, embryos were fixed in 4% formaldehyde for a certain amount of time corresponding with their age, see Table 3.

Embryo Age	Fixation time
E9.5	10 min
E10.5	20 min
E11.5	30 min
E12.5	50 min
E14.5	1hrs 20 min
E16.5	1hrs 45 min
E18.5	2hrs

Table 3 Fixation time for freshly isolated embryos

Stainings were performed on 12 µm thick sections. Slides with tissue samples were frozen at -20°C right after the last section was cut, not after 4 hours as has been custom in our lab in the past.

β-gal reporter gene expression was detected using X-Gal staining, see Protocol 1.

Immunohistochemistry (IHC) was performed as described in Protocol 2. Primary and secondary antibodies used for IHC, their concentrations and additional information to staining with these antibodies are listed in Table 4 and Table 5.

Some stainings needed to be performed within 2 weeks after sectioning and preservation at -20°C, as it appears that some proteins are degraded rapidly and cannot be detected by IHC after this time (marked “rapid deg.”). However, if slides are preserved at -80°C it is possible to stain for these proteins after a longer period of time, possibly 2-3 months.

Prior to IHC, cryo-sections were fixed for 30 seconds in 3.8% formaldehyde at room temperature. It is possible to fix for a longer period of time, but this could lead to the masking of binding sites, which inhibits proper binding of the primary antibodies. This is especially the case for transcription factors, in particular Sox10.

Antigen retrieval was only applied on tissue older than E11.5 unless stated otherwise in the additional information. Retrieval was performed using citrate buffer pH 6.

Usual blocking buffer was 1%BSA, 0.3% Triton X-100, in PBS (PBT) unless stated otherwise in Table 4. Moreover some primary antibodies cannot be incubated simultaneously, but rather serially as the primary antibodies cross react with other primary antibodies, again this is

marked in Table 4. Incubation for 2 hours at room temperature are equivalent to 4°C over night. In the case of Sox10 it is optimal to incubate for 4 hours at room temperature. Secondary antibodies can be incubated together, if there is no species interaction.

EdU was detected using the Click-iT® EdU Alexa Fluor® 488/647 Flow Cytometry Assay Kit from Invitrogen Molecular Probes. The staining was performed subsequently to the washing step after the incubation of the secondary antibodies.

Primary antibodies requiring amplification for IHC were amplified using the Tyramide Signal Amplification Plus TSA Plus Cy3/5 System from Perkin Elmer. Amplification was performed as described in Protocol 3. If an amplification staining was to be co-labeled for further markers, Protocol 3 was performed until step 16, subsequently slides were washed 2 times in PBS for ten minutes and normal staining procedures were continued starting from Protocol 2 step 4.

Protocol 1 X-Gal staining

- Fix whole embryos 5 min RT, cryosections 5min on ice in fixation solution:
  Fixation solution (always prepare fresh): 12.5 ml

2% Formaldehyde (37% stock)	675 µl stock
0.2% Glutaraldehyde (25% stock)	100 µl stock
0.02% NP40 (10% stock)	25 µl stock
in PBS	11.7 ml

- wash 3x5 min PBS at RT
- develop several hours in X-Gal staining solution at 37°C
  "**X- Gal reaction buffer**": can be stored at least one year at 4°C or RT in alu foil

1ml of 100mM K3Fe(CN)6 stock	final concentration 10mM
1ml of 100mM K4Fe(CN)6 stock	final concentration 10mM
1ml of 20mM MgCl2 stock	final concentration 2mM
in 10 ml PBS	

- **X-Gal staining solution**
  Add fresh to 10ml X-Gal reaction buffer
  20µl of 10% stock NP40 (final conc 0.02%)
  100 µl of 50mg/ ml X-Gal in DMF (aliquots stored at -20°C) = final conc. 0.5mg/ml
- after staining wash 3x5 min PBS at RT
- fix 4% PFA o.n. 4°C (embryos) or 15 min RT (sections)
- store Embryos in 70% EtOH at -20°C or mounts slides in Glycerol

Stock solutions	50ml
100mM K3Fe(CN)6 (329g/ mol)	1.645g
100mM K4Fe(CN)6 °3H2O (422.4g/ mol)	2.11g
20mM MgCl2 ° 6H2O (203.31g/ mol)	0.203g

Protocol 2 Immunohistochemistry staining

Experiment: **Embryo Age:** **Slide:** **Date:**

1. Warm up slides to RT
2. Fix for ___ @ RT in FA 1:10, 12.5 ml for 5 Slides
3. Wash 3x5' in PBS

   evtl Ag-retrieval (e.g. 5min 110°C citrate ph6, in high pressure microwave) cool down 15min, wash 1x 5min PBS
4. Block 30' blocking buffer

   □ 1% BSA + 0.3% Triton □ 0.1% BSA + 1% GS + 0.3% Triton

   □ Special:_____
5. Primary Antibodies

Pr. Ab 1) (# ; 1: ;) ➔ Scd. Ab 1) (# ; 1: ;)

Pr. Ab 2) (# ; 1: ;) ➔ Scd. Ab 2) (# ; 1: ;)

Pr. Ab 3) (# ; 1: ;) ➔ Scd. Ab 3) (# ; 1: ;)

□ 4°C over night □ 2 hrs @ RT □ 4hrs @ RT

□ Sequential □ Parallel

Wash 5' in PBST, 10' in PBS

- For sequential staining repeat steps 5 (for 2h) through 7 @ RT

6. Add secondary antibodies for 50' @ RT
   - Make sure the secondary antibody fits to the first antibody (*e.g. Pr.Ab: Antirabbit, 2nd.Ab: Goat antirabbit*)
7. Wash 5' in PBST, 10' in PBS

   □ 1h @ RT EdU Staining *
8. DAPI stain for 2' @ RT
9. Wash 3 x 5' in PBS
10. Mount

PBST: PBS 0.3% Triton

Citrate buffer:
Stock A = 4.2gr citric acid monohydrate (MW:210.14gr/mol) in 200mL ddH2O,
Stock B= 14.7gr tri-sodiumcitrate dehydrate (MW: 294.10gr/mol) in 500mL ddH2O,
Working Solution 18mL Stock A +82mL Stock B + 900mL ddH2O adjust pH 6.0

Comments on Staining:_____

*** EdU Staining**

219 µL	PBS	____ µL
5 µL	$CuSO_4$	____ µL
25 µL	Buffer Addative. (10x 1:10 in cell culture H_2O)	____ µL
1.25 µL	Alexa Fluo (□ Cy2 ; □ Cy5)	____ µL

Protocol 3 TSA staining amplification

1. Warm to RT for 20min
2. Fix in 4% FA for 30sec
3. Wash 3x5min PBS
4. Antigen retrieval in citrate buffer pH 6.0 with microwave at 110°C, 10min
5. Wash 1x PBS for 10min
6. Quenching 37°C H_2O_2 %0.3 (in PBS) for 5-6 min in plastic mailer. (37.5 µl 30% H_2O_2 in 12.5ml)
7. Wash 2x with PBS 10min
8. Wash 1x with TN 10min
9. Wash 2x with TNT 5min
10. Incubate in blocking buffer (TNTB) for 1 hour @RT
11. Add 200µl of 1st Ab (_____ 1:____) in TNTB onto sections and incubate at 4°C, o.n. or 2hrs @RT
12. Wash 3x with TNT for 10min
13. Add 200 µl of 2nd Ab (HRP anti-_____ 1:300) in TNTB and incubate @RT1hour
14. Wash 3x with TNT for 10min
15. Develop with CY3/5 TSA kit (2min 1:50 dilution in amplification diluent)
16. Wash 2x TNT for 10min
17. DAPI
18. Mount sections with Immuno Mount

Buffers

- TN ; Tris-HCL 0.1M, NaCl 0.15M pH 7.5
- TNT ; Tris-HCL 0.1M, NaCl 0.15M, Tween 0.05% pH 7.5 (0.5ml in 1L)
- TNTB ; (Blocking Reagent from PerkinElmer) %0.5 Reagent in TNT

Antibody Name	Species	Company	Ordering number	Conc.	Bl. Buffer	Infos
alpha-catenin	Rabbit	Sigma	C2081	1:200	PBT	
α-Ecatenin	Rabbit	Cell Signaling	3236	1:200	PBT	
β-catenin (C-term)	Rabbit	Sigma	c2206	1:250	PBT	
β-catenin (N-term)	Mouse	EnzoLifeScience	ALX-804-060-C100	1:200	PBT	
beta-galactosidase	Chick	Abcam	ab9361	1:2000	PBT	Cross-reacts
BrdU	Mouse	Sigma	B8434	1:200	PBT	
BrdU	Rat	Abcam	ab6326-250	1:100	PBT	
BrdU	Mouse	cell Signaling	5292	1:200	PBT	
Brn3a	Rabbit	Turner Lab		1:2000	PBT	
cCasp3	Rabbit	Cell Signaling	9661	1:200	PBT	
c-Myc	Rabbit	Abcam	ab32072	1:500	PBT	Rapid deg.
Cyclin D1	Mouse	Santa Cruz	sc-450	1:200	PBT	
DCX	Guinea Pig	Millipore	AB2253	1:400	PBT	
EGFR	Rabbit	Millipore	06-847	1:200	TNTB	2min Amp
EGFR phospo	Mouse	Cell signaling	2236	1:500	PBT	
EGFR	Rabbit	Cell Signaling	4267	1:200	TNTB	2min Amp
ERM (ETV5)	Rabbit	Santa Cruz	sc-22807	1:200	PBT	
FABP	Rabbit	Abcam	ab32423	1:200	PBT	
Plakoglobin	Mouse	BD	610253	1:200	PBT	
GFP	Chick	AVES	GFP-1020	1:400	PBT	
GFP	Rabbit	abcam	ab290-50	1:200	PBT	
GFP	Rabbit	MolecularProbes	A11122	1:200	PBT	
ID2	Rabbit	Sigma	HPA027612	1:3000	PBT	
IQGAP	Rabbit	Abcam	ab87262	1:200	PBT	
Islet 1/2	Mouse IgG1	Hybridoma	40.2D6	1:200	PBT	
Ki67	Rabbit	Abcam	ab15580	1:200	PBT	
Ki67	Rat	Biolegend	652402	1:100	PBT	
Krox20	Rabbit	D.N. Meijer		1:4000	PBT	
Lef1	Rabbit	Cell Signaling	2230	1:200	PBT	
MITF	Mouse	J. Debbache		1:2000	PBT	Retrieval
N-cadherin	Rabbit	Takara	M142	1:200	PBT	
Neurofilament-M	Mouse IgG2a	Invitrogen	13-0700	1:250	PBT	
Neurofilament 160	Mouse	Sigma	N5264	1:100	PBT	
Neurog1 (Ngn1)	Goat	Santa Cruz	sc-19231	1:100	PBT	Rapid deg.
Neurog2 (Ngn2)	Mouse	Anderson Lab		1:10	PBT	Rapid deg.
p44/42	Rabbit	Cell Signaling	9101	1:200	PBT	
Pax3	Rabbit	Invitrogen	38-1801	1:500	PBT	
Pax6	Rabbit	Covance	PRB-278P	1:200	PBT	
Phalloidin		MolecularProbes	A12379	1:40	PBS	1 hrs incub.
pHH3	Mouse	Cell Signaling	9706	1:200	PBT	
Pitx2	Rabbit	Capra Science	PA-1020-100	1:1000	PBT	

Table 4 Primary antibodies

Antibody Name	Species	Company	Ordering number	Conc.	Bl. Buffer	Infos
pSmad1/5/8	Rabbit	Cell Signaling	9511S	1:300	TNTB	3.5 min Amp
RET	Goat	Fitzgerald	70-RG002X	1:500	PBT	
RunX1	Rabbit			1:1000	PBT	Rapid deg.
RunX3	Rabbit	Abcam	ab68938	1:1000	PBT	
Sox2	Mouse	R&D system,Inc.	MAB2018	1:100	PBT	Cross-reacts
Sox10	Goat	Santa Cruz	sc-17342	1:200	PBT	Rapid deg. 4hrs incub.
TCF1	Rabbit	Cell Signaling	2203	1:200	TNTB	2min Amp
TCF3	Goat	Santa Cruz	sc-8635	1:200	TNTB	2min Amp
TCF4	Mouse	Gift from Tomas Valenta		1:200	TNTB	1.5 min Amp
TrkA	Rabbit	Reichardt Lab		1:500	PBT	
TrkB	Rabbit	Cell Signaling	4607	1:00	PBT	
TrkC	Goat	R&D system,Inc.	AF1404	1:50	PBT	
TRP2	Goat	Santa Cruz	sc-10451	1:200	PBT	
Wls (GPR177, Evi)	Rabbit	Seven hills bioreagents		1:1000	PBT	
Wnt5a	Rabbit	Abcam	ab72583	1:50	PBT	
ZO1	Mouse	Zymed	33-9100	1:200	PBT	

Table 4 Primary antibodies

Antibody Name	Species	Company	Ordering number	Concentration
Alexa Fluor 488 Goat anti-chicken IgG (H+L)	Goat	Jackson	103-545-155	1:500
Alexa Fluor 488 Goat anti-mouse IgG (H+L)	Goat	Invitrogen	A-11029	1:500
Alexa Fluor 488 Goat anti-mouse IgG_1	Goat	Invitrogen	A-21121	1:500
Alexa Fluor 488-conjugated AffiniPure Donkey anti-goat IgG (H+L)	Donkey	Jackson	705-545-147	1:500
Alexa Fluor 546 Goat anti-mouse IgG_2a	Goat	Invitrogen	A-21133	1:500
Alexa Fluor 647 Goat anti-chicken	Goat	Jackson	103-605-155	1:500
Alexa Fluor 647 Goat anti-mouse	Donkey	Jackson	715-605-150	1:500
Biotin-SP Goat anti-rabbit IgG (H+L)	Goat	Jackson	111-065-003	1:300
Cy2 Goat anti-guinea pig IgG	Goat	Jackson	706-225-148	1:500
Cy3 Donkey anti-goat IgG (H+L)	Donkey	Jackson	705-165-147	1:500
Cy3 Goat anti-mouse IgG (H+L)	Goat	Jackson	115-165-003	1:500
Cy3 Goat anti-rabbit IgG (H+L)	Goat	Jackson	111-165-003	1:500
Cy3 Goat anti-rat IgG (H+L)	Goat	Jackson	112-165-003	1:500
Cy3-AffiniPure Donkey Anti-Rat IgG (H+L)	Donkey	Jackson	712-165-153	1:500
DyLight 488 Goat anti-rabbit IgG (H+L)	Goat	Jackson	111-485-003	1:500
DyLight 649 Donkey anti-goat IgG (H+L)	Donkey	Jackson	705-495-147	1:500
DyLight 649 Goat anti-rabbit IgG	Goat	Jackson	111-495-003	1:500
HRP Streptavidin		Jackson	016-030-084	1:300
Perox-AffiniPure Donkey Anti-Rabbit IgG (H+L)	Donkey	Jackson	711-035-152	1:300
Perox-AffiniPure F(ab')2 Frag Donkey Anti-Goat IgG (H+L)	Donkey	Jackson	705-036-147	1:300

Table 5 Secondary antibodies

5. Results

5.1. Probing transcription-specific outputs of β-catenin *in vivo*

Genes Dev **25:** 2631-2643; 2011

Tomas Valenta, Max Gay, Sarah Steiner, Kalina Draganova, Martina Zemke, Raymond Hoffmans, Paolo Cinelli, Michel Aguet, Lukas Sommer, Konrad Basler

5.1.1. Abstract

β-catenin, apart from playing a cell adhesive role, is a key nuclear effector of Wnt-signaling. Based on activity assays in *Drosophila* we generated mouse strains where the endogenous β-catenin protein is replaced by mutant forms, which retain the cell adhesion function, but lack either or both the N- and the C-terminal transcriptional outputs. The C-terminal activity is essential for mesoderm formation and proper gastrulation, whereas N-terminal outputs are required later during embryonic development. By combining the double mutant *β-catenin* with a conditional null allele and a *Wnt1-Cre* driver we probed the role of Wnt/β-catenin signaling in dorsal neural tube development. While loss of β-catenin protein in the neural tube results in severe cell adhesion defects, the morphology of cells and tissues expressing the double mutant form is normal. Surprisingly, Wnt/β-catenin signaling activity only moderately regulates cell proliferation, but is crucial for maintaining neural progenitor identity and for neuronal differentiation in the dorsal spinal cord. Our model animals thus allow dissecting signaling and structural functions of β-catenin in vivo and provide the first genetic tool to generate cells and tissues that entirely and exclusively lack canonical Wnt pathway activity.

5.1.2. My contribution to this work

- Designing and performing the experiments presented in Figures 21 A, B, 22, 23, and 24
- Collection of the data for Figures 21 A, B, 22, 23, and 24
- Generation of Figures 21 A, B, 22, 23, and 24
- Generation of most reagents, including breeding, genotyping of the mice and collection of embryos needed for Figures 21 A, B, 22, 23, and 24
- Proofreading of the manuscript.

5.1.3. Introduction

β-catenin fulfils two key functions in metazoan organisms. First, it serves as an important component in the cadherin-based cell-cell adhesion system that is required for the structural integrity and functional polarization of epithelia. β-catenin binds the transmembrane protein E-cadherin and regulates actin filament assembly via α-catenin (Heuberger and Birchmeier, 2010). Experimental removal of β-catenin in the mouse embryo results in progressive body disintegration caused by the collapse of cadherin-based cell adhesiveness (Hierholzer and Kemler, 2010).

Second, β-catenin is the central regulator of gene expression in the canonical Wnt signal transduction pathway. In the absence of a Wnt signal, β-catenin is phosphorylated by a multiprotein degradation complex. Phosphorylation of β-catenin results in its ubiquitylation and subsequent degradation by the proteasome. Binding of Wnts to their cell surface receptors triggers a complex signaling cascade that leads to the inhibition of β-catenin-degradation and hence to increased levels of cytoplasmic β-catenin. Some of this β-catenin enters the nucleus and associates with transcription factors of the TCF/Lef family (Cadigan and Liu, 2006). On their own these factors possess only a limited ability to regulate transcription. Indeed, in the absence of Wnt signals, TCF/Lef proteins mediate transcriptional repression by forming a complex with Groucho/TLE repressors. The binding of β-catenin displaces Groucho, and converts TCF/Lef factors into activators, thereby translating the Wnt signal into a specific transcriptional program (Mosimann et al., 2009).

The β-catenin protein consists of a central region that is made up of 12 imperfect Armadillo repeats flanked by specific N- and C-terminal tails (Huber et al., 1997; Xing et al., 2008). Some mutations in the gene encoding the *Drosophila* ortholog of β-catenin, Armadillo (Arm), interfere with the adhesion function but not with its role in Wnt/Wingless (Wg) signaling, and vice versa, indicating that these two functions are independent and separable (Orsulic and Peifer, 1996). The signaling activity of Arm/β-catenin depends on different regions within the polypeptide sequence. The N-terminal domain of the first Arm repeat region is necessary and sufficient for recruitment of Legless (Lgs)/B-cell lymphoma 9 (BCL9) which in turn recruits Pygopus (Pygo). The latter appears to act as a transcriptional co-activator (Hoffmans and Basler, 2004; Hoffmans et al., 2005). The central Arm repeats mediate the interaction with TCF/Lef transcription factors. This region is also required for the binding to components of the adherens junctions, notably E-cadherin (Graham et al., 2000). Finally, a region comprising Arm repeats R11-12 and the C-terminal tail recruit a multitude of proteins involved in the transcription process, such as TATA-binding protein (TBP), Brahma/Brahma-related gene-1 (Brg-1), CREB-binding protein (CBP)/p300, Mediator subunit 12 (MED12) and Hyrax/Parafibromin. Many of these proteins are components of chromatin remodeling complexes or allow β-catenin to

connect with the basic transcription initiation and elongation machinery (reviewed in detail in Mosimann et al., 2009).

Despite the immense interest in deepening our understanding of canonical Wnt signaling, its roles in development and disease, as well as the in vivo activities of this pathway, are only poorly defined. Genetic investigations in vertebrates are confounded by the large size of the Wnt ligand and receptor families, the multiple roles played by the transduction components and the varied sign of action of the TCF/Lef transcription factors. Despite potential complications due to its dual role major attention has been focused on studying the in vivo requirements of β-catenin, the non-redundant pivot of the canonical pathway. In mice a large body of experiments has been generated using conditional ablation of β-catenin by using tissue specific Cre drivers (reviewed in Grigoryan et al., 2008). However, this approach does not reveal the contribution of defective cell adhesion to the observed phenotypes. For example, the loss of β-catenin in *Wnt1-Cre* expressing tissues severely affects midbrain and hindbrain development and also causes defects in the dorsal neural tube; but to what extent the signaling phenotypes are responsible for the observed defects is obscured by impaired epithelial integrity (Brault et al., 2001; Ille et al., 2007).

Here we exploit the molecular knowledge of β-catenin and assays for monitoring Wg and Wnt pathway activity to develop and validate a tool for the in vivo analysis specifically of canonical Wnt-signaling in the mouse. By depriving β-catenin of only its transcriptional activity, leaving its adhesive functions intact, we can generate cells and tissues that entirely lack canonical pathway activity. Moreover, the tools described here allow us to compare the contributions of BCL9/Legless and the C-terminal co-activators to Wnt/β-catenin-mediated transcription in different tissues at different times of development.

5.1.4. Results

5.1.4.1. The N- and C-terminal co-activators branches both contribute to the transcriptional output of β-catenin (Armadillo)

To discriminate between the transcriptional output of β-catenin and its structural role, we generated mutant forms of Arm and β-catenin, which lack the ability to bind N- and/or C-terminal co-activators. We introduced a single amino acid change into the first Arm repeat of β-catenin (D164A) blocking the interaction between β-catenin and its N-terminal co-activator BCL9/BCL9L. A C-terminal truncation (ΔC) in β-catenin abrogated the interaction with the multitude of co-activators that bind there. Finally, β-catenin-D164A-ΔC contains both the D164A mutation as well as the C-terminal deletion and is referred to as β-catenin-dm (for double-mutant). These mutations were validated biochemically (Figure 10). Equivalent forms of Arm were also generated (Arm D172 corresponds to D164 of mammalian β-catenin).

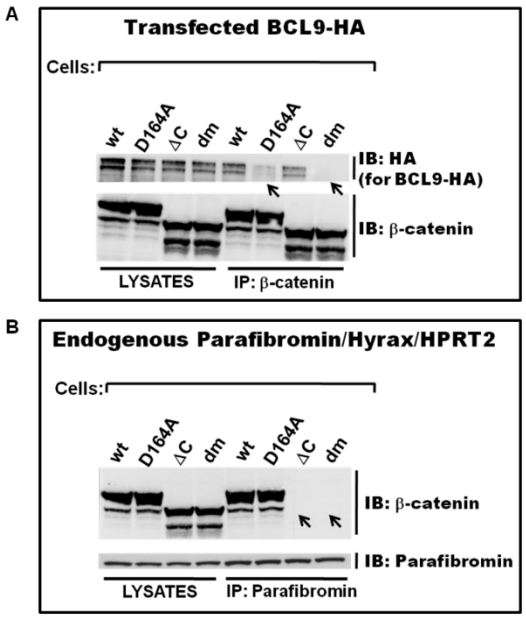

Figure 10 D164 is essential for the β-catenin/BCL9 interaction in mammalian cells, and the C-terminal truncation of β-catenin prevents association with the transcriptional co-activator Parafibromin/Hyrax/ HPRT2

A) Co-immunoprecipitations of different transfected mutant forms of β-catenin and exogenous BCL9 tagged by HA in MEF-β-catenin-ko cells. dm refers to double mutant.

B) Co-immunoprecipitations of endogenous Parafibromin and different transfected mutant forms of β-catenin in MEF-β-catenin-ko cells. dm refers to double mutant.

IP: immunoprecipitation; IB: immunoblotting; in lanes denoted as "lysates" 5% of total sample was loaded.

As an initial step we compared the functional consequences of the D172A/D164A mutation and the C-terminal truncation on Arm and β-catenin function in transactivation reporter assays. The effect of the mutations on the signaling capacities of constitutively active forms of Arm, Arm^{S10}, and β-catenin, β-$catenin^{S33Y}$, was assayed in *Drosophila* cells (Kc and clone-8, not shown) and mammalian HEK293 cells, respectively. Arm^{S10} strongly activates transcription of the Wg pathway-specific reporter *wf-Luc* (Figure 11). Similarly, β-$catenin^{S33Y}$ strongly activates expression of the mammalian Wnt-reporter *TOPFlash.* Only double mutant forms of either Arm^{S10} or β-$catenin^{S33Y}$ lacked any detectable transcription-inducing activity; single mutants retained transcription potential, especially in mammalian cells (Figure 11).

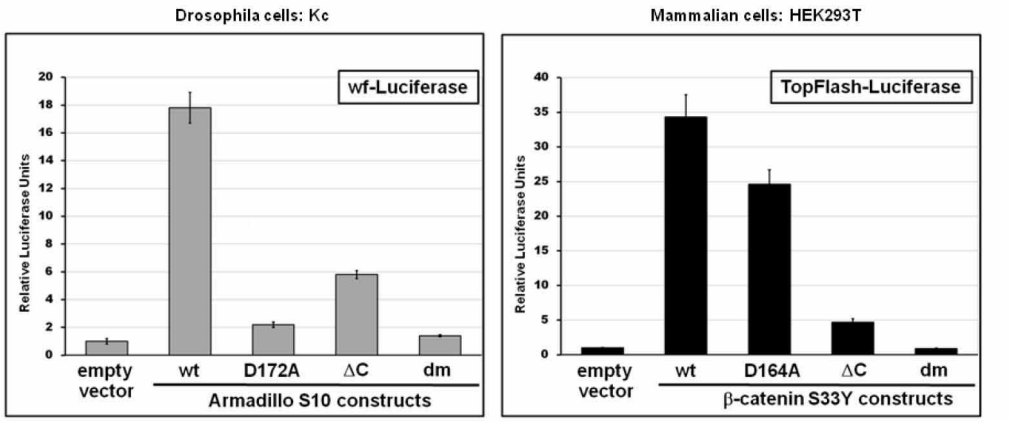

Figure 11 Requirements for N- and C-terminal co-activators for Arm- and β-catenin-mediated transcription-Part 1

The following mutant forms of Arm/ β-catenin were tested: wild type (wt), compromised in binding to Lgs/BCL9 (D172A for Arm, D164A for β-catenin), lacking the ability to interact with C-terminal co-activators (ΔC) and the composite of these two individual mutations (dm). Luciferase reporter assays in Drosophila Kc and mammalian HEK293T cells. The activity of Wnt/β-catenin transcription was determined in Kc cells by a wingful-Luciferase (wf-Luciferase) reporter, and in mammalian cells by TopFlash. The y-axes show relative luciferase units normalized to the levels of constantly expressed Renilla. Error bars represent standard deviations. Expression vectors are based on constructs encoding a constitutive active form of Arm (Arm^{S10}) or β-catenin (β-$catenin^{S33Y}$); the different mutant plasmids were transfected into Kc or HEK293T cells as indicated. Luciferase units shown were normalized relative to those from cells that were transfected in parallel with empty vector (and set to 1).

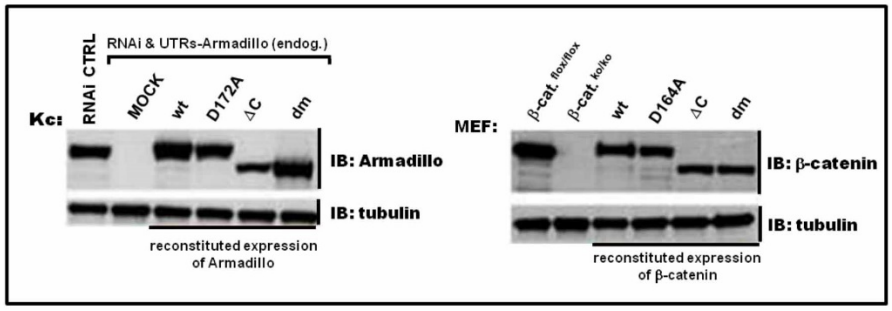

Figure 12 Replacement of endogenous Armadillo in Drosophila Kc cells to mutant forms and generation of MEF's expressing mutant forms as only source of β-catenin

Loading control to check replacement of endogenous Arm in Drosophila Kc cells or β-catenin in MEF-KO into mutant forms as indicated; dm refers to double mutant. Immunoblot (IB): Arm and β-catenin were detected by antibodies as indicated. Tubulin serves as an indicator of protein levels in the samples. For detailed descriptions see chapter experimental procedure.

The above reporter assays were based on constitutively active, overexpressed forms of Arm and β-catenin. We also examined the effect of the mutations in otherwise wild-type proteins that were expressed at normal levels and that constitute the only source of Arm and β-catenin, respectively (Figure 12). For mammalian β-catenin we started with mouse embryonic fibroblasts (MEFs) derived from conditional knock-out animals (*Ctnnb1*$^{flox/flox}$), eliminated endogenous β-catenin by infection with self-excising lentiviral Cre, and then re-installed expression of different β-catenin mutants by retroviral infection. In *Drosophila* cells we employed a highly effective dsRNA targeting the untranslated regions of *arm*, followed by transfection of expression constructs under control of the moderately active *tubulin*α*1* promoter. Expression of wild-type constructs rescued responsiveness of both mammalian and *Drosophila* cells to exogenously provided Wnt3a and Wg, respectively (Figure 13 A). The transcriptional activation of endogenous target genes was also restored: we analyzed *Axin2* and *Frizzled1* in MEFs and *Naked cuticle* and *dFrizzled3* in *Drosophila* cells (Figure 13 B). The behavior of the mutant forms of β-catenin and Arm in this more refined system confirmed that both the N- and C-terminal co-activators are important for proper transcriptional activity of β-catenin/Armadillo. Consistent with earlier results the individual contribution of the two branches seems to differ in *Drosophila* and mammals (Figure 13 A, B). Whatever the case, the double mutant proteins are transcriptionally inert both in *Drosophila* and mammals and hence provide a means to totally abrogate canonical Wnt-signaling activity in vivo.

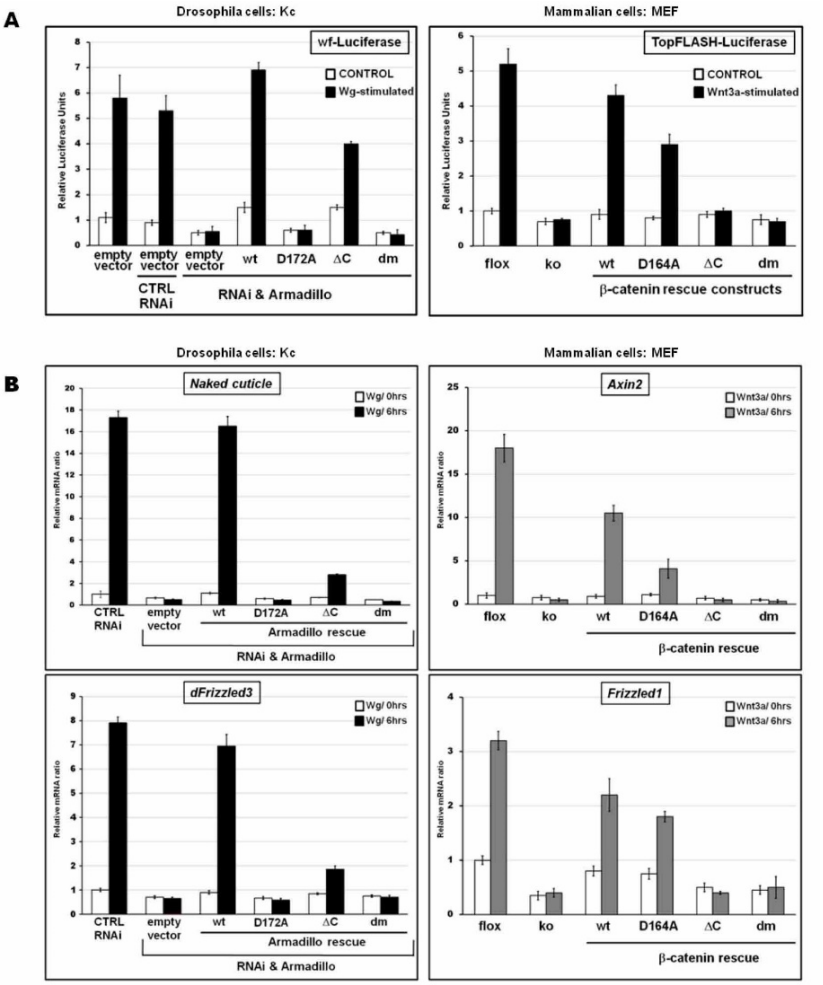

Figure 13 Requirements for N- and C-terminal co-activators for Arm- and β-catenin-mediated transcription-Part 2

A) Luciferase reporter assays in Drosophila Kc and mammalian MEF cells. Drosophila Kc cells were treated with dsRNA directed against untranslated regions of arm mRNA, or with control dsRNAi. Cells treated with dsRNAi were transfected with tubulinα1 promoter-driven mutant arm constructs to rescue Arm protein expression. All cells were cultivated with Wg conditioned medium or control medium. Mammalian MEFs containing a conditional knock-out allele of β-catenin (flox) were used for the generation of β-catenin null MEFs (ko). ko cells were infected with retroviral particles encoding different β-catenin rescue constructs as indicated. Cells were stimulated by Wnt3a-conditioned medium or control medium. Luciferase units shown were normalized relative to those from cells that expressed endogenous Arm or β-catenin in the Wnt-unstimulated situation.

B) Relative expression of the Wg targets Naked cuticle and dFrizzled3 in Drosophila Kc cells (which expressed different mutant forms or Arm instead of endogenous wild-type Arm) and relative expression levels of the Wnt/ β-catenin targets Axin2 and Frizzled1 upon Wnt3a-treatment in MEFs whose endogenous β-catenin expression was substituted with mutant forms. Cells were generated as in Fig. 1B. mRNA levels were normalized to those of the housekeeping genes SDHA and GAPDH. y-axes show normalized relative mRNA levels; Wnt-unstimulated cells expressing endogenous Arm and β-catenin, respectively, were set to 1. Error bars show standard deviations.

5.1.4.2. Double mutant Arm (Arm-D172A-ΔC) sustains adherens junctions but fully blocks Wg-mediated transcription in vivo

The most stringent assay to check if the double mutant form of either Arm or β-catenin lost its activity in signaling, but not its structural function in adherens junctions, is to test the mutant proteins in vivo. Using the attP/ΦC31 integration system we generated a series of *Drosophila* transgenic lines in which the *arm* transgenes were driven by the *tubulinα1*-promoter. All transgenes were integrated at the same predefined landing site and expressed equal levels of the Arm protein, comparable to those of the endogenous *arm* locus (Figure 14). We first analyzed to what extent the Arm variants can substitute for the wild-type form, in a rescue assay with the arm^{2a9} null allele. Hemizigous arm^{2a9} mutants die as embryos, but can be fully rescued to adulthood by a transgene encoding wild-type Arm (Table 6). In contrast, the N-terminally mutant form of Arm (Arm-D172A), as well as the double mutant Arm-D172A-ΔC failed to rescue the lethality of arm^{2a9} males. Only Arm-ΔC retains some modest rescuing function (1%). This assay indicates that in *Drosophila* the C-terminal co-activators are important for proper Arm function, while the N-terminal branch is essential.

TRANSGENE	RESCUED MALES (%)	RESCUED MALES n	MALES INHERITED WT ALLELE (n/wt)	MALES TOTAL (nΣ)
none	0,0	0	223	223
tub-arm-wt	96,4	189	196	385
tub-arm-D172A	0,0	0	238	238
tub-arm-ΔC	1,0	2	205	207
tub-arm-dm	0,0	0	242	242

Table 6 Rescue activity of arm transgenes

Contribution of both N-and C-terminal co-activators is required for proper Arm function. Females heterozygous for arm-null (arm^{2a9}) were crossed with males expressing tubulinα1 promoter-driven rescue constructs as indicated. Individual rescue constructs were integrated at the exact same position on the 3rd chromosome resulting in comparable expression levels. The percentage and exact numbers (n) of rescued males are shown that inherited the arm-null (arm^{2a9}) chromosome and the rescue transgene. n/wt denotes the number of male progeny that inherited the rescue construct together with the wild-type arm allele from the balancer chromosome (instead of arm^{2a9}); this number thus corresponds to the number of rescued males for a transgene expected to fully rescue the arm-null allele. Rescued males were tested for fertility and only fertile males were counted. ; dm refers to double mutant, nΣ denotes total number of males counted.

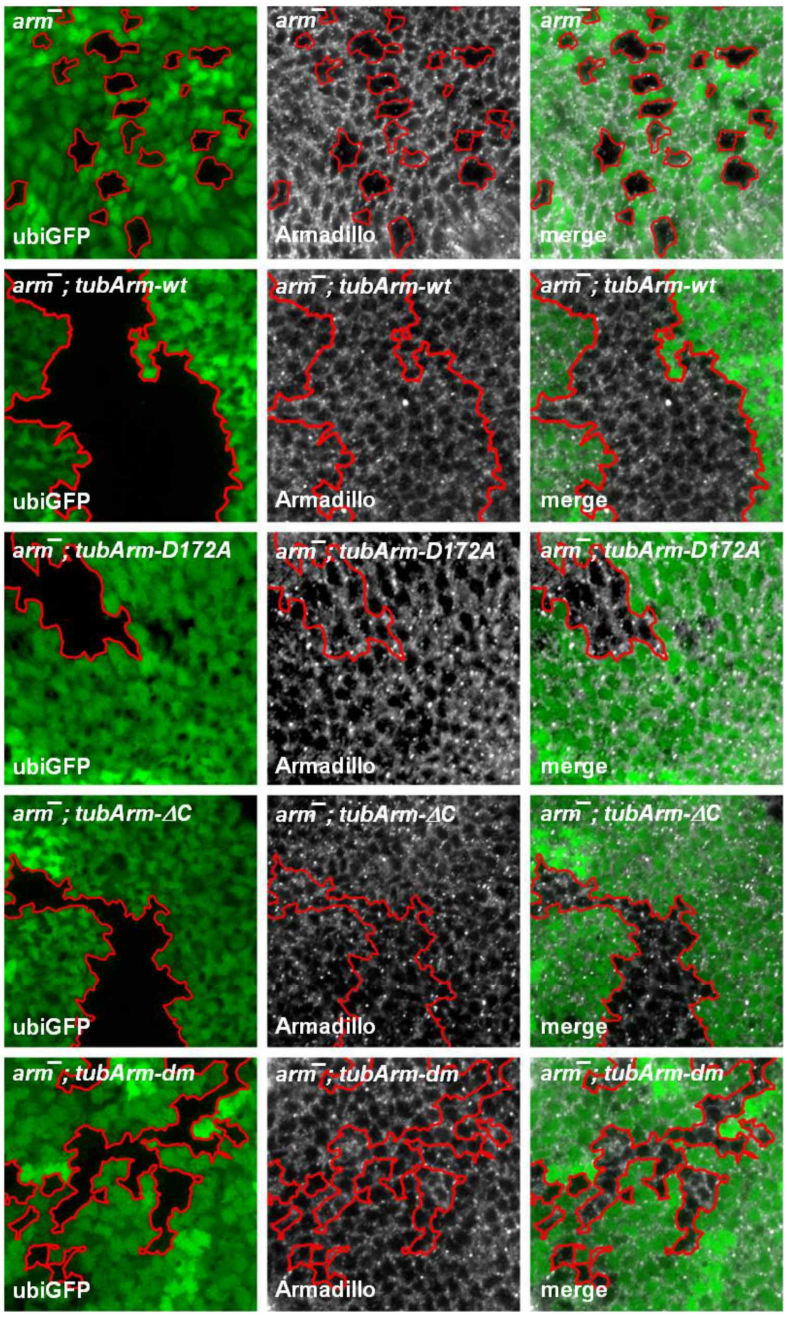

Figure 14 Mutant forms of Armadillo driven by tubulin-α1 promoter effectively replace loss of Armadillo in arm null clones

arm-null (arm$^-$) clones were generated in wing imaginal discs and marked by the loss of ubi-GFP expression. The particular form of ubiquitously expressed transgenic Arm is indicated in the upper corner. Left panels show the shape of the clones based on the expression of GFP, the middle panels show immunostainings of Arm, and the right panels show the merged images. In all cases, Arm expression and cell shapes within arm$^-$ clones are indistinguishable from surrounding wild-type tissue and the pattern of Arm is the same as in the wild-type (wt) control. Confocal sections of wing discs are shown.

To assess whether the cell-cell adhesive function is intact in our Arm mutants we induced *arm*-null (*arm^{2a9}*) clones in the wing imaginal discs of second instar larvae. *arm^{2a9}* clones remain small and often become eliminated roughly 48 hours after induction. In addition to being small, cells within the clone exhibit an irregular apical morphology. This disrupted epithelial shape is not seen in clones lacking other Wg pathway components and thus appears to be a consequence of the loss of Arm's structural function. In order to visualize the cell-cell adhesive junctions we stained wing discs with an antibody recognizing E-cadherin, which is the main binding partner of β-catenin in adherens junctions. In *arm^{2a9}* clones the pattern of E-cadherin is collapsed and E-cadherin is lost from the cell membranes, where it is normally localized, and it exhibits a diffuse distribution (Figure 15). In the presence of the *tub-arm-wt* transgene the expression levels of Arm are restored, leading to a rescue of cell shapes and the E-cadherin expression pattern (Figure 14 and Figure 15). The double mutant form of Arm (Arm-D172A-ΔC) also rescued the change in cell shape and the E-cadherin pattern in *arm^{2a9}* clones, indicating that Arm-D172A-ΔC retains its function as a building stone of epithelial adherent junctions (Figure 15). In these assays the single mutant transgenes did not significantly differ from the double mutant in the terms of rescuing clonal morphology and pattern of cell-cell contacts (not shown).

Using the same clonal system, we analyzed Wg-target gene expression to determine the Wg-transducing capacity of Arm mutants. *Senseless* (*Sens*) is a high threshold target expressed in two well-confined stripes of cells along the dorsoventral compartment boundary. Sens expression was completely lost in *arm^{2a9}* clones that overlap the Sens domain, but restored in clones from *tub-arm-wt* animals (Figure 15 B). Transgenes encoding Arm single mutants (*tub-arm-D172A*, *tub-arm-ΔC*) only partially rescued Sens expression, indicative of impaired Wg-signaling. Double mutant Arm (dm, i.e. Arm-D172A-ΔC) totally failed to rescue Sens expression. Thus, this genetic setup equals the Arm null situation in terms of lack of Wg transduction; however, as concluded above, it differs in its ability to restore epithelial integrity.

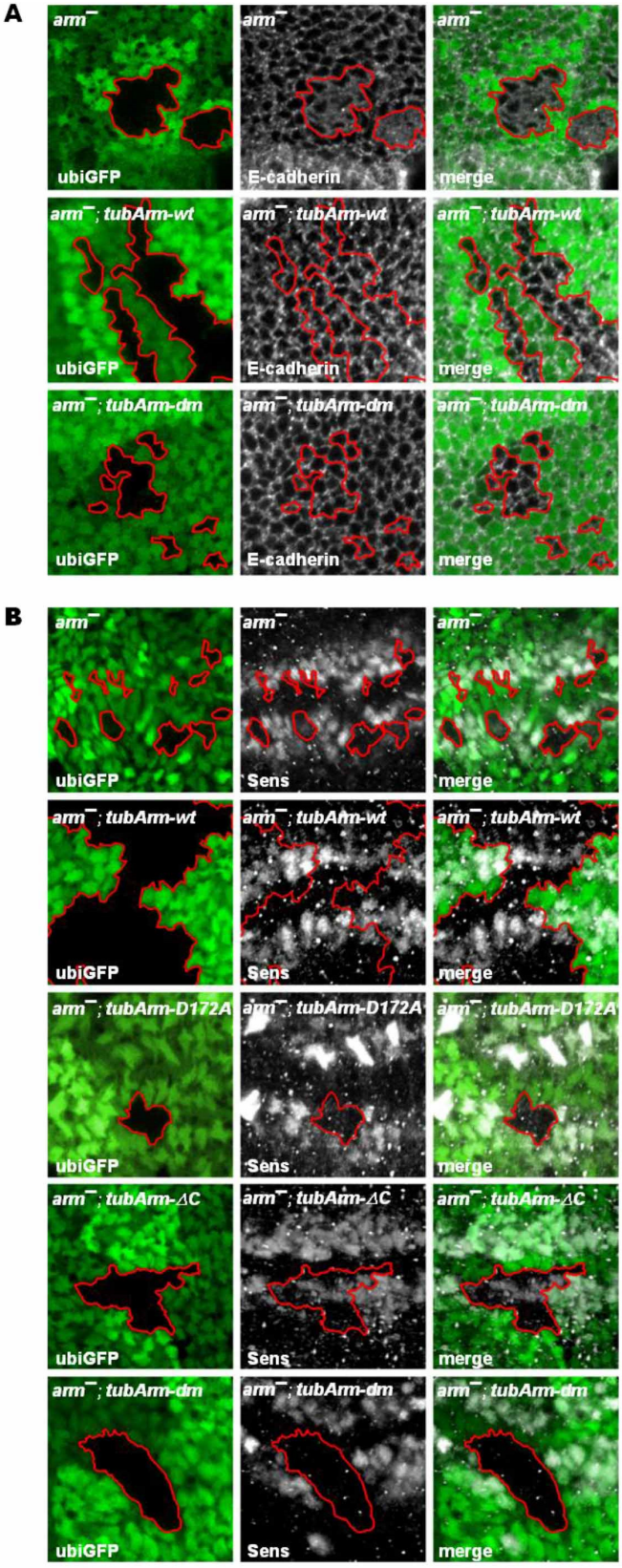

Figure 15 The double mutant form of Arm restores irregular adherens junctions of arm-null clones, but fails to rescue Wg-mediated transcription in vivo

(A-B) Confocal sections of wing discs are shown which contain arm null (arm$^-$) clones marked by the loss of ubi-GFP expression (borders of clones are highlighted). The particular form of ubiquitously expressed transgenic Arm is indicated in the upper corner. Panels to the left show the shape of the clones and the expression of GFP, the middle panels show immunostainings of proteins indicated in lower left corner, the panels to the right show the merged images.

A) Loss of Arm in arm$^-$ clones results in defective cell shapes and improper adherens junctions as revealed by the adherens junction component E-cadherin. Ubiquitous expression of wild-type Arm fully restores the normal cell adhesion pattern within arm null clones (arm$^-$, tubArm-wt). Expression of Arm lacking the ability to bind both Lgs and C-terminal co-activators sustains normal adhesivity, indistinguishable to the wild-type situation.

B) Arm$^-$ clones fails to express the Wg-target gene Senseless (Sens). Ubiquitous expression of wild-type Arm (tubArm-wt) fully restores the Sens expression pattern. Arm mutants lacking the ability to bind Lgs (tubArm-D172A) or missing the interaction domain with C-terminal co-activators (tubArm-ΔC) only partially restore Sens expression levels. The double mutant form of Arm (tubArm-dm) completely lacks the ability to restore Sens expression.

5.1.4.3. Generation of mouse strains with mutant β-catenin alleles

The successful separation of signaling and adhesive functions described above served as a rational for achieving the same in mammalian β-catenin. We replaced by homologous recombination in TC-1 (129Sv) mouse embryonic stem cells the endogenous *β-catenin* allele (*Ctnnb1*) with one of the three mutant variants that correspond to the mutants we tested in our tissue culture system (Figure 16 and Figure 17; for further details see Experimental Procedures): (1) A point mutation was introduced in the fourth exon of the *Ctnnb1* locus, resulting in a D164A mutation in the first Arm repeat that prevents binding to the N-terminal co-activator BCL9/BCL9L. (2) A stop codon was engineered yielding a C-terminally truncated *Ctnnb1*. In this allele, codon 673 in exon 13 was changed to a premature stop followed by a frame shift mutation. Moreover, in order to eliminate possible non-sense mediated RNA decay we fused exon 15 encompassing the *Ctnnb1* 3'UTR directly to exon 13 (Figure 16 and Supplemental Experimental Procedures Figure 26). (3) Finally, we also generated an ES cell line carrying the double mutant (dm) form of the *β-catenin* gene, which was created by two subsequent rounds of homologous recombination. These cells were then used to reconstitute mice of the same genotype. Upon successful elimination of the various selection markers we obtained three heterozygous strains harboring the mutant *Ctnnb1* alleles: $Ctnnb1^{D164A/wt}$; $Ctnnb1^{\Delta C/wtt}$ and $Ctnnb1^{dm/wt}$.

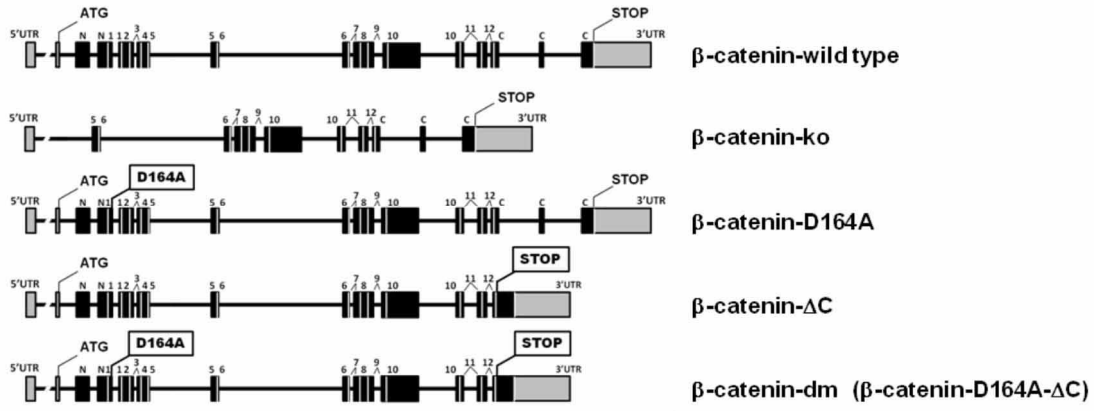

Figure 16 Schematic representation of the β-catenin loci of the mutant strains generated

*β-catenin-ko ($Ctnnb1^{ko}$) was generated by crossing a CMV-Cre line with a conditional β-catenin strain ($Ctnnb1^{flox/flox}$; i.e. B6.129-$Cnntb1^{tm2Kem/J}$); the resulting allele does not contain an in-frame ATG and exons 2 to 6, which encode domains essential for binding to E-cadherin and/or TCF/*Lef*, are eliminated. β-catenin-D164A ($Ctnnb1^{D164A}$) harbors a single amino acid exchange (D164A) in exon 4, preventing the interaction between the resulting β-catenin and BCL9/BCL9L. In the β-catenin-ΔC ($Ctnnb1^{\Delta C}$) locus a preliminary stop codon is followed by a frame shift introduced into exon 13; moreover, exon 15 was directly fused to exon 13, thus eliminating exon 14. β-catenin-dm ($Ctnnb1^{dm}$) strain carries both individual mutations. Boxes represent exons with black coding and gray non-coding; numbers denominate the Arm repeats.*

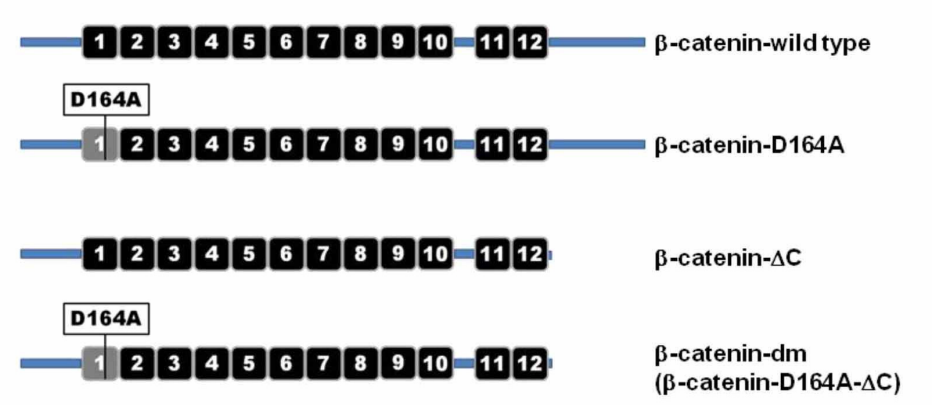

Figure 17 β-catenin forms expressed by mutant transgenic animals

Depiction of the β-catenin proteins expressed by the knock-in mouse strains represented in Figure 3A. The Ctnnb1^{ko} allele does not express any intact protein. Numbers denominate the Arm repeats.

5.1.4.4. Transcriptional output via β-catenin's C-terminus is essential for gastrulation

None of the three mutant *Ctnnb1* strains gave birth to homozygous animals. To determine the time point and cause of embryonic lethality we analyzed litters of such crosses. *Ctnnb1*$^{\Delta c/\Delta c}$ and *Ctnnb1*$^{dm/dm}$ embryos showed strong defects during gastrulation before E7.5, while *Ctnnb1*$^{D164A/D164A}$ animals developed normally until E10.0, when they exhibited first signs of developmental delay. The defects of *Ctnnb1*$^{\Delta c/\Delta c}$ and *Ctnnb1*$^{dm/dm}$ embryos resemble those described for the *Ctnnb1*$^{ko/ko}$ embryos (Haegel et al., 1995; Huelsken et al., 2000). While wild type and *Ctnnb1*$^{D164A/D164A}$ animals form mesoderm at the posterior side at E7.5 and are in a dynamic process of gastrulation, in *Ctnnb1*$^{\Delta c/\Delta c}$ embryos the majority of cells detached from the ectodermal cell layer and compact uniform cell masses form without any signs of mesoderm or other defined germ layers (Figure 18 A, B). Extraembryonic tissues do not seem to be affected, presumably because β-catenin is normally not expressed in these tissues (Figure 19 A). The total failure of embryonic development at E7.5 in *Ctnnb1*$^{\Delta c/\Delta c}$, as well as in *Ctnnb1*$^{dm/dm}$ and *Ctnnb1*$^{ko/ko}$ animals, mirrors the loss of Wnt/β-catenin mediated transcription as monitored by the β-galactosidase activity of the TCF/β-catenin reporter *BAT-gal* (Maretto et al., 2003). Wild-type or *Ctnnb1*$^{D164A/D164A}$ embryos have strong *BAT-gal* activity at the posterior side of the embryo in the primitive streak, the area where the mesoderm is formed. No such signal could be detected in embryos homozygous for a C-terminally truncated *Ctnnb1* allele (alone or as double mutant together with the D164A mutant), nor in embryos missing β-catenin entirely (Figure 18 B). The dramatic block in TCF/β-catenin transcriptional activity in *Ctnnb1*$^{\Delta c/\Delta c}$, *Ctnnb1*$^{dm/dm}$ and *Ctnnb1*$^{ko/ko}$ embryos could also be confirmed at E6.5 using

quantitative real-time PCR, for the *BAT-gal* reporter, or for the endogenous TCF/β-catenin target genes *Axin2* and Lef-*1* (Figure 18 C, and not shown). The disappearance of TCF/β-catenin-mediated transcription directly correlates with the failure in developing the mesodermal layer, as indicated by the loss of expression of the mesodermal marker *T/Brachyury* (Figure 18 C). The transcription factor T/Brachyury is not only encoded by a direct target of TCF/β-catenin-mediated transcription, but is also one of the key elements defining mesoderm formation in the primitive streak (Arnold et al., 2000; Yamaguchi et al., 1999). The lack of mesoderm was further confirmed by the absence of mRNA of the early mesodermal gene *Goosecoid* (Figure 18 C). We interpret our findings as an indication that the interactions of β-catenin with its C-terminal co-activators are essential for proper mesodermal formation and thus for gastrulation.

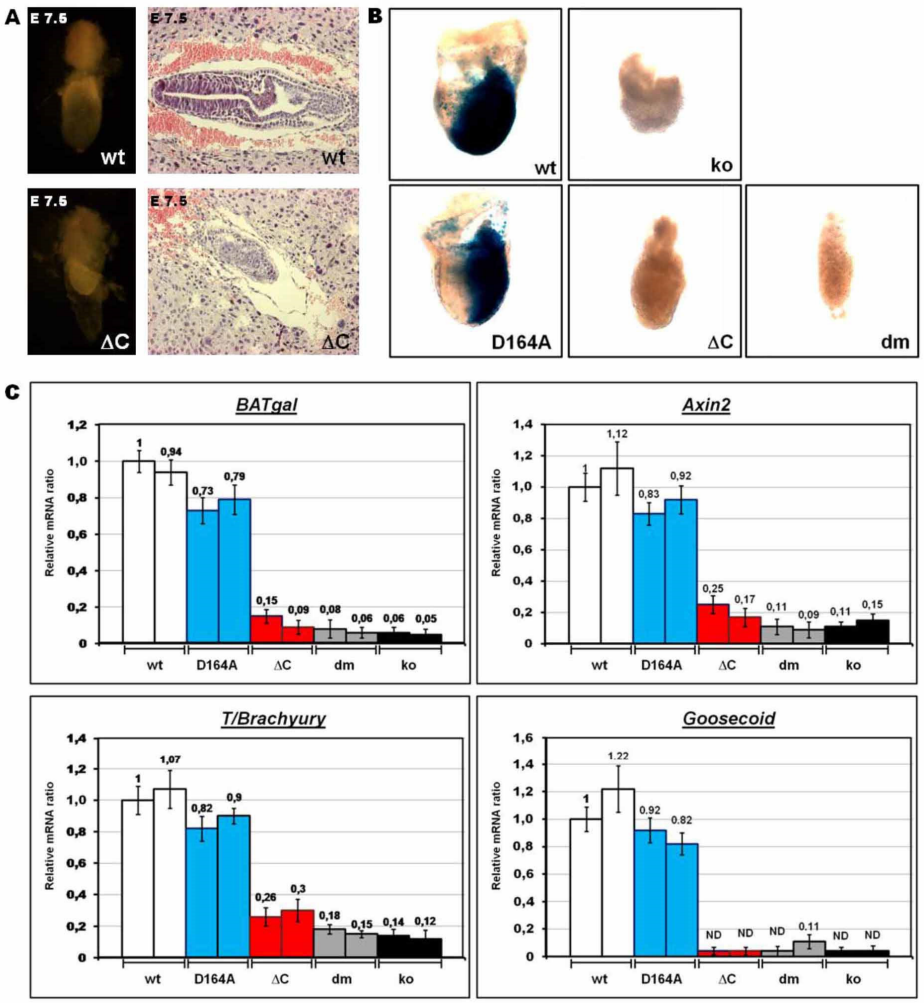

Figure 18 Contribution of the C-terminal β-catenin co-activators is essential for gastrulation

A) Morphology of wild-type (wt) and Ctnnb1$^{\Delta c/\Delta c}$ (ΔC) embryos at E7.5 including extraembryonic tissues. Right panels: embryos dissected from decidual tissues. left panels: sagittal sections of E7.5 embryos within the decidua stained by H&E.

B) Developmental failure during gastrulation caused by C-terminal truncation of β-catenin is associated with absence of TCF/β-catenin-mediated transcription, as monitored by the Wnt-specific reporter BAT-gal. Dissected embryos at E7.5; each individual embryo inherited one allele of the BAT-gal transcriptional reporter and is homozygous for the indicated mutant allele of β-catenin. ko represents total loss of β-catenin. β-gal expression from the BAT-gal reporter was determined using enzymatic staining based on X-gal (blue color).

C) Transcription of Wnt/β-catenin target genes (transgenic reporter BAT-gal, endogenous genes Axin2 and T/Brachyury) is strongly reduced in E6.5 embryos homozygous for the Ctnnb1 allele that prevents the binding of β-catenin to C-terminal transcription co-activators (ΔC). Expression of factors regulating mesoderm formation (T/Brachyury, Goosecoid) is also strongly affected in Ctnnb1$^{\Delta c/\Delta c}$ embryos. Levels of mRNA were determined by quantitative real time PCR and normalized to the housekeeping genes SDHA and GAPDH. The levels of a Ctnnb1$^{wt/wt}$ (wt) embryo are set as 1. Embryos from two independent litters were tested for each homozygous Ctnnb1 mutant as indicated; dm represents the double mutant form, ko the β-catenin null embryos. Each embryo carries one allele of the BAT-gal reporter. Error bars show standard deviation, ND stands for not-detectable levels.

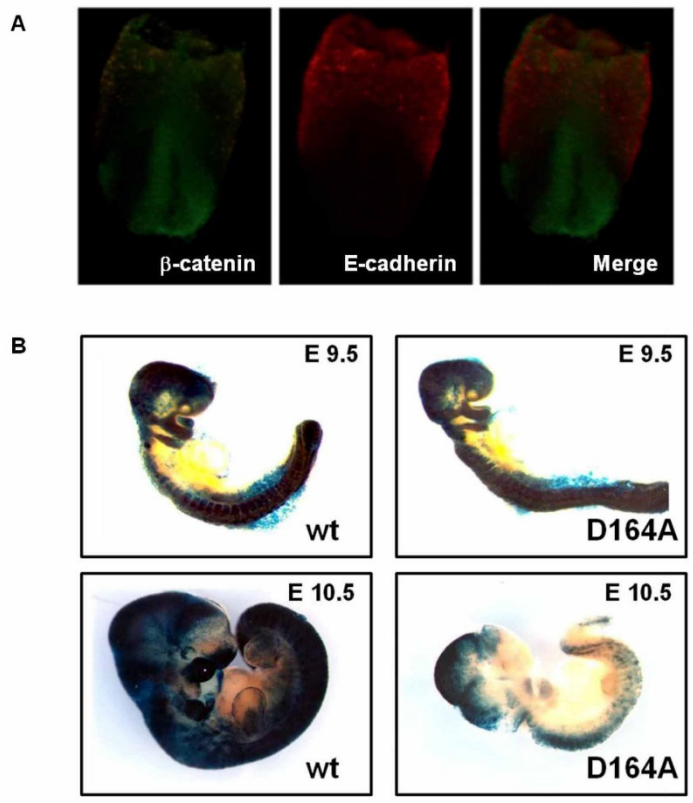

Figure 19 Embryos homozygous for the *Ctnnb1^{D164A}* allele develop normally until E9.5

A) Distinct expression patterns of E-cadherin and β-catenin in wild-type embryos at E7.5. Whole-mount immunohistochemical staining of wild-type embryos isolated at E7.5 with antibodies against β-catenin and E-cadherin. Whereas β-catenin is expressed mainly in the developing embryo, E-cadherin is primarily expressed in extra-embryonic tissues.

B) Dissected wild-type or Ctnnb1$^{D164A/D164A}$ embryos; each embryo expresses one copy of the BAT-gal transcription reporter. Embryos are stained with X-gal to monitor the expression of β-galactosidase from BAT-gal. At E9.5 there is no obvious difference in morphology and BAT-gal expression between wild-type and mutant embryos, whereas at E10.5 the mutants display severe developmental defect and reduced Wnt-signaling transcription.

In contrast to embryos expressing C-terminally truncated β-catenin, the development of embryos expressing the D164A form of β-catenin, which cannot bind BCL9/BCL9L, is indistinguishable to wild type until E10.0 (Figure 19 B). After this stage *Ctnnb1*$^{D164A/D164A}$ embryos are developmentally delayed and smaller than wild-type control embryos. At E10.5 their forebrain is not properly developed, pharyngeal arches are rudimentary and in 43% of the embryos (18/42 analyzed embryos) defects can be observed in craniofacial development (Figure 20A). These developmental defects are associated with reduced Wnt-signaling activity since *Ctnnb1*$^{D164A/D164A}$ embryos have strongly reduced *BAT-gal* expression in their pharyngeal arches and reduced reporter gene activity in the developing brain and throughout the body (Figure 19 B and Figure 20 A). The deficit in Wnt-signaling activity is the most likely reason for the developmental delay and the subsequent defects, since at E10.0, when no obvious phenotypic defects are detectable, *Ctnnb1*$^{D164A/D164A}$ embryos already exhibit a strong reduction of Wnt/β-catenin transcriptional activity, as assessed by qRT-PCR for the *BAT-gal* reporter (Figure 20 B). Endogenous *Axin-2* expression is also reduced, especially in pharyngeal arches (Figure 20 B). Thus it appears that N-terminal co-activators, represented by BCL9/BCL9L, are important regulators of the Wnt/β-catenin output during embryonic development independently of the C-terminal co-activator branch.

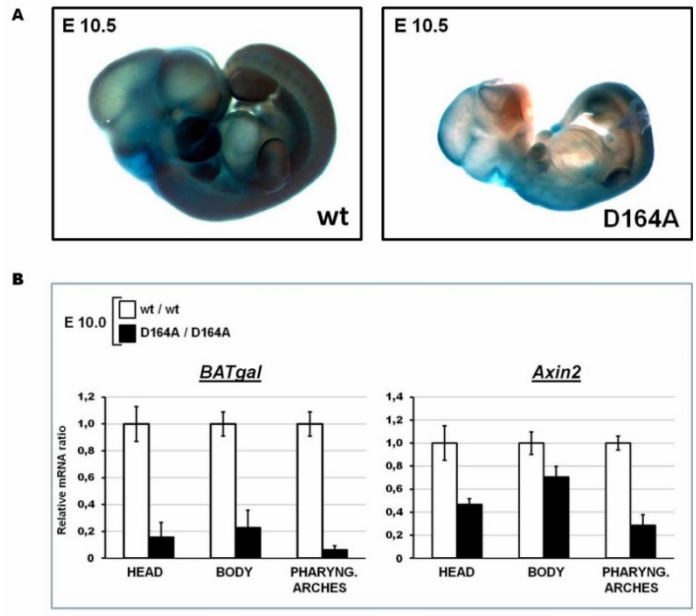

Figure 20 Developmental defects and reduction in β-catenin-mediated transcription in embryos expressing the D164A mutant form

A) Wild type (wt) and homozygous Ctnnb1$^{D164A/D164A}$ *(D164A) embryos at E10.5 carrying one allele of the Wnt/β-catenin-transcriptional reporter BAT-gal and stained for enzymatic activity with X-gal (blue color). The mutant embryos show severe defects in size and in the development of brain, craniofacial structures and pharyngeal arches. These defects are associated with reduced BAT-gal activity. Representative embryos are shown.*

B) Wnt/β-catenin transcription is reduced in such mutant embryos as determined by quantitative real-time PCR in the head and in the pharyngeal arches at E10.0. Expression of the BAT-gal reporter and of the endogenous Wnt/β-catenin target gene Axin2 in the head, pharyngeal arches and the rest of the body was monitored. Transcript levels are normalized to those of the housekeeping genes SDHA and GAPDH. Levels for wild-type (wt) embryos are set to 1. Error bars show standard deviations. Representative results are shown.

5.1.4.5. Replacing β-catenin with its signaling-defective variant in Wnt1 expressing tissues

To overcome the early embryonic lethality we placed the mutant *Ctnnb1* alleles over a conditional knock-out allele (*Ctnnb1*^{flox}), in combination with a Cre driver line. In Cre expressing cells that undergo mitotic recombination our mutant alleles are the only source for β-catenin, essentially replacing the wild-type protein with the mutant form of interest (for detailed crossing scheme see Supplemental Experimental Procedures Figure 25). As a model Cre driver we used *Wnt1-Cre* which is expressed in the early developing neural tube, resulting in recombination in the midbrain, dorsal spinal cord and in neural crest cells (Danielian et al., 1998). Previous reports showed that complete loss of β-catenin mediated by *Wnt1-Cre* dramatically affects the development of midbrain-hindbrain structures, the craniofacial apparatus and neural crest cell derivatives. However, for most of these phenotypes it is difficult to decipher what is due to the loss of Wnt-signaling activity as opposed to loss of adhesion (Brault et al., 2001; Hari et al., 2002).

To resolve this we used *Wnt1-Cre* in combination with our mutant *Ctnnb1* alleles. Upon *Wnt1-Cre*-mediated recombination, *Wnt1-Cre*; *Ctnnb1*$^{flox/flox}$ embryos exhibit severe phenotypes at E12.5: defective craniofacial structures, malformed telencephalic lobes and a missing mid-hindbrain boundary (MHB). The phenotypes of *Wnt1-Cre*; *Ctnnb1*$^{dm/flox}$ embryos are less drastic and comprise milder craniofacial and mesencephalic defects than the complete loss of β-catenin. The defects in *Wnt1-Cre*; *Ctnnb1*$^{dm/flox}$ are unvarying, while the *Wnt1-Cre*; *Ctnnb1*$^{flox/flox}$ embryos exhibit considerable phenotypic variability (Figure 21 A).

Embryos of the genotypes *Wnt1-Cre*; *Ctnnb1*$^{\Delta C/flox}$ and *Wnt1-Cre*; *Ctnnb1*$^{D164A/flox}$ resemble wild-type embryos and display less severe phenotypes (Figure 21 A), compared to those expressing double mutant β-catenin. This indicates that both the N- and the C-terminal co-activators contribute to the transcriptional output of β-catenin in Wnt1-expressing tissues, validating the approach of using the double mutant form to fully block the transcriptional output of β-catenin.

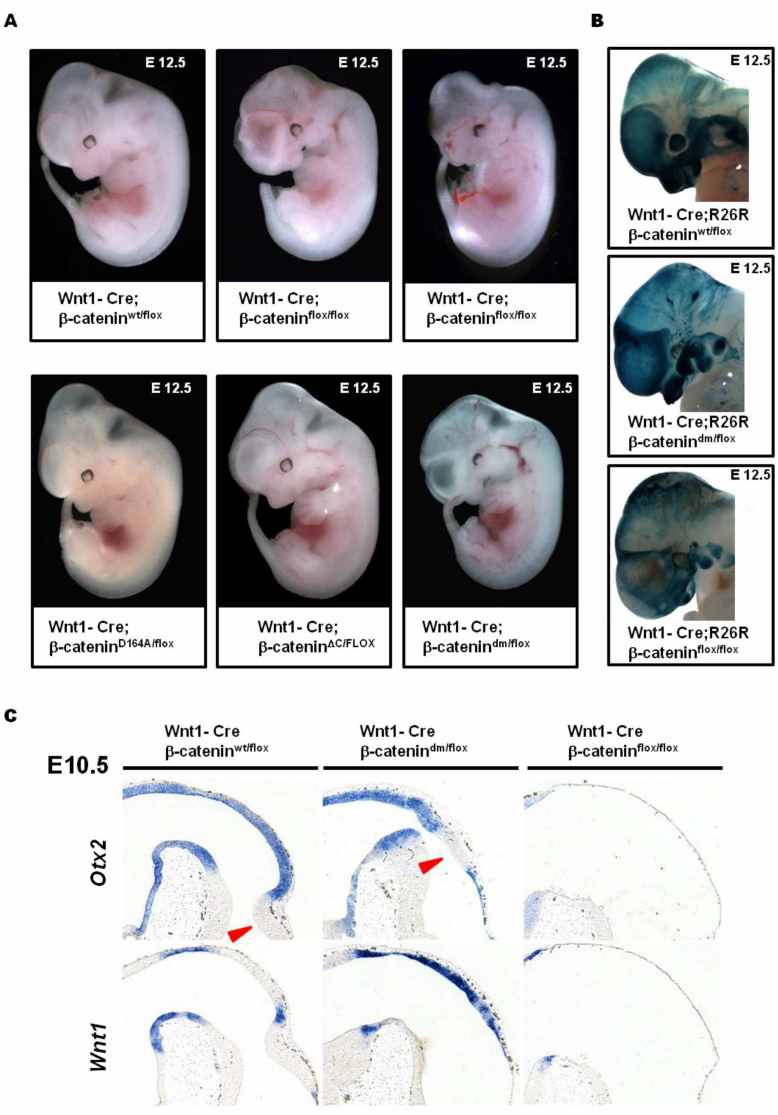

Figure 21 Total loss of β-catenin in *Wnt1-Cre* expressing tissues leads to more severe phenotypes than blocking the Wnt-signaling output of β-catenin

A) E12.5 embryos expressing Wnt1-Cre, one conditional allele of β-catenin (Ctnnb1^{flox}), and a second allele of Ctnnb1 as indicated. In Wnt1-Cre; Ctnnb1$^{flox/flox}$ embryos Cre activity results in the absence of β-catenin in Wnt1-expressing tissues. Such embryos show strong defects in craniofacial development, midbrain and hindbrain. The phenotype of Wnt1-Cre; Ctnnb1$^{dm/flox}$ embryos is milder compared to that of Wnt1-Cre; Ctnnb1$^{flox/flox}$, especially in the case of telencephalic lobes, midbrain and hindbrain areas. Representative embryos are shown.

B) X-gal staining visualizing Wnt1-Cre-mediated recombination using the ROSA26 (R26R) reporter in heads of embryos at E12.5. The strong dark blue signal in forming craniofacial structures (jaw/maxilla, meninges) and pharyngeal arches in wild type represents neural crest derivatives. Similarly strong signals could be partially observed in Wnt1-Cre/R26R; Ctnnb1$^{dm/flox}$, while in Wnt1-Cre/R26R; Ctnnb1$^{flox/flox}$ there are fewer, irregularly scattered X-gal-positive cells.

C) In situ hybridization with early midbrain-hindbrain junction markers on sagittal sections of embryonic heads at E10.5. In wild-type embryos the transcription factor Otx2 (upper panel) is expressed in the midbrain with a sharp boundary at the midbrain-hindbrain junction. In Wnt1-Cre; Ctnnb1$^{dm/flox}$ (middle panel) the midbrain-hindbrain junction marked by Otx2 expression is shifted and the prospective cerebellum is not developed. Wnt1 (lower panel) is expressed in wild type in the posterior midbrain and along the dorsal midline. Wnt1-Cre; Ctnnb1$^{dm/flox}$ animals show increased expression of Wnt1 along the dorsal midline (middle panel). In contrast, Wnt1-Cre; Ctnnb1$^{flox/flox}$ (ko) brains lack expression of both Otx2 and Wnt1, indicating absence of any midbrain and cerebellar structures (right panels). Arrowhead points to hindbrain structures (cerebellum). Scale bar represents 200 μm.

The significant differences between β-catenin double mutant and null phenotypes prompted us to examine the *Wnt1-Cre* recombined cells using the *ROSA26* reporter (*R26R*, (Soriano, 1999)). *Wnt1-Cre* activates *R26R* expression in the entire neural crest population, including the migrating pool of cells (Danielian et al., 1998). At E12.5 our control embryos exhibit strong *R26R* activity in the developing craniofacial structures, which are constituted from the pharyngeal arches into which neural crest cells migrate. In *Wnt1-Cre*; *R26R*; *Ctnnb1*$^{dm/flox}$ embryos the strong *R26R* expression in the craniofacial structures indicates that neural crest stem cells (NCSC) have migrated to form craniofacial skeletal structures, although these were hypoplastic and malformed. In contrast, *Wnt1-Cre*; *R26R*; *Ctnnb1*$^{flox/flox}$ embryos entirely lack maxillae and mandibles (Figure 21 B) and residual neural crest cells reside in rudimentary pharyngeal arches (Figure 21 B).

Closer examination of midbrain sagittal sections of mutant embryos at E10.5 revealed further differences between *Wnt1-Cre*; *Ctnnb1*$^{flox/flox}$ and *Wnt1-Cre*; *Ctnnb1*$^{dm/flox}$ animals. In wild-type embryos the expression domain of the transcription factor *Otx2* spreads throughout forebrain and midbrain with a sharp border at the midbrain-hindbrain boundary (MHB) (Millet et al., 1996). In null embryos the midbrain and hindbrain structures are entirely absent, while in *Wnt1-Cre*; *Ctnnb1*$^{dm/flox}$ animals the midbrain is present as a thin layer of *Otx2*-positive cells (Figure 21 C), but the prospective cerebellum is not developed. In both genotypes the MHB, demarcated by the expression of *FGF8*, is absent (data not shown). We also checked the distribution of *Wnt1*, which is expressed in a stripe along the dorsal neural tube with a gap at rhombomere 1 and as a transverse band dorsal to the MHB (Wilkinson et al., 1987). Upon total loss of β-catenin we did not detect any expression of *Wnt1* at the dorsal midline, where recombined cells are apoptotic (Brault et al., 2001), but increased expression laterally where the recombination rate decreases. Similarly, embryos expressing the double mutant β-catenin exhibit enhanced dorsal *Wnt1* expression (Figure 21 C), underscoring the importance of Wnt signaling for midbrain development and of distinguishing loss of signaling function versus lack of β-catenin.

5.1.4.6. Epithelial integrity in tissue with double mutant β-catenin (D164A-ΔC)

As described above, the *Wnt1-Cre* driver is active in the dorsal neural tube (Figure 22 A, (Ille et al., 2007)), an epithelial tissue well suited to analyse the capacity of different β-catenin forms to sustain cell-cell adhesion. Antibodies specific for either the N- or C-terminus of β-catenin allowed us to detect the presence of both termini in control spinal cord expressing wild-type β-catenin, a C-terminally truncated protein in *Wnt1-Cre; Ctnnb1*$^{dm/flox}$ and lack of β-catenin in *Wnt1-Cre*; *Ctnnb1*$^{flox/flox}$ (Figure 22 B). As expected, *Wnt1-Cre* -mediated loss of β-catenin in *Ctnnb1*$^{flox/flox}$ embryos caused the disruption of apical neural tube morphology and led to the

migration of cells into the neural canal as shown by immunostaining against the adherens junction components N-cadherin, α-catenin and the tight junction marker ZO-1 (Figure 22 C-E). In contrast to the *Wnt1-Cre*; *Ctnnb1*$^{flox/flox}$ embryos, the structure of *Wnt1-Cre; Ctnnb1*$^{dm/flox}$ neural tubes is intact and adherens junction components are distributed like in controls. Importantly, however, just like in the case of Arm, the double mutant form of β-catenin cannot provide transcriptional output for the canonical Wnt pathway, as the expression of the Wnt/β-catenin reporter *BAT-gal* and the direct target *CyclinD1* is severely reduced in the dorsal region of *Wnt1-Cre*; *Ctnnb1*$^{dm/flox}$ neural tubes (Figure 23 A,B). Taken together, we conclude that the mutations introduced into the β-catenin protein indeed ablate specifically the signaling roles of β-catenin independently of its adhesion function.

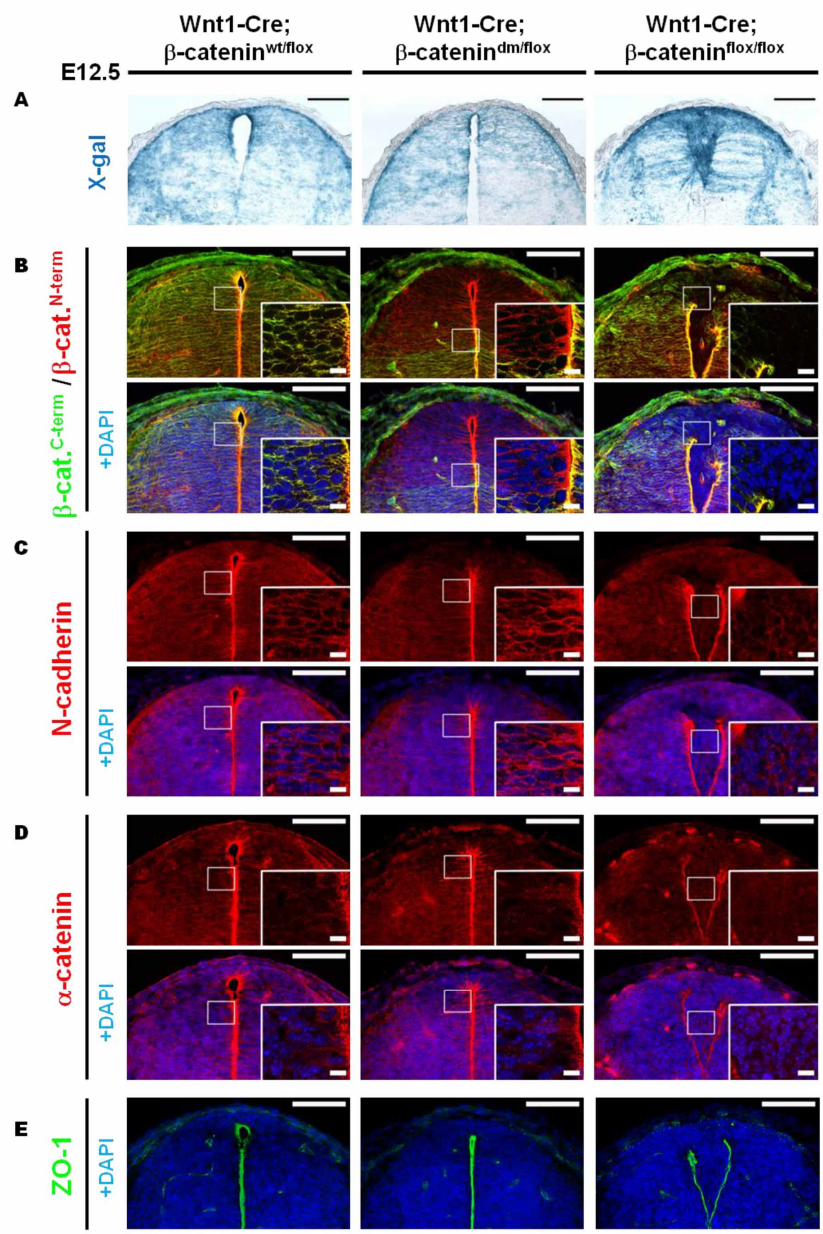

Figure 22 β-catenin-dm can fully restore the corrupted dorsal spinal cord morphology caused by defective adherens junctions in tissue lacking β-catenin

A) X-gal staining visualizing Wnt1-Cre-mediated expression of β-galactosidase from the ROSA26 reporter (R26R) in the dorsal spinal cord of E12.5 embryos. Wild-type embryos (Wnt1-Cre/R26R; Ctnnb1$^{wt/flox}$) and embryos expressing double mutant β-catenin (Wnt1-Cre/R26R; Ctnnb1$^{dm/flox}$) display normal morphology and shape of the dorsal spinal cord. On the other hand, absence of β-catenin (Wnt1-Cre/R26R; Ctnnb1$^{flox/flox}$) results in breakage of medial apical contacts and severe morphological defects.

B) Double mutant β-catenin effectively restores the adhesion defects caused by the loss of β-catenin in Wnt1-Cre positive tissues. Immunostaining with antibody recognizing either N- or C-terminus of β-catenin. The C-terminus is missing in the double mutant form, but protein expression is recognized by the antibody against the N-terminus. No β-catenin is detected in the recombination-prone region of Wnt1-Cre; Ctnnb1$^{flox/flox}$ neural tubes.

(C-E) N-cadherin (C), α-catenin (D) and ZO-1 (E) immunostainings for adherens and tight junctions do not show a significant difference between wild-type (Wnt1-Cre; Ctnnb1$^{wt/flox}$) and mutant (Wnt1-Cre; Ctnnb1$^{dm/flox}$) spinal cord. Lack of β-catenin (Wnt1-Cre; Ctnnb1$^{flox/flox}$) leads to adhesion defects associated with the breakdown of apical junctional complexes. Scale bar represents 100 μm, scale bar in inset is 10 μm.

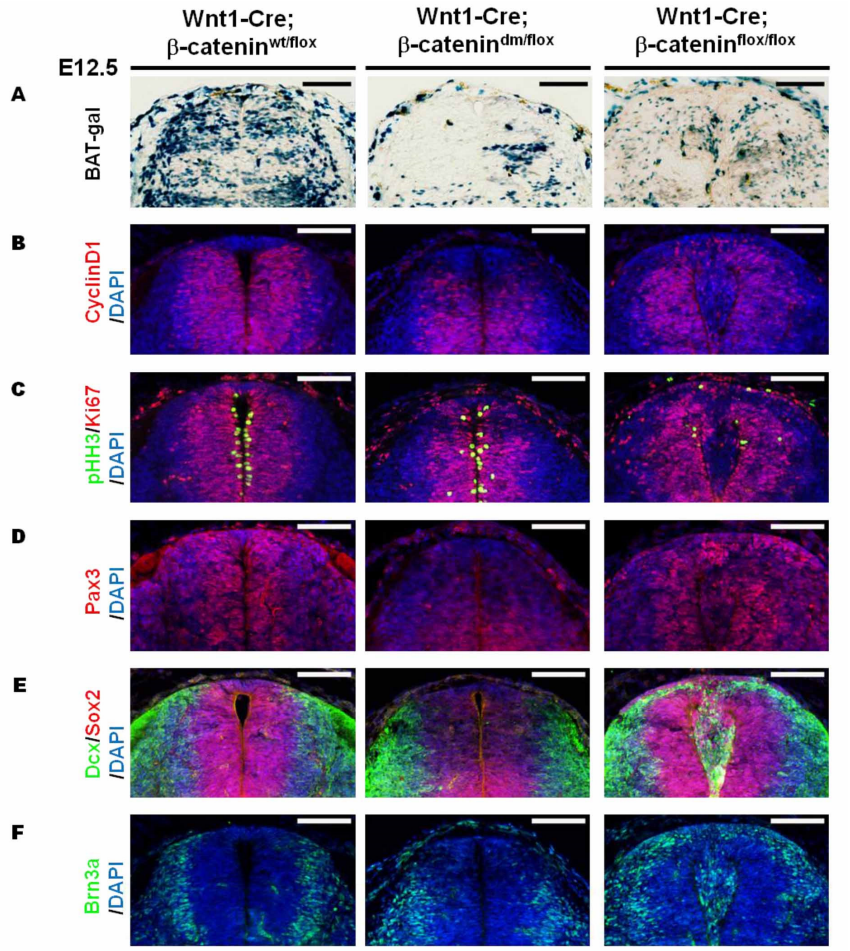

Figure 23 Block of Wnt-signaling output by double mutant β-catenin affects cell fate determination in the dorsal spinal cord

(A-F) Immunostaining of transversal sections of dorsal spinal cord isolated from E12.5 embryos. The double mutant form of β-catenin fully blocks expression of the Wnt-reporter BAT-gal (A) and of the endogenous Wnt-target gene CyclinD1 (B) in the dorsal spinal cord where Wnt1-Cre is active. Cells expressing the double mutant β-catenin are still proliferating, indicated by Ki67 and pHH3 expression (C). In contrast, cell proliferation was strongly reduced in Wnt1-Cre; Ctnnb1$^{flox/flox}$ animals. The spinal cord of Wnt1-Cre; Ctnnb1$^{dm/flox}$ animals is characterized by strongly reduced expression of Pax3 (D) and Sox2 (E), indicating a loss of undifferentiated precursor cells. Neuronal differentiation in the dorsal neural tube of these animals is affected as indicated by the absence of early neuronal markers: Dcx (E) and Brn3 (F). Scale bar represents 100 μm, scale bar in inset is 10 μm.

5.1.4.7. Block of transcriptional β-catenin output affects cell fate determination in the dorsal spinal cord

The rescued morphology of dorsal neural tube in E12.5 *Wnt1-Cre*; *Ctnnb1*$^{dm/flox}$ embryos enabled the analysis of progenitor in the absence of Wnt transduction. Blocking β-catenin-mediated transcription in the dorsal neural tube does not noticeably affect cell proliferation as determined by the expression of the proliferation marker Ki67 and the distribution of the mitotic marker phophorylated histone H3 (pHH3) in *Wnt1-Cre*; *Ctnnb1*$^{dm/flox}$ animals (Figure 23 C). Moreover, we did not observe any sign of increased apoptosis determined by caspase-3 staining in the dorsal neural tube of such embryos (Figure 24 A). However, when monitoring the differentiation of sensory neurons by pSmad1/5/8 activity we found this process severely affected (Figure 24 B). Furthermore, the expression of Pax3, a key transcription factor regulating the fate of neuronal precursor cells (Christova et al., 2010), as well as Sox2, normally expressed in spinal cord precursors (Wakamatsu et al., 2004), were strongly reduced (Figure 23 D, E). The severe decrease in expression of these transcription factors was accompanied by the disappearance of the neuronal marker Dcx and by a partial loss of dorsal interneurons marked with Brn3a (Fedtsova and Turner, 1995) (Figure 23 E, F). Thus Wnt/β-catenin transcription is essential for the maintenance and proper development of neuronal precursors in the dorsal neural tube.

In contrast to this phenotype, we found that β-catenin null cells underwent premature differentiation and often dispersed from the roofplate to the outer dorsal rim of the tube (Figure 23 E, F, right panels). These defects must be caused by the concurrent loss of β-catenin-mediated transcription and disruption of dorsal neural tube morphology (Figure 23 A-F, right panels). The loss of medial apical junctions in the dorsal spinal cord thus severely limits the possibility to determine the spatial and temporal fates of neurons in this tissue.

Together, our observations uncover the requirement of β-catenin-mediated transcription for maintenance of a neural progenitor state and for neuronal differentiation in the neural tube. They illustrate the importance of discriminating between the nuclear and adhesive roles of β-catenin when studying canonical Wnt signaling.

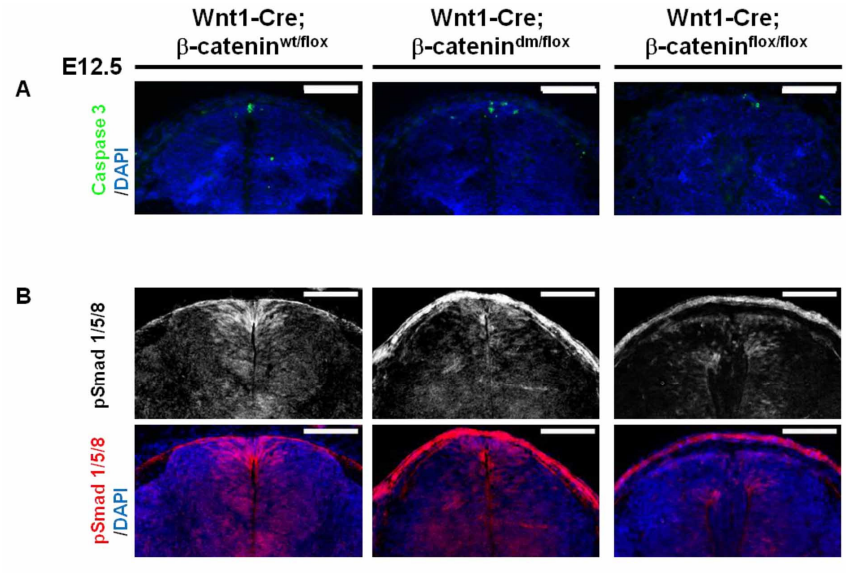

Figure 24 Blocking Wnt/β-catenin transcription in the dorsal spinal cord of *Wnt1-Cre*; β-catenin$^{dm/flox}$ embryos does not lead to increased apoptosis, but results in affected sensory neuron differentiation

(A-B) Immunostaining of transversal sections of the dorsal spinal cord isolated from E12.5 embryos. Activated caspase-3 staining does not show increased number of apoptotic cells in the Wnt1-Cre; Ctnnb1$^{dm/flox}$ dorsal neural tube (A). Altered differentiation of spinal cord precursors to sensory neurons in Wnt1-Cre; Ctnnb1$^{dm/flox}$ is monitored by the decrease in pSmad1/5/8 levels in those cells (B).

5.1.5. Discussion

5.1.5.1. The first specific model to study lack of canonical Wnt/β-catenin signaling

The importance of canonical Wnt/β-catenin signaling during development is only rivalled by the difficulty of studying it in vivo. The main obstacles for a genetic analysis of the transcriptional output of the canonical Wnt pathway are the following. First, mammalian genomes encode almost twenty different Wnt proteins. In many cases, their expression patterns are overlapping and the range of action is unknown. The elimination of canonical Wnt signaling at the level of the ligand thus not only faces the technical difficulty of removing the function of numerous genes at once, it is further complicated by the problem that each of these Wnts may additionally act in a non-canonical fashion. A similar complexity exists at the level of Wnt receptors (van Amerongen et al., 2008). The nuclear mediators of the canonical Wnt pathway, the TCF/Lef proteins, are somewhat better suited for the analysis of canonical Wnt output, as they are less numerous and have a better defined pathway specificity. However, there are still four family members existing as differently spliced variants that are all expressed in different combinations and at different stages of development (Najdi et al., 2011). Moreover some of these transcription factors have been shown to act - in addition to their role as activators - also as repressors of target genes in the absence of Wnt signaling. Their removal therefore, does not necessarily reflect the lack of canonical pathway activity, but rather a mixture of derepression and loss-of-activation states. Overexpressing a dominant negative form of TCF/Lef would also be problematic, as it might also elicit transcriptional repression in genomic regions that are not relevant for canonical Wnt signaling. Understandably therefore, much hope and attention has been focused on β-catenin, which is a non-redundant and essential component of the pathway. Indeed, loss-of-function studies with the *β-catenin* gene form the largest foundation for our current understanding of the canonical Wnt pathway.

A complication for using β-catenin to study Wnt signaling, however, is that it also acts as an organizer of polarized epithelia - an essential function that is independent of its signaling role. Accentuating this situation is the uncertainty about the extent to which the loss of β-catenin's adhesive function contributes to a particular phenotype; estimates of this contribution range from negligible to substantial at different stages in different tissues. Here we describe a genetic tool that resolves these issues. We have generated a *Ctnnb1* allele that is devoid of canonical Wnt signaling activity, yet retains cadherin-dependent cellular adhesion function. Using it we can now disentangle the consequences of loss-of-Wnt signaling from those of loss of cell adhesion. This relieves β-catenin of its sole significant drawback and enables to experimentally exploit its key position in the canonical Wnt pathway.

5.1.5.2. From Arm to β-catenin

The development of the signaling-defective form of β-catenin built on our understanding of Arm. The epithelium of the *Drosophila* wing imaginal disc served as a validation system for the separation of the signaling and the adhesive function. Clones of cells null mutant for Arm are eliminated 20-24 hours earlier than clones expressing the double mutant form of Arm. The loss of Arm's adhesive activity led to the destabilization of cadherin-based adherens junctions, as indicated by the delocalization of E-cadherin from the membrane. Clones with affected cadherin-based adhesion are rapidly extruded from the wing disc epithelium and eliminated (Widmann and Dahmann, 2009). Cells expressing the double mutant form of Arm, which preserves the adhesion function, survive longer than null clones, but are also smaller than clones rescued by the wild-type form of Arm, supporting previous observations that Wg/Arm signaling activity is essential for proper cell proliferation and survival (reviewed in (Gonsalves and DasGupta, 2008; Widmann and Dahmann, 2009)). Hence in the wing disc loss of Arm affects the behavior of mutant clones on two levels - adhesion and signaling.

After validating mutant mammalian β-catenin in biochemical and cell-based signaling assays, we introduced the mutations into the mouse germline. Using the resulting alleles in combination with tissue-specific knock-out of the *Ctnnb1* gene, cell populations could be generated that correspond to the *arm* clones in the *Drosophila* wing disc. With the *Wnt1-Cre* driver we observed in the dorsal neural tube corrupted adherens junctions, associated with morphological changes that would prevent studying the fate of cells lacking canonical Wnt output. Double mutant β-catenin, however, restores the cell and tissue structures and serves now as an adequate basis to assess the role of Wnt/β-catenin signaling as well as its crosstalk with other signaling pathways.

5.1.5.3. Early embryonic role of β-catenin

Embryos with transcriptionally inactive β-catenin die at E7.5, just like embryos with total loss of β-catenin. Therefore, β-catenin's role of mediating cadherin-dependent cellular adhesion does not seem to play an important function during gastrulation, although it is a dynamic process dominated by epithelial-to-mesenchymal transitions (EMT) and cell migrations (reviewed in (Arnold and Robertson, 2009)). Moreover, at these early stages β-catenin expression is more pronounced in areas where no E-cadherin is detected (E-cadherin is prominent in extra-embryonic tissues and β-catenin in the developing embryo). It appears, therefore, that mutant embryos are not significantly affected from the lack of β-catenin's adhesive role; rather, their phenotype results from the inability to form mesoderm. This in turn can be attributed to the loss of Wnt signaling-dependent expression of transcription factors that

are important for mesoderm formation. Indeed, embryos lacking MED12 die at E7.5, also from a failure to develop mesoderm (Rocha et al., 2010), and MED12 is an important co-activator of β-catenin (Kim et al., 2006).

5.1.5.4. Dual role of β-catenin in craniofacial and CNS development

Using *Wnt1-Cre* to remove wild-type β-catenin revealed situations where the consequences of total lack of β-catenin do not correspond to those of substituting it with the adhesion-competent form. Striking differences were observed in craniofacial and mesencephalic structures. Lack of β-catenin results in the absence of the midbrain and anterior hindbrain structures, yet when the signaling function is specifically ablated, the dorsal part of the midbrain develops. More posteriorly in the CNS, the specific removal of Wnt/β-catenin signaling seems to affect the ground state and the differentiation potential of precursors in the dorsal neural tube. As expected when Wnt signaling is blocked, expression of its downstream target *CyclinD1* is lost. However, the cell cycle of dorsal neural tube progenitors does not seem to be halted, as assessed by Ki67/pHH3 staining. Previous studies using the same *Wnt1-Cre* driver in conjunction with a constitutively active form of β-catenin indicated that Wnt signaling promotes proliferation while BMP signaling induces differentiation (Ille et al., 2007). Indeed, we also observed decreased differentiation of spinal cord precursors to sensory neurons, based on reduced pSmad1/5/8 activity in those cells. Thus, Wnt signaling plays an essential role not only for maintaining dorsal neural tube precursors in a proliferative state, but also affects their differentiation.

Our analysis of the developing neural tube demonstrates how the double mutant *Ctnnb1* allele can be used to specifically block canonical Wnt signaling and that it represents a powerful new tool to discriminate between the structural and signaling function of β-catenin. Additionally, our single mutant alleles will help to analyze the needs for individual β-catenin transcriptional co-activators during normal development and in disease, and could thus be invaluable to validate therapeutic strategies targeting the interaction of β-catenin with its co-activators.

5.1.6. Materials and methods

5.1.6.1. Vectors and constructs

Drosophila Arm expression constructs were based on pT2-attB(+) backbone driving protein expression under the control of *tubulinα1* promoter (Basler and Struhl, 1994). For mammalian expression constructs derived from pcDNA3.1 (Invitrogen) were used. Single amino acid change variant Armadillo-D172A or β-catenin-D164A was introduced using site directed mutagenesis (QuickChange, Stratagene). C-terminally truncated fragments of Arm (aa 1-691) or β-catenin (aa 1-673) were generated by PCR and cloned into particular vectors. Double mutant (dm) forms were created by combination of individual mutation using internal restriction site StuI conserved in both *arm* or *β-catenin*. For testing constitutive active forms of Arm, constructs arising from *arm^{S10}* in the pT2-attB(+) backbone with the same mutations as in the case of wild type Arm were generated (i.e. Armadillo^{S10}-wild type, Armadillo^{S10}-D172A, Armadillo^{S10}-ΔC, Armadillo^{S10}-dm). For the mammalian system corresponding constructs were prepared based on the constitutively active β-catenin^{S33Y} (β-catenin^{S33Y}-wt, β-catenin^{S33Y}-D164A, β-catenin^{S33Y}-ΔC, β-catenin^{S33Y}-dm).

5.1.6.2. Drosophila cell culture experiments

RNAi against the 5' and 3'-UTR of *arm* was performed as described previously by Mosimann et al. (2006) and Hofmanns et al. (2007), including dsRNA generation and application to Kc cells (for primer sequences see Supplementary table 2). Four hours after RNAi application cells were transfected using CellFectin (Invitrogen) with expression constructs encoding different Arm variants (0.5 μg of vector per 10^6 cells), eventually together with the luciferase reporter plasmids. Cells were incubated for 24 hours to allow turnover of endogenous Arm and replacement by exogenous mutant forms. After this cells were stimulated for additional 24 hours by Wg-conditioned medium (or control one) prepared from tubulin-Wg-S2 cells (*Drosophila* Genomic Resource Center, Stock No.165).

5.1.6.3. Mammalian cell culture experiments

HEK293T cells and Mouse Embryonic Fibroblasts (MEFs) were cultured at 37°C, 5%CO_2 in DMEM, 10%FCS, 1% P/S. MEFs were isolated from E13.5 *Ctnnb1$^{flox/flox}$* embryos according to standard protocols. MEFs lacking β-catenin (MEF-ko) were generated from MEF-*Ctnnb1$^{flox/flox}$* cells by infection with lentiviral particles encoding self-excising Cre recombinase as published by Cudre-Mauroux et al. (2003). Expression of β-catenin was reconstituted in MEF-ko cells through retroviral infection. Retroviral vectors based on the pBABE-Puro backbone were transfected into Phoenix-Eco (Orbigen) retrovirus producer cells via the Lipofectamine

transfection reagent (Invitrogen), and subsequent retroviral infection was performed as previously described (Valenta et al., 2003). Two days after infection MEF-ko cells were treated with Puromycin (5μg/ml) for five days to establish four different polyclonal cell lines: MEF-wt (expressing wild type β-catenin), MEF-D164A (expressing β-catenin-D164A), MEF-ΔC (expressing β-catenin-ΔC) and MEF-dm (expressing β-catenin-dm, i.e. D164A-ΔC). To activate Wnt/β-catenin-mediated transcription MEFs with reconstituted β-catenin expression (plus MEF-ko and parental MEF) were stimulated by Wnt3a-conditioned medium acquired from Wnt3a-producing L cells (L Wnt-3A; ATCC No. CRL-2647) as described by the supplier.

5.1.6.4. Luciferase assay

Drosophila Kc (or clone 8) cells were transfected in 96-well plates by CellFectin (Invitrogen) with a total amount of 300 ng plasmid mixture per three wells as follows: 50 ng wf-Luciferase reporter (Hoffmans and Basler, 2007), 30 ng tubulinα1-Renilla, 220 ng of empty vector or alternatively 100 ng of Arm^{S10}-based construct with 120 ng of empty vector. Luciferase reporter gene assays in mammalian cells were performed as described previously (Valenta et al., 2003). To assay Wnt/β-catenin-mediated transcription, firefly luciferase reporter pTOPFLASH was used. In both cases Luciferase activity was measured by the Promega Dual-Luciferase reporter system and firefly-luciferase levels were normalized to Renilla values to standardize the transfection efficiency.

5.1.6.5. Quantitative real time PCR

Total RNA was extracted from *Drosophila* Kc and mouse MEF cells and from embryos (whole E6.5 embryos or parts of E10.0 embryos) using Nucleospin RNAII kit (Marchery-Nagel). Quantitative real-time PCR reactions were performed in triplicates and monitored by the Applied Biosystems SYBR Green kit and the ABI Prism 7900HT System (Applied Biosystem). All experiments were repeated in parallel at least twice, in the case of mouse embryos RNA isolated from different litters at the same developmental stage was tested. Results were normalized to *Actin5C, β-tubulin,* and *GAPDH* in the case of *Drosophila* Kc cells. *SDHA*, *GAPDH* and *β-actin* were used for normalization of mouse samples (MEF, embryos). ΔΔCt method (Applied Biosystem user bulletin) was used for result calculations. For details concerning primers see Supplementary Table 2.

5.1.6.6. Fly stocks

Four transgenic fly lines expressing Arm under the control of *tubulinα1* promoter were generated using ΦC31 integration system developed previously in our lab (Bischof et al., 2007): *tub-Arm-wt*; *tub-Arm-D172A*, *tub-Arm-ΔC* and *tub-Arm-dm*. Constructs based on pT2-attB(+) vector backbone were injected into the *ZP-attP-86Fb* fly line harboring a landing site on the third chromosome.

5.1.6.7. Disc clones

Mutant imaginal disc clones were generated by crossing *arm^{2a9} FRT19/FM7* females with *hs-flp ubiGFP FRT19; tub-arm-R/TM6b* males, where R represents an individual variant of an *arm* rescue construct. 72 hours after egg laying larvae were heat shocked at 38°C for 45 minutes. Female third instar larvae that did not carry *TM6b* were dissected 48 hours after the heat shock. Imaginal discs were fixed and stained by standard techniques. Pictures were captured by a Zeiss LSM710 confocal microscope.

5.1.6.8. Generation of β-catenin knock-in mouse strains

To replace the endogenous *Ctnnb1* locus with mutant forms two independent targeting vectors for homologous recombination were cloned. The single point amino acid change D164A, blocking the interaction between β-catenin and BCL9/BCL9L, was introduced using pL-PGK#12(loxP-Hyg-loxPrev) (a gift from D. Shmerling) encoding the D164A mutation in exon 4 cloned in the 5' arm of the vector. For the C-terminal truncation vector pTargetVectorpBS-FRT-neo-TK was generated, which encodes in its 3' arm a preliminary stop codon at position of amino acid 673 followed by a frameshift mutation. Moreover, exon 13 harboring the premature stop codon was directly fused to exon 15 encoding the 3' UTR of *Ctnnb1* (exon 14 and the introns between exon 13,14 and 15 were thus eliminated. Electroporation of targeting vectors into TC-1 (129Sv) mouse embryonic cells, blastocyst injection and further generation of knock-in animals including verification was performed by Polygene (Rümlang, Switzerland). Double mutant animals were generated by two subsequent steps of homologous recombination; mES cells harboring C-terminal truncation were electroporated with targeting vectors encoding the D164A mutation and double mutant mES cells were further used for blastocyst injection. For the detailed information concerning targeting vectors and genotyping see Supplemental Experimental Procedures Table 7, Table 8, and Figure 26.

5.1.6.9. Mouse experiments

Mouse experiments were performed in accordance with Swiss guidelines and approved by the Veterinarian Office of the Kanton of Zürich, Switzerland. All animals were kept on a C57BL/6 background. Strains harboring the *Ctnnb1* null allele (*Ctnnb1*^{ko}) were generated by crossing a CMV-Cre line with the conditional β-catenin strain *Ctnnb1*$^{flox/flox}$ (B6.129-*Catnb*$^{tm2Kem/J}$; Jackson Laboratory, USA). To monitor Wnt/β-catenin transcription, compound animals heterozygous for the mutated forms of *Ctnnb1* were crossed with the *BAT-gal* reporter line (Maretto et al. 2003) and offsprings were further crossed to get *Ctnnb1*$^{mutant/mutant}$; *BAT-gal*$^{+/-}$ embryos, where 'mutant' represents: D164A, ΔC or dm (D164A-ΔC). The fate of neuroepithelial cells was followed in compound transgenic animals (*Ctnnb1*$^{mutant/flox}$) expressing Cre (*Wnt1-Cre*) and bred to the *ROSA26* mouse reporter *(R26R)* line (Soriano, 1999). Activity of β-galactosidase expressed in *BAT-gal* or *ROSA26* was determined by X-gal staining as described previously (Ille et al., 2007; Maretto et al., 2003).

5.1.6.10. Co-immunoprecipitations, staining of tissue sections

Co-immunoprecipitations

MEF-ko cells were transfected by Lipofectamine 2000 (Invitrogen), 24 hour after transfection cells were stimulated with Wnt3a conditioned medium for additional 24 hours. Cell were lysed in NP-40 lysis buffer (Mosimann et al., 2006) and further processed as described in Valenta et al. (2006).

Staining of tissue sections

For immunohistochemistry cryo-sections were fixed for 15 min in 4% paraformaldehyde (PFA)/PBS at room temperature (RT) and treated with 10% goat serum, 0.3% Triton-X-100 and 0.1%BSA in PBS for 60 minutes before incubation with primary antibody for 1 hour at RT or at 4°C overnight. Immunostainings were visualized by incubation with fluorescently labeled secondary antibody. Nuclei were stained by DAPI (1:1000, Sigma). Antibodies used in this study are indicated in Supplementary table S3. Non- radioactive in situ hybridizations with digoxigenin-labelled riboprobes and X-gal staining on cryo-sections were performed on cryo-sections as previously described (Ille et al., 2007). All stainings have been done at least on sections from 3 independent embryos of the relevant genotype.

5.1.7. Supplemental experimental procedure

This part contains additional detailed information concerning experimental procedure plus figures showing experimental crossing scheme and scheme of targeting vectors used for generation of *Ctnnb1* knock-in mouse strain.

5.1.7.1. Genotyping of Ctnnb1 knock-in mouse strains

To distinguish the the wild type allele of *Ctnnb1* from mutated ones we used the fact that in knock-in animals there is one remaining FRT site after the elimination of the Neomycin resistance cassette in the case of the *Ctnnb1*-ΔC transgene and one loxP site after elimination of Hygromycin resistance cassette in the *Ctnnb1*-D164A transgene (and both in the case of the *Ctnnb1*-dm transgene). Primer pairs flanking FRT or loxP sites can thus monitor the presence of the respective knock-in allele. *Ctnnb1*-D164A (i.e. loxP insertion) was detected by primers 5301.1 (5'- TCC CTG AGA CGC TAG ATG – 3') and 5301.2 (5'- GAG TCC CAG CAG TAC AAC– 3') which yields an amplicon of the size 475 bp for the wild-type and 628 bp for mutant alleles. *Ctnnb1*-ΔC (i.e. FRT insertion) was determined using primers 5301.3 (5'- GTG CAC ACG TCA TGC TTT AC– 3') and 5301.4 (5'- TGG CTT GTC CTC AGA CAT TCG– 3') generating an amplicon of size 349bp for the wild-type and 415 bp for mutant alleles.

5.1.7.2. Crossing scheme based on tissue-specific Cre-transgenes and a conditional Ctnnb1 null allele, allowing to overcome early embryonic lethality of the various point-mutant Ctnnb1 alleles

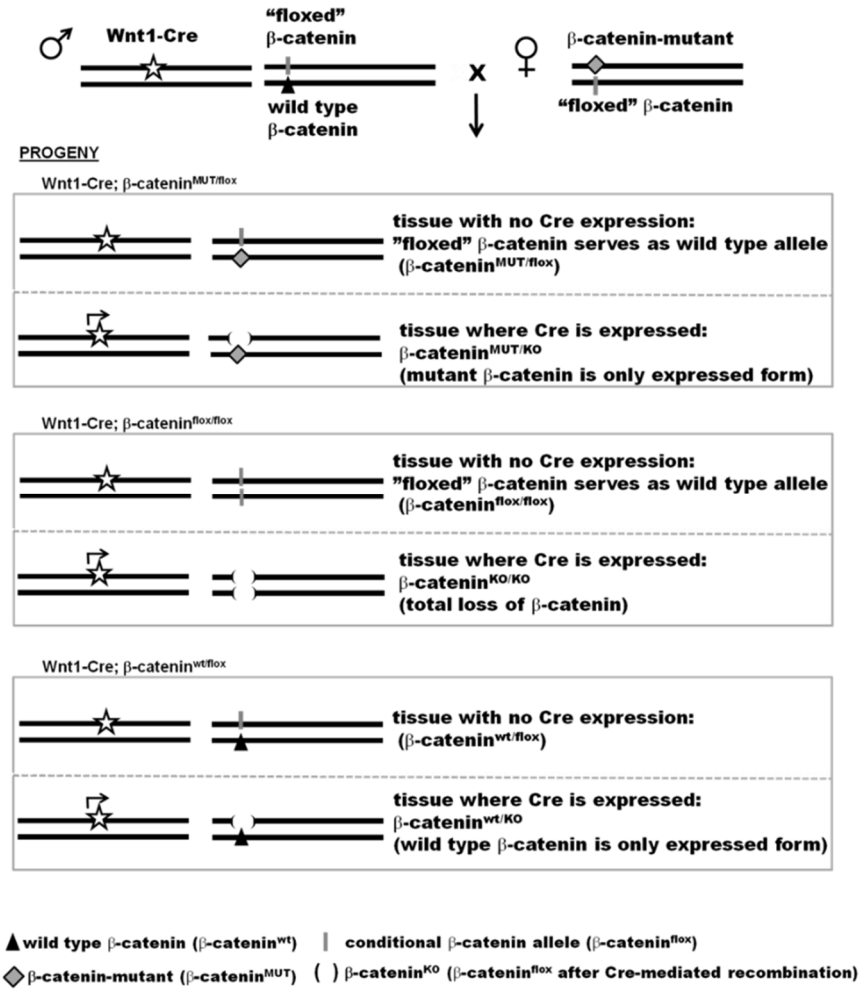

Figure 25 Crossing scheme based on tissue-specific Cre-transgenes

Wnt1-Cre; Ctnnb1$^{wt/flox}$ male is crossed to Ctnnb1$^{mutant/flox}$ female, where mutant represents D164A, ΔC or the double mutant combination. In progeny expressing Wnt1-Cre, and containing one mutant and one floxed Ctnnb1 allele, the mutant allele is resistant to Cre and thus serves as the only source of β-catenin in the Wnt1-positive tissues. Control animals inherit either a wild-type or a second Ctnnb1^{flox} allele. Wnt1-Cre; Ctnnb1$^{flox/flox}$ tissues absolutely lack any signaling- or adhesion-functional β-catenin (Ctnnb1^{ko}).

5.1.7.3. Targeting vectors used for the generation of the Ctnnb1 knock-in mice

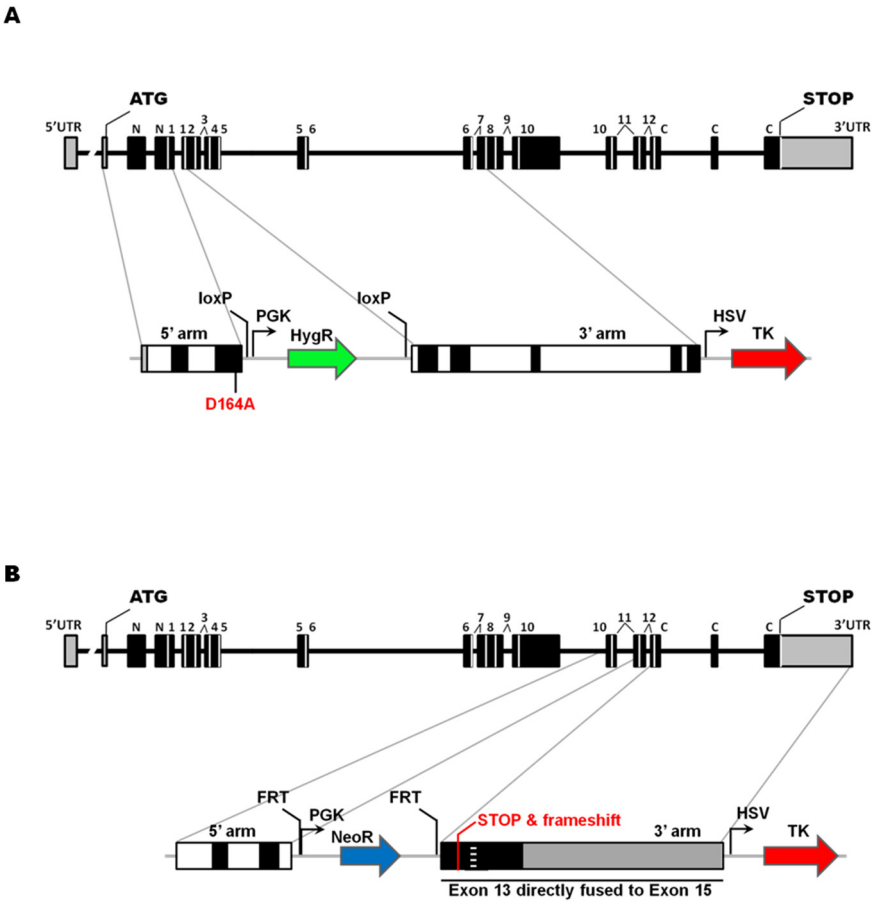

Figure 26 Targeting vectors used for the generation of the β-catenin knock-in mice

(A) The Ctnnb1-D164A targeting vector (pL-PGK-Hyg#12/loxP-Hyg-loxPrev). The 5' arm contains exons 2-4 and the 3' arm exon 5-8 and part of exon 9. In exon 4 the amino acid D164 is changed to alanine.

(B) The Ctnnb1-ΔC targeting vector (pTargetVector_pBS-FRT-neo-TK). The 5' arm contains exons 11-12 and the 3' arm exon 13 which is fused to exon 15 (exon 14 is deleted). In exon 13 the amino acid 673 is changed to a stop codon and is followed by a frame shift.

5.1.7.4. List of Primers

Region	Forward sequence (5'-3')	Reverse sequence (5'-3')
control(GFP)	T7-CTTTTCACTGGAGTTGTCC	T7-ATCCATGCCATGTGTAATCC
Arm(3'-UTR) #1	T7-AGCCGAGCTAAGGGTAAGGG	T7-CTTGCCGTTTCGTTCGCATT
Arm(3'-UTR) #2	T7 -ACAAGCCGAGCTAAGGGTAAG	T7-CATATGAAGGGAAATGTACG
Arm(5'-UTR)	T7-CTCCCAGTCTCTTTCCCTGTC	T7-TTAGCACTCTTTCAAATCTCATGC

-three generated dsRNA against Armadillo (Arm(3'-UTR)#1; Arm(3'-UTR)#2; and Arm(5'-UTR)) were mixed in equal ratio and applied to Kc cells in total amount as described in Experimental Procedure

Table 7 Primers for generation of templates used for dsRNA synthesis to knock-down endogenous Armadillo

A) Drosophila cells

Gene/mRNA	***Forward sequence (5'-3')***	***Reverse sequence (5'-3')***
Actin5C (Act5C)	CAAAGCGCAAAAAGAACACA	AGAGGAGAGGGCGAGGTTAG
beta-tubulin 56D	CAAGGCTTCCAACTCACACA	TGTCGATGCAGTAGGTCTCG
dFrizzled3 (Fz3)	GCAAAACTTTAGCGGCAGTC	TGTAGCACAGGCACAGGAAG
GAPDH1	ATCGTCGAGGGTCTGATGAC	CGGACGGTAAGATCCACAAC
Naked cuticle (Nkd)	GTTGCTGAGCGTGTACGTGT	TAAACTGGCGGCCATAGTTC
Succinate dehydrogenase B (SDHB)	CTACGAGCAGTACCGCAACA	CTACGAGCAGTACCGCAACA

B) Mouse cells and embryos

Gene/mRNA	***Forward sequence (5'-3')***	***Reverse sequence (5'-3')***
Axin2	GGGGGAAAACACAGCTTACA	ACTGGGTCGCTTCTCTTGAA
BAT-gal	CGATGATCCCGTCGTTTTAC	GGCCTCTTCGCTATTACGC
Beta-actin	GATCTGGCACCACACCTTCT	GGGGTGTTGAAGGTCTCAAA
Beta-galactosidase (lacZ)	TTGAAAATGGTCTGCTGCTG	TATTGGCTTCATCCACCACA
Frizzled1	CAAGGTTTACGGGCTCATGT	GTAACAGCCGGACAGGAAAA
GAPDH	AACTTTGGCATTGTGGAAGG	ATCCACAGTCTTCTGGGTGG
Goosecoid	CTCGGAGGAGTCAGAAAACG	TCGACTGTCTGTGCAAGTCC
LEF1	TGGTTAACGAGTCCGAAATCA	AGAGGACGGGGCTTGTCT
Succinate dehydrogenase A(SDHA)	AAGGCAAATGCTGGAGAAGA	TGGTTCTGCATCGACTTCTG
T/Brachyury (primer set1)	CAGCCCACCTACTGGCTCTA	GAGCCTGGGGTGATGGTA
T/Brachyury (primer set2)	GAACCTCGGATTCACATCGT	TTCTTTGGCATCAAGGAAGG

Table 8 Primers for real-time qRT-PCR

5.1.7.5. List of antibodies

Recognized protein	Generated in	Producer (Product Number)
Primary antibodies		
a-e-catenin	rabbit	CellSignaling (3236)
alpha-tubulin	mouse	CellSignaling (2144)
Armadillo	mouse	Hybridoma Bank (N2 7A1)
beta-catenin (N-terminus)	mouse	Alexis (ALX-804-060-c100)
beta-catenin (C-terminus)	rabbit	Sigma (a5316)
beta-catenin (C-terminus)	mouse	BD Trasduction Lab. (610153)
Brn3a	rabbit	gift from Turner Lab
Cleaved-Caspase3	rabbit	CellSignaling (9661)
Cyclin D1	mouse	Santa Cruz (sc-450)
Dcx	guinea pig	Milipore (Ab2253)
E-cadherin	mouse	BD Trasduction Lab. (610181)
E-cadherin(Drosophila)	mouse	Hybridoma Bank (DCAD2)
HA tag	mouse	Covance
HA tag	rabbit	ICL
Hyrax/Parafibromin	rabbit	Bethyl lab (A300-170A)
Ki67	rabbit	Abcam (ab15580)
N-cadherin	rabbit	Takara (M142)
Pax3	rabbit	Invitrogen (38-1801)
pHH3	mouse	Cell signaling (9706)
pSmad1/5/8	rabbit	Milipore (AB3848)
Senseless	guinea pig	kindly provided by Hugo Bellen
Sox2	mouse	R&D (MAB2018)
ZO1	mouse	Zymed (33-910)
Secondary antibodies		
Alexa Fluor 488 Goat anti-mouse IgG (H+L)	goat	Invitrogen (A11029)
Alexa Fluor 546 Goat anti-mouse IgG 2a	goat	Invitrogen (A21133)
Cy2 Goat anti-guinea pig IgG	goat	Jackson (106-225-003)
Cy3 Goat anti-mouse IgG	goat	Jackson (115-165-003)
Cy3 Goat anti-rabbit IgG	goat	Jackson (111-165-003)
DyLight 488 Goat anti-rabbit	goat	Jackson (111-485-003)
HRP Goat anti-rabbit IgG	goat	Chemicon (AP132P)
HRP Goat anti-mouse IgG	goat	Jackson

Table 9 List of antibodies used for publication

Antibodies were used for particular procedures (WB, IHC, IP) in dilution as recommended by supplier.

5.1.8. Acknowledgements

We thank H. Bellen, E. Wieschaus, T. Uemura and the Hybridoma Bank for antibodies, S. Piccolo for providing the *BAT-gal* strain, L.Hari, I. Miescher and D. Shmerling for help with mouse experiments, and G. Hausmann for critical reading of the manuscript. This work was supported by the European Research Council, the Swiss National Science Foundation and the Kanton of Zürich.

5.2. Distinct adhesion-independent functions of β-catenin control stage-specific sensory neurogenesis and proliferation

In press at BMC Biology; 2015

Max Hans-Peter Gay, Tomas Valenta, Patrick Herr, Lisette Paratore-Hari, Konrad Basler, Lukas Sommer

5.2.1. Abstract

Background: β-catenin plays a central role in multiple developmental processes. However, it has been difficult to study its pleiotropic effects, because of the dual capacity of β-catenin to coordinate cadherin-dependent cell adhesion and to act as a component of Wnt signal transduction. To distinguish between the divergent functions of β-catenin during peripheral nervous system development, we made use of a mutant allele of β−catenin that can mediate adhesion but not Wnt-induced TCF transcriptional activation. This allele was combined with various conditional inactivation approaches.

Results: We show that of all peripheral nervous system structures, only sensory dorsal root ganglia require β-catenin for proper formation and growth. Surprisingly, however, dorsal root ganglia development is independent of cadherin-mediated cell adhesion. Rather, both progenitor cell proliferation and fate specification are controlled by β-catenin signaling. These can be divided into temporally sequential processes, each of which depends on a different function of β-catenin.

Conclusions: While early stage proliferation and specific, Neurog2- and Krox20-dependent waves of neuronal subtype specification involve activation of TCF transcription, late stage progenitor proliferation and Neurog1-marked sensory neurogenesis are regulated by a function of β-catenin independent of TCF activation and adhesion. Thus, switching modes of β-catenin function are associated with consecutive cell fate specification and stage-specific progenitor proliferation.

5.2.2. My contribution to this work

- Designing and performing all experiments
- Collection of all the data
- Generation of all figures
- Generation of most reagents, including breeding, genotyping of the mice and collection of embryos
- Design of paper outline, together with L. Sommer. Writing of whole manuscript with corrections and contributions provided by L. Sommer. Discussion, modification and revision of manuscript.

5.2.3. Background

Canonical Wnt signaling is one of the most important evolutionarily conserved signaling pathways in embryonic development (Clevers, 2006; Klaus and Birchmeier, 2008; Logan and Nusse, 2004). There are 19 Wnt genes found in mammals and a multitude of receptors to which they bind. In the canonical Wnt signaling pathway the interaction between Wnt and the transmembrane receptor proteins Frizzled and LRP leads to recruitment of Axin and GSK-3 to the membrane, thus preventing degradation of β-catenin. This in turn results in the accumulation of β-catenin in the cytoplasm and its translocation into the nucleus, where it can interact with one of the members of the TCF/Lef family. In the absence of β-catenin, TCF/Lef transcription proteins act as transcriptional repressors by binding to Groucho/TLE co-repressors. Nuclear β-catenin physically displaces Groucho co-repressors and converts TCF/Lef into transcriptional activators (Daniels and Weis, 2005). In recent years, evidence has revealed that the purpose of some TCFs is not only their function to serve as trans-activators, but also their ability to act as repressors when bound by Goucho/TLE co-repressors. In this case, TCF targets become de-repressed upon removal of Groucho/TLE co-repressors due to the binding of nuclear β-catenin. The main TCF prone to act as a repressor is TCF3, whereas TCF4 and TCF1 have the capacity to fulfill both activator and repressor functions depending on the spatial and temporal context (Archbold et al., 2012; Chodaparambil et al., 2014; Lien et al., 2014; Nguyen et al., 2009; Shy et al., 2013; Wray et al., 2011; Wu et al., 2009; Yi et al., 2011).

β-catenin is the bottleneck of canonical Wnt signaling, as it is the central, non-redundant component of the pathway. This trait has made β-catenin especially attractive as a target for genetic manipulation to elucidate the impact of Wnt signaling in vivo. The β-catenin protein is composed of 12 Armadillo repeats and is flanked by an amino-terminal domain and a conserved helix-C next to a carboxy-terminal domain. Nuclear β-catenin interacting with TCF/Lef recruits transcriptional co-activators to the transcription complex by means of its N- and C-terminal, initiating TCF/Lef-mediated transcription (Valenta et al., 2012) (Figure 1A). However, apart from its role as a transcriptional co-activator, β-catenin also serves as a linking protein in cadherin-mediated adherens junction. In adherens junctions, transmembrane cadherins bind to the first eleven armadillo repeats of β-catenin, while actin-bound α-catenin binds to the amino-terminal domain. This dual role of β-catenin in mediating Wnt signaling and cell-cell adhesion made it difficult to collate a specific phenotype obtained upon β-catenin gene (*Ctnnb1*) manipulation to either or both functions of β-catenin. To distinguish between signaling and adhesion functions of β-catenin in the skin, a transgene has previously been used (DasGupta et al., 2002), which led to expression of a mutated form of β-catenin harboring a C-terminal truncation and lacking the first 87 amino acids. However, this version of β-catenin was non-degradable, unlike its physiological counterpart, and did not block interaction with N-

terminal co-activators. We recently generated another allele of β-catenin (*Ctnnb1^{dm}*) that results in expression of a mutated form of the protein from its endogenous locus. The protein expressed from this allele (β-catenin-dm) is degradable in the absence of Wnt, is fully functional in adherens junctions, and lacks known signaling properties as a transducer of Wnt-dependent transcriptional activation (Draganova et al., 2015; Valenta et al., 2011). Moreover, a dominant negative effect of the mutated protein can be excluded as heterozygous animals carrying *Ctnnb1^{dm}* display no phenotype (Valenta et al., 2011). This form of β-catenin has a single amino acid change in the first Armadillo repeat of β-catenin (D164A), which prevents the binding of the N-terminal transcriptional co-activators BCL9/BCL9L. These regulators are important independently of C-terminal co-activators. Indeed, homozygosity of the D164A mutation leads to lethality in mouse embryos at E10.5 (Valenta et al., 2011). Additionally, a truncation of its C-terminus blocks the association of β-catenin-dm with a multitude of co-activators acting as chromatin modifiers (CBP/p300, Brg1) or connecting β-catenin to RNApolII machinery (Paf1 complex, MEDIATOR complex). Importantly, β-catenin-dm is still able to bind to cadherins, α-catenin, and TCF/Lef (Figure 27 A'). Therefore, β-catenin-dm maintains the ability to mediate cellular adhesion and, likely, to de-repress TCF targets, allowing the identification of effects of β-catenin that are TCF-transactivation independent.

Neural crest cells (NCCs) are a population of multipotent cells that delaminate from the dorsal part of the neural tube during neurulation of vertebrate embryos (Le Douarin et al., 2008). Upon delamination, NCCs migrate along specific routes throughout the embryo to give rise to a broad variety of derivatives, such as the neuronal and glial cells of the peripheral and enteric nervous system as well as craniofacial bone, cartilage, smooth muscle, and melanocytes. Wnt signaling has been implicated at multiple developmental stages of the neural crest (Hari et al., 2002; Hari et al., 2012; Kléber et al., 2005; Lee et al., 2004; Rogers et al., 2012; Schmidt and Patel, 2005; Stuhlmiller and García-Castro, 2012). In particular, we have previously demonstrated the consequences of conditional ablation of β-catenin in the premigratory NCCs using Cre recombinase driven by the Wnt1 promotor (*Wnt1-Cre*) (Brault et al., 2001; Hari et al., 2002). Inactivation of β-catenin in *Wnt1-Cre Ctnnb1$^{flox/flox}$* embryos resulted in a drastic reduction of sensory neuronal and complete absence of glial lineages in the dorsal root ganglia (DRG), whereas other neural derivatives, such as sympathetic ganglia and the enteric nervous system, appeared to develop normally (Hari et al., 2002). Sensory neurogenesis involves the generation of multiple neuronal subtypes in three temporal waves and is tightly associated with the aggregation of NCCs in DRG. (Marmigère and Ernfors, 2007). However, it remains to be determined to what extent β-catenin transactivation signaling as opposed to other functions, such as β-catenin-mediated adhesion and TCF/β-catenin-mediated de-repression, controls sensory neuronal subtype specification and DRG formation. Here, we exploited our novel β-catenin signaling mutant allele, *Ctnnb1^{dm}*, together with β-catenin null and other conditional

knockout alleles, and reveal distinct requirements of β-catenin functions for sensory neurogenesis. Surprisingly, while β-catenin/α-catenin-mediated cellular adhesion plays a negligible role in sensory neuron formation, several steps in sensory neurogenesis require β-catenin, but only some of these are dependent on β-catenin-mediated transcriptional activation.

5.2.4. Results

5.2.4.1. Replacement of β-catenin with its signaling-defective variant in neural crest stem cells exhibits milder phenotypes in comparison to complete ablation of β-catenin

To investigate the role of β-catenin signaling during neural crest development independently of β-catenin-mediated cell adhesion, we generated *Wnt1-Cre Ctnnb1*$^{flox/dm}$ (*βcat-Sig*) animals. In these mice, Cre-mediated conditional deletion of β-catenin normally expressed from the *Ctnnb1*^{flox} allele leads to complete replacement of the endogenous β-catenin protein by the signaling mutant form derived from the *Ctnnb1*^{dm} allele (Figure 27 A'; (Valenta et al., 2011)). As a result, *Wnt1-Cre*-positive premigratory NCCs and their derivatives express mutant β-catenin that retains the cell adhesion function, but fails to activate TCF/Lef-dependent transcription (Figure 27 B''). For comparison, we also produced *Wnt1-Cre Ctnnb1*$^{flox/flox}$ (*βcat-Null*) embryos (Figure 27 B'''). Furthermore, to perform in vivo cell lineage tracing in both mouse models, we made use of the *ROSA26* Cre reporter line (*R26R*) (Soriano, 1999), which expresses β-galactosidase (*β-gal*) upon Cre-mediated recombination.

X-gal staining at embryonic day (E) 12.5 on whole-mount embryos carrying *R26R* revealed similar, but less severe phenotypes in *βcat-Sig R26R* embryos when compared to *βcat-Null R26R* embryos (Figure 27 C'-C'''). Craniofacial and mesencephalic defects were the most obvious macroscopic phenotype in both mutant embryos when compared to control embryos, as previously described (Valenta et al., 2011). Immunohistochemistry for *Cre*-dependent β-gal expression on transverse sections of E12.5 embryos revealed unaffected development of the enteric nervous system and the sympathetic ganglia in either mutant embryo (Figure 27 E'-E''', F'-F'''), in agreement with (Hari et al., 2002). In contrast, proper formation of the DRG was inhibited in E12.5 *βcat-Null R26R* embryos as evident by a reduction of DRG-populating cells by 91.7±0.6% (Figure 27 G'''), while the cell number in *βcat-Sig R26R* DRG was reduced by 74.9±3.8% (Figure 27 G'').

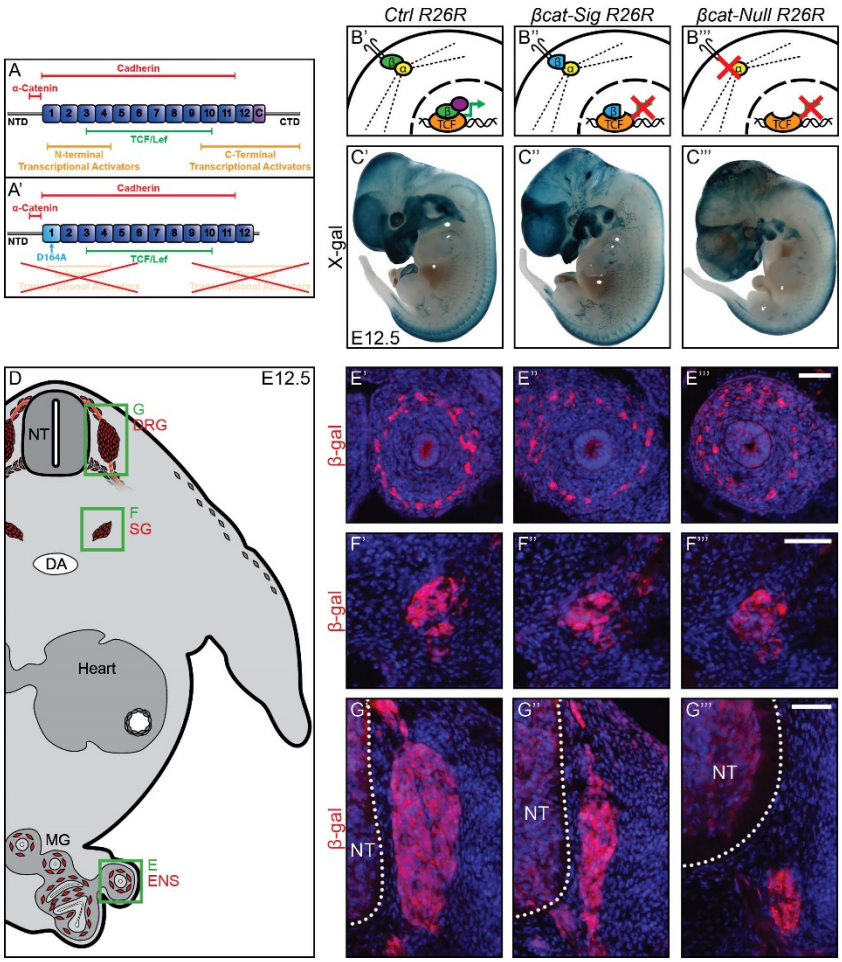

Figure 27 Total loss of β-catenin leads to a more severe phenotype in the dorsal root ganglia than inhibition of the TCF/Lef transcriptional output of β-catenin

(A) Diagram displaying binding regions of the β-catenin protein, consisting of 12 Armadillo repeats (numbered boxes) and conserved helix-C (C), flanked by an amino-terminal domain (NTD) and carboxy-terminal domain (CTD) (Valenta et al., 2011). Colored bars show binding sites for β-catenin interaction partners. Color code: red, components of adherens junctions; green, TCF/Lef transcription factors providing DNA binding; orange, transcriptional co-activators. (A') Diagram presenting the mutated β-catenin protein derived from the double mutated β-catenin allele (Ctnnb1^{dm}). D164A and truncation of CTD inhibits its association with multiple players of the transcription machinery. However, binding sites for TCF/Lef and components of adherens junctions are preserved.

(B'-B''') Schematic of Cre-recombined cells and the functional properties provided by the expressed β-catenin protein of the corresponding genotype. (B') β-catenin (green) of control animals induces transcription (green arrow) by binding with TCF/Lef (orange) in the nucleus and recruiting co-transcription factors (purple). Furthermore it links transmembrane cadherins via α-catenin (yellow) to the actin cytoskeleton (dotted line). (B'') The mutated β-catenin protein (blue) of βcat-Sig animals inhibits TCF/Lef-mediated transcription, but preserves cadherin-mediated adhesion. (B''') Cells of βcat-Null animals lose both TCF/Lef-mediated transcription and cadherin-mediated adhesion, as β-catenin is absent.

(C'-C''') In vivo fate mapping of neural crest cells by Wnt1-Cre on E12.5 whole-mount control and mutant embryos carrying the R26R reporter allele.

(D) Illustration of a transverse section of an E12.5 control animal displaying in red the neural derivatives of neural crest cells: dorsal root ganglia (DRG); sympathetic ganglia (SG); enteric nervous system (ENS). Green boxes display caption area for subfigures E-G.

(E'-G''') Immunohistochemistry for β-gal on transverse sections at E12.5. Normal migration and early development of the enteric nervous system (E'-E''') and the sympathetic ganglia (F'-F''') can be witnessed in both mutants. (G'-G'''). The size of the DRG of βcat-Sig R26R embryos is strongly reduced (G''), whereas DRG of βcat-Null R26R animals are virtually non-existent (G'''). NT, neural tube; DA, dorsal aorta; MG, mid gut. Scale bars: 50 µm.

The lineage-specific phenotypes observed in *βcat-Sig R26R* and *βcat-Null R26R* embryos might reflect distinct canonical Wnt signaling activity in derivatives of NCCs. Functional output of β-catenin was assessed using the *β-gal* expressing Wnt-reporter line *BAT-gal* (Maretto et al., 2003). In these mice, *Cre*-induced enhanced green fluorescent protein (EGFP) expression was used to be able to trace recombined *BAT-gal*-positive cells (Mao et al., 2001). Double immunofluorescent staining for β-gal and EGFP on transverse sections of E10.5 embryos revealed that NCCs giving rise to progenitors of the cardiac outflow tract, the enteric nervous system, and the sympathetic ganglia, were not subjected to canonical Wnt signaling post migration (Figure 28 A-C). However, EGFP-positive cells populating the pharyngeal arches (Figure 28 D) and DRG (Figure 29 B) strongly expressed the output of the *BAT-gal* reporter.

To verify the loss of wild type β-catenin in our mutant mouse models, antibodies specific for either the N- or C-terminus of β-catenin were used for immunohistochemistry. Triple immunofluorescent staining for EGFP and the N- and C-terminus of β-catenin on transverse sections of E10.5 embryos confirmed the loss of β-catenin in recombined cells of *βcat-Null* animals and substitution of wild type β-catenin by the double mutated form with a truncated C-terminus present in recombined cells of *βcat-Sig* mutants (Figure 29 E'-G''''). Moreover, on adjacent sections, double immunofluorescent staining for EGFP and β-gal of the *BAT-gal* reporter demonstrated the loss of Wnt/β-catenin-induced TCF/Lef-mediated transcription (Figure 29 B-D).

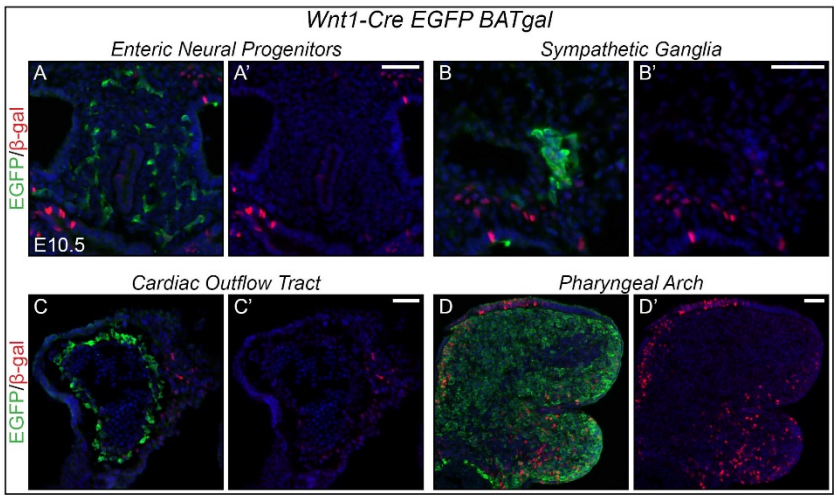

Figure 28 NCCs giving rise to the enteric nervous system, the sympathetic ganglia and the cardiac outflow tract are not subjected to canonical Wnt signaling as opposed to NCCs populating the pharyngeal arches

(A-D) Visualization of canonical Wnt activity using the β-gal expressing Wnt-reporter line BAT-gal in derivatives of NCCs, which were lineage traced using a Wnt1-Cre mouse line and Cre-induced EGFP. Double immunofluorescent staining β-gal and EGFP do not display co-localization of EGFP and β-gal in NCCs giving rise to progenitors of the enteric nervous system, the sympathetic ganglia, and the cardiac outflow tract at E10.5 (A-C). However, EGFP-positive NCCs populating the pharyngeal arches express β-gal expressed by the BAT-gal transgene (D). Scale bars: 50 µm.

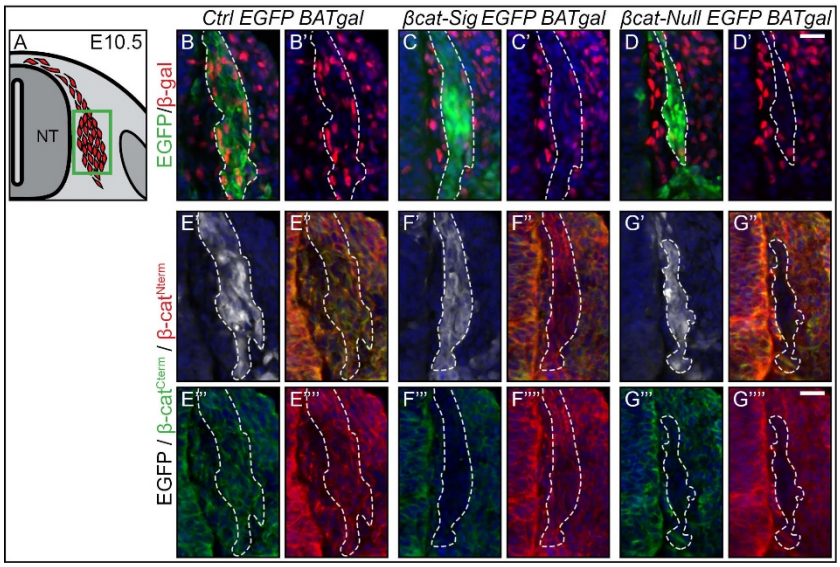

Figure 29 Proof of principle for the replacement of the endogenous β-catenin protein by the signaling mutant form in the DRG

(A) Illustration of a transverse section of an embryo at E10.5 displaying cells contributing to the DRG in red. Green box represents caption area for subfigures B-G. (B-D) Double immunofluorescent staining for β-gal expressed by the BAT-gal transgene and the Cre-induced EGFP lineage tracer at E10.5. Ctrl animals show many β-gal-positive cells in the developing DRG (B, B'). Both the βcat-Sig and βcat-Null animals display an almost complete loss of β-gal expression in EGFP-positive cells (C-D'). (E'-G', E'''-G''', F''''-G'''') Single channels of triple staining for EGFP and the N- and C-terminus of β-catenin at E10.5. (E''-G'') Overlay of channels of staining for the N- and C-terminus of β-catenin. Only a staining for the N-terminus of β-catenin can be detected in DRG progenitors of βcat-Sig embryos expressing EGFP, demonstrating that wild type β-catenin has been replaced in these cells by the double mutated form with the truncated C-terminus (F'-F''''). Furthermore, EGFP-positive cells of βcat-Null animals have completely lost expression of β-catenin (G-G''''). Scale bars: 25 µm.

5.2.4.2. Postmigratory proliferation of dorsal root ganglia precursors is temporally regulated by different functions of β-catenin

To determine the cause for the reduction of the sensory lineage in *βcat-Sig* and *βcat-Null* embryos, respectively, the presence of undifferentiated DRG progenitors during migration at E9.5 and post migration at E10.5 and E12.5 was analyzed by immunohistochemistry for the transcription factor Sox10 expressed by the multipotent NCCs (Kim et al., 2003) and β-gal expressed from the *R26R* lineage tracer (Figure 30 B-D, F-H, J-L). In comparison to control embryos, the number of Sox10-positive progenitors was retained in both mutants in migratory NCCs at E9.5 as well as in forming DRG at E10.5 (Figure 30 B-D, F-H). The reduction of the DRG size in both mutant embryos relative to control DRG was first observed after E10.5. Interestingly, from E10.5 to E12.5 the DRG of the *βcat-Sig R26R* embryos maintained a relatively constant size, whereas the size of the DRG of the *β-cat-Null R26R* mutants began to decrease (Figure 30 M).

It is well known that sensory neurons undergo apoptosis as of E11 (Wu et al., 2009). However, a normal distribution of apoptotic cells was observed in mutant DRG and their progenitors from E9 to E12.5, as revealed by staining for cleaved caspase 3 (data not shown). The presence of DRG progenitors and the exclusion of irregular apoptosis suggested a proliferation defect as cause for the reduced DRG size in both mutants. Unexpectedly, the expression of KI67, a marker for all phases of the cell cycle, was unchanged in both mutants at any time point from E9 to E12.5 (data not shown). Wnt signaling can coordinate cell cycle progression by regulating modulators of cell cycle checkpoints (Niehrs and Acebron, 2012). To investigate proper cell cycle progression, we labeled DRG progenitors entering or progressing through S-phase with a one hour EdU pulse. In migratory NCCs at E9, the ratio of EdU/Sox10-double positive cells per all Sox10-positive cells was similar in all three genotypes (Figure 30 B'-D', N). However, at E10.5 postmigratory Sox10 and EdU co-expressing DRG progenitors were significantly reduced in both mutant embryos (Figure 30 F'-H', N). Interestingly, in *βcat-Sig R26R* embryos, the percentage of EdU-positive cells in the Sox10-positive population started to recover after E10.5 and was rescued at E12.5 (Figure 30 J'-L', N). Taken together, we observed in both mutants a decrease in DRG progenitors correctly progressing through the cell-cycle at E10.5 This phenotype was maintained in *βcat-Null* embryos at later stages, whereas in *βcat-Sig* embryos mitotically active DRG progenitors slowly regained proper cell cycle progression over time and recuperated at E12.5. The loss of proper cell cycle progression in *βcat-Null* animals is probably the reason for the loss of DRGs in these animals at later developmental stages (Hari et al., 2002). In contrast, DRGs were detectable in *βcat-Sig* embryos at E16.5, although they were smaller than those of control animals (Figure 31). Presumably, this phenotype was due to a reduction of the DRG progenitor pool at earlier stages, even though cell cycle progression was rescued in the *βcat-Sig* animals from E12.5 onwards. This suggests that during early stages of DRG development normal proliferation of DRG progenitors depends on β-catenin as a co-transcription factor of TCF/Lef-mediated transcription. As time progresses, regulators of correct cell cycle progression apparently start to depend on an alternative function of β-catenin independent of mediating TCF/Lef transcription.

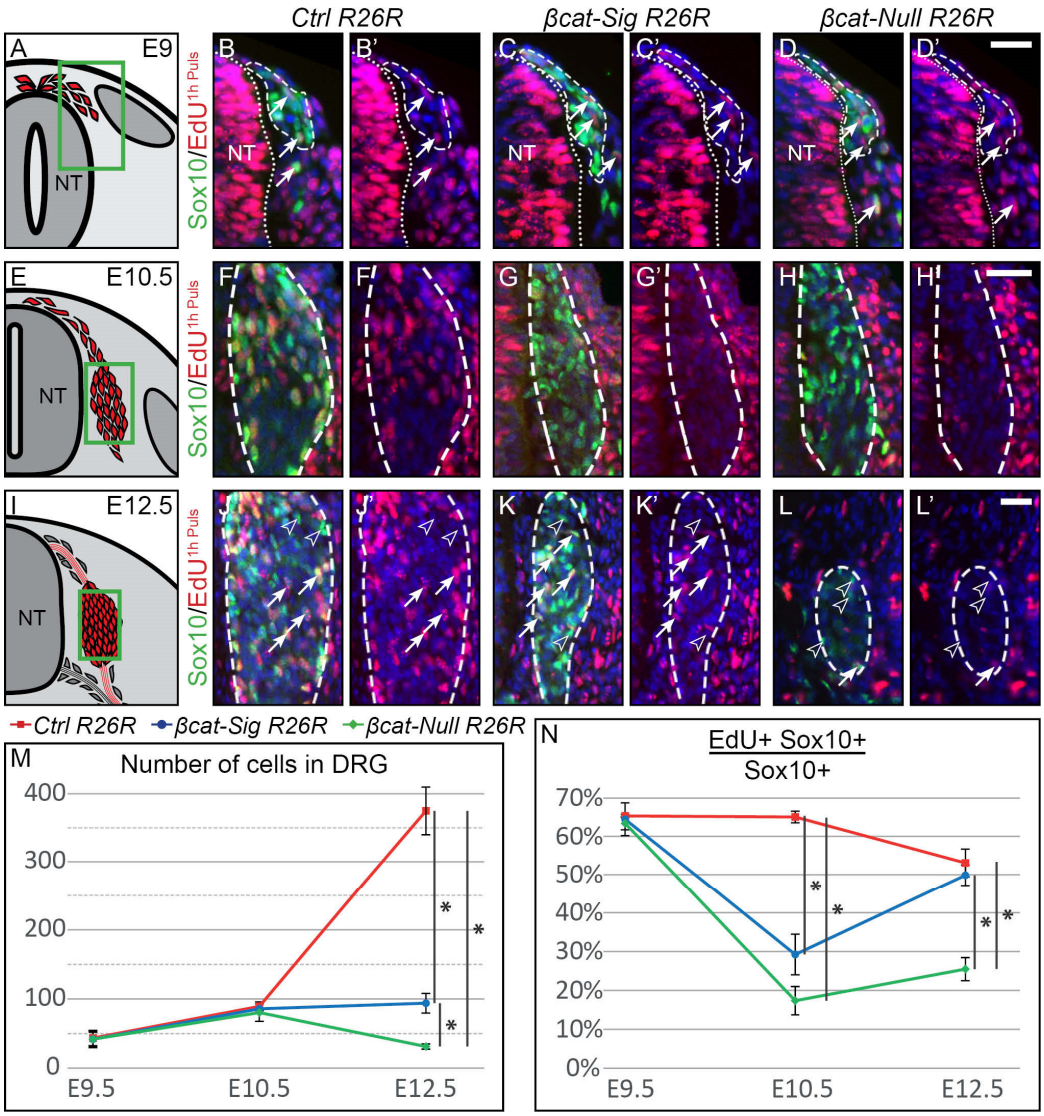

Figure 30 Rescue of proliferation defects in dorsal root ganglia precursors of *βcat-Sig* embryos

*(A, E, I) Illustration of a transverse section at E9, E10.5, and E12.5, respectively, displaying cells contributing to the DRG in red. Green box represents caption area for subfigures B-D, F-H and J-L, respectively. (B-D, F-H, J-L) Immunofluorescent staining for Sox10 and detection of EdU from a one-hour pulse. Dashed lines frame cells of the R26R reporter fate mapped in vivo, which were detected by an immunofluorescent co-staining for β-gal on the corresponding sections. (B-D, B'-D') No difference in the amount of Sox10- and EdU- double positive cells is apparent between the three types of embryos at E9. Arrows: Sox10 and EdU co-expressing cells. (F-H, F'-H') At E10.5, both mutant animals display reduced incorporation of EdU in Sox10-positive DRG progenitors. (J-L, J'-L') However, Sox10-positive cells of βcat-Sig R26R embryos recover the ability to incorporate EdU at E12.5, while Sox10-positive cells of βcat-Null R26R embryos of the same age do not. Arrows: Sox10 and EdU co-expressing cells, Arrowheads: Sox10-positive EdU-negative cells. (M) Quantification of the average numbers of R26R-positive cells contributing to the DRG at E9, E10.5 and E12.5 reveals no significant differences between mutant and control animals at E9 and E10.5. However, at E12.5 there is a statistically significant decrease of cells populating the DRG in both mutant animals. The decrease is significantly stronger in βcat-Null R26R embryos than in βcat-Sig R26R embryos. (N) Percentages of EdU-positive cells in the Sox10-positive population display a significant reduction of EdU incorporation in βcat-Null R26R animals at E10.5 and E12.5. Whereas βcat-Sig R26R animals exhibit similar statistically significant reduction as βcat-Null R26R animals at E10.5, they recover the ability to incorporate EdU by E12.5. NT, neural tube; * indicates $P < 0.05$; Scale bars: 25 µm.*

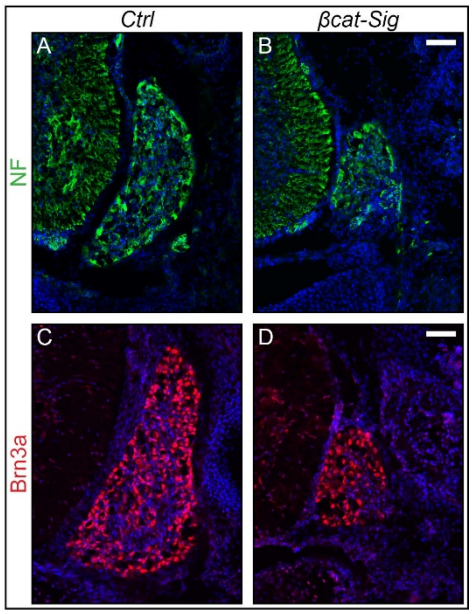

Figure 31 The DRGs of *βcat-Sig* mutants do not recover normal DRG size at later stages

(A-B) Staining for neurofilament (NF) as well as (C-D) Brn3a shows a reduced size of the DRG in βcat-Sig embryos at E16.5. Scale bars: 50 µm.

5.2.4.3. Diverse functions of β-catenin are required for subtype specification of the three waves of sensory neurogenesis

In peripheral sensory lineages, neuronal subtype specification occurs in sequential waves of neurogenesis driven by proneural transcription factors (Marmigère and Ernfors, 2007). The basic helix-loop-helix (bHLH) transcription factor neurogenin 2 (Neurog2) initiates a first wave of neurogenesis and is expressed in an early population of migratory NCCs. It is continuously expressed throughout their migration until they reach the forming DRG, after which it is largely down regulated (Ma et al., 1999; Sommer et al., 1996). Migratory cells expressing Neurog2 at high levels give rise to tyrosine receptor kinase (Trk) B- and TrkC-positive neurons (Ma et al., 1999). A later wave of neurogenesis is formed by Sox10-positive DRG progenitors, of which a subgroup will express the bHLH transcription factor neurogenin 1 (Neurog1) post migration within the coalesced DRG. This Neurog1-mediated wave mainly gives rise to neurons expressing TrkA (Ma et al., 1999), but can partially contribute to the TrkB and TrkC population. Furthermore, both waves of DRG progenitors generate glia. The third and final wave of neurogenesis produce the boundary cap cells (BCCs). BCCs give rise to peripheral glia, which appear in small clusters at the surface of the spinal cord, at prospective motor exit points and dorsal root entry zones. A fraction of cells surrounding the dorsal root entry zone migrate into the formed DRG and generate a small population of TrkA-positive neurons (Maro et al., 2004).

Previous work from our lab also using *Wnt1-Cre*-mediated ablation of β-catenin, demonstrated the requirement of β-catenin for the expression of Neurog2 and Neurog1. However, it was unclear whether the virtual absence of Neurog1 expression in the mutant reflected a role of β-catenin in Wnt signaling or in mediating cadherin-dependent cellular adhesion (Hari et al., 2002). Therefore, we analyzed protein expression of Neurog2 and Neurog1 in recombined

cells expressing β-gal from the *R26R* lineage tracer on transverse sections of our β-catenin mutant models at E9 and E10.5, respectively. A significant loss of Neurog2 expression was shown by immunohistochemistry in both mutant embryos at E9 (Figure 32 B-D, O), indicating that expression of Neurog2 is dependent on TCF/Lef mediated transcription. These results concur with previous findings that specified Neurog2 as a Wnt target (Backman et al., 2005).

Expression of Neurog1 was lost in *βcat-Null R26R* embryos at E10.5, as expected (Hari et al., 2002). Interestingly, however, Neurog1 expression was retained in *βcat-Sig* embryos (Figure 32 G-H, O). Considering that the mutated β-catenin-dm protein (expressed from *Ctnnb1*^{dm}) lacks the ability to attract transcriptional co-activators to TCF/Lef transcription factors (Valenta et al., 2011), the expression of Neurog1 in *βcat-Sig R26R* animals suggests that transcription of Neurog1 is not connected with the function of β-catenin as an activator of TCF/Lef-dependent transcription.

These data were supported by the results of co-stainings for early subtypes of DRG precursors and β-gal in control animals carrying the *BAT-gal* Wnt-reporter. Quantifications revealed that at least 40% of Neurog2- and Sox10-positive cells were positive for β-galactosidase at E9 (Figure 32 J-K, P) and that at E10.5 the percentage of the Sox10-positive population expressing β-gal was still about 30% (Figure 32 N, P). However, less than 15% of the Neurog1-positive cells were also positive for β-galactosidase (Figure 32 M, P). These findings revealed that β-catenin-TCF/Lef transactivation is rather active in the Sox10-positive DRG progenitors and the first sensory precursor wave expressing Neurog2. In contrast, Wnt-induced TCF/Lef-driven transcriptional activation is apparently less prominent during the second wave of sensory neurogenesis characterized by Neurog1 expression.

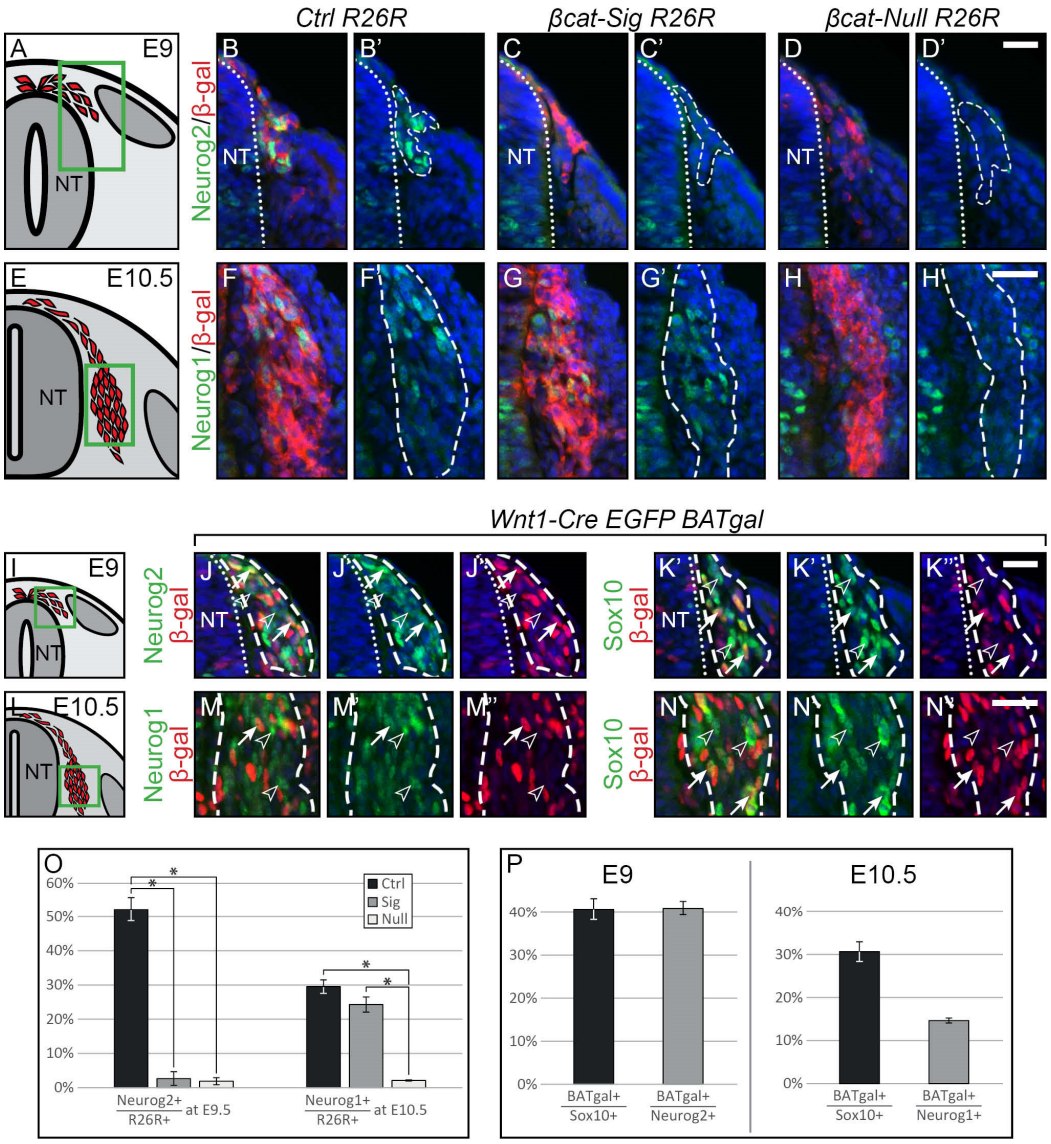

Figure 32 The first two waves of sensory neurogenesis depend on β-catenin

*(A, E, I, L) Illustration of a transverse section at E9 and E10.5, respectively, displaying cells, which contribute to the DRG in red. Green box represents caption area for subfigures B-D, F-H, J-K and M-N, respectively. (B-D, G-H) Double immunohistochemistry for β-gal expressed by the R26R reporter and the sensory neurogenesis transcription factors Neuog2 at E9 or Neurog1 at E10.5, respectively. (B'-D') Migrating DRG progenitors do not express Neurog2 in either of the two mutant types. (F'-H') Whereas βcat-Null R26R animals lose expression of Neurog1 in DRG progenitors, progenitors of βcat-Sig R26R animals maintain expression of Neurog1. (J-K, M-N) Double immunohistochemistry for β-gal expressed by the BAT-gal Wnt-reporter and the sensory neurogenesis transcription factors Neurog2 at E9 or Neurog1 at E10.5 as well as Sox10 at both stages, respectively. Arrows indicate double positive cells, arrowheads indicate BAT-gal-negative cells within the stained subpopulations. (O) Quantification of Neurogenin-positive cells per R26R-positive cells contributing to the DRG at E9 and E10.5 show an almost complete loss of Neurog2 in both mutants at E9 and a significant reduction of Neurog1 in the βcat-Null R26R mutant at E10.5. (P) Percentage of BAT-gal-positive cells in the subpopulations of DRG precursors displays that only small fraction of the Neurog1 population express BAT-gal, in comparison to the other subpopulations. NT, neural tube; Dashed lines frame in vivo fate mapped cells, * indicates $P < 0.05$; Scale bars: 25 µm.*

In addition to early markers of sensory neurogenesis, we also analyzed early subtype specification of the differentiating sensory neurons at E11.5, by staining for TrkA, TrkB, and TrkC, as well as a further tyrosine receptor kinase of sensory neurons RET. The relative contribution of the specific subtypes with the exception of TrkC varied between both mutant embryos to each other and the control (Figure 33 B-H), reflecting subtype specification regulated by both Neurog1 and Neurog2.

The earliest marker for BCCs, representing the third wave of sensory neurogenesis, is the zinc finger transcription factor Krox20 (respectively, EGR2). Triple staining for Krox20, neurofilament and the transcription factors Islet1/2, which mark motor and sensory neurons, showed a loss of dorsal as well as ventral Krox20-expressing BCCs at E12.5 in both β-catenin mutant embryos (Figure 33 J-L). Krox20 has been implied to be a Wnt target (Leclerc et al., 2008). Interestingly, Sox10-positive cells were observed at the dorsal entry zone and the motor exit point of both mutants at E12.5, suggesting that specification of BCCs rather than localization of their precursors was affected in β-catenin mutant embryos (seen later in Figure 38). Furthermore, emigration of motor neurons from the ventral neural tube was apparent in the ventral roots of the mutants (Figure 33 M-O). Such ectopic localization of motor neurons has been attributed to the loss of ventral BCCs or their secretion of constraining signals (Chauvet and Rougon, 2008; Mauti et al., 2007; Vermeren et al., 2003). As stated before, no irregular apoptosis was detected in DRG progenitors including BCCs (data not shown). These data indicated that BCC precursors are present, but that the formation of functional BCCs is dependent on β-catenin as inducer of TCF/Lef transcription.

In summary, the expression of the transcription factors Neurog2 and Krox20 depends on β-catenin as co-transcription factor for TCF/Lef-mediated transcription. In contrast, Neurog1 expression involves a co-transcription-independent function of β-catenin, indicating that sensory neuronal subtypes in the DRG are specified by distinct mechanisms.

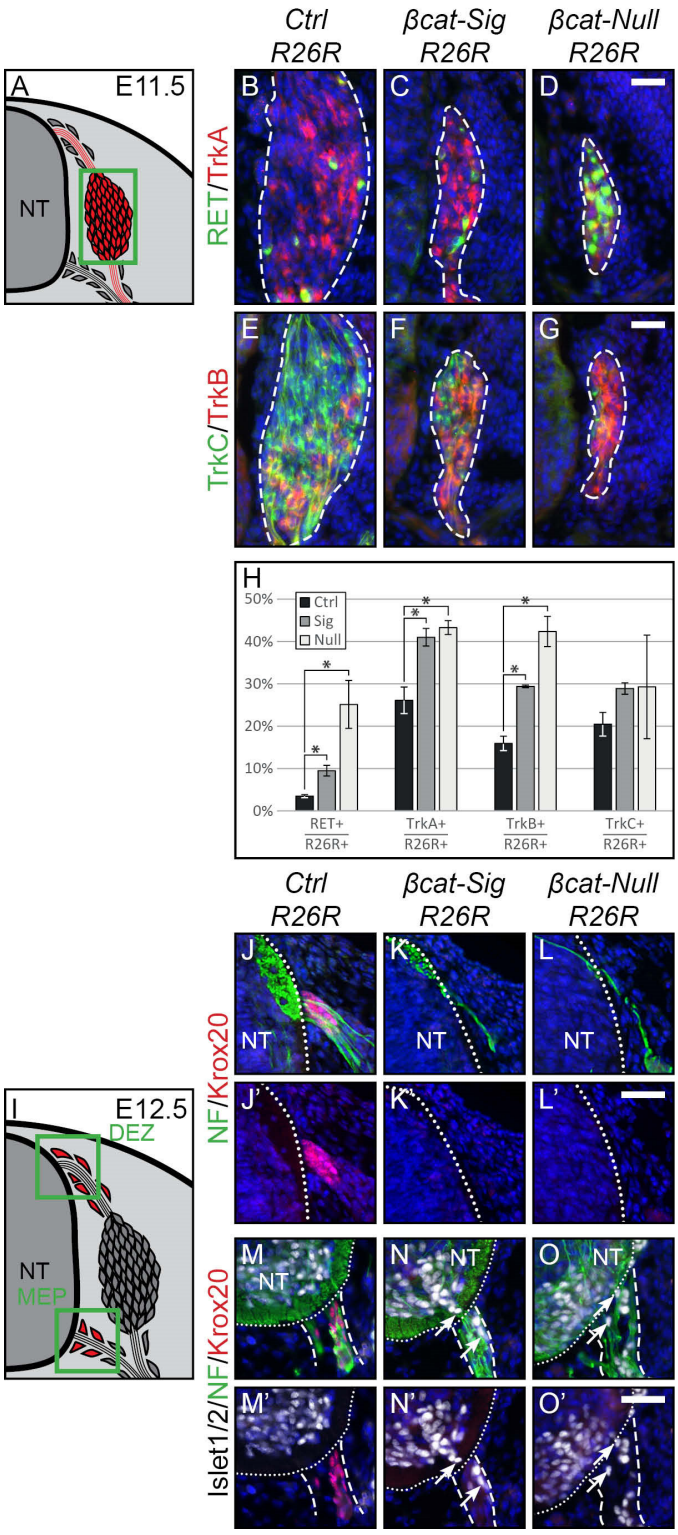

Figure 33 Late subtype specification is altered and boundary cap cell identity is lost in mutant animals

(A) Illustration of a transverse section at E11.5 displaying cells, which contribute to the DRG in red. Green box represents caption area for subfigures B-G. (B-G) Triple immunohistochemistry at E11.5 for β-gal expressed by the R26R reporter and for markers for subtype specification of sensory neurons: tyrosine receptor kinases RET and TrkA, TrkB and TrkC. Dashed lines surround the border of R26R-positive cells contributing to the DRG. (H) Quantifications of late sensory subtypes per DRG displays an altered distribution of sensory neuron subtypes in mutant animals. (I) Illustration of a transverse section at E12.5 displaying boundary cap cells in red. Green box represents caption area for subfigures J-O, respectively. (J-L) Double immunohistochemistry for Krox20 as a marker for differentiated boundary cap cells and neurofilament (NF) at E12.5. (M-O) Triple immunohistochemistry for Krox20, NF and Islet1/2 as a marker for motor neurons at E12.5. (J',M') In control animals, sensory axons invading the dorsal entry zone of the neural tube and motor axons penetrating the prospective motor exit point of the neural tube are surrounded by boundary caps cells. (K',L',N',O') Dorsal as well as ventral Krox20 expression is lost in both mutant animals. Arrows show migrating motor neurons, which are exiting or have already exited the ventral neural tube due to the loss of functional boundary cap cells. NT, neural tube; DEZ, dorsal entry zone; MEP, motor exit point; Scale bars: 25 µm.

5.2.4.4. Development of the dorsal root ganglia is independent of β- and α-catenin-encompassing cadherin adhesion junctions

As shown above, *βcat-Null* animals exhibited more severe phenotypes than *βcat-Sig* mutants, with first phenotypic variations manifested at E10.5 when the developing DRG coalesce laterally of the neural tube. The presence of N-cadherin and α-catenin at E12.5 (**Figure** 34 A-F) suggested that cadherin/β-catenin/α-catenin-mediated adhesion takes place in the DRG. Immunohistochemistry for β-catenin at the same stage confirmed the loss of β-catenin in the *βcat-Null* and only presence of the mutated form of β-catenin in the *βcat-Sig* mutant (**Figure** 34 G-I). Since cadherin-mediated adhesion is preserved in *βcat-Sig* but not *βcat-Null* mutants, the differences between mutant embryos might possibly be a consequence of insufficient adhesion in *βcat-Null* embryos. To test this idea, we also analyzed *Wnt1-Cre Ctnna1*$^{flox/flox}$ (*αcat-Adh*) mice, in which α-catenin is conditionally deleted in NCCs (Lien et al., 2006; Vasioukhin et al., 2001). α-catenin connects the actin-cytoskeleton with β-catenin bound to proteins of the cadherin family. Therefore, removing either α-catenin or β-catenin in the cadherin adhesion complex disrupts the connection of transmembrane-bound cadherins with the cytoskeleton, thus interfering with cell-cell adhesion. Accordingly, in both *βcat-Null* and *αcat-Adh* embryos, the epithelial integrity of the *Wnt1-Cre*-expressing dorsal neural tube was disturbed (Valenta et al., 2011) (Figure 35).

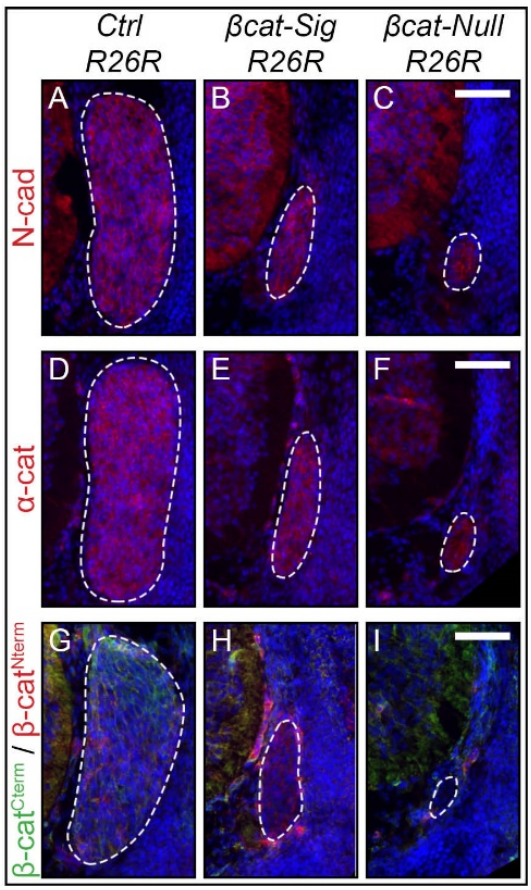

Figure 34 Presence of cadherin-adhesion complex components at E12.5

(A-F) Immunofluorescent staining for N-cadherin (N-cad) or α-catenin (α-cat) reveal no alteration of their expression in either mutant. (G-I) Overlay of channels of staining for the N- and C-terminus of β-catenin. Only a staining (red) for the N-terminus of β-catenin can be detected in DRG progenitors of βcat-Sig embryos, demonstrating that wild type β-catenin has been replaced in these cells by the double mutated form with the truncated C-terminus. Dashed lines frame R26R-lineage traced cells, Scale bars: 50 µm.

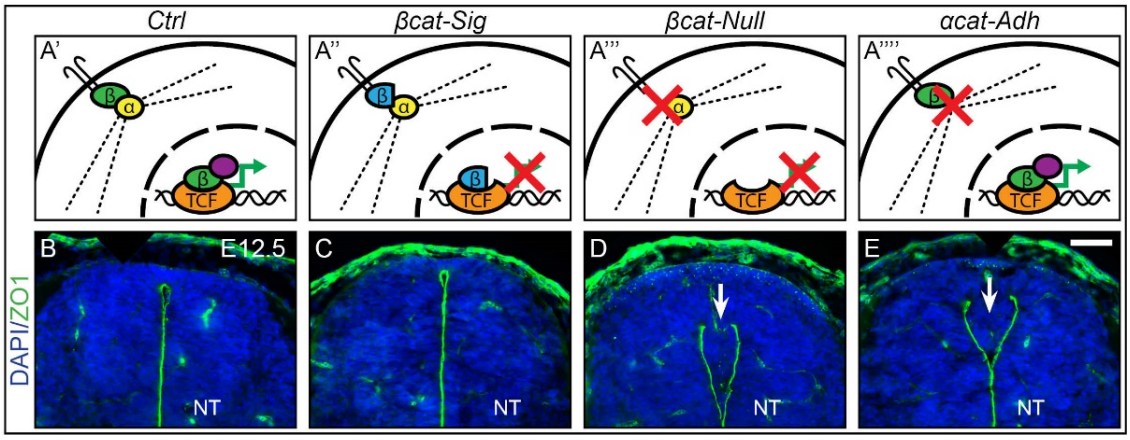

Figure 35 The dorsal neural tube upon loss of β-catenin or α-catenin displays identical loss of cell-cell adhesion

*(A'-A'''') Schematic of Cre-recombined cells and the functional output of the corresponding genotype. (A') β-catenin (green) of control animals induces transcription (green arrow) by binding with TCF/*Lef *(orange) in the nucleus and recruiting co-transcription factors (purple). Furthermore it links transmembrane cadherins via α-catenin (yellow) to the actin cytoskeleton (dotted line). (A'') The mutated β-catenin protein (blue) of βcat-Sig animals inhibits TCF/*Lef*-mediated transcription, but preserves cadherin-mediated adhesion. (A''') Cells of βcat-Null animals lose both TCF/*Lef*-mediated transcription and cadherin-mediated adhesion, as β-catenin is completely absent. (A'''') The loss of α-catenin in αcat-Adh animals prevents binding of cadherin to the actin cytoskeleton. (B-E) Staining for ZO1 a marker for tight junctions on transverse sections of E12.5 embryos shows that a complete loss of β-catenin or α-catenin causes a disruption of the epithelial integrity of the dorsal neural tube and leads to cells entering the neural tube lumen (arrows, D,E). In contrast, epithelial integrity is preserved in βcat-Sig animals (C). Scale bar: 100 µm.*

Intriguingly, unlike in *βcat-Null R26R* embryos at E10.5, DRG progenitors of *αcat-Adh R26R* embryos maintained expression of Neurog1 (Figure 36 D, H). Thus expression of Neurog1, indicative for the second wave of sensory neurogenesis, is not dependent on adhesion alone. Moreover, there is a possibility that initiation but not maintenance of Neurog1 expression could depend on multiple inputs such as TCF/Lef transcription as well as down-stream factors of stabilized adhesion in the coalescing DRG. To exclude this possibility, we generated *Wnt1-Cre Ctnna1*$^{flox/flox}$ *Ctnnb1*$^{flox/dm}$ (*αcat-Adh βcat-Sig*) double mutant embryos, which mimics *βcat-Null* embryos in respect to loss of adhesion and TCF/Lef transcription. If expression of Neurgo1 depends on additive effects of these two functions, *αcat-Adh βcat-Sig* double mutants should display the same phenotype as the *βcat-Null*. However, transverse sections through DRG of E10.5 *αcat-Adh βcat-Sig R26R* embryos revealed expression of Neurog1 comparable to control animals (Figure 36 C-E, H). Likewise, cell cycle progression as assessed by incorporation of EdU in Sox10-positive cells at E10.5 was normal in *αcat-Adh R26R* mutants (Figure 36 F-G, I). Furthermore, DRG size was not affected in *αcat-Adh R26R* embryos at E12.5, unlike in *βcat-Sig* mice (data not shown).

These data suggest that the DRG does not depend on the cadherin adhesion complex for proper formation. To further assess this assumption, we stained control animals at E9, E10.5, and E11.5 for tight junctions and desmosomes, other mediators of cell adhesion. Tight junctions were undetectable in DRG progenitors, as no expression for ZO1 was found (data not shown). In contrast, the expression of the essential desmosome component junction plakoglobin (JUP) was absent in migrating NCCs at E9, but became evident from E10.5 onwards and was readily detectable in DRG progenitors by E11.5 (Figure 36 K). However, neither proximal membrane localization nor protein presence of JUP was altered in *βcat-Sig R26R* or *βcat-Null R26R* embryos at E11.5 (Figure 36 L-M). Thus, loss of β-catenin has no effect on development or sustainability of cell-cell adhesion in DRG progenitors, possibly because adhesion in the developing DRG is sufficiently sustained by β- and α-catenin-independent desmosomes, rather than by cadherin/β-catenin/α-catenin-mediated adherens junctions.

In sum, our data indicate that all deviations of phenotypes of DRG development between *βcat-Null* and *βcat-Sig* mutants are not a result of intact cadherin-mediated adhesion in the *βcat-Sig* animals. Rather, Neurog1 expression as well as proliferation of postmigratory Sox10-positive progenitors in developing DRG require a function of β-catenin independent of its role in attracting transcriptional co-activators to activate TCF/Lef transcription or to sustain cadherin-based adhesion.

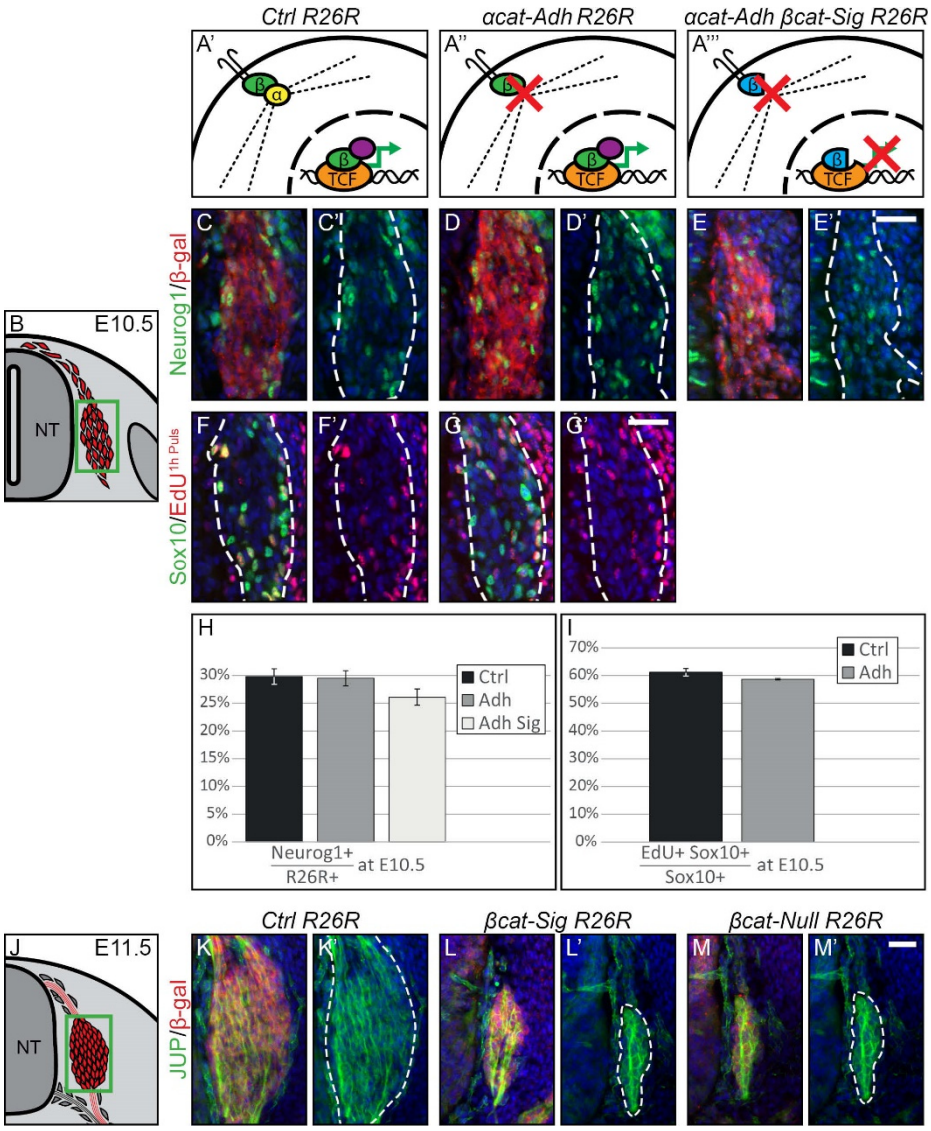

Figure 36 Development of the dorsal root ganglia does not depend on structural function of cadherin-mediated adherens junctions

*(A'-A''') Scheme representing functional properties of Cre-recombined cells in control and αcat-Adh and αcat-Adh βcat-Sig mutant animals. (A') β-catenin (green) of control animals induces transcription (green arrow) by binding with TCF/*Lef *(orange) and recruiting co-transcription factors (purple). Furthermore, it links transmembrane cadherins via α-catenin (yellow) to the actin cytoskeleton (dotted line). (A'') The loss of α-catenin in αcat-Adh animals prevents binding of cadherin to the actin cytoskeleton. (A''') In αcat-Adh βcat-Sig animals, the mutated β-catenin protein inhibits TCF/*Lef*-mediated transcription. Furthermore, the loss of α-catenin leads to an absence of cadherin-mediated adhesion. (B) Illustration of a transverse section at E10.5 displaying DRG progenitor cells in red. Green box represents caption area for subfigures C-G. (C-E) Double immunohistochemistry for Neurog1 and β-gal expressed by the R26R reporter. (C'-E') Expression of Neurog1 is maintained in both αcat-adh R26R and αcat-Adh βcat-Sig R26R animals. (F-G) Immunofluorescent staining for Sox10 and detection of a one hour EdU pulse. Dashed lines frame in vivo fate-mapped cells. (F'-G') EdU incorporation of Sox10-positive DRG progenitor cells is preserved in αcat-adh R26R embryos. (H) Quantification of Neurog1-positive cells per R26R-positive cells at E10.5 show no significant differences between control, αcat-Adh R26R, and αcat-Adh βcat-Sig R26R mutants. (I) Percentages of EdU-positive cells in the Sox10-positive population display no significant reduction of EdU incorporation in αcat-Adh R26R animals at E10.5. (J) Illustration of a transverse section at E11.5 displaying DRG in red. Green box represents caption area for subfigures K-M. (K-M) Double immunohistochemistry for β-gal expressed from the R26R reporter and junction plakoglobin (JUP), a linking protein in the desmosome adhesion complex, shows the same expression density of JUP in β-catenin mutant animals as in control animals. NT, neural tube; Scale bars: 25 μm.*

*5.2.4.5. Expression of TCF/*Lef *transcription factors during DRG development*

Previously, it has been shown that TCF family factors, such as TCF3 and TCF4, can also function as repressors, independent from Wnt-induced transcriptional activation (Archbold et al., 2012; Chodaparambil et al., 2014; Lien et al., 2014; Nguyen et al., 2009; Shy et al., 2013; Wray et al., 2011; Wu et al., 2009; Yi et al., 2011). In this case, target genes are de-repressed by binding of β-catenin to the repressing TCFs, followed by release of the complex from the DNA binding sites. It is conceivable that β-catenin expressed from the *Ctnnb1*^{dm} allele preserves this function, in addition to rescuing cadherin-mediated adhesion. To address whether expression of TCFs during DRG development is compatible with a role of β-catenin in de-repression, we first stained embryonic sections for TCF3 at stages E9, E10 and E11.5 in control embryos. TCF3 expression was present in virtually all migratory NCCs at the early stage of E9. Subsequently, however, TCF3 expression decreased, and only about 50% of all DRG cells expressed TCF3 at E10 and E11.5 (Figure 37 D-F, M). De-repression upon binding of β-catenin leads to partial TCF3 degradation, which is particularly evident in quantitative assays not applicable to β-catenin-mutant DRG (Shy et al., 2013). Using immunohistochemistry, TCF3 expression levels appeared to be generally low in the forming DRG and not altered in β-catenin-mutant embryos as compared to the control (Figure 37G-L, M).

At E10 and E11.5 triple immunohistochemistry for Sox10, TCF4, and Lef1 revealed that TCF4 and Lef1 were consistently expressed within the Sox10 population of the forming DRG in control animals (Figure 37 N, Q). De-repression mediated by TCF4 has not been shown to lead to its degradation. Accordingly, expression of TCF4 in Sox10-positive cells did not change in either mutant at any stage (Figure 37 N’’’-S’’’, T). In contrast, the percentage of Lef1-positive cells was decreased by more than 40% at E10 and was below 10% at E11.5 in both mutants (Figure 37 N’’-S’’, U). These data are in agreement with the known regulation of Lef1 by a positive feedback loop of Wnt signaling (Filali et al., 2002; Hovanes et al., 2001). Interestingly, as of E12.5, Lef1 was no longer expressed in DRG cells of wild type animals with the exception of the BCCs, which were, however, devoid of Lef1 expression in *βcat-Sig* and *βcat-Null* embryos (Figure 38).

In sum, the decrease of Lef1 expression from E10 to E11.5 in both mutants indicated that TCF/Lef transactivation is not essential for the induction of Lef1 expression, but necessary for its maintenance. Interestingly, Lef1 expression diminished in the DRG as of E12.5 in control animals, consistent with our finding that proliferation of DRG cells at later developmental stages is apparently not controlled by Wnt/β-catenin-induced transcriptional activation (Figure 30). Importantly, however, the expression of TCF3 and, in particular, TCF4 is compatible with an implication of β-catenin-dm in de-repression of TCF target genes.

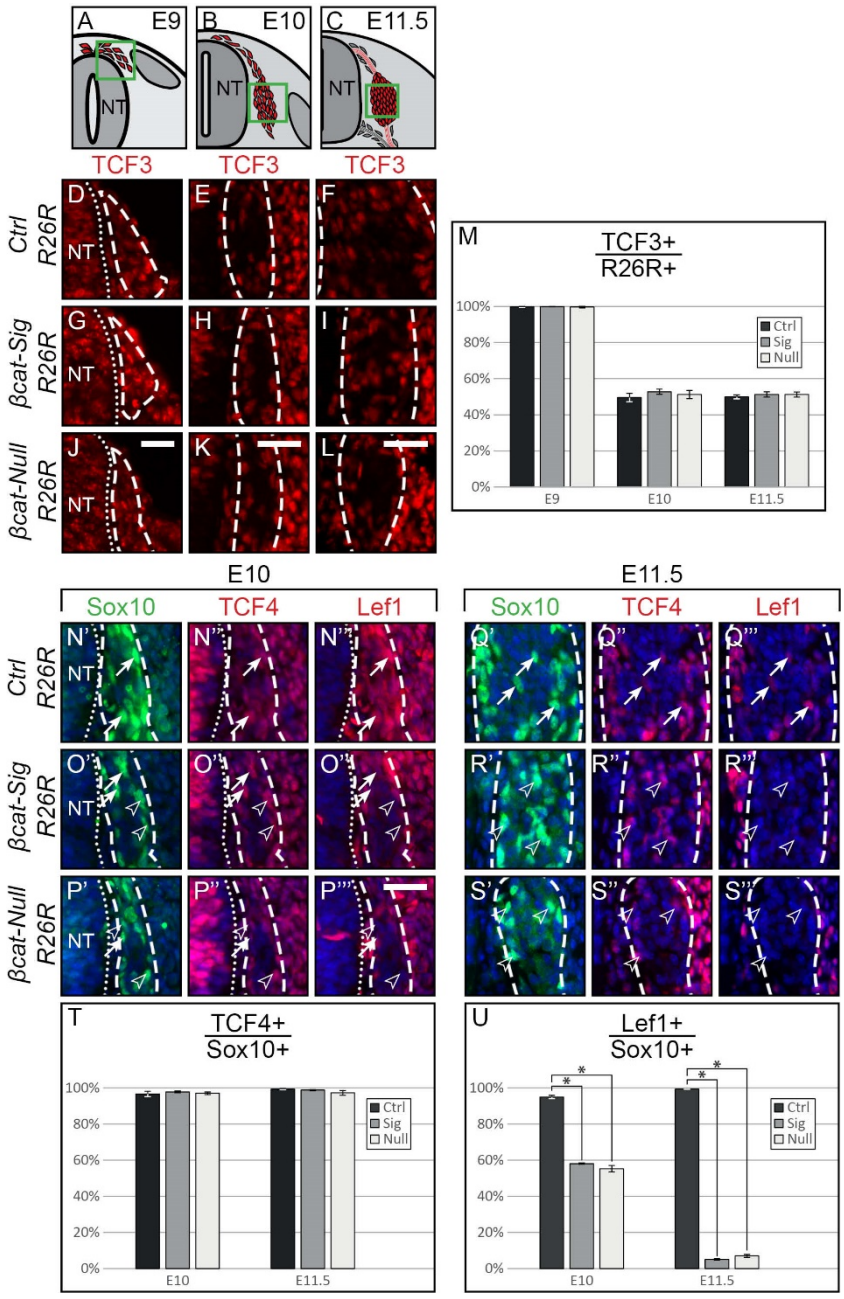

Figure 37 Expression of TCF3, TCF4, and Lef**1 in the developing DRG**

(A-C) Illustration of a transverse section at E9, E10 and E11.5, respectively, displaying cells, which contribute to the DRG in red. Green box represents caption area for subfigures D-L, and N-S respectively. (D-L) Immunohistochemistry for TCF3 shows decreased TCF3 expression in control and mutant animals at E10 and E11.5 as compared to the situation at E9, as verified by quantification (M). Dashed lines frame in vivo fate-mapped cells. (N-S) Triple immunohistochemistry for Sox10, TCF4 and Lef*1. (T) Quantification of TCF4 presence in Sox10-postive cells shows continuous expression in DRG cells and no difference between any of the three animals at both E10 and E11.5. (U) Quantification of Sox10- and* Lef*1-double positive cells shows reduced numbers in both mutants at E10 and a complete loss at E11.5. Dashed lines frame the outer border of cells which express Sox10 and thus roughly encompass the DRG area. Arrows point to cells expressing Sox10, TCF4 and* Lef*1. Arrow heads point to Sox10- and TCF4-positive,* Lef*1-negative cells. NT, neural tube; Scale bars: 25 µm.*

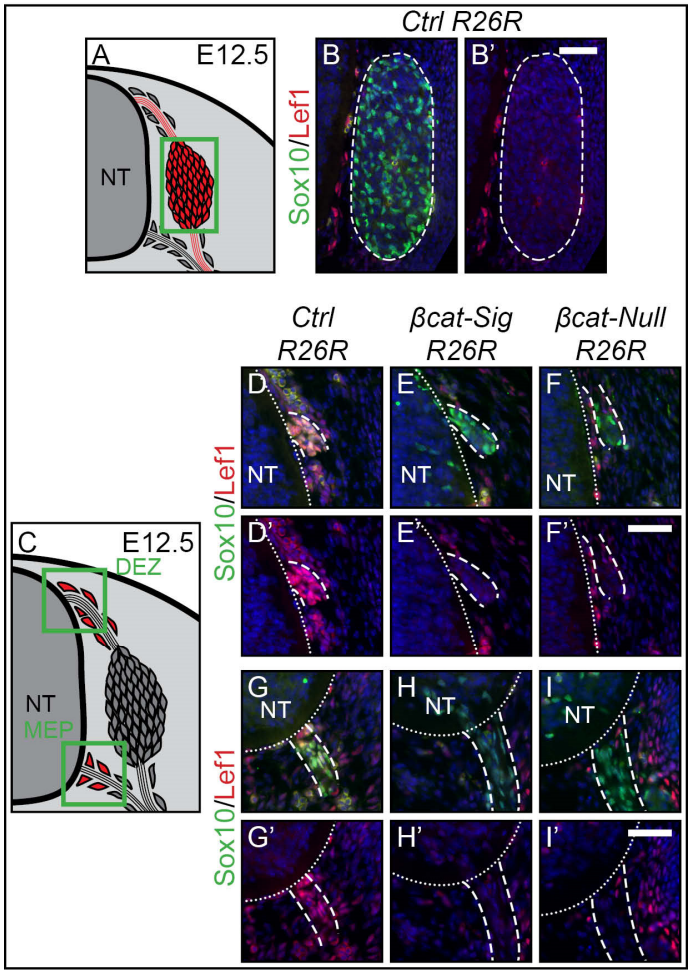

Figure 38 The absence of Lef1 expression at E12.5 in wild type DRGs and the loss of Lef1 expression in BCCs of mutant animals

(A) Illustration of a transverse section at E12.5 displaying cells of the DRG in red. Green box represents caption area for subfigure B. (B) Double-staining for Sox10 and Lef1 shows a loss of Lef1 expression in the entire DRG. Dashed lines frame lineage-traced cells. (C) Illustration of a transverse section at E12.5 displaying boundary cap cells in red. Green box represents caption area for subfigures D-I, respectively. (D-I) Double immunohistochemistry for Sox10 as a marker for boundary cap cell precursors and Lef1 at E12.5. (D'-I') In control animals, Sox10-positive cells in the vicinity of the dorsal entry zone and the motor exit point express Lef1. However, in both mutant animals, the same cell populations have lost Lef1 expression. (K',L',N',O'). Dashed lines border nerve bundles of the dorsal entry zone and the motor exit point, respectively. NT, neural tube; DEZ, dorsal entry zone; MEP, motor exit point; Scale bars: 25 µm.

5.2.4.6. The sensory lineage of neural crest cells depend on secreted Wnt of non-neural crest origin

The availability of the multipass transmembrane protein Wntless (Wls, respectively Gpr177) is vital for the secretion of all Wnt proteins (Bartscherer et al., 2006; Herr et al., 2012; Port and Basler, 2010), even though expression of Wnt proteins is controlled by various mechanisms depending on the developing tissue. Interestingly, however, immunohistochemistry for Wls displayed no expression in DRG progenitors at E10.5 or E12.5, but rather in the surrounding mesenchyme and the neural tube (Figure 40 B, D). DRG progenitors where visualized by co-staining for β-gal expressed from the *R26R* reporter allele recombined by *Wnt1-Cre*. To further assess that Wnt proteins necessary for sensory neurogenesis are not secreted by the DRG progenitors themselves, we utilized a mouse model, in which Wls was conditionally deleted (*Wls^{flox}*) (Figure 39) using *Wnt1-Cre*. Efficient deletion of Wls was determined by immunohistochemistry in *Wnt1-Cre*-recombined tissues, which express Wls, such as the roof plate (Figure 40 J, K). Interestingly, no phenotype could be observed in early DRG progenitors,

and the DRG of E12.5 mutant embryos were of normal size (data not shown). Surprisingly, however, identical to the phenotype observed in our β-catenin mutants, differentiated dorsal BCCs were missing upon ablation of Wls with *Wnt1-Cre*, as assessed by Krox20 staining (Figure 40 F-G). One possible explanation for this phenotype is that Wnts necessary for dorsal BCC formation are secreted from the dorsal neural tube, which is in close vicinity to BCCs and also recombined in the *Wnt1-Cre* mouse line. Indeed, confocal images of a double staining for Wls and β-gal showed that in *Wnt1-Cre R26R* control animals, Wls was expressed at the site of the dorsal entry point of sensory neurons in the dorsal neural tube (Figure 40 J'-J''). *Wnt1-Cre Wls$^{flox/flox}$* animals displayed a loss of Wls expression at the dorsal entry point (Figure 40 K'-K''). To address the implication of neural tube-derived Wnt in BCC formation, we used a *Sox10-Cre* mouse line that confers Cre-mediated recombination in NCCs only after their emigration from the neural tube (Hari et al., 2012; Matsuoka et al., 2005). Use of this mouse line allowed the preservation of Wls expression in the dorsal neural tube and thus its capacity to secret Wnt, despite conditional deletion of Wls in NCCs (Figure 40 L-M). Of note, Krox20 expression was rescued using the *Sox10-Cre Wls$^{flox/flox}$* mouse model in comparison with the *Wnt1-Cre Wls$^{flox/flox}$* model (Figure 40 H).

Taken together, our data and previous reports (Hari et al., 2002; Hari et al., 2012; Kléber et al., 2005; Lee et al., 2004; Rogers et al., 2012; Schmidt and Patel, 2005; Stuhlmiller and García-Castro, 2012) indicate that autocrine Wnt secretion is necessary in a short-time window for NCC delamination to occur. After delamination, however, the Wnt necessary for proper DRG development is not secreted by the DRG progenitors themselves. In particular, the development of dorsal BCCs depends on Wnt secreted from the dorsal neural tube.

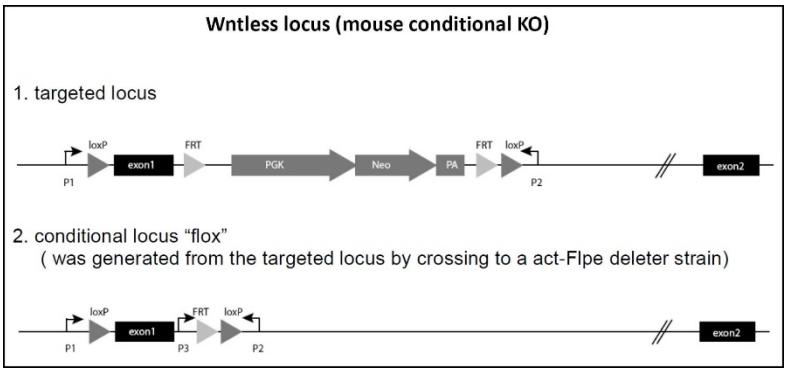

Figure 39 Generation of *Wls^{flox}* allele

For the generation of Wls^{flox} animals, the targeting vector was generated by assembling the 5' and 3' homology arms with the first exon flanked by loxP sites and the neomycin selection cassette flanked by FRT sites. Deletion of the FRT-flanked neomycin resistance cassette was verified by PCR and subsequent sequencing of positive Bl6 ES cell clones.

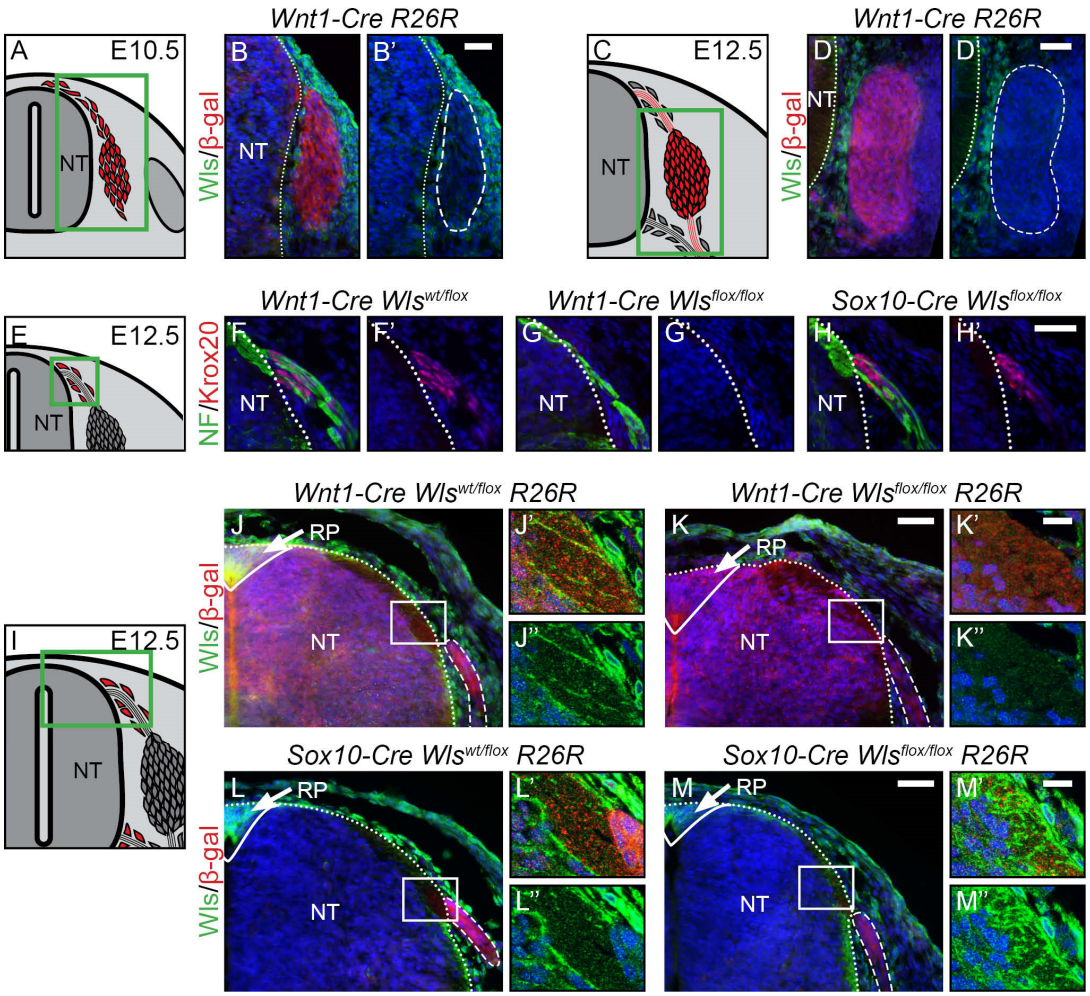

Figure 40 Development of boundary cap cells depends on neural tube-derived Wnt

(A, C) Illustration of a transverse section at E10.5 (A) and E12.5 (C) displaying cells contributing to the DRG in red. Green box represents caption area for subfigures B and D. respectively. (B, D) Double immunohistochemistry for Wls and β-gal expressed in Wnt1-Cre R26R mice at E10.5 and E12.5 shows that mesenchymal tissue and not cells populating the DRG express Wls. Dashed lines frame lineage-traced cells. (E, I) Illustration of a transverse section at E12.5 displaying BCCs in red. Green box represents caption area for subfigures F-H and J-M, respectively. (F-H) Double immunohistochemistry for Krox20 and neurofilament (NF) at E12.5. (G') Dorsal BCCs are lost upon conditional knock-out of Wls using Wnt1-Cre, which recombines the dorsal neural tube and derivatives of NCCs. (H') However, BCCs are rescued in conditional knockout of Wls using Sox10-Cre, which recombines NCCs only after their emigration and not the dorsal neural tube. (J-M) Double immunohistochemistry for Wls and β-gal expressed by the Cre reporter line R26R. J'-M' and J''-M'' are higher magnifications of the boxed areas in J-M, respectively. Dashed lines frame sensory axons. (J-J'', L-L'') Wls is expressed at the site where sensory axons enter the dorsal neural tube at the dorsal entry zone. Wls is also strongly expressed in the roofplate (arrow, J, L) of control animals carrying the respective Cre and one allele of Wlsflox. (K-K'') Expression of Wls is lost in dorsal neural tube upon conditional knock-out of Wls using Wnt1-Cre, as evident in the roofplate (arrow, K) and the dorsal entry zone (K',K''). (M-M'') Conditional ablation of Wls using Sox10-Cre does not affect expression of Wls in the dorsal neural tube in neither the roofplate (arrow, M) nor the dorsal entry zone (M',M''). NT, neural tube; Dotted line show NT border; RP, roofplate; Scale bars: 25 µm; 10µm in magnifications J'-M'.

5.2.5. Discussion

β-catenin is a multifaceted regulatory protein that apart from mediating β-catenin-dependent cellular adhesion elicits various transcriptional responses in a context-specific manner (Valenta et al., 2012). These signaling responses often involve activation of TCF/Lef transcription factors, but can also be independent of TCF/Lef activation. In the present study, we use sensory neurogenesis and ganglia formation as a model system to demonstrate how distinct facets of β-catenin function control cell proliferation and fate specification in a cell type- and stage-specific manner. Unexpectedly, the adhesion function of β-catenin is dispensable for sensory neurogenesis and the formation of DRG, as revealed by the comparison of conditional *βcat-Null*, *βcat-Sig*, and *αcat-Adh* embryos. β-catenin signaling, on the other hand, is essential for proper DRG development. However, β-catenin exploits both TCF activation-dependent and -independent signaling to regulate proliferation at different developmental stages as well as distinct cell fates associated with consecutive waves of sensory neurogenesis.

5.2.5.1. Sensory ganglia formation does not require β-catenin/α-catenin-mediated cellular adhesion

Cadherin adherens junctions associate transmembrane cadherin proteins with the actin cytoskeleton via a β-catenin - α-catenin complex. Cellular adhesion mediated by this process might conceivably be important for DRG formation, because DRG size and cellular composition were severely affected in conditional *βcat-Null* but much less so in *βcat-Sig* mutant animals. In the dorsal neural tube used as a control tissue, the deletion of either β-catenin or α-catenin resulted in loss of cell-cell adhesion and, thus, in the disruption of the epithelial integrity. In contrast, deletion of α-catenin did not affect DRG formation or growth, unlike loss of β-catenin in *βcat-Null* embryos. Crossing *αcat-Adh* with *βcat-Sig* animals also did not produce the phenotype of *βcat-Null* mutant DRG, excluding any compensatory mechanisms between TCF/Lef transcription and down-stream factors of stabilized adhesion. Additionally, we showed that DRG cells and their projecting axons commence to express plakoglobin as the DRG coalesces and maintain this expression with further development. Taken together, these findings substantiate that cadherin adhesion junctions are negligible for sensory neurogenesis and that cell-cell adhesion in the developing DRG might be mediated via desmosomes. Moreover, the differences in DRG formation observed in *βcat-Sig* vs. *βcat-Null* embryos can apparently not be attributed to an adhesion phenotype. This in turn suggests, that the mutated form of β-catenin in *βcat-Sig* mice not only maintains the ability to preserve cadherin-mediated adhesion, but also rescues a function of β-catenin independent of its function as an activator of TCF/Lef transcription.

5.2.5.2. Different functions of β-catenin regulate stage-specific proliferation of dorsal root ganglia progenitor cells

NCCs at different stages of development are subject to distinct mechanisms of proliferation control (Fuchs et al., 2009). This most probably reflects the changing environment NCCs encounter in the tissue they migrate through and the niches they reside in post-migration. At early stages of migration, NCC proliferation was neither affected in *βcat-Sig* nor in *βcat-Null* embryos, consistent with earlier reports that canonical Wnt signaling does not regulate proliferation of early NCCs (Hari et al., 2002; Lee et al., 2004). However, at E10.5, post-migratory DRG progenitors of *βcat-Sig* and *βcat-Null* mutant embryos failed to incorporate EdU after a one hour pulse even though they expressed KI67. These results indicate that DRG progenitors in both mutant animals are stuck in cell cycle, most probably in G1 phase. Wnt signaling has been shown to regulate cell proliferation by promoting G1 progression (Niehrs and Acebron, 2012). Moreover, we found Lef1 to be expressed at E10 and E11.5 within the Sox10 population of control animals, while its expression was lost at E12.5 within the DRG. Furthermore, reduction of Lef1 in both *βcat-Sig* and *βcat-Null* mutants was observed at E10 and E11.5. Therefore, at a stage during development when NCCs coalesce to form DRG, cell cycle progression of DRG progenitors is controlled by Wnt/β-catenin-dependent transcriptional activation, possibly mediated by Lef1 (Figure 41, green arrow). Intriguingly, at somewhat later stages of DRG development (E11.5 onwards), the DRG progenitors of the *βcat-Sig* mutants recovered their capacity to progress through the cell cycle, whereas the *βcat-Null* mutant cells were still incapable to do so. Thus, the mutant form of β-catenin expressed in *βcat-Sig* animals is apparently able to rescue DRG progenitor proliferation at later developmental stages.

As described above, the differences in the phenotype between *βcat-Sig* and *βcat-Null* mutant DRG are not due to changes in cadherin-mediated adhesion. We propose, therefore, that an alternative, adhesion- and TCF/Lef-transactivator-independent function of β-catenin regulates one or multiple factors responsible for the induction of a second wave of proliferation in DRG (Figure 41 A, red arrow). The expression of the known repressors TCF3 and, in particular, TCF4 (Archbold et al., 2012; Chodaparambil et al., 2014; Lien et al., 2014; Nguyen et al., 2009; Shy et al., 2013; Wray et al., 2011; Wu et al., 2009; Yi et al., 2011) in the developing DRG allows us to speculate, that this function likely involves the ability of β-catenin to de-repress TCF-bound target genes. In summary, NCC proliferation during migration and in specific NC target structures appears to be dynamically controlled by stage- and location-specific mechanisms that involve β-catenin-independent factors (Fuchs et al., 2009) as well as diverse β-catenin-dependent signaling pathways.

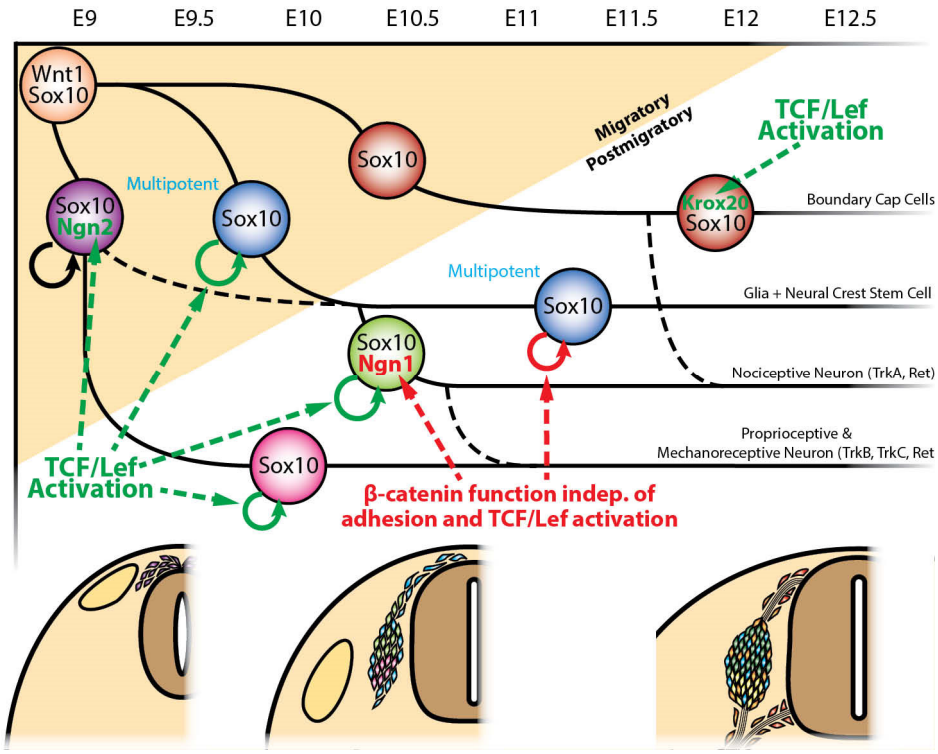

Figure 41 Development of the dorsal root ganglia depends on varying functions of β-catenin during sensory neurogenesis

*Simplified scheme illustrating the genetic cascades that control sensory neurogenesis (Marmigère and Ernfors, 2007) and their dependency on functions of β-catenin. The expression of Neurog2 specific for the first wave of neurogenesis and expression of Krox20 specific for the third wave depends on β-catenin to induce TCF/*Lef*-mediated transcription (green dashed line arrows). Furthermore, proliferation for late migratory and early postmigratory cells depends on one or more downstream factors of TCF/*Lef *transactivation (green dashed line arrows). Expression of Neurog1 as well as proliferation of postmigratory cells from E11 onwards depend on a function of β-catenin independent of its role to induce TCF/*Lef *transcription or to constitute cadherin-mediated cell-cell adhesion.*

5.2.5.3. Specification of the three waves of sensory neurogenesis depend on distinct β-catenin signaling functions

Subtype specification of sensory neurons is driven by proneural transcription factors, which regulate the three sequential waves of neurogenesis. The first wave is initiated in mice at around E9 and consists of migratory Sox10- and Neurog2-double positive cells fated to become mechano- or proprioceptive neurons expressing TrkB, TrkC and RET (Marmigère and Ernfors, 2007). However, lineage tracing revealed that some Neurog2-positive cells also give rise to TrkA-expressing neurons (Zirlinger et al., 2002). The second wave of neurogenesis is characterized by the continuous expression of Sox10 throughout migration and thereafter in the coalescing DRG. These multipotent DRG progenitors divide at a very high rate (Montelius et al., 2007) and then either give rise to a subpopulation of sensory neurons or glial cells, or remain DRG progenitors. The subgroup designated to become sensory neurons express Neurog1 post-migration and bias cells to become nociceptive neurons expressing TrkA and

Ret, but they can also give rise to mechano- and proprioceptive neurons (Ma et al., 1999). The third and final wave of sensory neurogenesis refers to the generation of BCCs. These cells express Krox20 and produce peripheral glia along the sensory axons entering the dorsal entry zone and motor axons exiting the ventral neural tube at prospective motor exit points (Maro et al., 2004). However, a subgroup of these cells loses their Krox20 expression, migrate into the developing DRG and give rise to nociceptive neurons (Maro et al., 2004).

In both *βcat-Sig* and *βcat-Null* animals, expression of Neurog2 and Krox20 was absent, indicating that these transcription factors are regulated by TCF/Lef-mediated transcription (Figure 41, green arrows). In the case of Krox20, which has been proposed to be a TCF/Lef transcriptional target (Leclerc et al., 2008), the responsible transcription factor likely is Lef1, which is strongly expressed within the BCCs. In contrast, Neurog1 was lost in *βcat-Null* mutants, but was still expressed in *βcat-Sig* animals. The expression of Neurog1 was not dependent on the capacity of the *βcat-Sig* mutant to preserve cadherin-mediated adhesion, as expression of Neurog1 was neither lost in *αcat-Adh* nor in *αcat-Adh βcat-Sig* embryos. Promoter binding studies performed in CNS progenitor cells have previously indicated that β-catenin can regulate Neurog1 gene expression (Hirabayashi et al., 2004; Israsena et al., 2004). Thus, given the normal expression of Neurog1 in *βcat-Sig* DRG, a function of β-catenin independent of its role in adhesion and TCF/Lef-induced transcriptional activation is responsible for Neurog1 expression. In support of this, *BAT-gal* reporter activity was low in Neurog1-expressing cells, in contrast to Neurog2-positive cells. Although this remains to be proven, Neurog1 is likely a target gene of TCF3/4-mediated repression released upon binding of β-catenin.

Collectively, these findings indicate that the proneural transcription factors specific for each of the three waves of sensory neurogenesis depend on β-catenin independent of its role in the cadherin adhesion complex. Importantly, the expression of Neurog2 and Krox20 are dependent on the ability of β-catenin to attract transcriptional co-activators to initiate TCF/Lef transcription, whereas Neurog1 expression does not require β-catenin to function as a TCF-transactivator (Figure 41, red arrows).

Our data show that both stage-specific proliferation as well as progressive fate determination in DRG involve β-catenin functions. The successive waves of sensory neurogenesis could be regulated by spatiotemporal Wnt ligand expression in the DRG itself or by changing Wnt expression in the tissues adjacent to the growing DRG. In agreement with previous studies (Carpenter et al., 2010; Fu et al., 2011), *Wnt1-Cre*-mediated conditional deletion of *Wls* – which prevents secretion of any Wnts in NCCs and their derivatives – did not result in overt DRG malformation. Previous work has shown that non-conditional double knock-out of Wnt1 and Wnt3a, the mayor known Wnts expressed in the dorsal neural tube and premigratory NCCs,

leads to major deficiencies in NCC derivatives, including the DRG (Ikeya et al., 1997; Muroyama et al., 2002). The *Wnt1-Cre Wls*$^{flox/flox}$ might not mimic this phenotype, because deletion of *Wls* occurs only after activation of the *Wnt1*-promotor. Our findings show that DRG progenitors are not subject to autocrine Wnt signaling after delamination. Rather, they depend on Wnt secretion from the surrounding tissue. In particular, BCCs emerge in close proximity to the neural tube, which is known to express various Wnt ligands (Agalliu et al., 2009). Indeed, a thorough comparison between *Wnt1-Cre Wls*$^{flox/flox}$ embryos (in which secretion of Wnts is lost in the dorsal neural tube and in NCCs) and *Sox10-Cre Wls*$^{flox/flox}$ animals (in which secretion of Wnts is exclusively depleted from NCCs; (Hari et al., 2012)), revealed that Wnts derived from the neural tube promote the generation of BCCs, while Neurog2- and Neurog1-dependent sensory lineages require other Wnt sources, most likely provided by the mesenchyme adjacent to NCCs and the forming DRG. Thus, the different subpopulations of sensory progenitors not only depend on different β-catenin functions but also on distinct sources of Wnt ligands.

5.2.6. Conclusions

5.2.6.1. Adhesion and signaling independent function of β-catenin during DRG development

Although canonical Wnt signaling has previously been implicated in neural crest development and, in particular, sensory neurogenesis (Hari et al., 2002; Ikeya et al., 1997; Kléber et al., 2005; Lee et al., 2004), the dual function of β-catenin in mediating cell-cell adhesion and Wnt signaling made it difficult to study the actual contribution of this signaling pathway to peripheral ganglia formation and cell type specification. Therefore, we designed an animal model, which allowed us to dissect adhesion and signaling roles of β-catenin in vivo (Valenta et al., 2011). To definitely attribute phenotypic changes to defective adhesion, we also performed an analysis of *β-catenin*-deficient DRG. Surprisingly, however, our study reveals that several processes underlying DRG formation do neither depend on a structural role of β-catenin in adherens junctions nor solely to attract transcriptional co-activators for initiating TCF/Lef mediated transcription. Recently it has been shown that some TCFs also act as repressors for other modes of transcription (Archbold et al., 2012; Lien et al., 2014; Nguyen et al., 2009; Shy et al., 2013; Wray et al., 2011; Wu et al., 2012; Yi et al., 2011). The binding of β-catenin to these TCFs displaces the co-repressors and de-represses the TCF-target genes, allowing transcription by other transcription complexes. Although for technical reasons we were unable to address this hypothesis directly, it is conceivable that the mutated form of β-catenin present in *βcat-Sig* embryos is capable to maintain the capacity to de-repress the TCF/Lef Groucho repression complexes, as its TCF/Lef-binding domain is preserved. This theory is supported by the fact that Neurog1 is expressed in the DRG progenitors of *βcat-Sig* animals, even though consensus sequences for TCF binding are located close to the transcription start site of the mouse Neurog1 gene (Hirabayashi et al., 2004) and β-catenin is directly involved in regulation of Neurog1 (Israsena et al., 2004). In any case, our findings demonstrate that the double mutated form of β-catenin in cells of *βcat-Sig* mice, although defective in TCF/Lef activation, preserves a specific signaling function of β-catenin, next to its ability to maintain proper formation of the cadherin adhesion complex. This made it possible to reveal that distinct β-catenin signaling functions regulate DRG size and cellular composition in a spatiotemporal manner. The interaction partners and targets mediating these stage-specific functions remain to be identified.

5.2.7. Methods

5.2.7.1. Animals and genotyping

Mouse experiments were performed in accordance with Swiss guidelines and approved by the Veterinarian Office of the Kanton of Zürich, Switzerland. The Cre-loxP system was used to conditionally knockout various genes. The generation of mutant mice has been reported previously: *Wnt1-Cre* mice (Danielian et al., 1998), *Sox10-Cre* mice (Matsuoka et al., 2005), *Ctnnb1*^{tm2Kem} (*Ctnnb1*^{flox}) mice (Brault et al., 2001), *Ctnnb1*^{dm} mice (Valenta et al., 2011), and *Ctnna1*^{tm1Efu} (*Ctnna1*^{flox}) mice (Vasioukhin et al., 2001). In vivo fate mapping was performed utilizing either the *ROSA26* reporter expressing β-galactosidase (*R26R*) (Soriano, 1999) or the *ROSA26* reporter expressing enhanced green fluorescent protein (*EGFP*) (Mao et al., 2001) mouse lines. Embryos carrying one allele for lineage tracing are indicated as *R26R* or *EGFP*. To monitor Wnt/β-catenin transcription, animals were crossed with the *BAT-gal* reporter line (Maretto et al., 2003).

To study the role and importance of Wls in the mouse, a conditional allele of *Wls* (*Wls*^{flox}) was generated (Ozgene, Bentley, Australia). The targeting approach was to flank the first exon with loxP sites. The first exon encodes the transcriptional start and the complete signal sequence. Excision of the “floxed” region therefore leads to a *Wls* null-allele. Bl6 was used as background strain. The targeting vector was generated by assembling the 5’ and 3’ homology arms with the loxP site flanked first exon and the FRT site flanked neomycin selection cassette (Additional file 1: Figure S7). Deletion of the FRT flanked Neomycin resistance cassette was verified by PCR and subsequent sequencing of positive Bl6 ES cell clones. *Wls* conditional homozygous mice are viable and fertile and do not show any abnormalities. Deletion of the loxP flanked first exon to generate the *Wls* knockout allele was verified by PCR and sequencing.

Genotyping for the floxed *Wls* allele was performed by PCR with primers Wls-up (5'-CCCCCTTTCCCTCTCGGTTCC-3') and Wls-lo (5'- GGCGGCATGGAAGCCAAGGGC -3') and 34 cycles of 94°C for 30 seconds, 57°C for 30 seconds and 72°C for 1 minute, to amplify a wild type fragment of 267bp length and respectively a mutant fragment 353bp in length.

5.2.7.2. X-Gal staining and immunohistochemistry

β-gal reporter gene expression was detected using X-Gal staining (Hari et al., 2002). For immunohistochemistry, cryo-sections were fixed for 30 seconds in 4%formaldehyde at room temperature and treated with blocking buffer (1%BSA, 0.3% Triton X-100, in PBS) for 30 minutes. Primary antibodies were used as follows: chicken anti-β-galactosidase (1:2000; Abcam ab9361), rabbit anti-GFP(1:500; Abcam ab290), goat anti-Sox10 (1:200; Santa Cruz sc-17342), mouse anti-Neurog2 (1:10; gift from D. J. Anderson, California Institute of

Technology, Pasadena, CA, USA), anti-Neurog1 (1:200; Santa Cruz sc-19231), goat anti-RET (1:500; Fitzgerald 70R-RG002X) rabbit anti-TrkA (1:500; gift from L.F. Reichardt, University of California, San Francisco, CA, USA), rabbit anti-TrkB (1:100; Cell signaling 4607), goat anti-TrkC (1:50; R&D system Inc. AF1404), mouse anti-NF (1:250; Invitrogen 13-0700), rabbit anti-Krox20 (1:4000 gift from D. Meijer, Erasmus University Medical Center, Rotterdam, NL), mouse anti-JUP (1:200, BD Transduction laboratories 610253), rabbit anti-Wls(1:1000 Seven Hills Bioreagents WLAB-177), rabbit anti-Ki67 (1:200, Abcam ab15580),mouse anti-β-catenin N-terminus (1:200; Enzo Life Sceince ALX-804-060-C100), rabbit anti-β-catenin C-terminus (1:200; Sigma c2206), rabbit anti-cCasp3 (1:200; Cell Signaling 9661), mouse anti-Islet1/2 (1:200; Hybridoma 40.2D6), goat anti-TCF3 (1:200; Santa Cruz sc-8635) mouse anti-TCF4 (1:200; gift from Basler Lab; University of Zurich, Zurich, Switzerland), rabbit anti-Lef1 (1:500; Cell Signaling C12A5), rabbit anti-Brn3a (1:5000; gift from Turner Lab, Seattle Children's Research Institute, Seattle, WA 98101, USA) rabbit anti-Ncad (1:200; Takara M142) rabbit anti-αcat (1:200; Sigma C-2081) mouse anti-ZO1 (1:200; Zymed 33-9100). Secondary antibodies were from Jackson Immuno Research or Invitrogen. Tyramide Signal Amplification (TSA) kit from PerkinElmer was used for amplification of TCF3 and TCF4. EdU incorporation was stained using "click" chemistry and was performed as described (Salic and Mitchison, 2008).

5.2.7.3. Statistical analysis

All quantifications were performed on 12 µm transverse sections. Three control and three mutant embryos were quantified at each stage for each type of mutant. To determine rostral-caudal differences quantifications were performed in each embryo on levels of the upper and lower limbs as well as on an intermediate level between the two, collecting 2-3 sections for each level. As relative proportions were consistent on all three levels in all animal types, we averaged the output of 8 sections per embryo. Statistical analyses was performed using the two-tailed unpaired Student's t-test between control and mutant animals with Microsoft Excel. All results are shown as mean ± standard deviation. Pictures in figures were chosen from the intermediate sections between the upper and lower limbs.

5.2.8. Authors' contributions

MG participated in the design of the study, carried out experiments, analyzed the data, and drafted the manuscript. LP-H conceived the study and participated in its design. TV designed the β-catenin-dm mouse model and participated in the design of the study. PH designed the *Wls*^{flox} animals. KB conceived the study and participated in its design. LS conceived the study,

participated in its design and helped drafting the manuscript. All authors read and approved the final manuscript.

5.2.9. Acknowledgements

We thank R. Kemler, S. Piccolo, E. Fuchs, McMahon and P. Soriano for providing transgenic animals, and L.F. Reichardt, D. Meijer, E. Turner and D. J. Anderson for sharing antibodies, and Iris Miescher, Annika Geminn, Jessica Häusel for technical support, and past and current members of the Sommer lab for critical comments. This work was supported by the Swiss National Science Foundation (SNF).

5.3. The role of β-catenin in the development of neural crest cells in the eye

Masterarbeit zur Erlangung des akademischen Grades Master of Dental Medicine (M Dent Med) der Medizinischen Fakultät der Universität Zürich; unpublished 2015

Yvonne Ambühl, Betreuung Max Gay, Leitung der Masterarbeit Prof. Dr. Lukas Sommer

5.3.1. Abstract

Background: During embryonic development, neural crest cells generate various derivatives, including specific structures of the eye. The Wnt/β-catenin pathway is very important in eye development, but it is unclear to what extend Wnt signaling activity in neural crest derivatives controls proper eye development. The two main known functions of β-catenin are a signaling and an adhesive one, but it was not possible to study them separately until recently. Therefore, we sought to use novel genetic tools in order to distinguish these two functions of β-catenin in neural crest cells giving rise to features of the eye.

Methods: We combined different mouse lines to distinguish the functions of β-catenin. The Cre-loxP-system was used for conditional knock-out. On one hand we bred mice with a mutated β-catenin protein, which was able to perform the adhesion function, but not the signaling one in neural crest cells (*βcat-Sig*). On the other hand mice were also bred, in which β-catenin had been entirely ablated in neural crest cells (*βcat-Null*). As controls we used mice of these breedings, which had intact β-catenin function. Mouse embryos were sampled at embryonic day (E) 12.5 and 18.5. Immunhistochemistry was used for protein detection. One mouse for every breeding type at each age was evaluated.

Results: Early in the development malformations in the eye were observable in both mutants. The optic fissure was not fused in either mutant and therefore the optic cup did not inflate. The cornea was completely missing in the *βcat-Null* mutant at E18.5, whereas in the *βcat-Sig* mutant the corneal endothelium and a possibly week stroma were maintained. The retinal pigmented epithelium was not properly pigmented despite MITF expression in both mutants at early and late time-points. Retinal layering is perturbed in both mutants as horizontal cells are strongly reduced. In addition there is an increase in Pax6-positive retinal progenitor cells in both mutants. Furthermore, at E18.5 an increase of apoptotic cells was observed in the retina in both mutants.

Conclusion: The Wnt/β-catenin pathway has great effects in the eye development. A lot of connections between the Wnt pathway and other pathways seem to exist, but still a lot of work will be needed to verify them. We can contribute by stating that the loss of Wnt signaling in neural crest cells does not only have an effect on neural crest derivatives, but also on neighboring structures such as the retina, retinal pigmented epithelium and lens. Furthermore, at a first glance it appears as if there are no relevant differences in the eye development between the two different mutants, which indicates that the main phenotypes are a result of the loss of Wnt signaling and not the loss of β-catenin-mediated adhesion.

5.3.2. My contribution to this work

- Designing all experiments
- Supervision of all experiments
- Supervision of all data collection
- Generation of most reagents, including breeding, genotyping of the mice and collection of embryos
- Design of thesis outline, together with Y. Ambühl. Proofreading, modification and discussion of manuscript.

5.3.3. Background

5.3.3.1. Neural crest cells

The neural crest cells (NCCs) are a transient unique embryonic cell population located between the neural tube and the epidermis in the vertebrate embryo (Figure 42). They originate in the ectoderm at the margins of the neural tube. After epithelial-mesenchymal transition and migration, they settle down in different parts of the body to contribute to a lot of tissues and organs (Shakhova and Sommer, 2010). In vertebrates NCCs generate the neuronal and glial cells of the peripheral nervous system as well as pigment, smooth muscle-like cells and cartilage (Hari et al., 2002).

Migrated NCCs are important for eye development as they give rise to a large part of the anterior eye segment (Hari et al., 2002). They form the corneal endothelium, stromal keratinocytes, ciliary body (Shakhova and Sommer, 2010) and the neural melanocytes, which form a part of the iris (Hari et al., 2002).

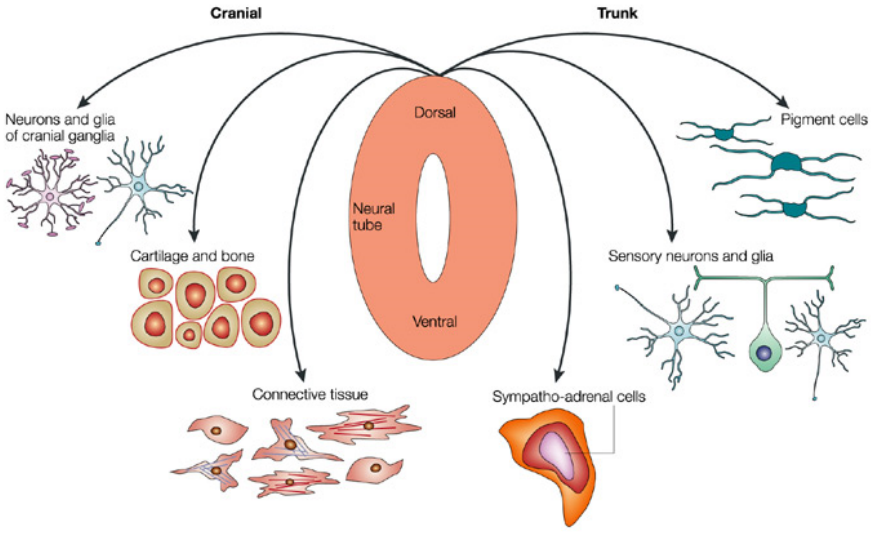

Figure 42 Neural crest cells migration

Neural crest cells migrate from the neural tube and form many different mesodermal and ectodermal cell populations (Knecht and Bronner-Fraser, 2002).

5.3.3.2. Eye development

To describe the postnatal eye structures look at Figure 43. Behind the cornea we will see the lens between the anterior and posterior chamber. Posterior of the lens, the secondary vitreous is found, surrounded by the retina, choroidea and sclera. The nervus opticus leaves the eye at the papilla nervi optici. Inside it the arteria centralis retinae continues as a single artery for the blood supply in the eye.

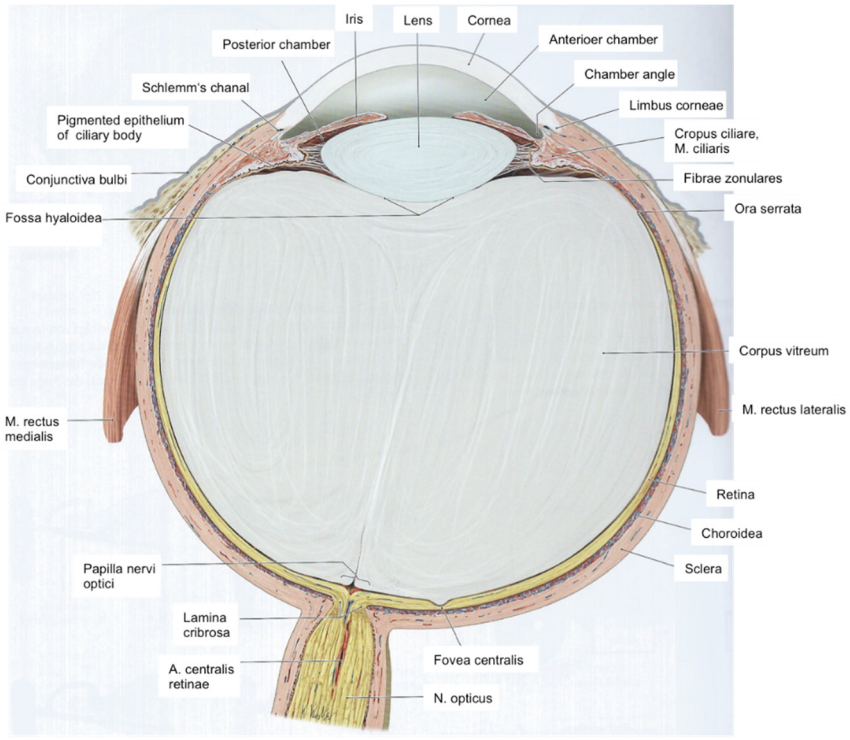

Figure 43 Structures of the postnatal eye

(Schünke et al., 2012).

The eye development starts with two flat grooves on each side of the prosencephalon (the first brain vesicle). With the closing of the neural tube these grooves bulge outwards of the prosencephalon and build the optic vesicles, which contact the surface ectoderm. This contact induces the formation of lens placodes by thickening the surface ectoderm locally. Thereafter, the optic vesicles start to invaginate and develop the double-layered optic cups. The outer layer of the eye cup evolves into the pigment epithelium of the retina. The inner layer will form the mantle layer of the neuroblasts, which will give rise to the retina and the marginal zone with axons of the nerve cells (Cvekl and Tamm, 2004; Sadler, 2008). Parallel to the development of the optic cup, the lens placode enlarges and sinks below the level of the surrounding ectoderm, forming the lens pit and then the lens vesicle, which finally detaches from the surface ectoderm and invaginates into the optic cup (Figure 44) (Cvekl and Tamm, 2004).

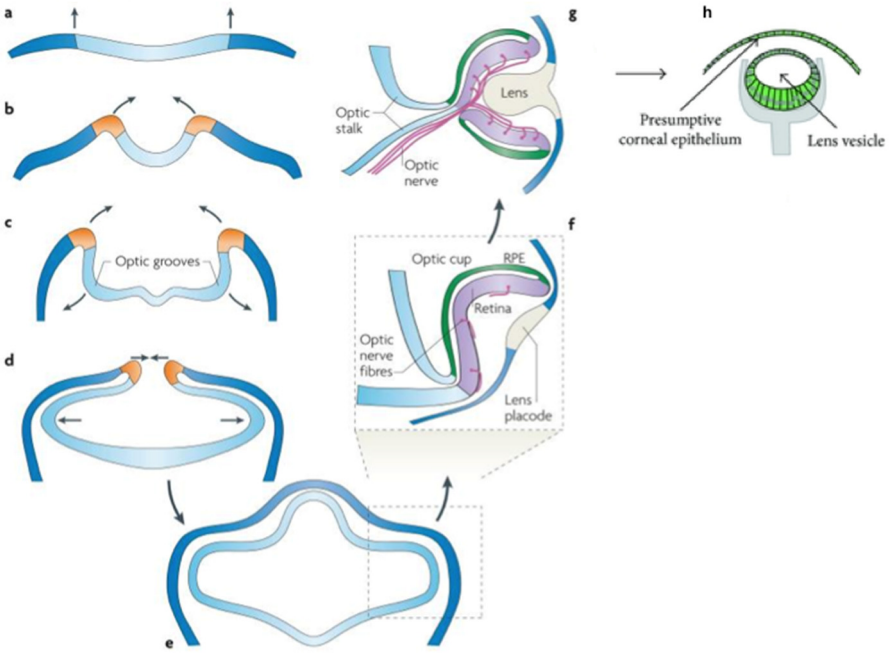

Figure 44 Eye development

Optic grooves bulge outwards of the prosencephalon (a, b, c) building the optic vesicle (d, e) and then the optic cup (f). The lens placode starts forming themselves and out of that the lens will develop (g, h). RPE: retinal pigmented epithelium modified after Lamb et al., 2007; Swamynathan, 2013.

As the optic cup invaginates, a cleft called embryonic (optic) fissure is formed at the inferior part of the optic cup and the ventral inferior part of the optic stalk, which will eventually fuse for proper development of the eye. The optic fissure is used by the hyaloid artery to pass into the optic cup to transport the nutrients to the lens and vitreous during embryonic development (Figure 45) (Cvekl and Tamm, 2004; Sadler, 2008).

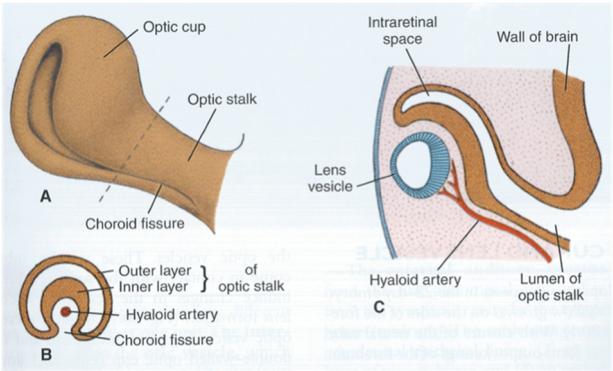

Figure 45 Optic stalk

Through the optic stalk the arteria hyaloidea is transporting nutrients to lens and vitreous (Sadler, 2012).

Mesenchyme cells, derived from the cranial NCCs, surround not only the outer part of the eye, but also migrate through the embryonic fissure into the optic cup. They take part in building the vasa hyaloidea, a vascular layer on the inner surface of the retina, which generates a fine network of fibers between lens and retina and supports the lens. The interstitial rooms of this network will later be filled with a transparent, thickened substance to form the vitreous (Sadler, 2008).

The corneal endothelium is formed by posterior NCCs. The surface ectoderm that covers the anterior side of the mesenchyme will become the corneal epithelium. Corneal stroma fibroblasts and keratinocytes differentiate between these two structures (Figure 46) (Cvekl and Tamm, 2004).

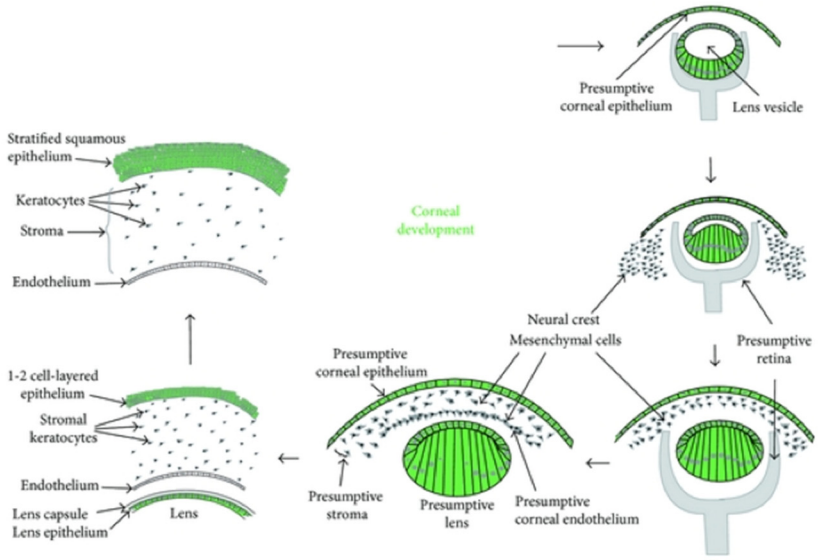

Figure 46 Corneal development

Neural crest cells migrate and form the corneal endothelium and the corneal stromal keratinocytes besides the periocular mesenchyme (Swamynathan, 2013).

As the corneal endothelium differentiates, the lens and the future cornea separate allowing a new group of NCCs to migrate into the anterior eye, precisely to the angle between the future cornea and the anterior edge of the optic cup. When the anterior edges of the optic cup start forming iris and ciliary body, these NCCs will migrate along the epithelial layers of both structures and finally differentiate into the stroma of the iris and ciliary body. As a consequence of this, the anterior and posterior chambers develop and the trabecular meshwork and Schlemm's canal arise in the chamber angle (Figure 47) (Cvekl and Tamm, 2004).

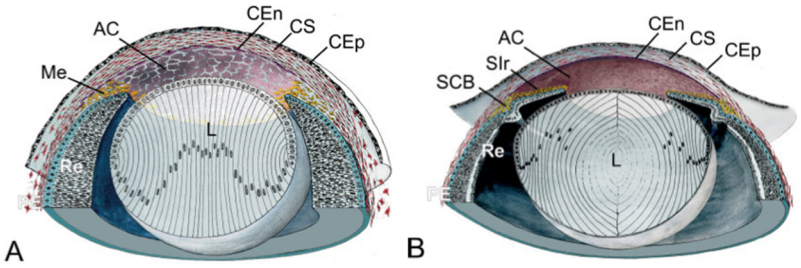

Figure 47 Cells of cornea and chamber angle development

A new group of mesenchyme cells at the angle between the future cornea and the anterior edge of the optic cup gives rise to iris and ciliary body. CEn: corneal endothelium, CS: corneal stroma, CEp: corneal epithelium, AC: anterior chamber, Me: mesenchyme cells, Sir: stroma of the iris, SCB: ciliary body, Re: retina, L: lens (Cvekl and Tamm, 2004).

The loose mesenchyme that surrounds the eye changes in an inner layer building the future choroidea and an outer layer, called sclera, which continues in the dura mater of the nervus opticus (Figure 48) (Sadler, 2008).

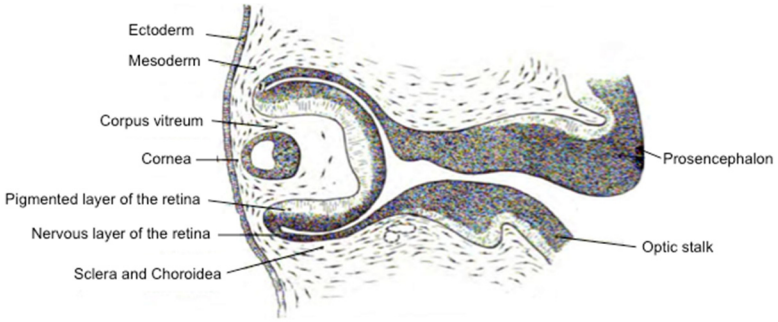

Figure 48 Sclera development

The loose mesenchyme around the optic cup starts building the sclera and choroidea(Hill, 2012).

The optic stalk, with the optic fissure on its ventral side, builds the connection between the eyecup and the brain. Between the cells of the inner layer, nerve fibers continue from the retina to the brain. When the optic fissure closes, there will only remain a small canal in the optic stalk. As nerve fibers grow the inner layer of the optic stalk thickens and the two layers get fused. So the nervus opticus will arise from the optic stalk (Figure 49). It will be surrounded by a continuation of the choroidea and the sclera. The hyaloid artery, seated in the centrum of the optic stalk, will reform its peripheral part in the vitreous and remain as the arteria centralis retinae supplying the retina from there on (Figure 50) (Sadler, 2008).

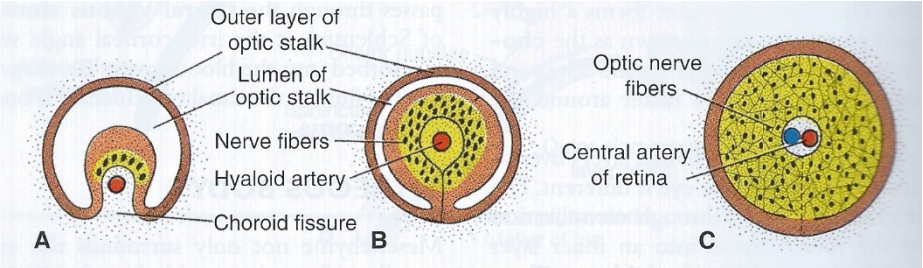

Figure 49 Development of the nervus opticus

Development of the nervus opticus by growing of the nerve fibers and correspondent thickening of the inner layer of the optic stalk and the following fusion of both layers (Sadler, 2012).

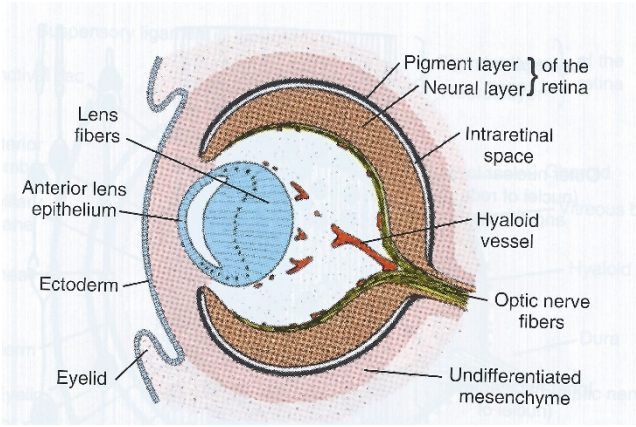

Figure 50 Development of arteria centralis retinae

The vessels of the arteria hyaloidea reform the peripheral part and remain as arteria centralis retinae, at the same time the nervus opticus will arise from the optic stalk (Sadler, 2012).

5.3.3.3. The β-catenin protein

The β-catenin (Armadillo in *Drosophila*) protein consists of a central region with 12 imperfect Armadillo repeats, flanked by a structurally flexible N- respectively C-terminus. A conserved Helix-C is located proximally to the C-terminus next to the last Armadillo repeat and is very important for the signaling activity of β-catenin. Only a small number of co-activators bind N-terminally to the first repeat. The central part forms a relatively rigid scaffold, which serves as an interaction platform for many β-catenin binding partners (Valenta et al., 2012).

5.3.3.4. Wnt/β-catenin signaling

Wnt signaling is a crucial pathway in development and has been shown to be very important in NCCs in the development of the eye (Zacharias and Gage, 2010). This fact is not surprising as Wnt is involved early in the neural crest development (Hari et al., 2002). Already NCC

precursors need to directly receive a Wnt signal to become NCCs (Raible and Ragland, 2005). In all stages of NCC development, Wnt signaling pathway is used reiteratively, from induction, delamination and proliferation to eventual differentiation or as survival factor. NCCs respond differently to Wnt signals depending on their development stage (Taneyhill and Bronner-Fraser, 2005).

Almost 20 different Wnt proteins are encoded by the mammalian genome. Wnts are produced and secreted by a defined subset of cells. They can travel about 20 cells diameters from their source of production (Port and Basler, 2010). In their trafficking heparan sulfate proteoglycans, a component of the extracellular matrix, is implicated (Hausmann et al., 2007). For secretion as well as for signaling activity, lipid adducts are required. Also proteins and glycosylation play a role. After secretion they spread in the tissues to form a concentration gradient (Port and Basler, 2010). The gradient leads to subtle but crucial differences in the repertoire and the level of Wnt-target-gene expression (Hausmann et al., 2007). Additionally, their expression patterns are often overlapping (Valenta et al., 2011). β-catenin is a very important protein in the canonical Wnt cascade. It is responsible for the transduction of signals to the nucleus and triggers the transcription of Wnt-specific genes, which control cell fate decisions in various cell types (Valenta et al., 2012).

In absence of a Wnt stimulus, the majority of β-catenin is located at the cytoplasmic side of the membrane as a cadherin-based cell-cell connection (Figure 51). It associates with newly synthesized E-cadherin in the endoplasmatic reticulum. Together they move to the cell membrane. Without binding to E-cadherin, β-catenin is targeted through glycogen synthase-3β (GSK-3β) amongst others for ubiquitination and proteasomal degradation (Nelson and Nusse, 2004; Valenta et al., 2012).

Signaling is initiated by Wnt ligand binding to Frizzled protein and the lipoprotein receptor-related protein 5 and 6 (LRP5/6). The following binding of GSK-3β leads to its inactivity (Nelson and Nusse, 2004). The inhibition of β-catenin destruction leads to an accumulation in the cytoplasm and then to a translocation into the nucleus. It can shuttle dynamically between the two compartments. Since β-catenin has no DNA-binding domain, it needs DNA binding partners to bring it to the target gene promoters. T-cell factor/Lymphoid enhancer-binding factor (TCF/Lef) is the main nuclear partner of β-catenin (Valenta et al., 2012).

Without β-catenin, TCF/Lef acts as a transcriptional repressor through its binding to Groucho/Thrombin-like enzyme (TLE). Availability of nuclear β-catenin initiates its binding to TCF/Lef. This process leads to the displacement of Groucho/TLE, converting TCF/Lef into a transcriptional activator. In addition, co-activators are necessary, which are general initiators of transcription and not specific for β-catenin. There is also growing evidence that β-catenin interacts with other DNA-binding transcription factors. However, most of them can start

transcription themselves or in association with other co-factors. But these interactions lead to competition for β-catenin and affect TCF/Lef-β-catenin-mediated transcription (Valenta et al., 2012).

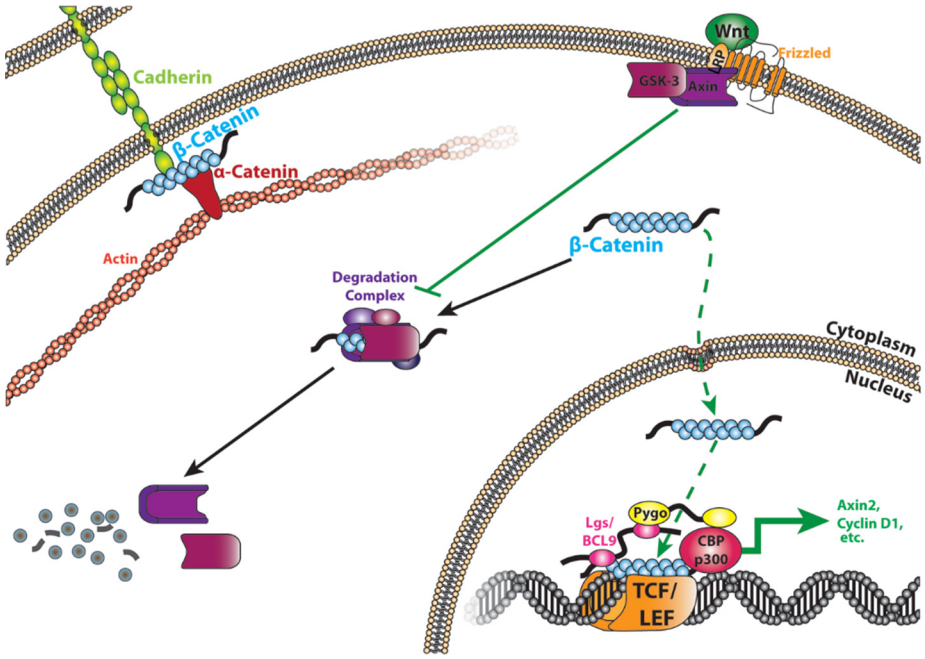

Figure 51 Wnt signaling pathway

The binding of Wnt to the transmembrane Frizzled receptor inactivates the formation of the GSK-3 and Axin degradation complex. This process leads to a stabilization of β-catenin in the cytoplasm from where it translocates into the nucleus. Cadherin bound β-catenin cannot be degraded, therefore in the presence of Wnt, β-catenin can perform transcription in the nucleus, as well as serve as an adhesion molecule. Unpublished schematic by M. Gay.

5.3.3.5. Which function of β-catenin is needed by neural crest cells of the developing eye

As previously mentioned Wnt signaling has been shown to be very important in the development of the eye (Zacharias and Gage, 2010). However, in that study β-catenin was ablated in all NCCs, which leads to not only the loss of canonical Wnt signaling, but also cadherin mediated adhesion. Due to this it is difficult to assign phenotypes to singular functions of β-catenin. With the new generated mouse line by Tomas Valenta et al. (Valenta et al., 2011), it is now possible to replace endogenous β-catenin with a mutated form that enables the induction of signaling, but can preserve adhesion. Therefore the main target for this master thesis is to analyze, which function of β-catenin could be important in the different NCC derived structures of the developing eye. This preliminary investigation was performed with the goal to generate a basis for a possible dissertation, depending on the magnitude of the results.

5.3.4. Materials and methods

5.3.4.1. Settings

Male and female mice of specific genotypes were caged together for one night and separated the next morning. Upon separation females were examined for the presence of a plug, which indicates previous mating. If a plug was observed the female was expected to be pregnant and that day was marked as embryonic day (E) 0.5, as animals expect to mate in the middle of the night. When pregnancy reached the date for the desired embryo age, females were sacrificed and embryos extracted. Mouse experiments were performed in accordance with Swiss guidelines and approved by the Veterinarian Office of the Kanton of Zurich, Switzerland. Experimentation as well as animal breeding and care were performed in the mouse facility of the Institute of Anatomy of the University of Zurich.

5.3.4.2. Mating of mouse embryos

The used transgenic mouse lines

To generate mutant embryos, five transgenic mouse lines were used. Some of them required a conditional knock out, achieved using the Cre-LoxP system.

The Cre-loxP system works as follows: By transgenic technology the Cre recombinase is inserted in the DNA of one mouse line after a gene, which should be responsible for that activation respectively works as a promoter for the Cre recombinase. In a second mouse line two loxP sites are introduced in the same direction around a gene that is wished to be eliminated. These two mouse lines get crossbred so that their littermates have both components in their genome. Although all cells of one animal contain the whole and identical DNA, not every cell expresses the same proteins, which means that not the same genes are transcribed in each cell. Therefore in some cells the transcription of the gene before Cre is activated and therefore Cre will be expressed as well. The Cre protein will locate to the two loxP sites in the distant DNA in the same cell and cut the sequence between these two sites. In other cells no transcription of the appropriate gene before Cre takes place and therefore the Cre recombinase will not be transcribed and no Cre protein will be expressed. This means that the floxed DNA will not be cut and therefore no changes in the DNA will take place in these cells (Figure 52).

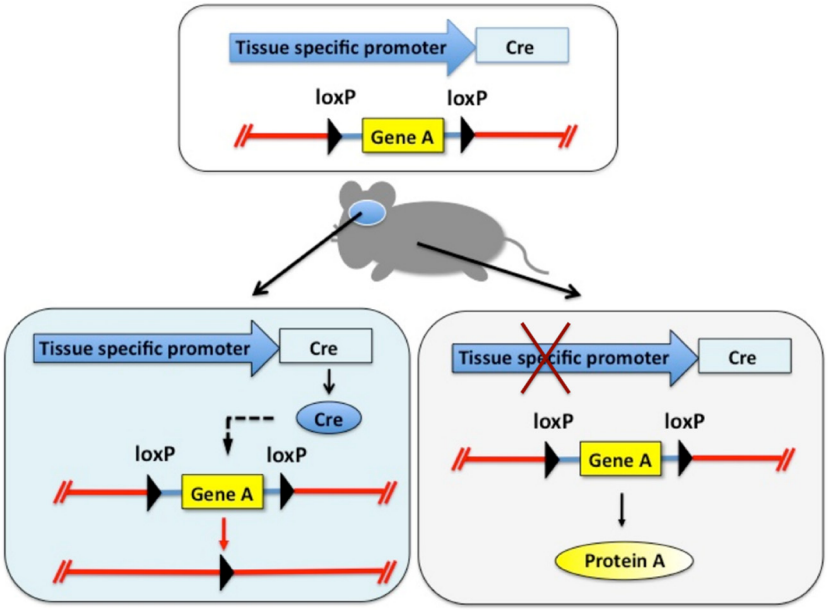

Figure 52 Function of the Cre-loxP system

Is the tissue specific promoter activated, Cre protein will be produced and deletes the floxed DNA (MediaWiki, 2012).

Mice were generated and described in earlier publications (Table 10).

In our models, for Cre recombination we used the *Wnt1-Cre* mouse line (Nagy, 2000). This meant, when *Wnt1* was to be transcribed, the transcription of *Cre* was also induced.

With the *β-catenin* floxed mouse line (*Ctnnb1*^{flox}) in combination with the *Wnt1-Cre* mouse line we were able to delete the floxed DNA of β-catenin, which led to mice with complete loss of β-catenin function (Brault et al., 2001; Valenta et al., 2011).

In the β-catenin double mutant mouse line (*Ctnnb1*^{dm}) a point mutation was introduced in the fourth exon of the first Armadillo repeat of the β-catenin locus resulting in D164A. Through this mutation the adhesive function of β-catenin was still intact whereas the signaling role got lost (Valenta et al., 2011).

In the mouse line *R26R*^{GFP} a green fluorescent protein (GFP) was introduced in addition to a loxP sites flanked stop codon behind the *R26R* promotor. Whenever Cre was active, the stop codon was deleted and therefore GFP was expressed (Mao et al., 2001). Since *R26R* was ubiquitously expressed, all cells, which initiated *Wnt1* transcription would produce GFP.

In the *BAT-gal* mouse line β-galactosidase (β-gal) was expressed under the control of mulitmerized TCF/Lef-binding sites. The Wnt/β-catenin stimulation led to activation of that

construct. The *BAT-gal* mouse unveiled the dynamic pattern of the Wnt/β-catenin activation, meaning if the Wnt stimulus was removed β-gal expression would fade (Maretto et al., 2003).

Name	Genetic	
Wnt1-Cre	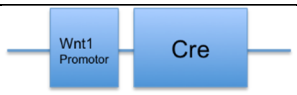	(Nagy, 2000)
Ctnnb1^{flox}		(Brault et al., 2001)
Ctnnb1^{dm}		(Valenta et al., 2011)
R26R^{GFP} (Lineage tracer)	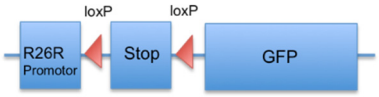	(Mao et al., 2001)
BAT-gal (Wnt Reporter)	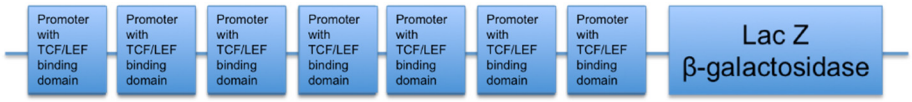	(Maretto et al., 2003)

Table 10 Mouse lines of the first generation used in experiment

Breeding

For time-matings the previously described mice were crossed to get the following second generation (Table 11):

Male	Female
Wnt1-Cre x Ctnnb1$^{flox/wt}$	*Ctnnb1*$^{flox/flox}$ *x BAT-gal*$^{-/-}$ *x R26R*$^{GFP/GFP}$
Wnt1-Cre x Ctnnb1$^{dm/wt}$	

Table 11 Second generation of male and female mice

This meant, the second-generation males still had one wild type (wt) allele of *Ctnnb1* and therefore would not have any mutations. Second-generation females were homozygous for the floxed *Ctnnb1* and the *R26R GFP* Cre-reporter allele, as well as for the *BAT-gal* Wnt reporter.

However, they had no Cre-recombinase, so they would not have mutations in β-catenin and no expression of GFP. They did however express β-gal, as it was independent of Cre recombinase.

Time mating was used to get the third generation, which we used in this experiment (Table 12).

Control	**Signaling mutant**	**Null-mutant**
Wnt1-Cre x Ctnnb1$^{flox/wt}$ x BAT-gal$^{+/-}$ x R26R$^{wt/GFP}$	*Wnt1-Cre x Ctnnb1$^{dm/flox}$ x BAT-gal$^{+/-}$ x R26R$^{wt/GFP}$*	*Wnt1-Cre x Ctnnb1$^{flox/flox}$ x BAT-gal$^{+/-}$ x R26R$^{wt/GFP}$*
Wnt1-Cre x Ctnnb1$^{dm/wt}$ x BAT-gal$^{+/-}$ x R26R$^{wt/GFP}$		

Table 12 Third generation of mice for analyzing in the experiment
Male and female are identical.

All used embryos were heterozygous for *Wnt1-Cre*, *R26R^{GFP}* and *BAT-gal*. Control animals still were unaffected upon Cre-recombinase as they still had one wt allele of the β-catenin gene.

Recombined cells of the *Wnt1-Cre* x *Ctnnb1$^{dm/flox}$* , Signaling mutant (*βcat-Sig*) produced β-catenin that was not able to activate transcription in the nucleus, because Cre cut the loxP sites of the floxed allele, so only the mutated allele was left, which only maintained the adhesion function.

Recombined cells in the *Wnt1-Cre* x *Ctnnb1$^{flox/flox}$* , Null-mutant (*βcat-Null*) animals produced no β-catenin, meaning that transcription in the nucleus was inhibited, as well as the adhesion at the cell membrane was perturbed.

Since the Cre-recombinase was driven under a *Wnt1* promotor, all cells producing Wnt1 would express GFP in all analyzed animals. Since Wnt1 was expressed in the NCCs, we were able to detect all cells, which originated from them, because they expressed GFP. Thus we were able to detect changes in the morphology due to β-catenin mutations as they were activated by *Wnt1-Cre*.

Moreover, β-gal of the *BAT-gal* reporter would be expressed in all cells exposed to a canonical Wnt signal. Through this combination we had the possibility to look at cells originating from the NCCs in the eye and to determine if they were prone to Wnt-signaling.

We analyzed one of each animal, control respectively mutants, at E12.5 and E18.5.

5.3.4.3. Laboratory procedures

Removal and storing of the embryos respectively tissue samples

The uteri containing embryos were taken out of the mother at E12.5 respectively E18.5. Uteri were held on ice in DEPC-PBS, before we extracted the embryos (using the Binocular to get an increase in size). Extracted embryos were put back in DEPC-PBS on ice. From the embryonic uterus of each embryo we took a tissue sample for the later following genotyping. Tissue samples were purified in 50µl embryonic tissue lyses buffer with 2µl Proteinase K (kept at 4°C). The Proteinase K was activated at 55°C and incubated for 90 minutes by 500 revolutions per minute to induce the reduction of proteins. Thereafter inactivation was initiated at 95°C for 15 minutes (no rotation). Isolated DNAs were stored at 4°C until further use.

Macroscopic phenotypes of whole mount embryos were photographed under a binocular magnification. The heads of the embryos were cut by a forceps or scissors and placed in 3.8% Formaldehyd in DEPC-PBS on ice, 50 minutes for E12.5 and 1 hour 45 minutes for E18.5. Then followed two washing steps in DEPC-PBS for 5 minutes and 10 minutes. Afterwards heads were put in a 30% sucrose solution in DEPC-PBS in 2ml Eppendorf tubes. When embryos sank to the bottom of the Eppendorf tubes, they had reached the same density as the sucrose solution and thus the same density as the imbedding solution. If embryos would not have that density they could not be properly imbedded, as they would float on the imbedding media. The heads were imbedded in casting mold with OCT-Tissue-Teq and then frozen at -80°C.

PCR with following gel-separation

For genotyping we used the polymerase chain reaction (PCR). All tissue samples and used substances were kept on ice. Depending on the type of PCR different kits were needed. Detecting the *Wnt1-Cre* transgene required a Quiagen kit, whereas the double mutant allele *Ctnnb1*^{dm} demanded the one from Invitrogen.

We made a 2%-Agarose-gel (2g Agarose in 100ml TBE-buffer). Per 100ml of gel we used 3µl Redsafe (binds and colors DNA). The mixed gel was brought to boil in a microwave. The still warm gel was poured in the form with the combs and cooled down. The DNA-probes were diluted with 6X DNA-Dye (6µl per probe; weighs down DNA to the bottom and helps mark the beginning and ending of the probe after separation). A 100bp DNA-ladder gave us the reference for evaluating the length of our DNA-fragments. The gel chambers were filled with 30µl of the probing material. Afterwards the separation took place by 100V for a 100ml and 200V for a 200ml gel (size depended on the amount of probes).

Sectioning of the embryos

The embedded heads were cut in the cryostat into 12µm thick slices and mounted on slides. Afterwards the slides were kept at -20°C until we used them for stainings.

Stainings

Immunohistochemistry was performed using different antibodies for varying proteins. Primary antibodies and corresponding secondary antibodies, as well as their species, dilution, dissolvent and product information are listed in Table 13.

Slides were warmed up from -20°C to room temperature for 20 minutes and fixed for one minute in 3.8% Formaldehyd at room temperature. Afterwards we washed them with our standard washing procedure of a 5 minutes washing step in PBST followed by a 10 minutes washing step in PBS. Epitope-retrieval was performed using a pressure cooker microwave to improve detection of antigens. The epitope-retrieval protocol consisted of heating slides to 110°C under high-pressure conditions and maintaining the temperature at 110°C for 5 minutes. Afterwards slides were cooled down and washed once in PBS for 5 minutes. Slides were then covered with blocking buffer consisting of 1% BSA and 0.3% Tritron in PBS for 30 minutes. Primary antibodies diluted in blocking buffer were then given on the slides and incubated at 4°C over night. After one standard washing procedure, we added the secondary antibodies for 50 minutes at room temperature. Another standard washing procedure followed, after which DAPI was used for 2 minutes to get a fluorescent staining of the nucleus, more exactly adenosine-thymidine rich parts of the DNA (Kapuscinski, 1995). A last wash in PBS for 5 minutes followed. To finish our staining procedure we mounted the slides with DAKO Immunofluorescent Mounting Media. Three to four drops of the mount solution were given onto the slide, covered by a cover glass and let to dry at room temperature for 30 minutes. At the end we covered the border of the coverslip with nail polish to ensure stabilization.

To get a better overview one Hematoxylin-Eosin (HE) staining was made for E 18.5. The standard procedure was used (Groscurth, 2011).

HE-staining were observed using a Zeiss Mirax Midi Slide Scanner. For detection of immunohistochemistry a Leica DMI6000 Fluorescent microscope was used.

Primary Antibody	Firm	Product number	Dissolvent	Dilution	Species
Rabbit Anti-Pitx2^{ABC} Antidody	CAPRA SCIENCE	PA-1020-100	Blocking buffer (0.3% Triton in PBS + 1% BSA)	1:1000	Rabbit
MITF	Heinz Arnheiter's laboratorium			1:2000	Mouse
Anti-GFP	Avés labs, Inc.	GFP-1020		1:400	Chicken
GFP antibody	abcam	ab290		1:500	Rabbit
beta-Galactosidase antibody	abcam	ab9361		1:2000	Chicken
Monoclonal anti-neurofilament 160 clone NN18	Sigma-Adrich	N 5264		1:400	Mouse
Anti-Brn3a	Gift from Turner Lab			1:200	Rabbit
Cleaved Caspase-3 (Asp175) Antibody	Cell Signaling Technology	9661		1:400	Rabbit
Pax-6 Polyclonal Antibody, Purified	Covance	PRB-278P		1:200	Rabbit
Secondary Antibody	**Firm**	**Product number**	**Dissolvent**	**Dilution**	**Species**
Alexa Fluor 488-AffiniPure Goat Anti-Chicken IgY (IgG) (H+L)	Jackson ImmunoResearch Laboratories, Inc.	103-545-155	Blocking buffer (0.3% Triton in PBS + 1% BSA)	1:500	Goat
Cy^{TM}3-conjugated AffiniPure Goat Anti Rabbit IgG (H+L)	Jackson ImmunoResearch Laboratories, Inc.	111-165-003		1:500	Goat
Alexa Fluor 647-AffiniPure Donkey Anti-Mouse IgG (H+L)	Jackson ImmunoResearch Laboratories, Inc.	715-605-150		1:500	Donkey
Dylight^{TM}488-conjugated AffiniPure Goat Anti-Rabbit IgG (H+L)	Jackson ImmunoResearch Laboratories, Inc.	111-485-003		1:500	Goat
Cy3-AffiniPure Goat Anti-Chicken IgY (IgG) (H+L)	Jackson ImmunoResearch Laboratories, Inc.	103-165-155		1:500	Goat

Table 13 Primary and secondary antibodies for immunohistochemistry with the dissolvent, dilution and species used in our experiment

5.3.4.4. Statistics

We looked for possible phenotypes in the developing eye with stainings for Brn3a and Neurofilament (NF), respectively Pax6 and NF and for cleaved caspase 3 (cCasp3) by comparing control (*Ctrl*) with *βcat-Sig* and *βcat-Null* animals. The previously mentioned stainings were performed on sections, which originated from one embryo for each type of embryo. Six stained sections of 20µm radial length each of each animal type were counted manually using the imageJ software. Mean value, standard deviation and standard error for the variance within one animal were calculated for the controls respectively mutants using Microsoft Excel. Analysis for significance was not performed, as the animal sample number was n=1.

5.3.5. Results

5.3.5.1. First overview of the embryos

At E12.5, differences in phenotype between *Ctrl*, *βcat-Sig* and *βcat-Null* embryos could be seen under the binocular in bright field (BF) as well as with fluorescence microscopy (Figure 53). The black coloration of the pigmented epithelium was only observed in half of the mutants' eye, whereas in *Ctrl* embryo, it was pronounced circularly. Also an altered form of the head was apparent in both mutants.

At E18.5 the impact of the mutations was even more distinct (Figure 54). In both mutants the eye could not clearly be distinguished and the snout did not develop correctly.

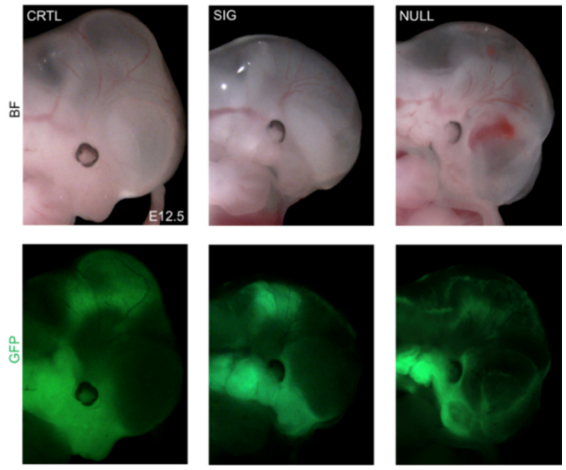

Figure 53 Macroscopic view of embryo heads at E12.5

Bright field (BF) and GFP of the control (Crtl), Signaling- (Sig) and Null-mutant (Null) at E12.5. The black coloration of the pigmented epithelium was observed in half of the mutants' eye, whereas it was pronounced circularly in control embryo. An altered form of the head was apparent in both mutants.

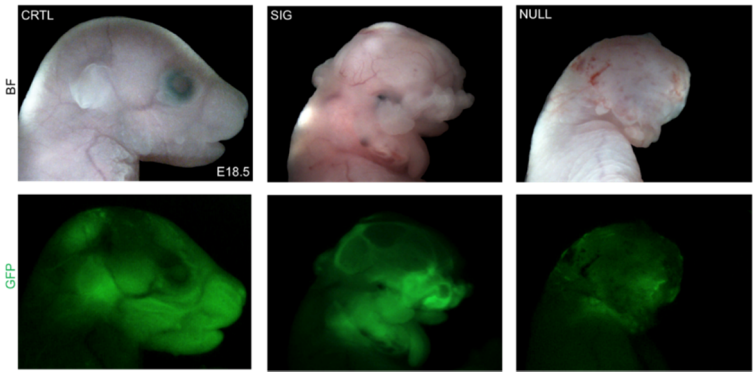

Figure 54 Macroscopic view of embryo heads at E18.5

Bright field (BF) and GFP of the control (Crtl), Signaling- (Sig) and Null-mutant (Null) at E18.5. In both mutants the eye could not clearly be distinguished. Also the snout did not develop correctly.

HE-stainings at E18.5 allowed more detailed observations. Compared to *Ctrl* embryo, the eyes of *βcat-Sig* and *βcat-Null* animals were positioned more medial. In *Ctrl* animal the retina was fused and thus the eye expanded. Expansion of the eye did not happen in *βcat-Sig* or *βcat-Null* embryos, which suggested that the embryonic fissure had not fused and remained open (Figure 55, yellow arrows). Moreover, the retina was pulled longitudinal in both mutants.

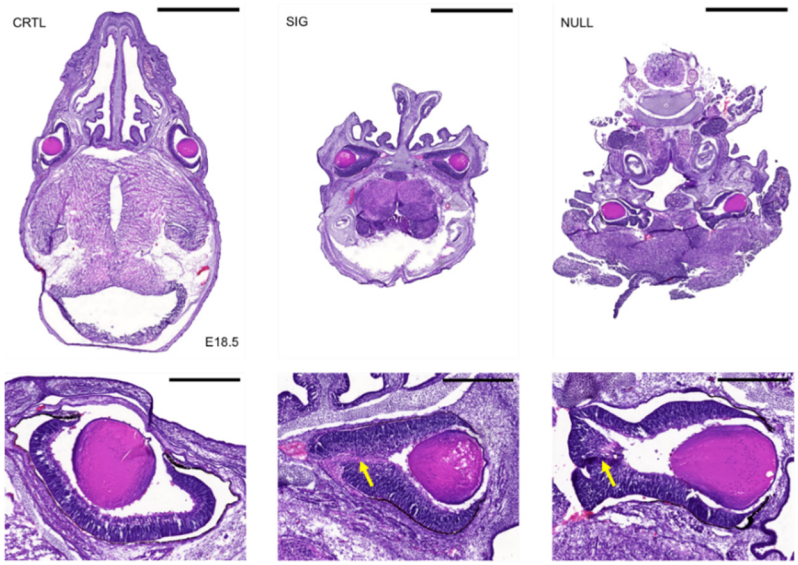

Figure 55 H&E sections of embryo eye ate E18.5

Hämatoxylin-Eosin-stainings of the control (Crtl), Signaling- (Sig) and Null-mutant (Null) at E18.5. The more medial positioned eyes of the mutants had no fused retina and were not expanded (yellow arrows), scale bars 2mm, detail 400µm.

5.3.5.2. *Improper development of the cornea and inhibition of the optic fissure closure*

The expression of GFP lineage tracer is activated by *Wnt1-Cre*, which is expressed in NCCs and the dorsal neural tube (Ittner et al., 2005). Expression of GFP allowed us to track the migration of recombined cells. At E12.5, GFP producing NCCs were located equally in all three animals at the locations in the eye to give rise to the primary vitreous (between retina and lens) and the periocular mesenchyme, which indicated that the cells in *βcat-Sig* and *βcat-Null* mutants seemed to migrate properly. However, in the future cornea differences already appeared: Whereas in *βcat-Sig* mutant, there were still three cell layers observed, the same as in *Ctrl* embryo (Figure 56, white arrows), in *βcat-Null* mutant only two could be discriminated (Figure 56, red arrows).

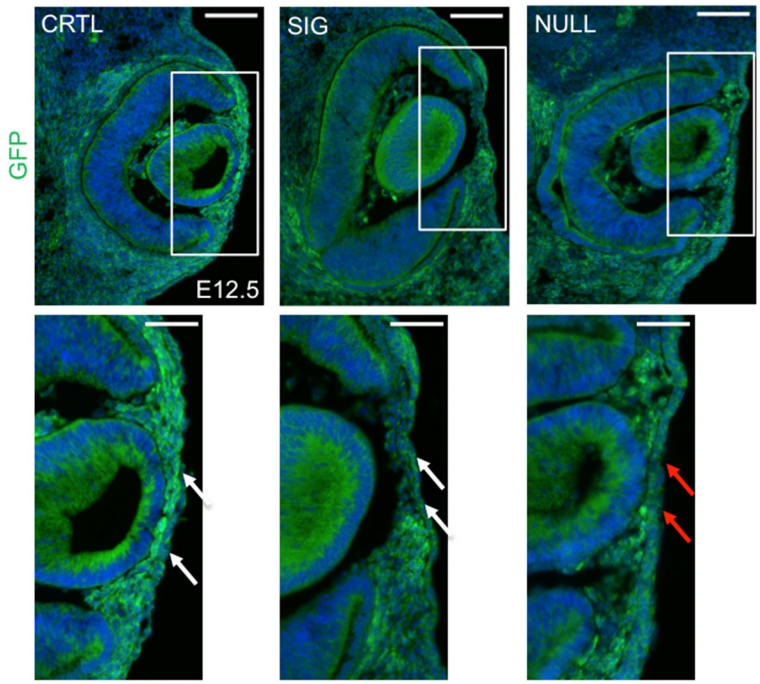

Figure 56 Cornea precursors are reduced in *βcat-Null* mutants at E12.5

GFP staining with corneal detail of the control (Crtl), Signaling- (Sig) and Null-mutant (Null) at E12.5. In the Signaling-mutant three cell layers were still observed as in the control embryo (white arrows). In the Null-mutant only two layers could be discriminated (red arrows). Scale bars 100µm, detail 50µm.

Pitx2 is a transcription factor expressed in the periocular mesenchyme, the presumptive cornea, the eyelids and the extraocular muscles, but not in the retina or lens (Cvekl and Tamm, 2004). When co-staining for Pitx2 and GFP at E12.5 the expression pattern was of a salt and pepper distribution in the *Ctrl* embryo containing double positive cells (Figure 57, grey arrows). Interestingly, expression pattern in mutant animals appeared to be more separated with few double positive cells at the border between the two (Figure 57, red arrows).

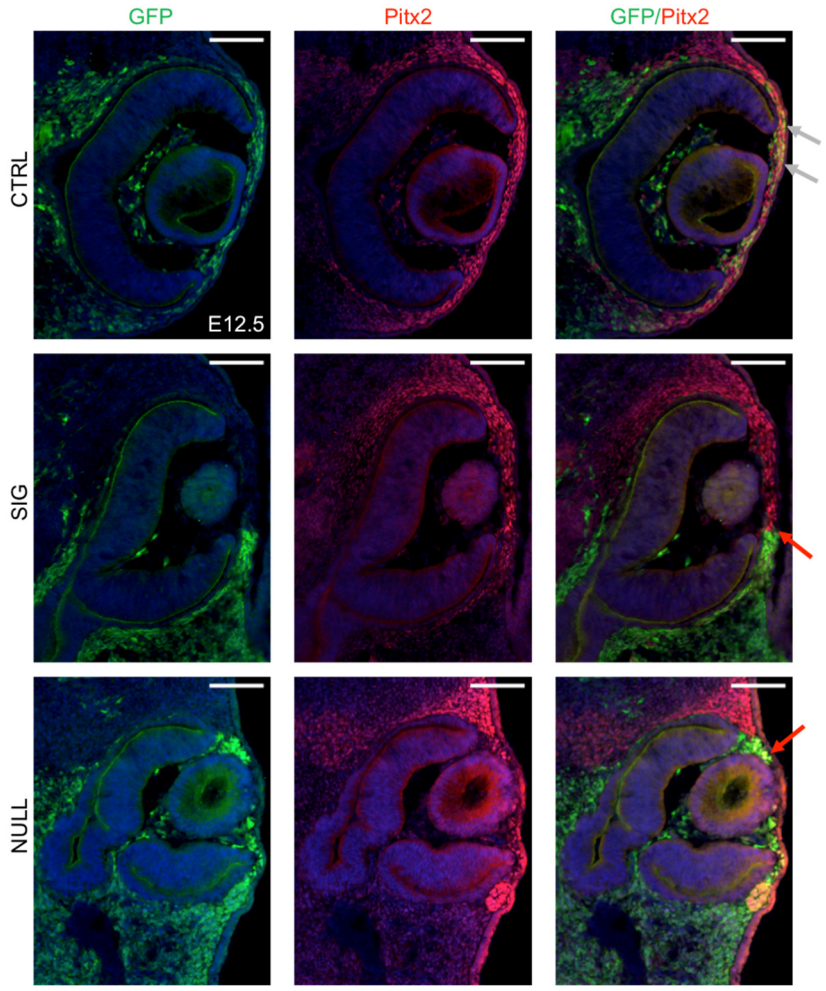

Figure 57 Expression of Pitx2 is lost in neural crest stem cells in both mutants at E12.5

Staining for GFP and Pitx2 in the control (Crtl), Signaling- (Sig) and Null-mutant (Null) at E12.5. The co-staining for Pitx2 and GFP contained double positive cells in the control embryo (grey arrows). The expression pattern in mutant animals seemed more separated with few double positive cells (red arrows). Scale bars 100µm.

At E18.5, in *βcat-Sig* and *βcat-Null* mutants the GFP-positive cells were not arranged in a thin layer on top of the retina near the vitreous or around the lens as in *Ctrl* embryo. However, a large amount of GFP-positive cells were found clumped in what appeared to be the open optic fissure (Figure 58 B, red arrows) or observed in the ganglion cell layer (Figure 58 B, yellow arrows) of the retina.

In *βcat-Null* embryo GFP expressing cells giving rise to any aspects of the cornea were totally missing (Figure 58 C, orange arrows).

In eyes of *βcat-Sig* animal however a cornea-like structure was observed, as an intact corneal endothelium could be recognized (Figure 58 C, white arrows). However, a clear stroma could not be distinguished and the corneal epithelium was missing.

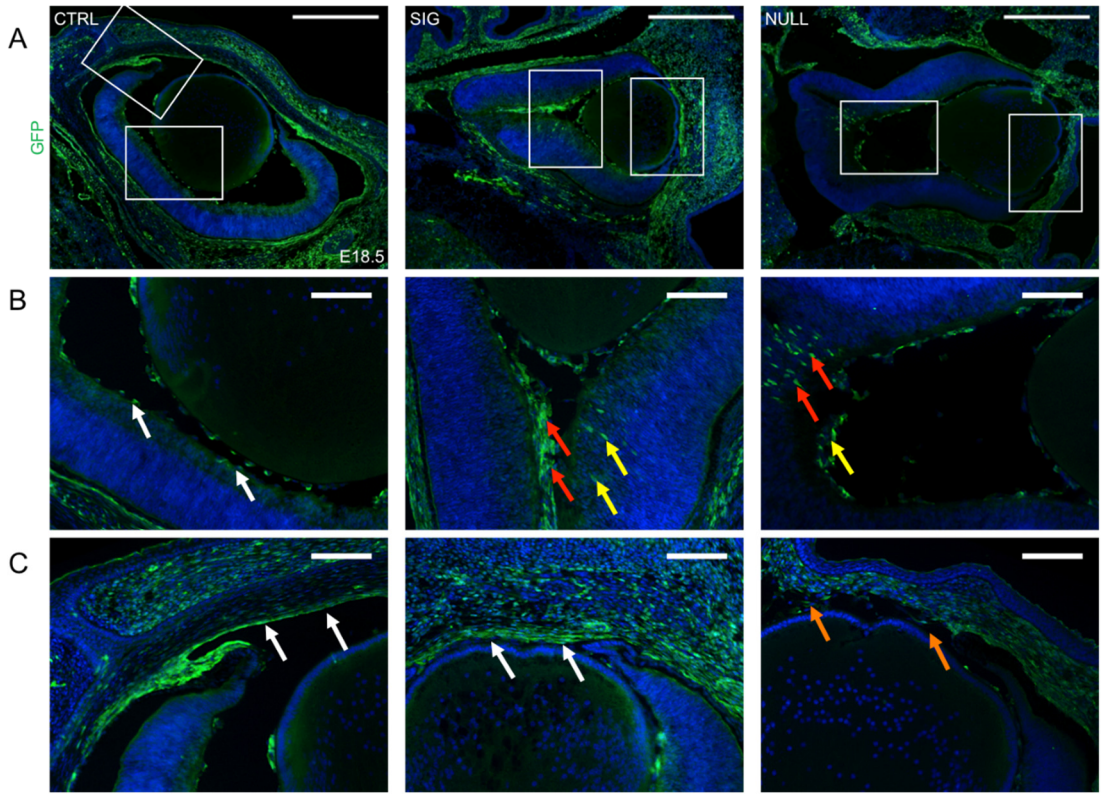

Figure 58 Phenotypes of mutant cornea and vitreous at E18.5

Staining for GFP at E18.5 in the control (Crtl), Signaling- (Sig) and Null-mutant (Null) (A) with details from the embryonic fissure (B) and the chamber angle (C). A large amount of GFP-positive cells were found clumped in the open optic fissure (red arrows) and in the ganglion cell layer (yellow arrows). In Null-embryo GFP expressing cells giving rise to any aspects of the cornea were totally missing (orange arrows). Scale bars 400µm, detail 100µm; white arrows: correct expression.

At E18.5, GFP and Pitx2 co-expressing cells were found in the corneal stroma, corneal endothelium and the chamber angle in *Ctrl* animal (Figure 59, white arrows). In *βcat-Null* animal the corneal structures were lost (Figure 59, green arrow) and the chamber angle could not be properly determined (Figure 59, red arrow), however Pitx2 and GFP double positive cells were observed in the vicinity of where the chamber angle could be (Figure 59, yellow arrow). In *βcat-Sig* animal the corneal stroma was undistinguishable, the chamber angle was deformed (Figure 59, orange arrow), but the corneal endothelium was present (Figure 59, white arrow). However, the corneal endothelium and chamber angle of *βcat-Sig* animals were Pitx2-negative.

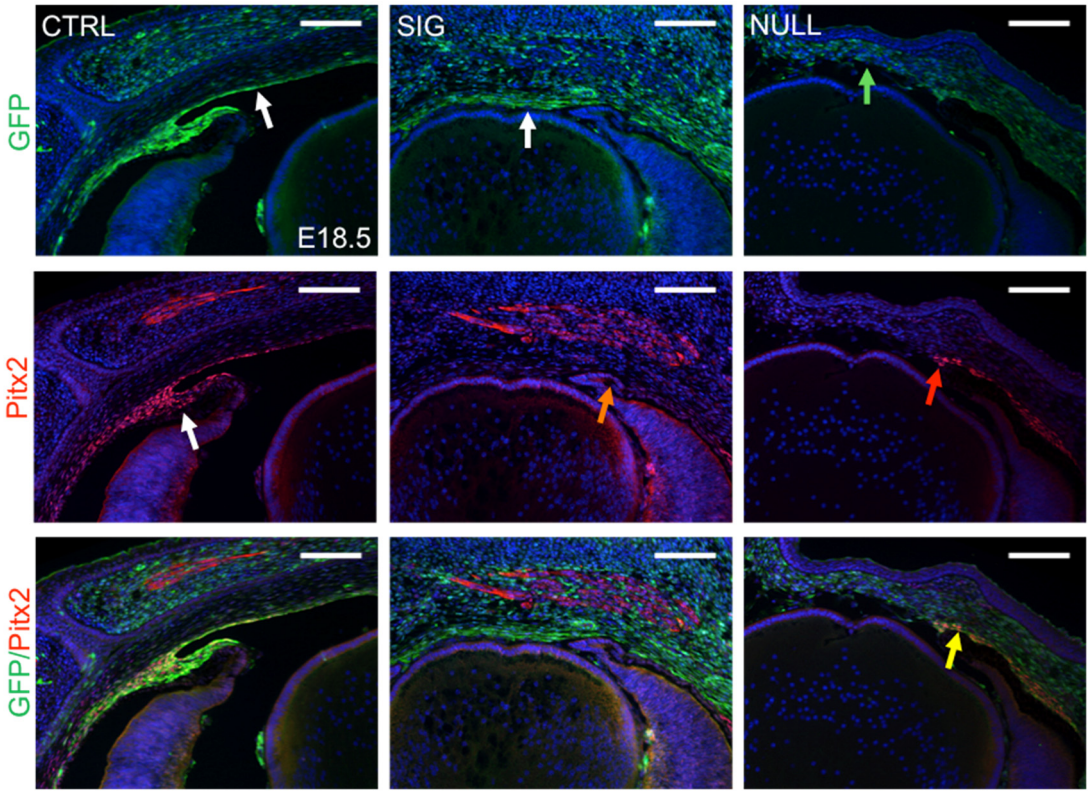

Figure 59 Signaling mutant corneal stroma does not express Pitx2

Staining for GFP and Pitx2 in the control (Crtl), Signaling- (Sig) and Null-mutant (Null) at E18.5. In Signaling-mutant the corneal stroma was undistinguishable and the chamber angle was deformed (orange arrow). The corneal endothelium and chamber angle were Pitx2 negative. In Null-mutant the corneal structures were lost (green arrow) and the chamber angle could not be properly determined (red arrow), but Pitx2/GFP double positive cells were observed in the vicinity of the chamber angle (yellow arrow). Scale bars 400µm, detail 100µm; white arrows: correct expression.

5.3.5.3. *The retinal pigmented epithelium partially loses pigmentation*

As described previously in the overview, proper pigmentation of the Retinal pigmented epithelium (RPE) was lost in both mutants (Figure 60, BF).

MITF is a transcription factor, which controls production of the pigment melanin in pigment-producing cells. Even though pigmentation of the RPE was not homogenous in *βcat-Sig* and *βcat-Null* animals at E12.5, RPE cells still expressed MITF (Figure 60). Compared to *Ctrl* embryo, MITF-positive cells of mutant animals decreased MITF expression intensity in the RPE in the region of the future exit of the nervus opticus (Figure 60, orange arrows), respectively the open embryonic fissure. Nevertheless, the expression of MITF seemed to be equally anterior and posterior, except from the part of the open embryonic fissure.

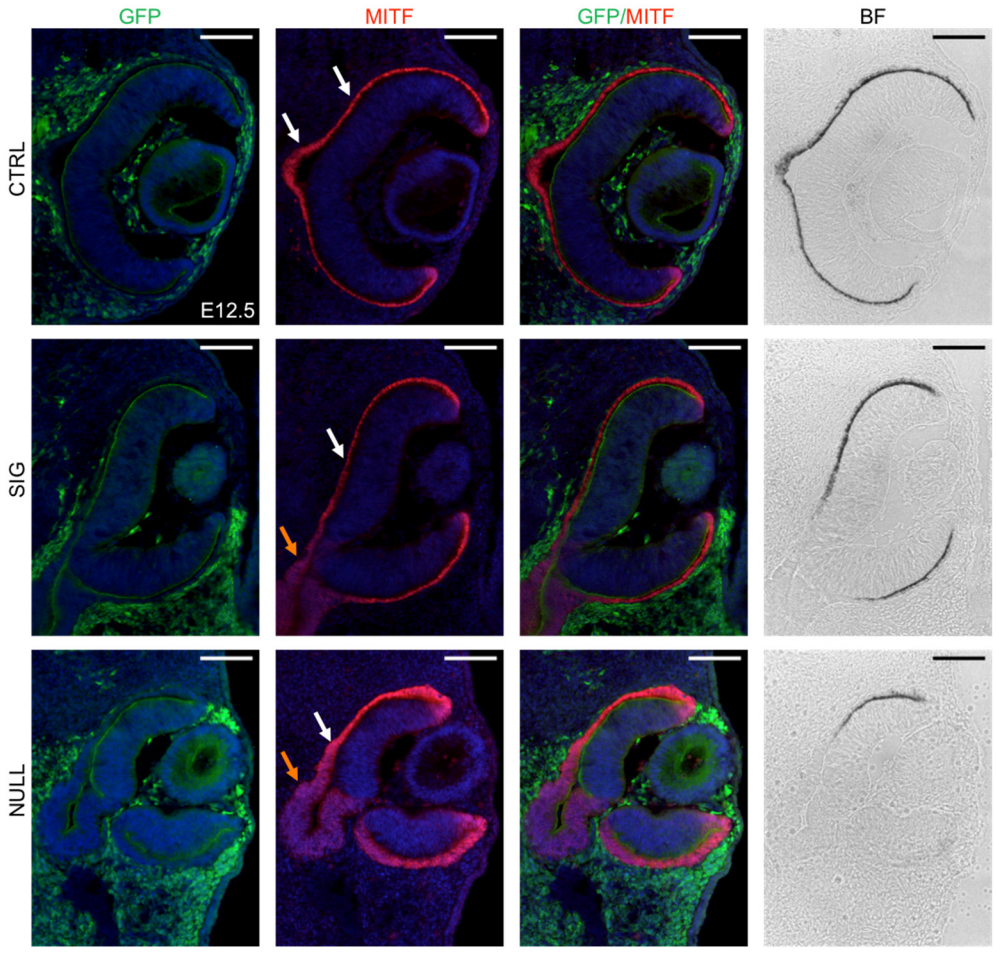

Figure 60 Loss of retinal pigmented epithelium pigmentation despite MITF expression at E12.5

GFP and MITF stainings and bright field (BF) for the control (Crtl), Signaling- (Sig) and Null-mutant (Null) at E12.5. MITF-positive cells of mutant embryos decreased MITF expression intensity in the retinal pigmented epithelium in the region of the open embryonic fissure (orange arrows). Scale bars 100µm; white arrows: correct expression.

At E18.5, intensity of MITF expression appeared weaker in *Ctrl* animal. *βcat-Null* embryo displayed a quite high expression of MITF in the RPE anterior (Figure 61, yellow arrows), which was lost in the posterior region, whereas *βcat-Sig* mutant preserved MITF expression of the entire RPE (Figure 61, orange arrows). As already observed at E12.5, black coloration of the pigment was also missing in the posterior part of the eye in *βcat-Sig* and *βcat-Null* embryos at E18.5, which meant the fluorescence was not masked by the pigmentation in the posterior region, what led to the high fluorescent signal compared to *Ctrl* embryo.

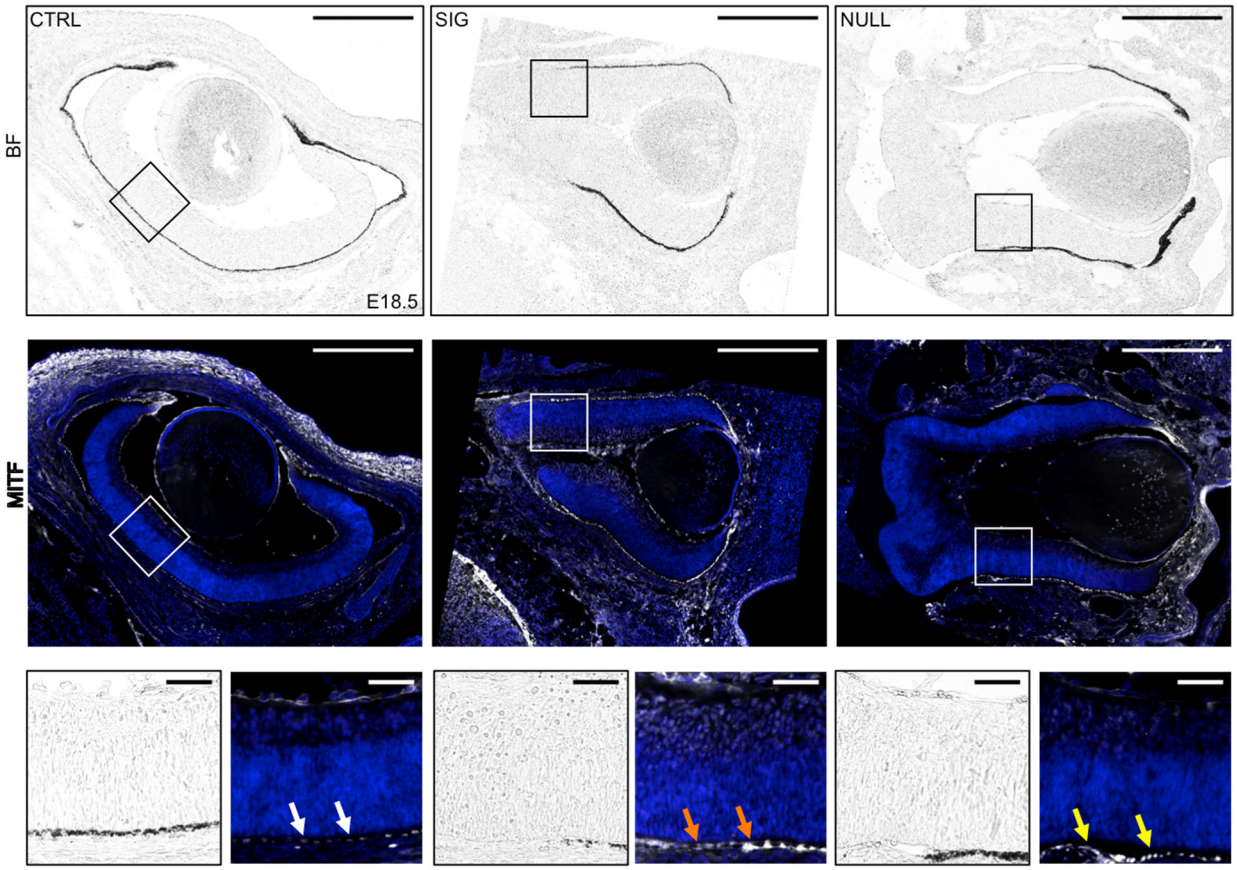

Figure 61 Loss of pigmentation persists at E18.5

MITF staining and bright field (BF) for the control (Crtl), Signaling- (Sig) and Null-mutant (Null) at E18.5. The Signaling-mutant preserved MITF expression of the entire Retinal pigmented epithelium (orange arrows), whereas the Null-mutant displayed a high expression in the Retinal pigmented epithelium anterior (yellow arrows), which was lost in the posterior region. Scale bar 400µm, detail 50µm; white arrows: correct expression.

To check whether pigmentation of the RPE depended on active canonical Wnt signaling from NCCs neighboring the RPE, we stained for β-gal of the Wnt-reporter gene *BAT-gal*. Interestingly, β-gal was only expressed in the RPE at E12.5 in *Ctrl* animal and not in migrating NCCs (Figure 62, white arrows). Furthermore, these β-gal expressing cells of the RPE were extremely reduced in *βcat-Sig* and *βcat-Null* mutants (Figure 62, orange arrows).

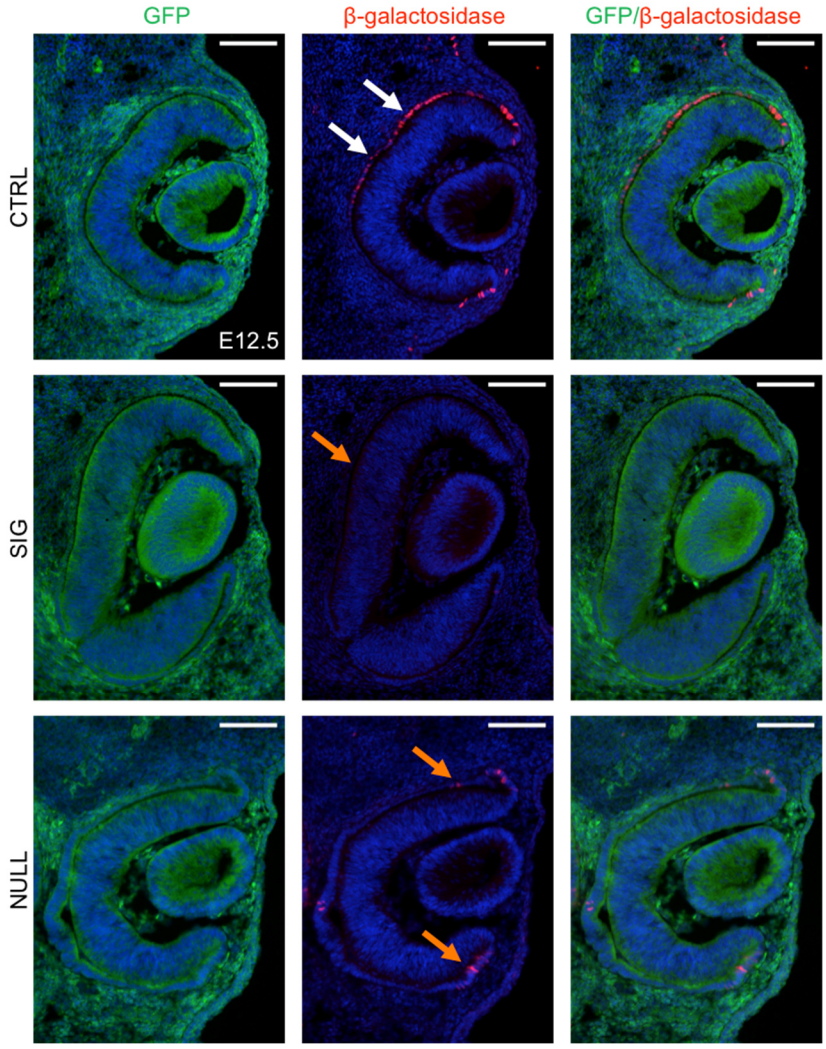

Figure 62 Loss of Wnt reporter activity in retinal pigmented epithelium of mutant animals at E12.5

Stainings for GFP and β-gal in the control (Ctrl), Signaling- (βcat-Sig) and Null-mutant (βcat-Null) at E12.5. The β-gal expressing cells of the Retinal pigmented epithelium were extremely reduced in both mutants (orange arrows). Scale bars 100µm; white arrows: correct expression.

At E18.5, RPE cells in *Ctrl* embryo maintained their expression of β-gal (Figure 63). As already observed at E12.5, these cells were strongly reduced in *βcat-Sig* and *βcat-Null* animals. Furthermore, β-gal expressing cells were found overlaid with the cytoplasmic GFP of NCCs of the vascular layer. We could not distinguish, whether the β-gal expressing cells were in fact the GFP expressing vascular cells or blood cells within the lumen of the vasculature. The fact that in mutant embryos GFP, *BAT-gal* double positive cells were rarely found in the vitreous, does not help in this assessment, as *BAT-gal* signal was expected to be absent in both mutants, because of the insufficient reporter protein β-catenin.

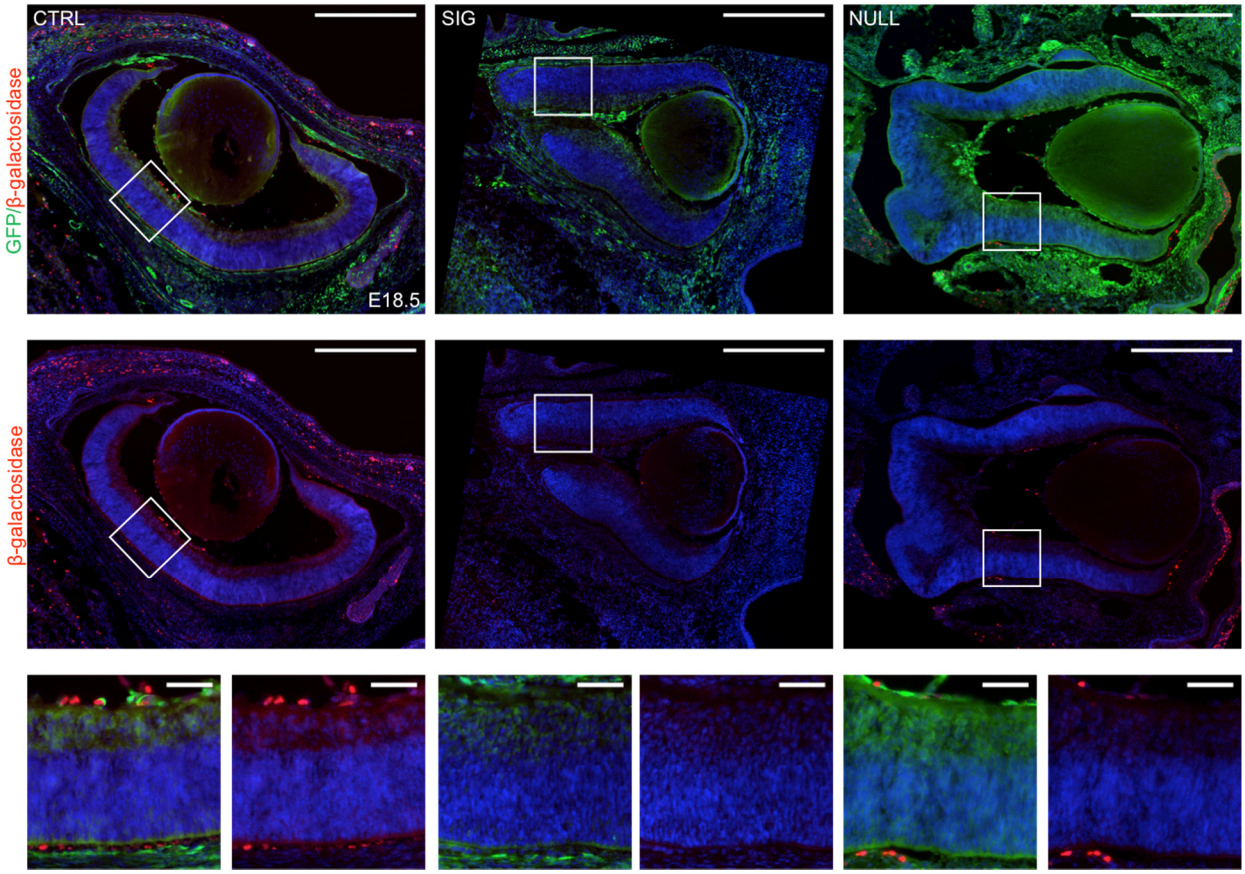

Figure 63 Retinal pigmented epithelium does not regain Wnt signaling activity at E18.5

Stainings for GFP and β-gal n the control (Crtl), Signaling- (Sig) and Null-mutant (Null) at E18.5. β-gal expressing cells were strongly reduced in both mutants. In addition they were found overlaid with the cytoplasmic GFP of Neural crest cells of the vascular layer. Scale bars 400µm, detail 50µm.

5.3.5.4. Perturbed retinal layering

We analyzed retinal layering in both of our mutants at E18.5 since NCCs gave rise to the primary vitreous. In a grown-up eye the retina is built up in the following layers (Figure 64):

1: Ganglion cell layer with multipolar ganglion cells and amacrine cells

2: Inner plexiform layer

3: Inner nuclear layer with bipolar ganglion cells and horizontal and amacrine cells

4: Outer plexiform layer

5: Outer nuclear layer with cones and rods

6: Layer of photoreceptors outer segments

7: Pigmented epithelium

8: Choroidea

(after (Maake, 2011/12))

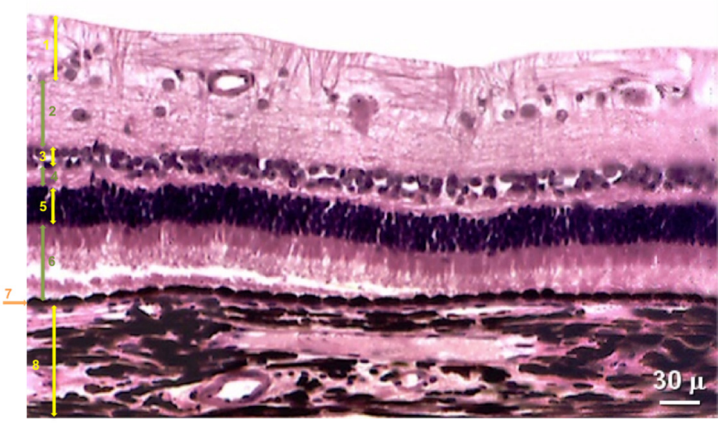

Figure 64 Layers of the retina in an adult eye

1: ganglion cell layer, 2: inner plexiform layer, 3: inner nuclear layer, 4: outer plexiform layer, 5: outer nuclear layer, 6: layer of photoreceptors outer segments, 7: pigmented epithelium, 8: choroidea. (Groscurth et al., 2010-2013).

Brn3a can be used as a marker in retinal ganglion cells (Nadal-Nicolás et al., 2009). NF is found in horizontal cells (Shaw and Weber, 1984) in the inner nuclear layer and in a subset of ganglion cells of the ganglion cell layer (Dräger and Hofbauer, 1984).

At E18.5 in *βcat-Null* and *βcat-Sig* embryos, hardly any NF stained cells were found in the inner layer, but rather in the ganglion cell layer and even more at the border to the inner layer (Figure 65, orange arrows; Figure 66).

Retinal ganglion cells expressing Brn3a were located at the same place in *βcat-Sig* and *βcat-Null* animals as in *Ctrl* embryo (Figure 65) and their cell number did not change either (Figure 67).

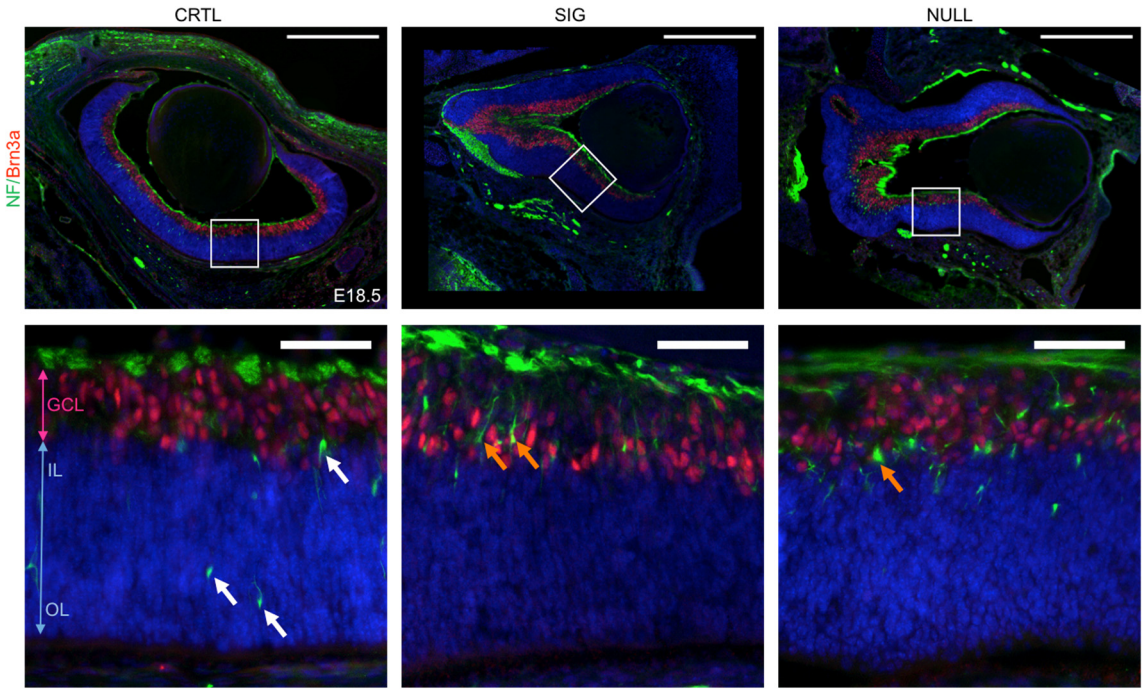

Figure 65 Retinal layering is perturbed in mutant animals at E18.5

Staining for NF and Brn3a in the control (Crtl), Signaling- (Sig) and Null-mutant (Null) at E18.5. NF stained cells were found in the ganglion cell layer and even more at the border to the inner layer (orange arrows). Retinal ganglion cells expressing Brn3a were located at the same place in all embryos. GCL: ganglion cell layer, IL: inner layer, OL: outer layer. Scale bars 400µm, detail 50µm; white arrows: correct expression.

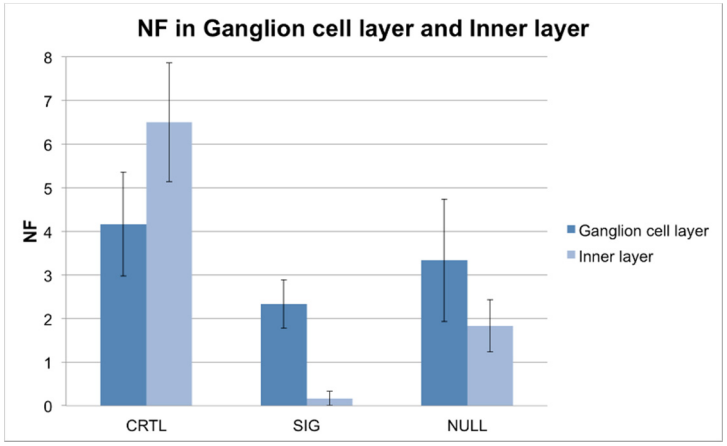

Figure 66 Quantification of horizontal cells

Quantification of the NF stained nuclei in the Ganglion cell layer and Inner layer of the retina in the control (Crtl), Signaling- (Sig) and Null-mutant (Null) at E18.5.

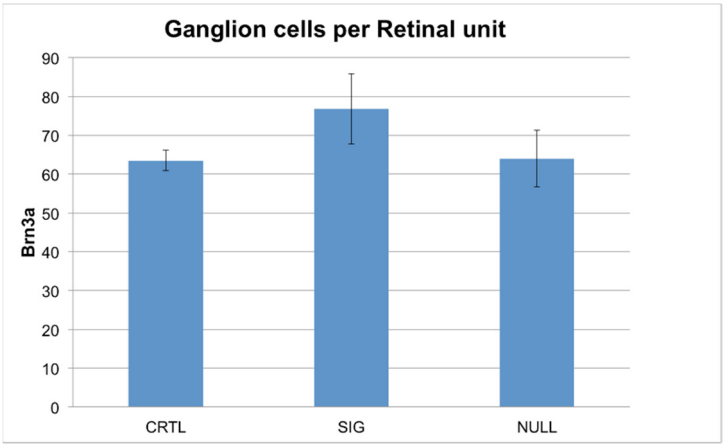

Figure 67 Quantification of ganglion cells

Quantification of the Brn3a stained Ganglion cells in the retina in the control (Crtl), Signaling- (Sig) and Null-mutant (Null) at E18.5. No change in number was found.

The regulation for differentiation in the RPE as well as in the retina is complicated. The predicted retina and RPE are both derived from the same optic neuroepithelium and maintain the capacity to switch from one into the other during development (Bharti et al., 2012).

Pax6 is a transcription factor, which plays an important role in the vertebrate eye development as in structures derived from the surface ectoderm such as cornea and lens, and in those derived from the neuroepithelium, such as iris, ciliary body and retina (Bharti et al., 2012). The role of Pax6 in the retina is to promote the maturation of retinal progenitor cells and their eventual differentiation to all of the retinal cell types (Oron-Karni et al., 2008). Pax6 was initially expressed in the distal and proximal optic vesicle. At first it remained high in the future retina

and the RPE, but later faded away in the RPE (Bharti et al., 2012). In both *βcat-Sig* and *βcat-Null* embryos we quantified more Pax6-positive cells in the developing retina than in *Ctrl* animal at E18.5 (Figure 68).

Furthermore, in *βcat-Sig* and *βcat-Null* embryos Pax6 expression in the anterior lens epithelium was similar to *Ctrl* animal. As Pax6 is a marker for the corneal epithelium and the epithelium of conjunctiva palpebrae (Figure 69, white arrows), the absence of Pax6-positive cells implied both structures to be missing in *βcat-Sig* and in *βcat-Null* mutants.

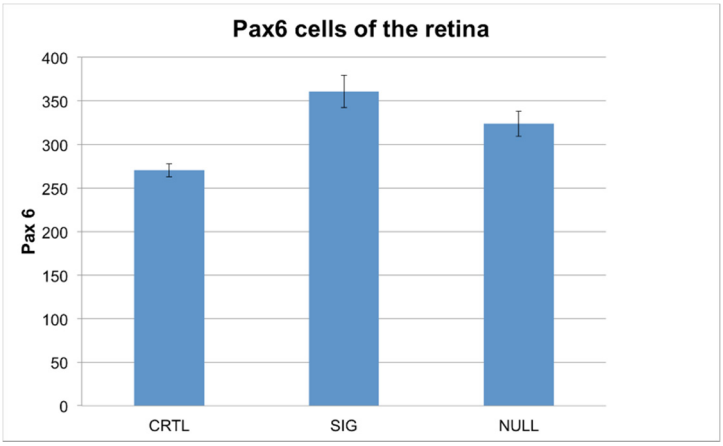

Figure 68 Quantification of Pax6 cells

Quantification of the Pax6 stained cells in the retina in the control (Crtl), Signaling- (Sig) and Null-mutant (Null) at E18.5. In both mutants we quantified more Pax6-positive cells.

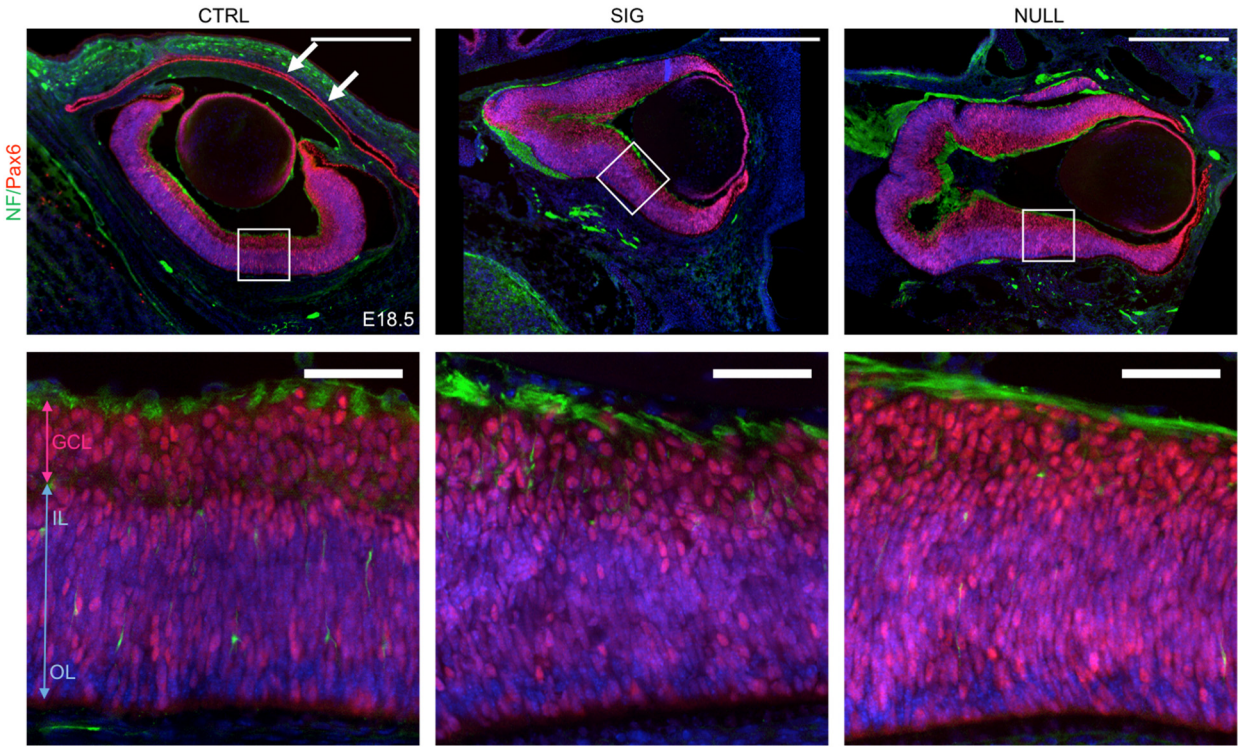

Figure 69 Pax6 expression

Pax6 expression at E18.5 Stainings for NF and Pax6 for the control (Crtl), Signaling- (Sig) and Null-mutant (Null) at E18.5. In both mutanexpression in the anterior lens epithelium was similar to the control, whereas the absence of Pax6-positive cells implied to be missing the corneal epithelium and epithelium of conjunctiva palpebrae in both mutants. GCL: ganglion cell layer, IL: inner layer, OL: outer layer; Scale bars 400µm, detail 50µm; white arrows: correct expression.

5.3.5.5. Irregular apoptosis in the retina

The cleavage of Caspase 3 plays a central irreversible role in the execution-phase of cell apoptosis, due to this cleaved Caspase 3 (cCasp3) is a suitable marker for apoptotic cells.

At E12.5, there was no apoptosis in NCCs. However, a slight increase of apoptotic cells was witnessed in the developing retina and optic stalk of mutant animals (Figure 70).

At E18.5 the differences were more pronounced. In the *Ctrl* animal no apoptotic cells in the developing eye were observable, with exception of single cells in the retina. In mutant embryos cell death was also only observed in the retina, but to a higher degree. In the *βcat-Null* embryo cell death was seen more frequently than in the *βcat-Sig* animal (Figure 71). Interestingly, the cells in apoptosis were located in the ganglion cell layer at the border to the primary vitreous in *βcat-Sig* as well as in *βcat-Null* mutants (Figure 70).

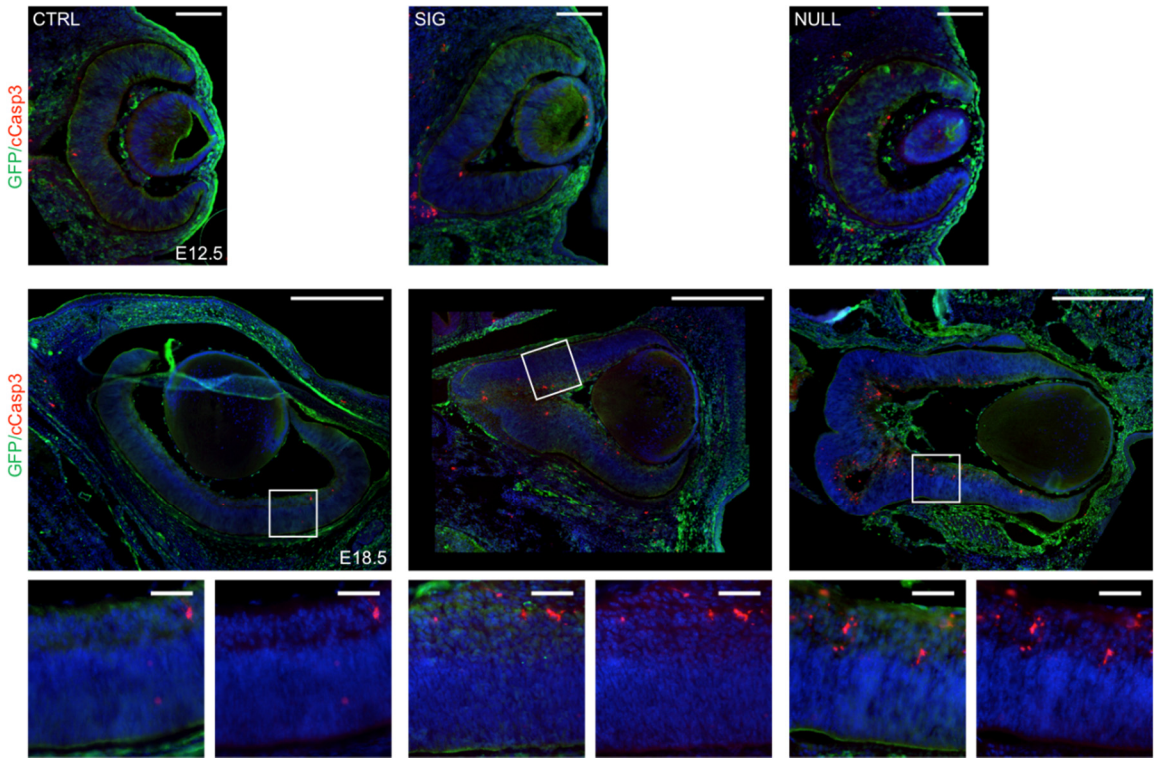

Figure 70 Apoptosis in the retina is increased in Null-mutants at E18.5

The staining for GFP and cCasp3 in the control (Crtl), Signaling- (Sig) and Null-mutant (Null) at E12.5 and E18.5. A slight increase of apoptotic cells was observed in the developing retina and optic stalk of the mutants at E12.5. At E18.5, in mutant embryos cell death was also only observed in the retina. The cells in apoptosis were located in the ganglion cell layer at the border to the primary vitreous. Scale bars E12.5 100µm, E18.5 400µm, detail 50µm.

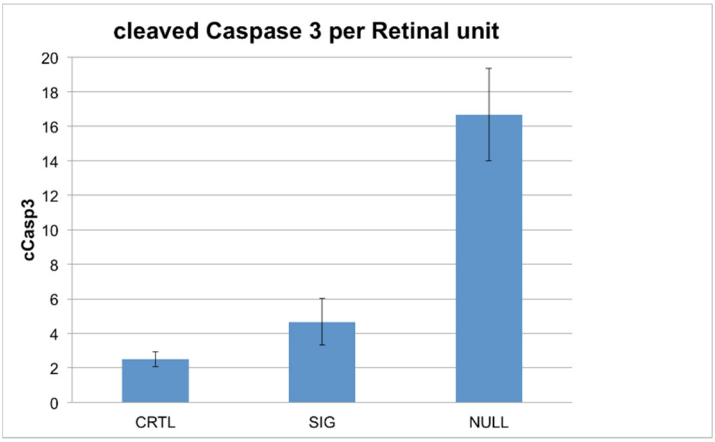

Figure 71 Quantification of the cleaved Caspase 3

Quantification of the cleaved caspase 3 (cCasp3) stained nuclei in the control (Crtl), Signaling- (Sig) and Null-mutant (Null) at E18.5. In the Null-mutant cell death was seen more frequently than in the Signaling one.

5.3.6. Discussion

5.3.6.1. Most important results

NCCs giving rise to the primary vitreous and its hyaloid vascular system migrate correctly in both mutants. However, the optic fissure did not fuse in eyes of either of the mutants and therefore the optic cup did not properly inflate. However, due to the loss of the fusion of the optic fissure in both mutants the secondary vitreous did not replace the primary vitreous as it still persisted at E18.5 in both mutants.

The pigmentation of the RPE was not expressed correctly despite MITF expression in both of the mutants.

The corneal endothelium, stroma and epithelium were totally missing in the *βcat-Null* animal, whereas in the *βcat-Sig* embryo the corneal endothelium was preserved.

In the developing retina of E18.5, animals of different phenotypes could be observed. Horizontal cells of both mutants were reduced and retinal progenitor cells were increased. Additionally, irregular apoptotic cells were observed in the inner layer of the retina of both mutants with the phenotype being more severe in *βcat-Null* than in *βcat-Sig* animal.

5.3.6.2. Comparison with the literature

Improper development of the primary vitreous inhibits the optic fissure to fuse

The NCCs arrived correctly at the margins of the primary vitreous in both mutants at the early stage of E12.5, but were still observed as a clump of cells in the unfused optic fissure at E18.5. It is probable that this clump is the preserved primary vitreous, in which cells were neither replaced by the secondary vitreous nor did they differentiate into the hyaloid vascular system. These first findings lead us to believe that the fusion of the optic fissure is dependent on extra cellular signals from NCCs and that these factors are downstream targets of Wnt signaling in NCCs. Furthermore, it is likely that the open optic fissure induces a feedback signal, which leads to an altered environment in the eye, which influences the proper progression of the vitreous development. In addition, it could be possible that a Wnt signal from tissue surrounding the primary vitreous, such as lens or retina, is necessary for the proper maturing of the hyaloid vascular system.

Cornea development depends on both functions of β-catenin

Even though NCCs were found at the site of the future cornea at E12.5 in both mutants, at E18.5 the cornea was completely missing in the *βcat-Null* animal. In the *βcat-Sig* embryo, however, the corneal endothelium could be observed. This phenotype could be due to the mutated β-catenin protein function to preserve adhesion. Interesting was, however, that even though the corneal endothelium was formed, a clear stroma could not be distinguished and the corneal epithelium was missing altogether.

Pitx2 is a transcription factor expressed in the periocular mesenchyme and is important for the development of the presumptive cornea, the eyelids and the extraocular muscle, but does not exist in the retina or the lens (Cvekl and Tamm, 2004). Amanda L. Zacharias and Philip J. Gage analyzed the effects of conditional knock-out of β-catenin in NCCs contributing to eye development using the *Wnt1-Cre* mouse line. In their research they could show that production of Pitx2 is dependent on retinoic acid (RA), but β-catenin is required for the maintenance of Pitx2 expression in NCCs (Gage et al., 2008). Furthermore, they showed using a Pitx2 conditional knock-out mouse, that at a later time point Pitx2 expression initiates production of Dkk2, which is an extracellular antagonist of canonical Wnt/β-catenin signaling (Figure 72) (Gage et al., 2008; Kumar and Duester, 2010).

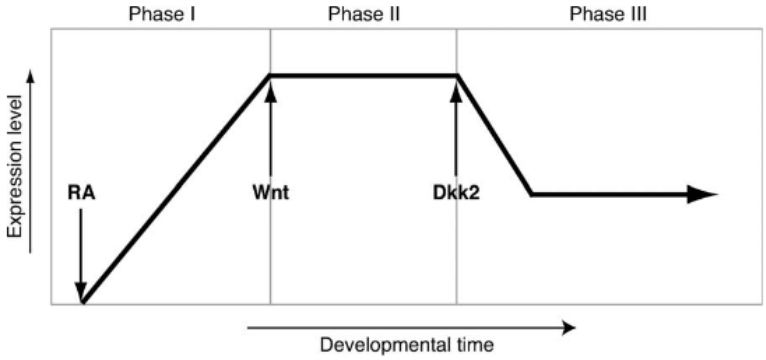

Figure 72 Expression level of Pitx2 in ocular neural crest stem cells

Expression level of Pitx2 during developmental time in dependence of retinoid acid (RA), Wnt and Dkk2 (Zacharias and Gage, 2010).

Intact production of Pitx2 was confirmed by our data as it is expressed in *βcat-Sig* and *βcat-Null* embryos similar to the *Ctrl* animal at E12.5. Pitx2 was however missing in the corneal endothelium of the *βcat-Sig* embryo at E18.5. Zacharias and Gage's work stated "that early Pitx2 expression in the neural crest activates a mechanism for bonding anterior segment elements together" (Zacharias and Gage, 2010).

Taken together the presented findings and our own suggest that the adhesion function of β-catenin is not necessary for correct migration of NCCs giving rise to the cornea. However, β-catenin mediated adhesion is necessary for the coalescing corneal endothelium. Why the corneal stroma and epithelium do not properly form could have two explanations. Either the development of the stroma and the endothelium depend on Wnt signaling for their proper proliferation and differentiation, or the mode of adhesion varies from β-catenin mediated adhesion in corneal endothelium to an alternate mode of adhesion depending on Pitx2 expression in the corneal epithelium.

Incorrect eye inflation and lens formation as a result of persisting primary vitreous and remaining open embryonic fissure

In both mutants the margins of the optic fissure did not fuse, therefore the embryonic fissure remained open. As a result of that the inner eye could not establish increased pressure for the proper inflation of the eye. It is likely that NCCs giving rise to the primary vitreous release or display signals necessary for the fusion of the optic fissure and that the expression of these signals are induced by Wnt-signaling.

The more triangular appearance of the lens may be a result of the changed respectively lower pressure in the optic cup. It is however also possible, that it is a result of the persistent primary vitreous, which did not properly form vessels of the hyaloid vascular structure. The loss of these vessels would inhibit the transmission of signals between the lens and the retina. It may also be a combination of pressure and signal loss.

Induction of pigmentation of the Retinal pigmented epithelium results from Wnt signaling pathway

Cells from the RPE in control animals at both E12.5 and E18.5 expressed β-gal induced by the Wnt-reporter *BAT-gal*. Therefore there was a signal that led to TCF/Lef transcription activity, which required nuclear β-catenin activity (Valenta et al., 2012). In both of our mutants at either time point the expression of β-gal was heavily reduced.

Interestingly, Naoko Fujimura et al. acquired similar results to ours upon conditionally knock-out of β-catenin using the *Trp1-Cre*, which is specific for the RPE. Their results not only showed a significant downregulation of the *BAT-gal* reporter and Lef1 genes in the presumptive RPE, but their mutant RPE was not pigmented either (Figure 73) (Fujimura et al., 2009).

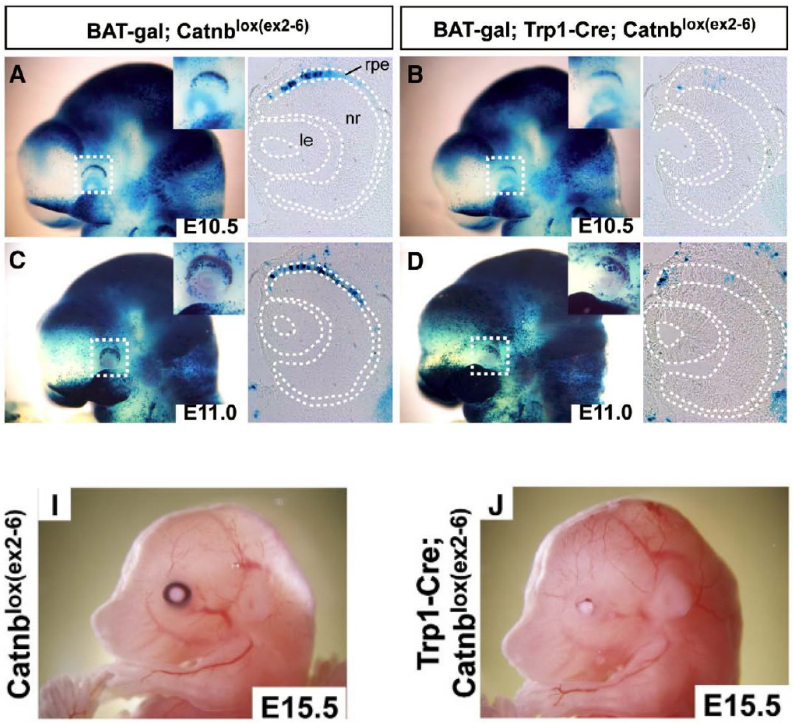

Figure 73 RPE requires Wnt-signaling for pigmentation

Similar results Fujimura et al. acquired upon conditionally knock-out of β-catenin using the Trp1-Cre, which is specific for the RPE. A significant downregulation of the BAT-gal reporter and Lef1 *genes in the presumptive RPE was shown and also their mutant RPE was not pigmented (Fujimura et al., 2009).*

Taken together with our findings, this would suggest that the Wnt signal needed by the RPE is supplied by neighboring NCCs and that these NCCs require canonical Wnt signaling themselves to supply the Wnt signal to the RPE. A similar mechanism was observed in the experiments by L. Henry Goodnough et al., in which they showed that cranial surface ectoderm secrets Wnts, which activates a β-catenin signaling response in the underlying cranial mesenchyme required for its own induction of Wnt expression (Figure 74) (Goodnough et al., 2014).

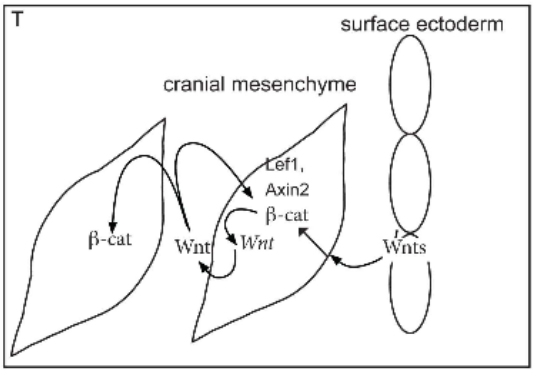

Figure 74 Wnt driving Wnt

Wnts from the surface ectoderm activate β-catenin (β-cat), which in turn activate Wnt signals in the underlying cranial mesenchyme (Goodnough et al., 2014).

Moreover, studies by Kapil Bharti et al. suggested that „BMP, ACTIVIN and WNT signaling in or around the dorso-proximal optic vesicle may stimulate MITF in the dorso-proximal neuroepithelium and initiate the retina pigmented epithelium developmental program“ (Bharti et al., 2012). MITF is a transcription factor, which has a fundamental function in the development of melanin-producing cells, including the neural-crest-derived melanocytes and the RPE (Martínez-Morales et al., 2004). During vertebrate eye development MITF is expressed in the whole optic vesicle, but later it is restricted to the RPE (at 29-30 somite stage (Tachibana, 2000) ≈ E10 (Baldock et al., 2002)), the ciliary body and the iris (Fujimura et al., 2009). The hypothesis of Bharti et al. in consideration with our hypothesis, that a Wnt signal is supplied from the NCCs, would suggest that the initiation of RPE developmental program by stimulating MITF expression does not depend on the Wnt secreted by the NCCs since we did not observe a change in expression of MITF in the RPE at any time point in either mutant. However, it appears as if the Wnt signal and a functional β-catenin for transcription, which is supplied by the NCCs is necessary for the induction of the pigmentation of the RPE.

Canonical Wnt signaling in the primary vitreous is necessary for correct development of the retina

At E18.5, staining for Brn3a, Pax6 and NF revealed the expected patterning of the retina in control eyes and an altered distribution in β-catenin mutant embryos.

In both mutants the NF expressing horizontal cells were reduced in the inner layer of the retina. However, the ganglion cell layer in all mouse types had the same amount of ganglion cells marked by Brn3a. Moreover, an increase in Pax6-positive retinal progenitor cells could be observed in both mutants.

Furthermore cCasp3 staining at E18.5 showed that there were more dying cells present in the retina of either mutant. These cells were located in the inner layer of the retina in both mutants.

These findings put together with the fact that the primary vitreous persists, what in turn has to be the result of an incorrect β-catenin respectively Wnt signaling pathway, let us speculate that the environment of cells within the retina is not suitable. Possibly this could be due to circumstances such as that there is decreased pressure in the eye or that the blood supply and the signals it carries are insufficient due to the not correctly built primary vitreous hyaloid vascular system.

It could however, also be plausible that the persistent primary vitreous emits signals that influence the proper retina development.

5.3.6.3. Potency and limitations

The mouse line created by Tomas Valenta et al. (Valenta et al., 2011) gave the new possibility to look at differences between the adhesion and transcription function of β-catenin. The aim of this project was to determine if phenotypes derived from complete loss of β-catenin in NCCs giving rise to structures of the eye differ from those in which Wnt-signaling was inhibited, but β-catenin adhesion was preserved. No obvious difference in the displayed phenotypes could be determined between the two mouse models in this respect, with exception of the preserved corneal endothelium. In the discussion a lot of “hand-waving” hypothesis were presented. We tried to explain the results of our findings by comparing them to existing literature. Most literature looked at a wide range of time points, whereas we only looked at E12.5 and E18.5. Therefore a comparison with other results was often difficult. Nevertheless, we described the end result of the eye development in these two mutants as well as we could. Since we only looked at a single mouse for every type at each age in this experiment to acquire a first impression of the differences between the two mutants, the results were not evaluated statistically. Due to the given time quota of this thesis we did not have the possibility to increase the number of analyzed embryos or look at any further developmental stages.

5.3.6.4. Importance of the study / Implications

Below are described two inherited diseases, which have a known connection to some of the tested factors in our experiment. The connection to the canonical Wnt/β-catenin pathway may have a relevant influence on the expression of the factors in the equivalent disease. With the understanding of the development may also arise possibilities for a treatment pre-birth.

Axenfeld-Rieger syndrome

In the Axenfeld-Rieger syndrome (ARS) the anterior eye segment shows structural malformations at birth (1:200'000 birth (Kunze, 2010), autosomal-dominant (Schlote and Rohrbach, 2004)), for example: Iridocorneal adhesions, megalocornea, loss of retinal ganglion cells, local degradation of the retina, completely degenerated optical nervehead (Figure 75). Defects in teeth and umbilicus are often part of ARS. 50%-75% (Kunze, 2010) of the patients develop glaucoma in addition. Pitx2 seems to be the major gene associated to ARS, despite relevance of Foxc1 and Pax6. There is also a wide range of variability in severity and manifestation. 40% of the patients lack any of the known chromosomal aberrations or known gene mutations, so there is evidence in finding more associated factors (Hjalt and Semina, 2005).

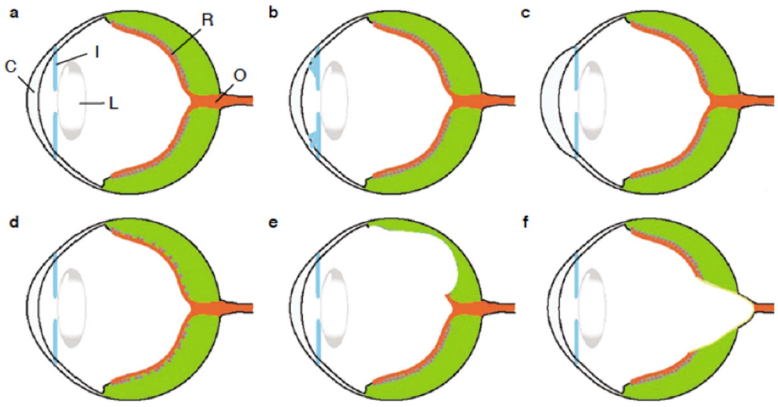

Figure 75 Ocular phenotypes of Axenfeld-Rieger syndrome

Some ocular phenotypes of Axenfeld-Rieger syndrome: (a) healthy eye, (b) iridocorneal adhesions, (c) megalocornea, (d) loss of retinal ganglion cells, (e) local degradation of the retina, (f) completely degenerated optical nervehead. C: cornea, I: iris, L: lens, R: retina, O: optical nervehead (Hjalt and Semina, 2005).

Persistent hyperplastic primary vitreous

This congenital disease occurs in infancy and childhood (Zhang et al., 2008), is very rarely and mostly unilateral (Lang, 2014). A pigmented retrolental mass tissue is caused by a persistent hyperplastic primary vitreous vasculature in the vitreous body. The retrolental mass tissue attaches to the inner neuroretina and/or to the posterior surface of the lens. That leads to abnormalities, such as retinal folds, retinal detachment, abnormal retinal lamination and lens destruction, resulting in vision loss up to blindness (Zhang et al., 2008). The pathogenesis is still unclear (Zhang et al., 2008).

5.3.6.5. Unanswered questions

It must be pointed out that β-catenin is an important factor of the Wnt pathway, so that our work only scratches the surface of what could be found in the eye region in the future. According to this, the questions give also only a rough overview.

Is the fusion of the embryonic fissure a downstream target of Wnt signaling in NCCs and important for the proper progression of the secondary vitreous? Is the hyaloid vascular system development depending on further Wnt signals from lens and/or retina? How is the correct appearance of the lens involved in transmission of signals between lens and retina respectively correct pressure in an inflated eye?

Does the proper development of the endothelium and stroma of the cornea depend on Wnt signaling or does the mode of adhesion vary from a β-catenin mediated adhesion in corneal endothelium to a Pitx2 mediated in the epithelium?

Is Wnt signaling the initiator of pigmentation of the RPE?

To answer these questions and thereby verify the development of the eye further experiments are needed, which may help to treat inherited diseases in the future.

5.3.7. Acknowledgements

First I would like to thank Prof. Dr. Lukas Sommer for the opportunity to do this interesting thesis in his research group, even though the conditions from my faculty were very different to those of their own master students of the MNF.

A big thanks is also given to Max Gay (Doctoral student PhD), who supported me well and with a lot of motivation.

For helping me in several technical things I would also like to thank Arianna Baggiolini (Doctoral student PhD), Charlotte Burger, Annika Geminn and Jessica Häusel (Technicians).

6. Discussion and outlook

6.1. The β-catenin-dm protein can preserve cadherin mediated cell-cell adhesion and inhibit TCF/Lef transactivation, but can it do more?

We were able demonstrate that the mutated version of the β-catenin protein, β-catenin-dm, maintains the ability to participate in the cadherin adhesion complex and thus preserve integrity of epithelial tissue dependent on this form of adhesion, such as the dorsal neural tube. Furthermore, we could show that downstream targets of Wnt signaling, which are either induced or maintained by TCF transcription, are lost in tissues only expressing the β-catenin-dm. These factors include CyclinD1 and Pax3 in the dorsal neural tube, Krox20, Lef1 and Neurog2 in the sensory lineage of trunk NCSCs as well as Pitx2 in ocular NCSCs. In addition the output from the Wnt-reporter *BAT-gal* was also lost in these tissues. These findings validated what was hoped to be achieved through this model. Interestingly, it appears as if the β-catenin-dm protein preserves at least one further function of the wild type protein. We concluded this notion by showing that we could not reproduce the sensory phenotype of *βcat-Null* animals in *βcat-Sig αcat-Adh* embryos, such as the loss of Neurog1 at E10.5 and the deficit of correct cell cycle progression at E12.5 in DRG progenitors. We excluded the possibility of β-catenin-dm having a dominant negative effect as heterozygous animals for the *Ctnnb1*^{dm} allele displayed no phenotype. We believe, however, that β-catenin-dm preserves the ability to de-repress genes, which are repressed by TCFs. This is due to the fact that the mutated β-catenin has an unimpaired binding site for TCF, in addition to the presence of TCF3 and TCF4, two known repressive TCFs, in DRG progenitors. We attempted to validate our hypothesis by biochemical studies.

We had to quickly exclude performing a Western blot on neural crest explants of *βcat-Sig* mutants as the yield of cell numbers of a single neural crest explant is very low and we would have needed to pool a massive amount of embryos. In respect to this, we considered applying our model to the replacement of β-catenin in the entire embryo using the inducible system of the *ROSA26-CreERT2* mouse line (Hameyer et al., 2007). The idea was to perform a Western blot using the tissue of the entire embryo. Cells of the embryos were dissociated using a protocol for the dissociation of planarians. We applied this protocol as we afterward wanted to fractionize the cells and a member in our lab had good working experience with this procedure during her previous work. Cell fractioning was performed using the Thermo Scientific "Subcellular Protein Fractionation Kit" to isolate cytoplasmic, membrane, cytoskeletal, nuclear free floating and chromatin bound proteins from the cells. With this protocol we would have shown whether or not β-catenin-dm and the repressors TCF3 and TCF4 are free floating in the nucleus or chromatin bound. Moreover, we would have performed immunoprecipitation to verify the binding of the mutated β-catenin to TCFs, as well as cadherins and α-catenin in a

biochemical manor. As informative and demonstrative these findings could have been, we were not able to obtain proper samples that gave any results until the last day of my work in the lab. We believe this was due to the samples yielding to little protein for detection by Western blot. We can only speculate where the error occurred in our procedures, as we did not have sufficient time to fully establish optimal procedure conditions.

In summary, aside from preventing TCF transactivation and mediating adhesion the β-catenin-dm mouse model preserves an unknown function of β-catenin. Modest biochemical experiments did not bear any useful results for the determination of this function. It is, however, very probable that further experiments will be dedicated to determining the rescued function of the β-catenin-dm by our lab or that of Konrad Basler, which generated the mouse model. We strongly expect the results from these experiments to verify our hypothesis that β-catenin-dm has the capacity of de-repressing genes repressed by TCFs. It is however thinkable that additional functions of β-catenin could come to light by an extended analysis of this mouse model. Even though this further possibility exists, I will from now refer to the unknown rescued function of β-catenin-dm as “TCF de-repression”.

6.2. Proper development of various tissues depend on the coordination of separate β-catenin functions

Our analysis of multiple embryonic tissues has made it clear that their development requires more than one function of β-catenin per tissue. Further investigation of these structures indicates that their development depends on the separate functions of β-catenin to different degrees.

6.2.1. Does the dorsal neural tube relies on all three functions of β-catenin?

The dorsal neural tube depends on β-catenin as a linking protein in the cadherin adhesion complex to preserve epithelial integrity of the dorsal neural tube and furthermore, as a TCF transactivator for the expression of the transcription factors Pax3 and Sox2, which maintain cells in an undifferentiated precursor state. In addition to this, TCF transcription also contributes to cell cycle progression by promoting expression of CyclinD1. Furthermore, we can consider that TCF de-repression also plays a part in regulating certain processes in the dorsal neural tube. In our first publication we pointed out that cells, which migrate into the neural canal upon disruption of the apical neural tube morphology in *βcat-Null* embryos, have a tendency to differentiate into neurons as they express the neuronal markers Brn3a and Dcx.

We suspected that this premature differentiation of the prior dorsal cells was due to their exposure to the different gradients of signaling factors, which regulate neural tube patterning. We did not consider that this phenotype could have been related to a further function of β-catenin, as there was no strong public awareness of TCF de-repression at the time. Looking back however it is reasonable to assume that genes necessary for neural differentiation are possibly repressed by TCF, as both TCF3 and TCF4 are expressed in the vicinity of undifferentiated precursors in the dorsal neural tube, but not in the area of differentiated neurons at E12.5 (Figure 76). To exclude the old theory of exposure to different signaling gradients for neural tube patterning, it would make sense to repeat the immunohistochemistry of the first publication on *αcat-Adh* and *αcat-Adh βcat-Sig* embryos at the corresponding ages.

Reassessment of the previously published data, now considering that β-catenin-dm maintains TCF de-repression and expression of TCF3 and TCF4 are present in the dorsal neural tube, indicates that for correct development of the dorsal neural tube to occur all three functions of β-catenin are essential. Adhesion is vital to preserve epithelial integrity, TCF transactivation is necessary for the maintenance and proliferation of undifferentiated precursors, and TCF de-repression is required to allow cells to adopt a neural fate. However, to fully validate the last assumption, further experiments would be required.

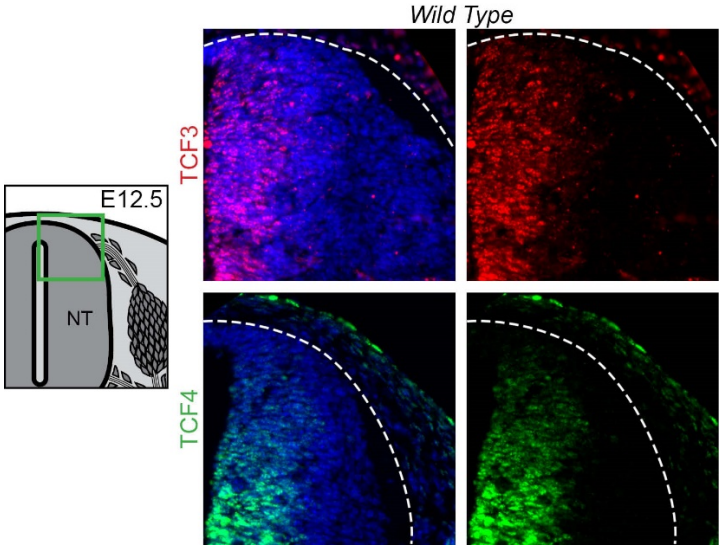

Figure 76 TCF expression in dorsal neural tube

Dashed lines frames neural tube border. Unpublished data from M. Gay

6.2.2. Distinct processes of sensory neurogenesis require different adhesion independent-functions of β-catenin

We successfully demonstrated that β-and-α-catenin encompassing cadherin adhesion junctions are not crucial for the coalescing of DRGs or for sensory fate specification. The expression of junction plakoglobin, cadherin, β-catenin and α-catenin in the DRG suggests that both desmosomes and cadherin adhesion junctions are present. However, the loss of α-catenin did not mimic ablation of β-catenin in DRGs, which indicates that the coalescing and maintenance of adhesion of the developing DRG is sufficiently sustained by desmosomes. Furthermore, no differences were determined in DRG development when comparing *αcat-Adh* to Ctrl animals or, respectively, when comparing *αcat-Adh βcat-Sig* to *βcat-Sig* embryos. These findings demonstrate that the function of β-catenin to mediate adhesion is negligible in DRG development. Identical phenotypes in both β-catenin mutants substantiated the importance of β-catenin to transactivate TCF transcription factors. The absence of the transcription factors Neurog2 and Krox2 indicated that the latter are regulated by TCF transactivation. Data from other labs further validate these conclusions, as TCF binding sites were found on the promoters of both Neurog2 and Krox20 by means of ChiP analysis (Leclerc et al., 2008; Qu et al., 2013). Moreover, cell cycle progression of an early mechanism of proliferation appeared to depend also on TCF-mediated transcription. However, even though the capability of β-catenin-dm to preserve adhesion was inconsequential, deviations of phenotypes between *βcat-Null* and βca-Sig did exist. We attributed these dissimilarities to TCF de-repression such as the expression of Neurog1 in the *βcat-Sig* and the lack thereof in the *βcat-Null*. Furthermore, we attributed the appearance of a reduced DRG in *βcat-Sig* embryos to the rescue of a mode of proliferation, which is regulated by factors, which genes depend on being de-repressed of TCFs.

6.2.2.1. Possible mechanisms of proliferation in DRG development regulated by Wnt/β-catenin signaling

We strived to determine the downstream factors of Wnt-stabilized β-catenin, which would be required for the proper execution of the early and late mechanism of proliferation of DRG progenitors. In previous work acquired in our lab, epithelial growth factor receptor (EGFR) was recognized as a regulator of late proliferation in DRG progenitors. In addition, it was shown that EGFR is very weakly present in the DRG at E10.5 and that its expression increases over time (Fuchs et al., 2009). Studies in cancer by other labs could demonstrate that EGFR is a downstream target of Wnt stabilized β-catenin and that its promoter possess two consecutive TCF4 binding sites (Guturi et al., 2012; Tan et al., 2005). The fact that in EGFR expression arises in the time window in which proper cell cycle progression is rescued in the *βcat-Sig* and

that its promoter contains binding sites of repressive TCFs made it to an optimal candidate as the cell cycle regulator was lost in *βcat-Null* animals. We attempted to stain for EGFR, the phosphorylated active form of EGFR (pEGFR) and phosphorylated extracellular-regulated kinase1/2 (pERK1/2), which serves a nuclear downstream readout of EGFR activation, in our β-catenin models. Even though we invested a lot of time in establishing functional immunohistochemistry for these factors, we were not able to acquire a usable protocol by the end of my PhD work in the lab. Members of our lab are establishing staining procedures for these factors for their own work. When proper immunohistochemistry has been established it would be nice to verify this possibility.

To narrow down likely mechanisms, which promote cell cycle progression in DRG progenitors at early stages we conducted an expanded literature search. Assessment of the literature implied transcription factor c-Myc as a conceivable Wnt-downstream target (He et al., 1998; van de Wetering et al., 2002), which regulates proliferation. c-Myc performs a dual role in G1 progression, one of which is the repression of *p21* and *p27*, whose respective proteins promote cell-cycle exit and entry into quiescence (Gartel et al., 2001; van de Wetering et al., 2002; Yang et al., 2001). In addition, c-Myc promotes Cyclin D expression (Daksis et al., 1994), which is also a Wnt target (Tetsu and McCormick, 1999), as well as a regulator of many events in G1. Accumulation of Cyclin D leads to the inhibition of Retinoblastoma (Rb) complex. The Rb inhibition increases levels of a further Wnt-target, Cyclin E. The increase of Cyclin E acts as a G1/S checkpoint, which promotes transition from G1 to S-phase (Baldin et al., 1993; Malumbres et al., 2009).

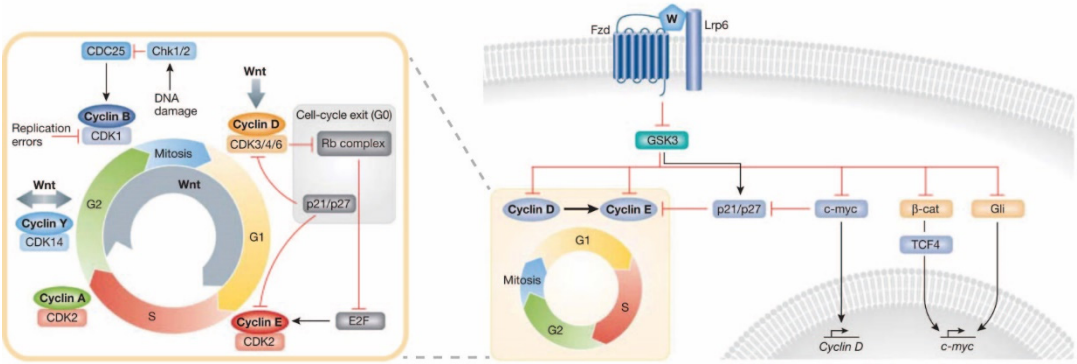

Figure 77 Overview of Wnt in cell-cycle regulation and G1- to S-phase progression

Inhibition of GSK3 by Wnt signaling regulates a central node for G1 control. GSK3 inhibits or activates the indicated proteins, all of which can contribute to G1- to S-phase progression. Adapted from Niehrs and Acebron, 2012.

We stained for c-Myc at E10.5 and E12.5 (Figure 78). Surprisingly, c-Myc was not expressed in the forming DRG at E10.5 in any of the animals. However c-Myc was present in both Ctrl and mutant animals at E12.5. Even though we did not quantify this, it appears as if the relative numbers of c-Myc-positive DRG cells is higher in the *βcat-Sig* and *βcat-Null* as in the Ctrl. At a first glance the data suggested that c-Myc expression in DRG progenitors is regulated by other mechanisms than Wnt-signaling. In addition, the relative increase of c-Myc-positive cells in mutant animals could suggest that these c-Myc expressing cells in the DRG are prone to be maintained when cut off from Wnt-signaling. Reevaluation of the reviewed literature revealed that the c-Myc promoter contains binding sites for TCF4 (He et al., 1998). Reinterpretation of the data would now suggest that c-Myc is rather a target of TCF de-repression as it is so widely expressed in the *βcat-Sig*. However, the few c-Myc-positive cells in the *βcat-Null* suggest that expression of c-Myc could be mildly promoted by alternative signaling pathways such as the one from Sonic Hedge Hog (Shh) of which c-Myc has also been shown to be a target of (Borycki et al., 2000). The responsible Shh signal could possibly be secreted from the notochord, which lies under the neural tube. If this was the case it would clarify why the virtually non-existent DRGs of the β-cat-Null are located so ventrally. As c-Myc promotes DRG progenitor maintenance, *c-Myc* transcription relies on the de-repression of TCFs. In the case of the *βcat-Null* where de-repression is also lost, Shh secreted from the notochord initiates some c-Myc expression in cells of close vicinity. I was not able to further analyze this concept due to the limited time I had left in the lab. I am aware that this hypothesis is implied by a lot of “hand-waving” assumptions. However, I still wanted to mention it to share my theoretical thoughts with others that may continue this work in the future.

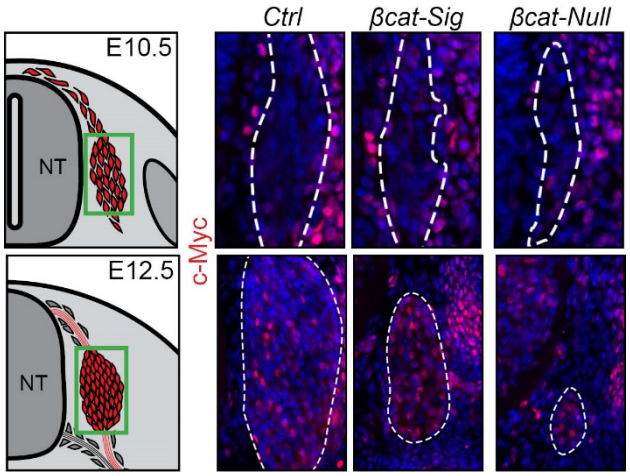

Figure 78 Expression of c-Myc in the DRG

c-Myc is not expressed in DRG progenitors at E10.5 in any of the three animals. However at E12.5 it appears as if there are relatively more c-Myc-positive cells in mutant animals as in Ctrl. Dashed lines frame in vivo fate-mapped cells. Unpublished data from M. Gay.

Despite the fact that c-Myc was not the protein we were looking for at E10.5, it should be considered as a possible further candidate for the rescue of late proliferation mechanism at E11.5. For this reason it would be profitable to analyze whether expression of c-Myc arises at this developmental stage.

Even though, we were not able to determine the definitive downstream targets of Wnt, which regulate cell cycle progression of DRG progenitors, we indicated two factors, c-Myc and EGFR, which are promising candidates of controlling late proliferation. In addition to these factors the analysis of Wnt downstream targets Cyclin D, Cyclin E and Cyclin Y (Niehrs and Acebron, 2012) could also prove profitable to consider. Diminishing levels of Lef1 in the forming DRG from E10 to E12.5, make it appealing to assume that possible factors regulating early cell cycle progression are downstream targets of Lef1 transcription. Taking this into account reduces the possible targets to be considered for researchers who would like to follow up on this work.

6.2.2.2. Is sensory neuron subtype specification directly controlled by Wnt signaling?

Aside from the previously described DRG progenitor phenotypes, the subtype specification of sensory neurons was also perturbed in mutant animals at E11.5. Subtype specification has been shown to be regulated by the expression of Neurog1 and Neurog2. These assessments were made based on Neurog1 and Neurog2 knockout studies (Ma et al., 1999). Analysis of Neurog2 knockout mice indicated that the Neurog1-mediated wave mainly gives rise to neurons expressing TrkA, but also generate TrkB- and TrkC-positive neurons (Ma et al., 1999). This was the same presetting as in the *βcat-Sig* mutant, which lost Neurog2, but preserved expression of Neurog1. The expression of all three Trks in this case was not surprising, in contrast to their presence in *βcat-Null* embryos. In the study of Ma et al. (1999), DRGs were absent due to irregular apoptosis at early stages in double knockout mice for Neurog1 and Neurog2. In our study, the βcat-null mice mimicked the loss of Neurog1 and Neurog2 expression, nonetheless these animals still expressed Trks at E11.5 and their DRGs first vanished after E12.5. The possible explanation for this unexpected phenotype required further insight into circumstances of subtype specification. Analysis of Neuog1 knockout mice gave rise to the assumption that migratory cells expressing Neurog2 would only generate TrkB- and TrkC-positive neurons (Ma et al., 1999). However, follow-up Neurog2 lineage tracing studies provided evidence that cells expressing low levels of Neurog2 later could also contribute to TrkA-positive neurons (Zirlinger et al., 2002). Taken together the data show that both waves contribute to all three subtypes to a certain degree. Moreover, the studies imply that TrkA-positive neurons that derive from cells expressing low levels of Neurog2, need to be able to express the Neurog1 transcription factor to acquire this fate. Projecting these observations

onto our results suggested that the observed loss of Neurog1 and Neurog2 in *βcat-Null* embryos, did not replicate a loss of both transcription factors to the same extent as a complete knockout did. This premise was also supported by the fact that increased apoptosis could be observed upon double knockout of Neurog1 and Neurog2 in DRG progenitors, which was not the case in the *βcat-Null* animals. In summary, we assume that expression of Neurog1 is decreased to a level at which detection was not possible by means of immunohistochemistry in *βcat-Null* animals. However, the reduced level was sufficient to promote cell survival and induce subtype specification.

We decided to further analyze the expression of the tyrosine receptor kinases Trk A, B and C at the later stages. Stainings for these factors showed that their presence varied over time in β-catenin mutant animals (Figure 79 and Figure 80). Surprisingly, even though TrkA-positive cells were present at E11.5, expression of TrkA protein as well as *TrkA* mRNA were lost in both mutant animals at E12.5 (Figure 79, data not shown). However, presence of *TrkA* mRNA was detected again in *βcat-Sig* mutants at E16.5 (Figure 80).

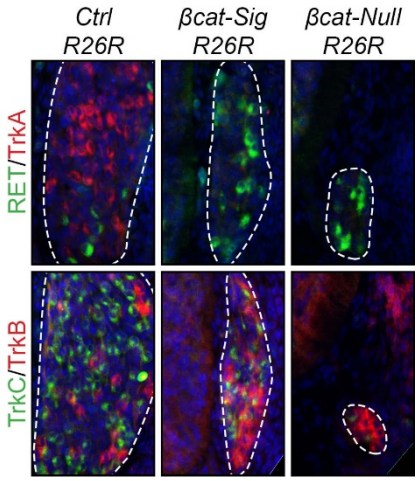

Figure 79 Sensory subtype specification at E12.5

Expression of TrkA is lost in both βcat-Sig and βcat-Null mutant embryos at E12.5. Dashed lines frame in vivo fate-mapped cells. Unpublished data from M. Gay.

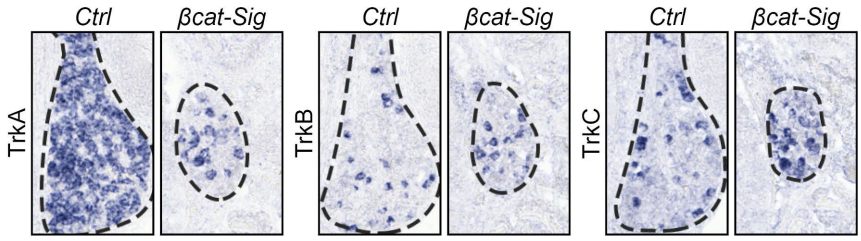

Figure 80 Sensory subtype specification at E16.5

TrkA-positive sensory neurons are present again in βcat-Sig mutants at E16.5. Dashed lines frame DRG. Unpublished data from M. Gay.

A previous study has shown that early sensory neurons express different combinations of the Trk receptors and that over time they dynamically change their expression levels (Karchewski et al., 1999). It is possible to consider that Wnt signaling is involved in the dynamic process of changing Trk expression in sensory neurons. However, analysis of Trk expression in embryos with *Wnt1-Cre* conditional ablation of Wls displayed no diffrences in Trk expression in comparison to the control (Figure 81). These results imply that if Wnt/βcatenin signaling is involved in the determination of subtype specification, the Wnt ligand is not from an autocrine source. It is likely that the possible regulating Wnt is secreted at the tissue in which the sensory axon terminals reside. However, the dorsal neural tube, where the afferent neurons enter the central nervous system could be excluded as a source, as Wnt1cre also recombines this tissue region.

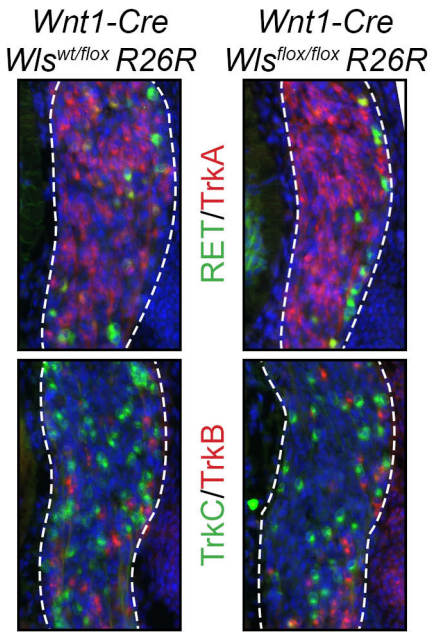

Figure 81 Sensory subtype specification of *Wnt1cre Wls* animals at E12.5

Subtype specification of sensory neurons is normal in animals in which Wls is ablated using the Wnt1-Cre recombinase. Dashed lines frame in vivo fate-mapped cells. Unpublished data from M. Gay.

It is possible, however, that canonical Wnt signaling does not directly contribute to the determination of sensory subtypes. A preceding publication has reported that neurotrophins have an instructive role in sensory specification. Furthermore they demonstrated that early manipulation of Trk receptor expression leads altered sensitivity of the cells to neurotrophic factors. The change in neurotrophin stimulation leads these cells to acquire an alternative sensory fate to the one they were supposed to assume (Moqrich et al., 2004). When considering these findings, it is possible that the sensory neurons of the *βcat-Sig* mutant dynamically change their subtype specification, because they have an altered Trk expression

at early developmental stages due to the misregulation of Neurog1 and Neurog2. To follow up on this, we attempted to ablate and/or replace β-catenin in the migratory rather than premigratory NCSCs using the *Sox10-Cre* mouse line, in hopes of rescuing expression of Neurog1 and Neurog2. Immunohistochemistry for Neurog2 at E9 and Neurog1 at E10.5 showed that the expression of these factors was preserved in both mutants (Figure 82), making it an adequate model to determine whether the Wnt signaling influences subtype specification directly independent without an altered expression of Neurog1 and Neurog2.

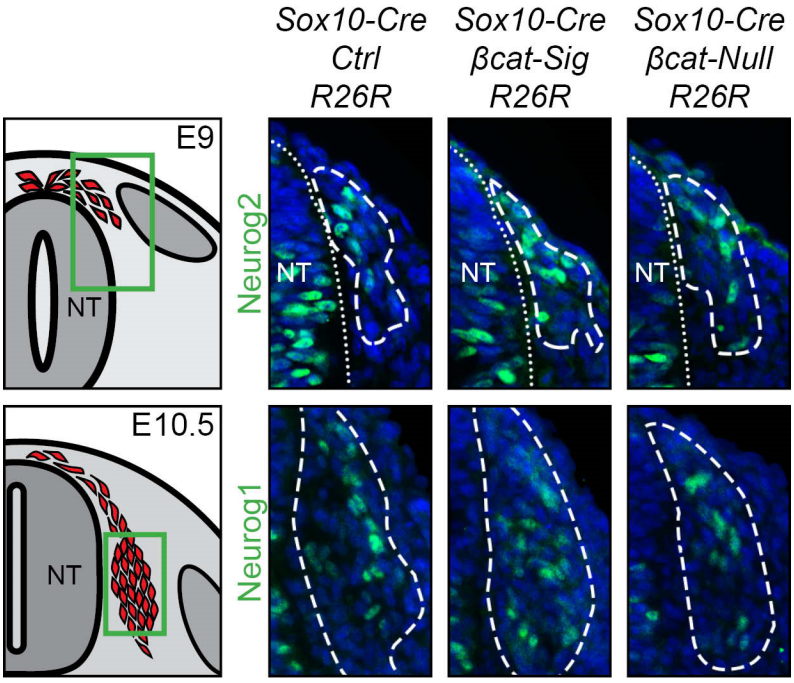

Figure 82 Neurog1 and Neurog2 are rescued when using *Sox10-Cre* mouse model

Dashed lines frame in vivo fate-mapped cells. Unpublished data from M. Gay.

Embryos at ages E12.5 and E16.5 of these *Sox10-Cre* animals were extracted and cryo-preserved for analysis. Due to limited amount of time, it was never possible to prepare sections of these animals for further examination. These embryos would also be of value for the analysis to determine the rescued proliferation mechanism at late stages, as early cell cycle progression appears to proceed regularly at E10.5 (Figure 83).

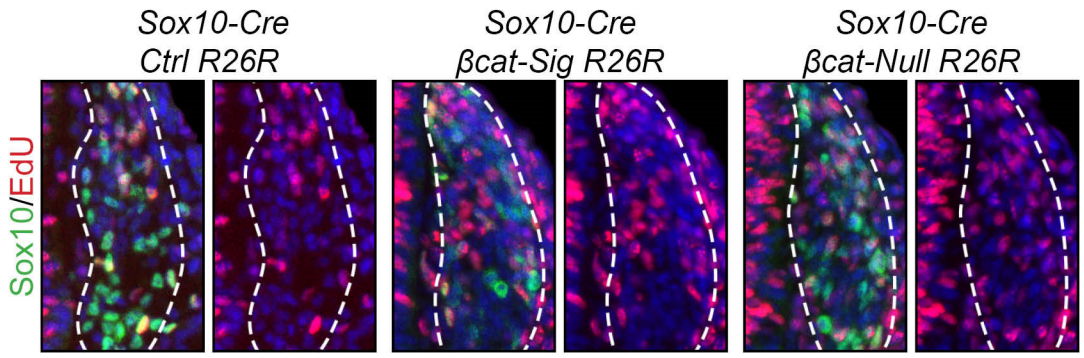

Figure 83 Early cell cycle progression is rescued in the *Sox10-Cre* mutants

Dashed lines frame in vivo fate-mapped cells. Unpublished data from M. Gay

Even though we have not verified whether late cell cycle progression is also perturbed in the *Sox10-Cre βcat-Null* animals at later stages, preliminary data from my predecessor Lisette Paratore-Hari suggests that this is the case. Her work showed that the DRG of *Sox10-Cre βcat-Null* mutants are reduced in size at E11.5. We expect that the DRGs of *Sox10-Cre βcat-Sig* animals will be normal in size, as the late proliferation mechanism is rescued in these animals. Overall, analysis of the Sox10cre embryos would offer a more in-depth insight of late DRG development in terms of DRG cell cycle progression and the presence of different sensory sublineages.

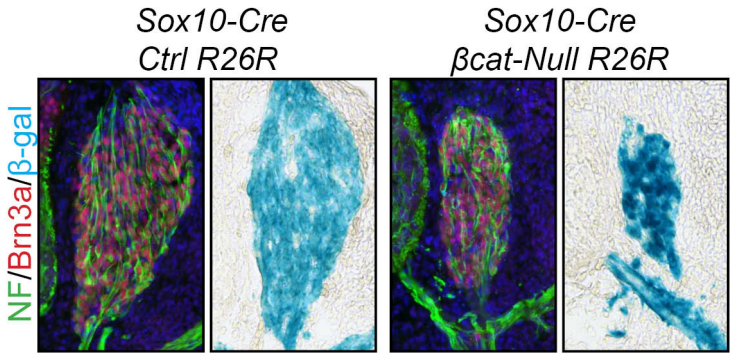

Figure 84 DRGs of *Sox10-Cre βcat-Null* embryos are reduced in size at E11.5

Unpublished data from L. Paratore-Hari

6.3. Functions of β-catenin in ocular NCSCs is important for NCSC derived tissue, as well as for non-NCSC derived tissue

Our data of Wnt/β-catenin signaling in ocular NCSCs at early stages was consistent with previous published work in which Wnt signaling was shown to be important for the maintenance of Pitx2 expression (Zacharias and Gage, 2010). Moreover, the authors related the inhibition of the fusion of the optical neural fissure to the loss of Pitx2. In our study we could perceive the same phenotype in both mutant animals. Furthermore, we observed a loss of pigmentation in the RPE, which is a structure not recombined by *Wnt1-Cre*. Activity of the Wnt-reporter *BAT-gal* was also lost in the RPE, which lead us to associate the inexistent pigmentation with the loss of Wnt activity in these cells, since Wnt signaling in the RPE has been shown to be necessary for pigmentation (Fujimura et al., 2009). In our work we associated this phenotype to a possible loss of Wnt secretion from the NCSCs which give rise to the choroid sclera. Moreover, we speculated that the initiation of the Wnt secretion depends on the capability of NCSCs to respond to a Wnt signal themselves. However, preliminary analysis of whole mounted *Wnt1-Cre* $Wls^{flox/flox}$ animals was performed after the completion of the master Thesis. The observations did not display a change in RPE pigmentation as in β-catenin mutants (Figure 85). This suggested that the NCSCs are not supplying Wnt to the RPE. These results give us reason to assume, that Wnt signaling is important for NCSCs to secrete factors, which induce, support, maintain or amplify the response of RPE cells to Wnt. One of these factors could possibly be R-spondins, which bind to Lgr transmembrane proteins to amplify Wnt signals on responding cells (Barker et al., 2013; Birchmeier, 2011) (Figure 86).

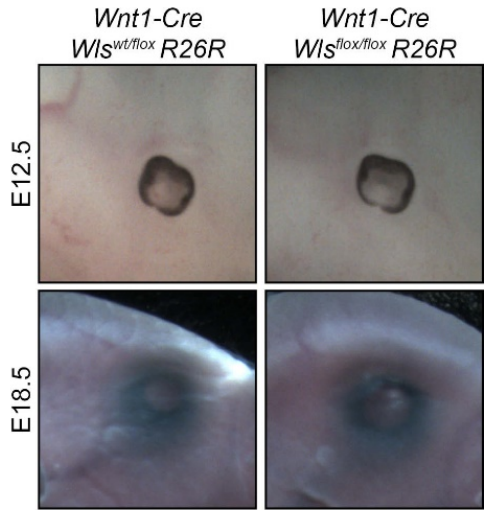

Figure 85 Pigmentation of RPE is not lost in *Wnt1cre* $Wls^{flox/flox}$ animals

Unpublished data from M. Gay

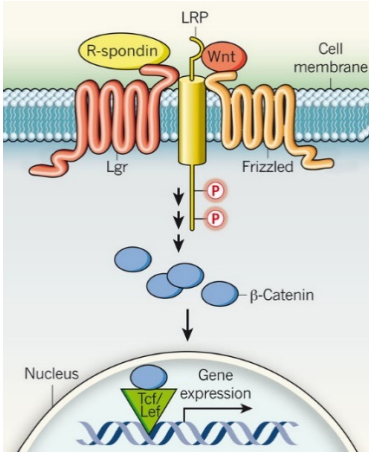

Figure 86 R-spondin reinforces Wnt signaling

R-spondins activate Lgr membrane proteins to recruit the LRP–Frizzled receptor complex, which leads them to bind to Wnt ligands, reinforcing Wnt signaling following phosphorylation of LRP (Birchmeier, 2011).

Investigation of more mature developmental stages have demonstrated that the *βcat-Sig* mouse model shows great promise in determining the importance of Wnt signaling in ocular NCSCs at late stages. In the past analysis of cranial NCSC derivatives was very difficult at late stages of development in *βcat-Null* animals, as distinguishing cranial structures becomes increasingly harder with time from E14.5 on. The *βcat-Sig* mutant preserved more distinct cranial structures than the *βcat-Null* at E18.5. The preservation of structural components such as bone and cartilage could have an important impact on eye development independent of Wnt-signaling. The preservation of these structures could be due to both preserved adhesion as well as TCF de-repression, however to determine this a separate study would have to be performed, which includes the comparison to *αcat-Adh* and *αcat-Adh βcat-Sig* mutants.

There were three main differences in ocular development between the two β-catenin models. First of all, the corneal epithelium and a weak corneal stroma were present in the *βcat-Sig* in contrast to *βcat-Null* animals in which we could find no corneal-like structures. Secondly, we observed increased apoptosis in the ganglion cell layer of the *βcat-Null* embryos. In addition, we noted a loss of the Horizontal cells in the retina of *βcat-Sig* mutants. These cells were however present in the *βcat-Null* animals. We believe that the rescue of the corneal structures is related to the property of the *βcat-Sig* cells to preserve cadherin mediated adhesion. The other two divergences could possibly be due to the alteration of instructive signals designated for the retina, which are supplied by the vitreous. These instructive signals from the vitreous derived from ocular NCSCs would then be regulated by genes, which are repressed by TCF. The preliminary discussion of these results is very hypothetical. We suggest that further investigation of the β-catenin mutants and α-catenin adhesion mutants could be performed for a more substantial analysis of the importance of β-catenin in ocular NCSC development.

6.4. Spin-off projects

In this section of this thesis I will present additional data, which we acquired from our experiments, but never followed up on, due to the lack of time.

6.4.1. What are the functions of β-catenin in melanocyte differentiation?

Melanocytes are also derivatives of the trunk NCSC. It has been shown that melanoblasts, the precursors of melanocytes are lost when conditional ablation of β-catenin is performed using the *Wnt1-Cre* (Hari et al., 2002). In this respect we performed a preliminary analysis using our β-catenin-dm mouse model to see whether there was a difference in this corresponding phenotype. Lineage tracing with additional immunohistochemistry for the melanoblast markers Sox10 and MITF show that at E11.5 melanoblasts are not lost in the *βcat-Sig* mutant (Figure 87). The number of melanoblasts in the *βcat-Sig* was slightly less than in the Ctrl. Furthermore, these melanoblasts did not lose their expression of other melanoblast markers such as Pax3 or DCT (data not shown). It is plausible to consider that de-repression of TCF is the regulating factor for trunk NCSCs to adapt a melanoblast fate. Of course cadherin mediated adhesion could be necessary for the emigration of precursor cells from the neural tube, but as earlier NCSCs did not have reduced migratory numbers we believe it is safe to assume that cadherin mediated adhesion is neither vital for emigration of NCSCs nor crucial for the differentiation of NCSCs into melanoblasts. In situ hybridization analyses at E12.5 for DCT performed by my predecessor Lissette Paratore-Hari displayed a decrease in melanocyte numbers throughout *βcat-Sig* mutants (Figure 88). These findings would suggest that proliferation of melanoblasts depend on TCF transactivation during and after migration. These hypotheses are educated guesses meant to advice the subsequent researchers of this project in which direction one should pursue this work.

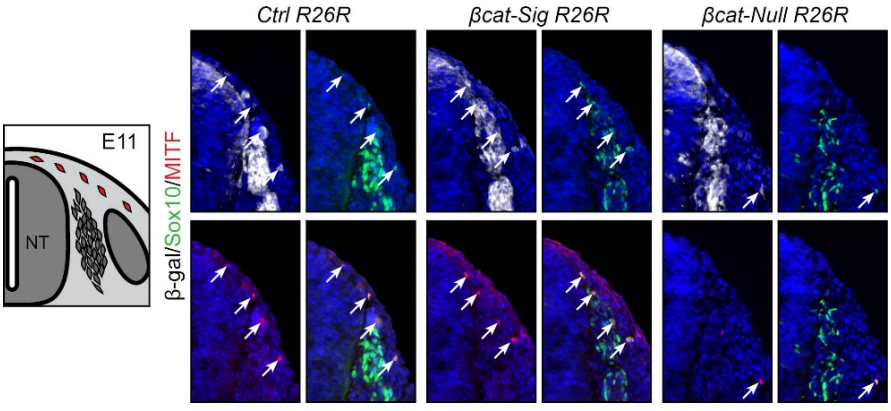

Figure 87 The melanocyte lineage is rescued in the *βcat-Sig* mutant animals at E11.5

Immunohistochemistry for Sox10 and MITF shows that melanoblasts are present almost to the same extent in βcat-Sig mutants as in Ctrl animals. Furthermore, the almost complete loss of melanoblasts in the βcat-Null is consensus with previously published work. Unpublished data M.Gay.

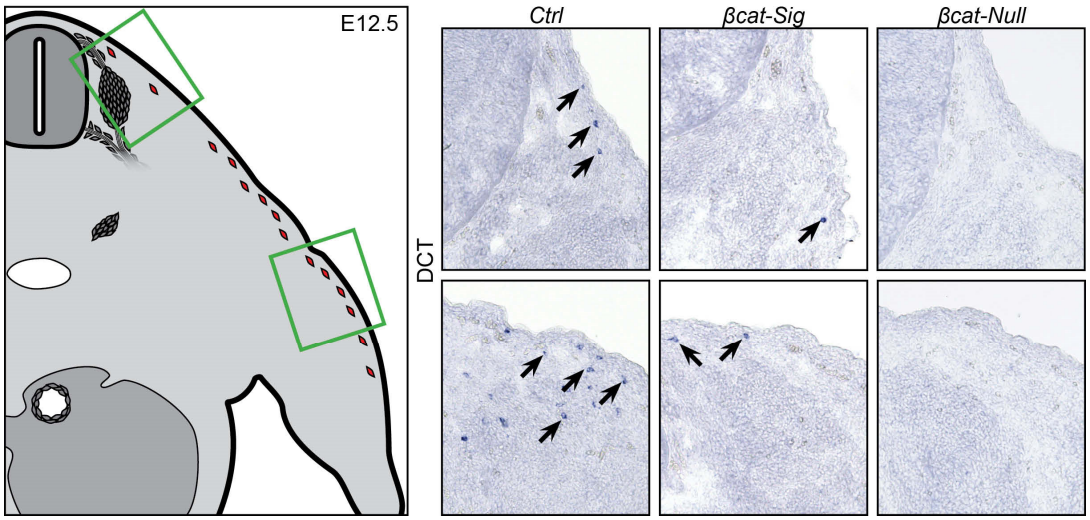

Figure 88 Melanoblasts are reduced in number in *βcat-Sig* mutants at E12.5

In situ hybridization analyses with melanoblast-specific DCT riboprobe, shows that less melanoblast can be found throughout the βcat-Sig embryos at E12.5, whereas in βcat-Null animals no melanoblasts could be located. Unpublished data L. Paratore-Hari.

6.4.2. Adhesion versus signaling in development of the mid- and hindbrain

The *Wnt1-Cre* mouse line also recombines the dorsal neural tube, which will give rise to structures of the brain, such as the hind- and midbrain. In this section we will point out the obvious phenotype that we observed in the β-catenin mutants compared to the α-catenin mutants at E12.5 (Figure 89). When looking at the whole mount embryos it is not possible to distinguish the border between the mid-and hindbrain in the *βcat-Sig* mutant. Even though these structures appear to be inadequately developed, they have a size comparable to those of *Ctrl* animals, as opposed to the *βcat-Null* animals which display a severe decrease in mid- and hindbrain size. The *αcat-Adh* mutant displays a completely different phenotype. In these embryos a tumor-like clump could be seen in the regions of the mid- and hindbrain. Interestingly, however, this growth does not arise when the *αcat-Adh* is crossed with the *βcat-Sig* mutant.

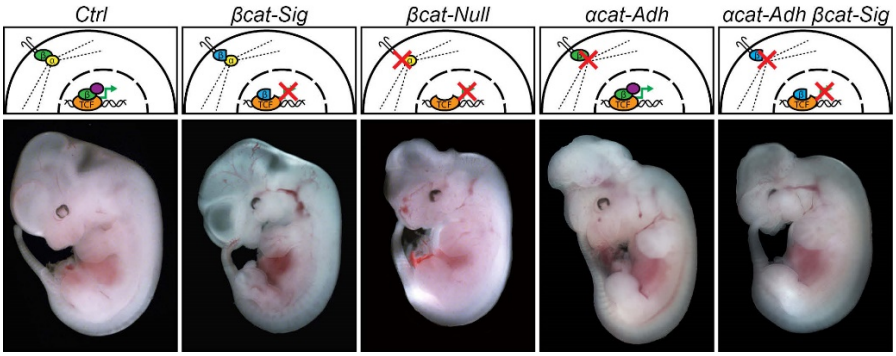

Figure 89 β-catenin and α-catenin mutant embryos at E12.5

Unpublished data M. Gay.

Without going into detail, we would like to suggest another possible direction which could show promise. Previous work in which α-catenin was deleted using a nestin-promoter-driven Cre recombinase, which is expressed in the central nervous system progenitors starting at E10.5 was the bases for our hypothesis (Lien et al., 2006). Lien et al. witnessed a massive hyperplasia in the mutant animal brains and related this phenotype to a negative feedback loop model, which regulates the cell proliferation in the cerebral cortex (Figure 90). In this model increase in cell density is translated into a down regulation of hedgehog (Hh) signaling, which in turn decreases cell proliferation. Abnormal decrease in cell density by the loss of α-catenin translates into activation of the Hh pathway and cell proliferation is accelerated subsequently. It is tempting to think that the same "crowd control" model is responsible for the phenotype, which we observed in the *αcat-Adh* mutant. If this is the case then it is plausible to assume that the cell proliferation is regulated by factors down stream of TCF transactivation, as *αcat-Adh βcat-Sig* mutants display a visual identical phenotype as βcat-null animals. In respect to this project it would be also interesting to verify this hypothesis and assess the possible regulator of cell proliferation down stream of TCF transactivation.

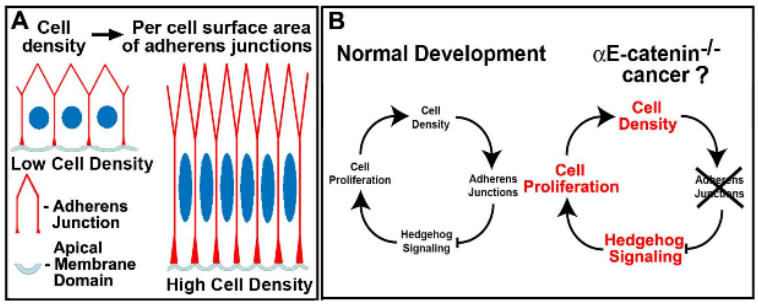

Figure 90 Model of "crowd control" negative feedback signaling loop regulating cell proliferation

(A) Model showing linear relationship between cell density and per cell surface area occupied by adherens junctions.(B) "crowd control" model": Increase in cell density is sensed by extension of adherens junctions, which negatively regulate the hedgehog pathway and decrease cell proliferation. The denser the crowd, the lower the rates of cellular accumulation. The sparser the crowd, the higher the rates of cellular accumulation (Lien et al., 2006)

7. References

Agalliu, D., Takada, S., Agalliu, I., McMahon, A.P., and Jessell, T.M. (2009). Motor neurons with axial muscle projections specified by Wnt4/5 signaling. Neuron *61*, 708-720.

Angers, S., and Moon, R.T. (2009). Proximal events in Wnt signal transduction. Nat Rev Mol Cell Biol *10*, 468-477.

Archbold, H.C., Yang, Y.X., Chen, L., and Cadigan, K.M. (2012). How do they do Wnt they do?: regulation of transcription by the Wnt/β-catenin pathway. Acta Physiologica (Oxford, England) *204*, 74-109.

Arnold, S.J., and Robertson, E.J. (2009). Making a commitment: cell lineage allocation and axis patterning in the early mouse embryo. Nat Rev Mol Cell Biol *10*, 91-103.

Arnold, S.J., Stappert, J., Bauer, A., Kispert, A., Herrmann, B.G., and Kemler, R. (2000). Brachyury is a target gene of the Wnt/beta-catenin signaling pathway. Mech Dev *91*, 249-258.

Backman, M., Machon, O., Mygland, L., van den Bout, C.J., Zhong, W., Taketo, M.M., and Krauss, S. (2005). Effects of canonical Wnt signaling on dorso-ventral specification of the mouse telencephalon. Dev Biol *279*, 155-168.

Baggiolini, A., Varum, S., Mateos, J.M., Bettosini, D., John, N., Bonalli, M., Ziegler, U., Dimou, L., Clevers, H., Furrer, R.*, et al.* (2015). Premigratory and migratory neural crest cells are multipotent in vivo. Cell Stem Cell *16*, 314-322.

Baldin, V., Lukas, J., Marcote, M.J., Pagano, M., and Draetta, G. (1993). Cyclin D1 is a nuclear protein required for cell cycle progression in G1. Genes & development *7*, 812-821.

Baldock, R., Bard, J., Davidson, D., and Lawson, K. (2002). 3D digital Atlas | Staiging Criteria (The Medical Research Council & University of Edinburgh).

Banziger, C., Soldini, D., Schutt, C., Zipperlen, P., Hausmann, G., and Basler, K. (2006). Wntless, a conserved membrane protein dedicated to the secretion of Wnt proteins from signaling cells. Cell *125*, 509-522.

Barker, N., Tan, S., and Clevers, H. (2013). Lgr proteins in epithelial stem cell biology. Development *140*, 2484-2494.

Baroffio, A., Dupin, E., and Le Douarin, N.M. (1991). Common precursors for neural and mesectodermal derivatives in the cephalic neural crest. Development *112*, 301-305.

Bartscherer, K., Pelte, N., Ingelfinger, D., and Boutros, M. (2006). Secretion of Wnt ligands requires Evi, a conserved transmembrane protein. Cell *125*, 523-533.

Basler, K., and Struhl, G. (1994). Compartment boundaries and the control of Drosophila limb pattern by hedgehog protein. Nature *368*, 208-214.

Bharti, K., Gasper, M., Ou, J., Brucato, M., Clore-Gronenborn, K., Pickel, J., and Arnheiter, H. (2012). A regulatory loop involving PAX6, MITF, and WNT signaling controls retinal pigment epithelium development. PLoS genetics *8*, e1002757.

Birchmeier, W. (2011). Stem cells: Orphan receptors find a home. Nature *476*, 287-288.

Bischof, J., Maeda, R.K., Hediger, M., Karch, F., and Basler, K. (2007). An optimized transgenesis system for Drosophila using germ-line-specific phiC31 integrases. Proceedings of the National Academy of Sciences of the United States of America *104*, 3312-3317.

Borycki, A., Brown, A.M., and Emerson, C.P., Jr. (2000). Shh and Wnt signaling pathways converge to control Gli gene activation in avian somites. Development *127*, 2075-2087.

Brault, V., Moore, R., Kutsch, S., Ishibashi, M., Rowitch, D.H., McMahon, A.P., Sommer, L., Boussadia, O., and Kemler, R. (2001). Inactivation of the beta-catenin gene by Wnt1-Cre-mediated deletion results in dramatic brain malformation and failure of craniofacial development. Development (Cambridge, England) *128*, 1253-1264.

Bronner-Fraser, M., and Fraser, S. (1989). Developmental potential of avian trunk neural crest cells in situ. Neuron *3*, 755-766.

Bronner-Fraser, M., and Fraser, S.E. (1988). Cell lineage analysis reveals multipotency of some avian neural crest cells. Nature *335*, 161-164.

Bronner, M. (2015). Confetti clarifies controversy: neural crest stem cells are multipotent. Cell Stem Cell *16*, 217-218.

Bronner, M.E. (2012). A career at the interface of cell and developmental biology: a view from the crest. Mol Biol Cell *23*, 4151-4153.

Cadigan, K.M., and Liu, Y.I. (2006). Wnt signaling: complexity at the surface. J Cell Sci *119*, 395-402.

Carpenter, A.C., Rao, S., Wells, J.M., Campbell, K., and Lang, R.A. (2010). Generation of mice with a conditional null allele for Wntless. Genesis (New York, NY: 2000) *48*, 554-558.

Chauvet, S., and Rougon, G. (2008). Semaphorins deployed to repel cell migrants at spinal cord borders. J Biol *7*, 4.

Chodaparambil, J.V., Pate, K.T., Hepler, M.R., Tsai, B.P., Muthurajan, U.M., Luger, K., Waterman, M.L., and Weis, W.I. (2014). Molecular functions of the TLE tetramerization domain in Wnt target gene repression. EMBO J *33*, 719-731.

Christova, T., Mojtahedi, G., and Hamel, P.A. (2010). Lymphoid enhancer factor-1 mediates loading of Pax3 to a promoter harbouring lymphoid enhancer factor-1 binding sites resulting in enhancement of transcription. Int J Biochem Cell Biol *42*, 630-640.

Clevers, H. (2006). Wnt/beta-catenin signaling in development and disease. Cell *127*, 469-480.

Cordero, D.R., Brugmann, S., Chu, Y., Bajpai, R., Jame, M., and Helms, J.A. (2011). Cranial neural crest cells on the move: their roles in craniofacial development. Am J Med Genet A *155A*, 270-279.

Crane, J.F., and Trainor, P.A. (2006). Neural crest stem and progenitor cells. Annu Rev Cell Dev Biol *22*, 267-286.

Cvekl, A., and Tamm, E.R. (2004). Anterior eye development and ocular mesenchyme: new insights from mouse models and human diseases. Bioessays *26*, 374-386.

Daksis, J.I., Lu, R.Y., Facchini, L.M., Marhin, W.W., and Penn, L.J. (1994). Myc induces cyclin D1 expression in the absence of de novo protein synthesis and links mitogen-stimulated signal transduction to the cell cycle. Oncogene *9*, 3635-3645.

Danielian, P.S., Muccino, D., Rowitch, D.H., Michael, S.K., and McMahon, A.P. (1998). Modification of gene activity in mouse embryos in utero by a tamoxifen-inducible form of Cre recombinase. Current biology: CB *8*, 1323-1326.

Daniels, D.L., and Weis, W.I. (2005). β-catenin directly displaces Groucho/TLE repressors from Tcf/Lef in Wnt-mediated transcription activation. Nature Structural & Molecular Biology *12*, 364-371.

DasGupta, R., Rhee, H., and Fuchs, E. (2002). A developmental conundrum: a stabilized form of beta-catenin lacking the transcriptional activation domain triggers features of hair cell fate in epidermal cells and epidermal cell fate in hair follicle cells. J Cell Biol *158*, 331-344.

Draganova, K., Zemke, M., Zurkirchen, L., Valenta, T., Cantu, C., Okoniewski, M., Schmid, M.T., Hoffmans, R., Gotz, M., Basler, K.*, et al.* (2015). Wnt/beta-catenin signaling regulates sequential fate decisions of murine cortical precursor cells. Stem Cells *33*, 170-182.

Dräger, U.C., and Hofbauer, A. (1984). Antibodies to heavy neurofilament subunit detect a subpopulation of damaged ganglion cells in retina. Nature *309*, 624-626.

Fedtsova, N.G., and Turner, E.E. (1995). Brn-3.0 expression identifies early post-mitotic CNS neurons and sensory neural precursors. Mech Dev *53*, 291-304.

Filali, M., Cheng, N., Abbott, D., Leontiev, V., and Engelhardt, J.F. (2002). Wnt-3A/beta-catenin signaling induces transcription from the LEF-1 promoter. The Journal of biological chemistry *277*, 33398-33410.

Fu, J., Ivy Yu, H.-M., Maruyama, T., Mirando, A.J., and Hsu, W. (2011). Gpr177/mouse Wntless is essential for Wnt-mediated craniofacial and brain development. Developmental Dynamics: An Official Publication of the American Association of Anatomists *240*, 365-371.

Fuchs, S., Herzog, D., Sumara, G., Büchmann-Møller, S., Civenni, G., Wu, X., Chrostek-Grashoff, A., Suter, U., Ricci, R., Relvas, J.B.*, et al.* (2009). Stage-specific control of neural crest stem cell proliferation by the small rho GTPases Cdc42 and Rac1. Cell Stem Cell *4*, 236-247.

Fuhrmann, S. (2008). Wnt signaling in eye organogenesis. Organogenesis *4*, 60-67.

Fujimura, N., Taketo, M.M., Mori, M., Korinek, V., and Kozmik, Z. (2009). Spatial and temporal regulation of Wnt/beta-catenin signaling is essential for development of the retinal pigment epithelium. Dev Biol *334*, 31-45.

Gage, P.J., Qian, M., Wu, D., and Rosenberg, K.I. (2008). The canonical Wnt signaling antagonist DKK2 is an essential effector of PITX2 function during normal eye development. Dev Biol *317*, 310-324.

Gage, P.J., Rhoades, W., Prucka, S.K., and Hjalt, T. (2005). Fate maps of neural crest and mesoderm in the mammalian eye. Invest Ophthalmol Vis Sci *46*, 4200-4208.

Gartel, A.L., Ye, X., Goufman, E., Shianov, P., Hay, N., Najmabadi, F., and Tyner, A.L. (2001). Myc represses the p21(WAF1/CIP1) promoter and interacts with Sp1/Sp3. Proceedings of the National Academy of Sciences of the United States of America *98*, 4510-4515.

Gonsalves, F.C., and DasGupta, R. (2008). Function of the wingless signaling pathway in Drosophila. Methods Mol Biol *469*, 115-125.

Goodnough, L.H., Dinuoscio, G.J., Ferguson, J.W., Williams, T., Lang, R.A., and Atit, R.P. (2014). Distinct requirements for cranial ectoderm and mesenchyme-derived wnts in specification and differentiation of osteoblast and dermal progenitors. PLoS genetics *10*, e1004152.

Graham, T.A., Weaver, C., Mao, F., Kimelman, D., and Xu, W. (2000). Crystal structure of a beta-catenin/Tcf complex. Cell *103*, 885-896.

Grigoryan, T., Wend, P., Klaus, A., and Birchmeier, W. (2008). Deciphering the function of canonical Wnt signals in development and disease: conditional loss- and gain-of-function mutations of beta-catenin in mice. Genes & development *22*, 2308-2341.

Groscurth, P. (2011). Praktikum Histologie I - Kursunterlagen (Anatomisches Institut der Universität Zürich).

Groscurth, P., Filgueira, L., and Slomianka, L. (2010-2013). Histologie (OLAT - VAM der Universität Zürich: Anatomisches Institut Universität Zürich, Unité d' Anatomie Université de Fribourg).

Guturi, K.K., Mandal, T., Chatterjee, A., Sarkar, M., Bhattacharya, S., Chatterjee, U., and Ghosh, M.K. (2012). Mechanism of beta-catenin-mediated transcriptional regulation of epidermal growth factor receptor expression in glycogen synthase kinase 3 beta-inactivated prostate cancer cells. The Journal of biological chemistry *287*, 18287-18296.

Haegel, H., Larue, L., Ohsugi, M., Fedorov, L., Herrenknecht, K., and Kemler, R. (1995). Lack of beta-catenin affects mouse development at gastrulation. Development *121*, 3529-3537.

Hameyer, D., Loonstra, A., Eshkind, L., Schmitt, S., Antunes, C., Groen, A., Bindels, E., Jonkers, J., Krimpenfort, P., Meuwissen, R.*, et al.* (2007). Toxicity of ligand-dependent Cre recombinases and generation of a conditional Cre deleter mouse allowing mosaic recombination in peripheral tissues. Physiological genomics *31*, 32-41.

Harada, T., Harada, C., and Parada, L.F. (2007). Molecular regulation of visual system development: more than meets the eye. Genes & development *21*, 367-378.

Hari, L., Brault, V., Kléber, M., Lee, H.-Y., Ille, F., Leimeroth, R., Paratore, C., Suter, U., Kemler, R., and Sommer, L. (2002). Lineage-specific requirements of beta-catenin in neural crest development. The Journal of cell biology *159*, 867-880.

Hari, L., Miescher, I., Shakhova, O., Suter, U., Chin, L., Taketo, M., Richardson, W.D., Kessaris, N., and Sommer, L. (2012). Temporal control of neural crest lineage generation by Wnt/β-catenin signaling. Development (Cambridge, England) *139*, 2107-2117.

Hausmann, G., Bänziger, C., and Basler, K. (2007). Helping Wingless take flight: how WNT proteins are secreted. Nat Rev Mol Cell Biol *8*, 331-336.

He, T.C., Sparks, A.B., Rago, C., Hermeking, H., Zawel, L., da Costa, L.T., Morin, P.J., Vogelstein, B., and Kinzler, K.W. (1998). Identification of c-MYC as a target of the APC pathway. Science *281*, 1509-1512.

Heanue, T.A., and Pachnis, V. (2007). Enteric nervous system development and Hirschsprung's disease: advances in genetic and stem cell studies. Nat Rev Neurosci *8*, 466-479.

Herr, P., Hausmann, G., and Basler, K. (2012). WNT secretion and signalling in human disease. Trends in Molecular Medicine *18*, 483-493.

Heuberger, J., and Birchmeier, W. (2010). Interplay of cadherin-mediated cell adhesion and canonical Wnt signaling. Cold Spring Harb Perspect Biol *2*, a002915.

Hierholzer, A., and Kemler, R. (2010). Beta-catenin-mediated signaling and cell adhesion in postgastrulation mouse embryos. Dev Dyn *239*, 191-199.

Hill, M. (2012). UNSW Embryology - File:Kollmann699.jpg.

Hirabayashi, Y., Itoh, Y., Tabata, H., Nakajima, K., Akiyama, T., Masuyama, N., and Gotoh, Y. (2004). The Wnt/beta-catenin pathway directs neuronal differentiation of cortical neural precursor cells. Development (Cambridge, England) *131*, 2791-2801.

Hjalt, T.A., and Semina, E.V. (2005). Current molecular understanding of Axenfeld-Rieger syndrome. Expert Rev Mol Med *7*, 1-17.

Hoffmans, R., and Basler, K. (2004). Identification and in vivo role of the Armadillo-Legless interaction. Development *131*, 4393-4400.

Hoffmans, R., and Basler, K. (2007). BCL9-2 binds Arm/beta-catenin in a Tyr142-independent manner and requires Pygopus for its function in Wg/Wnt signaling. Mech Dev *124*, 59-67.

Hoffmans, R., Stadeli, R., and Basler, K. (2005). Pygopus and legless provide essential transcriptional coactivator functions to armadillo/beta-catenin. Curr Biol *15*, 1207-1211.

Hovanes, K., Li, T.W., Munguia, J.E., Truong, T., Milovanovic, T., Lawrence Marsh, J., Holcombe, R.F., and Waterman, M.L. (2001). Beta-catenin-sensitive isoforms of lymphoid enhancer factor-1 are selectively expressed in colon cancer. Nat Genet *28*, 53-57.

Huang, H., and He, X. (2008). Wnt/beta-catenin signaling: new (and old) players and new insights. Curr Opin Cell Biol *20*, 119-125.

Huber, K. (2006). The sympathoadrenal cell lineage: specification, diversification, and new perspectives. Dev Biol *298*, 335-343.

Huber, O., Krohn, M., and Kemler, R. (1997). A specific domain in alpha-catenin mediates binding to beta-catenin or plakoglobin. J Cell Sci *110 (Pt 15)*, 1759-1765.

Huelsken, J., Vogel, R., Brinkmann, V., Erdmann, B., Birchmeier, C., and Birchmeier, W. (2000). Requirement for beta-catenin in anterior-posterior axis formation in mice. J Cell Biol *148*, 567-578.

Ikeya, M., Lee, S.M.K., Johnson, J.E., McMahon, A.P., and Takada, S. (1997). Wnt signalling required for expansion of neural crest and CNS progenitors. Nature *389*, 966-970.

Ille, F., Atanasoski, S., Falk, S., Ittner, L.M., Marki, D., Buchmann-Moller, S., Wurdak, H., Suter, U., Taketo, M.M., and Sommer, L. (2007). Wnt/BMP signal integration regulates the balance between proliferation and differentiation of neuroepithelial cells in the dorsal spinal cord. Dev Biol *304*, 394-408.

Israsena, N., Hu, M., Fu, W., Kan, L., and Kessler, J.A. (2004). The presence of FGF2 signaling determines whether beta-catenin exerts effects on proliferation or neuronal differentiation of neural stem cells. Developmental Biology *268*, 220-231.

Ittner, L.M., Wurdak, H., Schwerdtfeger, K., Kunz, T., Ille, F., Leveen, P., Hjalt, T.A., Suter, U., Karlsson, S., Hafezi, F.*, et al.* (2005). Compound developmental eye disorders following inactivation of TGFbeta signaling in neural-crest stem cells. J Biol *4:11*.

Jiang, X., Rowitch, D.H., Soriano, P., McMahon, A.P., and Sucov, H.M. (2000). Fate of the mammalian cardiac neural crest. Development *127*, 1607-1616.

Kapuscinski, J. (1995). DAPI: a DNA-specific fluorescent probe. Biotech Histochem *70*, 220-233.

Karchewski, L.A., Kim, F.A., Johnston, J., McKnight, R.M., and Verge, V.M. (1999). Anatomical evidence supporting the potential for modulation by multiple neurotrophins in the majority of adult lumbar sensory neurons. The Journal of comparative neurology *413*, 327-341.

Kim, J., Lo, L., Dormand, E., and Anderson, D.J. (2003). SOX10 Maintains Multipotency and Inhibits Neuronal Differentiation of Neural Crest Stem Cells. Neuron *38*, 17-31.

Kim, S., Xu, X., Hecht, A., and Boyer, T.G. (2006). Mediator is a transducer of Wnt/beta-catenin signaling. The Journal of biological chemistry *281*, 14066-14075.

Klaus, A., and Birchmeier, W. (2008). Wnt signalling and its impact on development and cancer. Nature Reviews Cancer *8*, 387-398.

Kléber, M., Lee, H.-Y., Wurdak, H., Buchstaller, J., Riccomagno, M.M., Ittner, L.M., Suter, U., Epstein, D.J., and Sommer, L. (2005). Neural crest stem cell maintenance by combinatorial Wnt and BMP signaling. The Journal of cell biology *169*, 309-320.

Knecht, A.K., and Bronner-Fraser, M. (2002). Induction of the neural crest: a multigene process. Nat Rev Genet *3*, 453-461.

Krispin, S., Nitzan, E., Kassem, Y., and Kalcheim, C. (2010). Evidence for a dynamic spatiotemporal fate map and early fate restrictions of premigratory avian neural crest. Development *137*, 585-595.

Kumar, S., and Duester, G. (2010). Retinoic acid signaling in perioptic mesenchyme represses Wnt signaling via induction of Pitx2 and Dkk2. Dev Biol *340*, 67-74.

Kunze, J. (2010). Wiedmanns Atlas klinischer Syndrome Phänomenologie - Ätiologie - Differentialdiagnose, 6 edn (Schattauer GmbH).

Lamb, T.D., Collin, S.P., and Pugh, E.N., Jr. (2007). Evolution of the vertebrate eye: opsins, photoreceptors, retina and eye cup. Nat Rev Neurosci *8*, 960-976.

Lang, G.K. (2014). Augenheilkunde, 5 edn (Georg Thieme Verlag KG).

Le Douarin, N.M., Calloni, G.W., and Dupin, E. (2008). The stem cells of the neural crest. Cell Cycle (Georgetown, Tex) *7*, 1013-1019.

Leclerc, N., Noh, T., Cogan, J., Samarawickrama, D.B., Smith, E., and Frenkel, B. (2008). Opposing effects of glucocorticoids and Wnt signaling on Krox20 and mineral deposition in osteoblast cultures. J Cell Biochem *103*, 1938-1951.

Lee, H.-Y., Kléber, M., Hari, L., Brault, V., Suter, U., Taketo, M.M., Kemler, R., and Sommer, L. (2004). Instructive role of Wnt/beta-catenin in sensory fate specification in neural crest stem cells. Science (New York, NY) *303*, 1020-1023.

Lien, W.-H., Klezovitch, O., Fernandez, T.E., Delrow, J., and Vasioukhin, V. (2006). alphaE-catenin controls cerebral cortical size by regulating the hedgehog signaling pathway. Science (New York, NY) *311*, 1609-1612.

Lien, W.-H., Polak, L., Lin, M., Lay, K., Zheng, D., and Fuchs, E. (2014). In vivo transcriptional governance of hair follicle stem cells by canonical Wnt regulators. Nature cell biology *16*, 179-190.

Logan, C.Y., and Nusse, R. (2004). The Wnt signaling pathway in development and disease. Annual Review of Cell and Developmental Biology *20*, 781-810.

Ma, Q., Fode, C., Guillemot, F., and Anderson, D.J. (1999). Neurogenin1 and neurogenin2 control two distinct waves of neurogenesis in developing dorsal root ganglia. Genes & development *13*, 1717-1728.

Maake, C. (2011/12). Auge, Orbita und ihr Inhalt (OLAT - VAM der Universität Zürich).

Malumbres, M., Harlow, E., Hunt, T., Hunter, T., Lahti, J.M., Manning, G., Morgan, D.O., Tsai, L.H., and Wolgemuth, D.J. (2009). Cyclin-dependent kinases: a family portrait. Nature cell biology *11*, 1275-1276.

Mao, X., Fujiwara, Y., Chapdelaine, A., Yang, H., and Orkin, S.H. (2001). Activation of EGFP expression by Cre-mediated excision in a new ROSA26 reporter mouse strain. Blood *97*, 324-326.

Maretto, S., Cordenonsi, M., Dupont, S., Braghetta, P., Broccoli, V., Hassan, A.B., Volpin, D., Bressan, G.M., and Piccolo, S. (2003). Mapping Wnt/beta-catenin signaling during mouse development and in colorectal tumors. Proceedings of the National Academy of Sciences of the United States of America *100*, 3299-3304.

Marmigère, F., and Ernfors, P. (2007). Specification and connectivity of neuronal subtypes in the sensory lineage. Nature Reviews Neuroscience *8*, 114-127.

Maro, G.S., Vermeren, M., Voiculescu, O., Melton, L., Cohen, J., Charnay, P., and Topilko, P. (2004). Neural crest boundary cap cells constitute a source of neuronal and glial cells of the PNS. Nature neuroscience *7*, 930-938.

Martínez-Morales, J.R., Rodrigo, I., and Bovolenta, P. (2004). Eye development: a view from the retina pigmented epithelium. Bioessays *26*, 766-777.

Matsuoka, T., Ahlberg, P.E., Kessaris, N., Iannarelli, P., Dennehy, U., Richardson, W.D., McMahon, A.P., and Koentges, G. (2005). Neural crest origins of the neck and shoulder. Nature *436*, 347-355.

Mauti, O., Domanitskaya, E., Andermatt, I., Sadhu, R., and Stoeckli, E.T. (2007). Semaphorin6A acts as a gate keeper between the central and the peripheral nervous system. Neural Dev *2*, 28.

MediaWiki (2012). Cre/loxP システム.

Millet, S., Bloch-Gallego, E., Simeone, A., and Alvarado-Mallart, R.M. (1996). The caudal limit of Otx2 gene expression as a marker of the midbrain/hindbrain boundary: a study using in situ hybridisation and chick/quail homotopic grafts. Development *122*, 3785-3797.

Montelius, A., Marmigère, F., Baudet, C., Aquino, J.B., Enerbäck, S., and Ernfors, P. (2007). Emergence of the sensory nervous system as defined by Foxs1 expression. Differentiation; Research in Biological Diversity *75*, 404-417.

Moon, R.T., Kohn, A.D., De Ferrari, G.V., and Kaykas, A. (2004). WNT and beta-catenin signalling: diseases and therapies. Nat Rev Genet *5*, 691-701.

Moqrich, A., Earley, T.J., Watson, J., Andahazy, M., Backus, C., Martin-Zanca, D., Wright, D.E., Reichardt, L.F., and Patapoutian, A. (2004). Expressing TrkC from the TrkA locus causes a subset of dorsal root ganglia neurons to switch fate. Nature neuroscience *7*, 812-818.

Mosimann, C., Hausmann, G., and Basler, K. (2006). Parafibromin/Hyrax activates Wnt/Wg target gene transcription by direct association with beta-catenin/Armadillo. Cell *125*, 327-341.

Mosimann, C., Hausmann, G., and Basler, K. (2009). Beta-catenin hits chromatin: regulation of Wnt target gene activation. Nat Rev Mol Cell Biol *10*, 276-286.

Muroyama, Y., Fujihara, M., Ikeya, M., Kondoh, H., and Takada, S. (2002). Wnt signaling plays an essential role in neuronal specification of the dorsal spinal cord. Genes & development *16*, 548-553.

Nadal-Nicolás, F.M., Jiménez-López, M., Sobrado-Calvo, P., Nieto-López, L., Cánovas-Martínez, I., Salinas-Navarro, M., Vidal-Sanz, M., and Agudo, M. (2009). Brn3a as a marker of retinal ganglion cells: qualitative and quantitative time course studies in naive and optic nerve-injured retinas. Invest Ophthalmol Vis Sci *50*, 3860-3868.

Nagy, A. (2000). Cre recombinase: the universal reagent for genome tailoring. Genesis *26*, 99-109.

Najdi, R., Holcombe, R.F., and Waterman, M.L. (2011). Wnt signaling and colon carcinogenesis: beyond APC. J Carcinog *10:5*.

Najdi, R., Proffitt, K., Sprowl, S., Kaur, S., Yu, J., Covey, T.M., Virshup, D.M., and Waterman, M.L. (2012). A uniform human Wnt expression library reveals a shared secretory pathway and unique signaling activities. Differentiation *84*, 203-213.

Nelson, W.J., and Nusse, R. (2004). Convergence of Wnt, beta-catenin, and cadherin pathways. Science *303*, 1483-1487.

Nguyen, H., Merrill, B.J., Polak, L., Nikolova, M., Rendl, M., Shaver, T.M., Pasolli, H.A., and Fuchs, E. (2009). Tcf3 and Tcf4 are essential for long-term homeostasis of skin epithelia. Nature Genetics *41*, 1068-1075.

Niehrs, C., and Acebron, S.P. (2012). Mitotic and mitogenic Wnt signalling. The EMBO journal *31*, 2705-2713.

Oron-Karni, V., Farhy, C., Elgart, M., Marquardt, T., Remizova, L., Yaron, O., Xie, Q., Cvekl, A., and Ashery-Padan, R. (2008). Dual requirement for Pax6 in retinal progenitor cells. Development *135*, 4037-4047.

Orsulic, S., and Peifer, M. (1996). An in vivo structure-function study of armadillo, the beta-catenin homologue, reveals both separate and overlapping regions of the protein required for cell adhesion and for wingless signaling. J Cell Biol *134*, 1283-1300.

Paratore, C., Goerich, D.E., Suter, U., Wegner, M., and Sommer, L. (2001). Survival and glial fate acquisition of neural crest cells are regulated by an interplay between the transcription factor Sox10 and extrinsic combinatorial signaling. Development *128*, 3949-3961.

Port, F., and Basler, K. (2010). Wnt trafficking: new insights into Wnt maturation, secretion and spreading. Traffic (Copenhagen, Denmark) *11*, 1265-1271.

Prasad, M.S., Sauka-Spengler, T., and LaBonne, C. (2012). Induction of the neural crest state: control of stem cell attributes by gene regulatory, post-transcriptional and epigenetic interactions. Dev Biol *366*, 10-21.

Qu, Q., Sun, G., Murai, K., Ye, P., Li, W., Asuelime, G., Cheung, Y.T., and Shi, Y. (2013). Wnt7a regulates multiple steps of neurogenesis. Molecular and cellular biology *33*, 2551-2559.

Raible, D.W., and Ragland, J.W. (2005). Reiterated Wnt and BMP signals in neural crest development. Semin Cell Dev Biol *16*, 673-682.

Rocha, P.P., Scholze, M., Bleiss, W., and Schrewe, H. (2010). Med12 is essential for early mouse development and for canonical Wnt and Wnt/PCP signaling. Development *137*, 2723-2731.

Rogers, C.D., Jayasena, C.S., Nie, S., and Bronner, M.E. (2012). Neural crest specification: tissues, signals, and transcription factors. Wiley Interdisciplinary Reviews Developmental Biology *1*, 52-68.

Ruhrberg, C., and Schwarz, Q. (2010). In the beginning: Generating neural crest cell diversity. Cell Adh Migr *4*, 622-630.

Sadler, T.W. (2008). Medizinische Embryologie (Georg Thieme Verlag KG: Thieme).

Sadler, T.W. (2012). Langman's Medical Embrylogy, 12 edn (Lippincott Williams & Wilkins).

Salic, A., and Mitchison, T.J. (2008). A chemical method for fast and sensitive detection of DNA synthesis in vivo. Proceedings of the National Academy of Sciences of the United States of America *105*, 2415-2420.

Sauka-Spengler, T., and Bronner-Fraser, M. (2008). A gene regulatory network orchestrates neural crest formation. Nat Rev Mol Cell Biol *9*, 557-568.

Schlote, T., and Rohrbach, J.M. (2004). Sekundärglaukome Komplizierte Glaukome in Theorie und Praxis (Schattauer GmbH).

Schmidt, C., and Patel, K. (2005). Wnts and the neural crest. Anatomy and Embryology *209*, 349-355.

Schünke, M., Schulte, E., Schumacher, U., Voll, M., and Wesker, K. (2012). Prometheus - Lernatlas der Anatomie, Kopf und Hals und Neuroanatomie, 3. Auflage edn (Georg Thieme Verlag KG).

Shakhova, O., and Sommer, L. (2010). Neural crest-derived stem cells. In The Stem Cell Research Community (stembook.org: StemBook).

Shaw, G., and Weber, K. (1984). The intermediate filament complement of the retina: a comparison between different mammalian species. Eur J Cell Biol *33*, 95-104.

Shy, B.R., Wu, C.-I., Khramtsova, G.F., Zhang, J.Y., Olopade, O.I., Goss, K.H., and Merrill, B.J. (2013). Regulation of Tcf7l1 DNA binding and protein stability as principal mechanisms of Wnt/β-catenin signaling. Cell Reports *4*, 1-9.

Sieber-Blum, M. (2004). Cardiac neural crest stem cells. Anat Rec A Discov Mol Cell Evol Biol *276*, 34-42.

Sieber-Blum, M., and Cohen, A.M. (1980). Clonal analysis of quail neural crest cells: they are pluripotent and differentiate in vitro in the absence of noncrest cells. Dev Biol *80*, 96-106.

Sommer, L., Ma, Q., and Anderson, D.J. (1996). neurogenins, a novel family of atonal-related bHLH transcription factors, are putative mammalian neuronal determination genes that reveal progenitor cell heterogeneity in the developing CNS and PNS. Molecular and Cellular Neurosciences *8*, 221-241.

Soriano, P. (1999). Generalized lacZ expression with the ROSA26 Cre reporter strain. Nature genetics *21*, 70-71.

Southard-Smith, E.M., Kos, L., and Pavan, W.J. (1998). Sox10 mutation disrupts neural crest development in Dom Hirschsprung mouse model. Nat Genet *18*, 60-64.

Stemple, D.L., and Anderson, D.J. (1992). Isolation of a stem cell for neurons and glia from the mammalian neural crest. Cell *71*, 973-985.

Stuhlmiller, T.J., and García-Castro, M.I. (2012). Current perspectives of the signaling pathways directing neural crest induction. Cellular and molecular life sciences: CMLS *69*, 3715-3737.

Swamynathan, S.K. (2013). Ocular surface development and gene expression. Journal of ophthalmology *2013*, 103947.

Tachibana, M. (2000). MITF: a stream flowing for pigment cells. Pigment Cell Res *13*, 230-240.

Tan, X., Apte, U., Micsenyi, A., Kotsagrelos, E., Luo, J.H., Ranganathan, S., Monga, D.K., Bell, A., Michalopoulos, G.K., and Monga, S.P. (2005). Epidermal growth factor receptor: a novel target of the Wnt/beta-catenin pathway in liver. Gastroenterology *129*, 285-302.

Taneyhill, L.A., and Bronner-Fraser, M. (2005). Recycling signals in the neural crest. J Biol *4*, 10.

Tetsu, O., and McCormick, F. (1999). Beta-catenin regulates expression of cyclin D1 in colon carcinoma cells. Nature *398*, 422-426.

Trainor, P.A. (2005). Specification and patterning of neural crest cells during craniofacial development. Brain Behav Evol *66*, 266-280.

Valenta, T., Gay, M., Steiner, S., Draganova, K., Zemke, M., Hoffmans, R., Cinelli, P., Aguet, M., Sommer, L., and Basler, K. (2011). Probing transcription-specific outputs of β-catenin in vivo. Genes & development *25*, 2631-2643.

Valenta, T., Hausmann, G., and Basler, K. (2012). The many faces and functions of β-catenin. The EMBO journal *31*, 2714-2736.

Valenta, T., Lukas, J., and Korinek, V. (2003). HMG box transcription factor TCF-4's interaction with CtBP1 controls the expression of the Wnt target Axin2/Conductin in human embryonic kidney cells. Nucleic Acids Res *31*, 2369-2380.

van Amerongen, R., Mikels, A., and Nusse, R. (2008). Alternative wnt signaling is initiated by distinct receptors. Sci Signal *1*.

van de Wetering, M., Sancho, E., Verweij, C., de Lau, W., Oving, I., Hurlstone, A., van der Horn, K., Batlle, E., Coudreuse, D., Haramis, A.P.*, et al.* (2002). The beta-catenin/TCF-4 complex imposes a crypt progenitor phenotype on colorectal cancer cells. Cell *111*, 241-250.

Vasioukhin, V., Bauer, C., Degenstein, L., Wise, B., and Fuchs, E. (2001). Hyperproliferation and defects in epithelial polarity upon conditional ablation of alpha-catenin in skin. Cell *104*, 605-617.

Vermeren, M., Maro, G.S., Bron, R., McGonnell, I.M., Charnay, P., Topilko, P., and Cohen, J. (2003). Integrity of developing spinal motor columns is regulated by neural crest derivatives at motor exit points. Neuron *37*, 403-415.

Wakamatsu, Y., Endo, Y., Osumi, N., and Weston, J.A. (2004). Multiple roles of Sox2, an HMG-box transcription factor in avian neural crest development. Dev Dyn *229*, 74-86.

Widmann, T.J., and Dahmann, C. (2009). Wingless signaling and the control of cell shape in Drosophila wing imaginal discs. Dev Biol *334*, 161-173.

Wilkinson, D.G., Bailes, J.A., and McMahon, A.P. (1987). Expression of the proto-oncogene int-1 is restricted to specific neural cells in the developing mouse embryo. Cell *50*, 79-88.

Wray, J., Kalkan, T., Gomez-Lopez, S., Eckardt, D., Cook, A., Kemler, R., and Smith, A. (2011). Inhibition of glycogen synthase kinase-3 alleviates Tcf3 repression of the pluripotency network and increases embryonic stem cell resistance to differentiation. Nature cell biology *13*, 838-845.

Wu, C.-I., Hoffman, J.A., Shy, B.R., Ford, E.M., Fuchs, E., Nguyen, H., and Merrill, B.J. (2012). Function of Wnt/β-catenin in counteracting Tcf3 repression through the Tcf3-β-catenin interaction. Development (Cambridge, England) *139*, 2118-2129.

Wu, H.-H., Bellmunt, E., Scheib, J.L., Venegas, V., Burkert, C., Reichardt, L.F., Zhou, Z., Fariñas, I., and Carter, B.D. (2009). Glial precursors clear sensory neuron corpses during development via Jedi-1, an engulfment receptor. Nature neuroscience *12*, 1534-1541.

Xing, Y., Takemaru, K., Liu, J., Berndt, J.D., Zheng, J.J., Moon, R.T., and Xu, W. (2008). Crystal structure of a full-length beta-catenin. Structure *16*, 478-487.

Xu, W., and Kimelman, D. (2007). Mechanistic insights from structural studies of β-catenin and its binding partners. Journal of Cell Science *120*, 3337-3344.

Yamaguchi, T.P., Takada, S., Yoshikawa, Y., Wu, N., and McMahon, A.P. (1999). T (Brachyury) is a direct target of Wnt3a during paraxial mesoderm specification. Genes & development *13*, 3185-3190.

Yang, W., Shen, J., Wu, M., Arsura, M., FitzGerald, M., Suldan, Z., Kim, D.W., Hofmann, C.S., Pianetti, S., Romieu-Mourez, R.*, et al.* (2001). Repression of transcription of the p27(Kip1) cyclin-dependent kinase inhibitor gene by c-Myc. Oncogene *20*, 1688-1702.

Yi, F., Pereira, L., Hoffman, J.A., Shy, B.R., Yuen, C.M., Liu, D.R., and Merrill, B.J. (2011). Opposing effects of Tcf3 and Tcf1 control Wnt stimulation of embryonic stem cell self-renewal. Nature cell biology *13*, 762-770.

Yu, J., Chia, J., Canning, C.A., Jones, C.M., Bard, F.A., and Virshup, D.M. (2014). WLS retrograde transport to the endoplasmic reticulum during Wnt secretion. Dev Cell *29*, 277-291.

Zacharias, A.L., and Gage, P.J. (2010). Canonical Wnt/beta-catenin signaling is required for maintenance but not activation of Pitx2 expression in neural crest during eye development. Dev Dyn *239*, 3215-3225.

Zhang, J., Fuhrmann, S., and Vetter, M.L. (2008). A nonautonomous role for retinal frizzled-5 in regulating hyaloid vitreous vasculature development. Invest Ophthalmol Vis Sci *49*, 5561-5567.

Zirlinger, M., Lo, L., McMahon, J., McMahon, A.P., and Anderson, D.J. (2002). Transient expression of the bHLH factor neurogenin-2 marks a subpopulation of neural crest cells biased for a sensory but not a neuronal fate. Proceedings of the National Academy of Sciences of the United States of America *99*, 8084-8089.

8. Publications

1. Valenta, T., **Gay, M.**, Steiner, S., Draganova, K., Zemke, M., Hoffmans, R., Cinelli, P., Aguet, M., Sommer, L., and Basler, K. (2011). Probing transcription-specific outputs of β-catenin in vivo. Genes & development *25*, 2631-2643.

2. **Gay M.**, Vatenta, T., Herr P., Paratore-Hari L., Basler K., and Sommer L. (2015) Distinct adhesion-independent functions of β-catenin control stage-specific sensory neurogenesis and proliferation. BMC Biology, in press.

3. Zemke M., Draganova K., Geminn A., Schöler A., Zurkirchen L., **Gay M.**, Cheng P, Koseki H., Valenta T., Schübeler D., Basler K., and Sommer L. (2015) Ezh2 represses cell cycle exit and forebrain identity in neural progenitor cells in the midbrain. Submitted to EMBO Journal

9. Curriculum vitae

Name	Max Hans-Peter Gay
Date of birth	27th February 1984
Place of Origin	Birmingham, Alabama, USA
Nationality	Swiss, German and American

Education

Since 12/2009	**PHD studies in Cell Biology, University of Zurich Switzerland** Prof. Dr. L. Sommer, Institute of Anatomy: "Distinguishing the Influence of Singular β-catenin Functions in Development Using a Novel In Vivo Approach."
10/2007 - 10/2009	**Master of Sciences, ETH Zurich, Switzerland** Focus on Biomedical Engineering, Biomechanics
10/2003 - 10/2008	**Bachelor of Sciences, ETH Zurich, Switzerland** Focus on Mechanical Engineering, Structural mechanics
08/1999 – 09/2003	**Matura Typus C, Mathematics and Natural Science Gymnasium (MNG) Ramibuhl, Zurich, Switzerland** Focus on Math and Physics

10. Acknowledgements

This chapter is probably the most satisfying to write. Not only is it the last chapter of this thesis, but the drafting of this section allows me to commemorate the people, who have helped, supported, challenged and guided me in the five years of my PhD studies. I would not have succeeded without them.

First, I would like to express my gratitude to Prof. Dr. Lukas Sommer who gave me the opportunity to do my PhD studies in his lab. He encouraged me to be self-reliant in decisions concerning the progression of my projects, but was always available for assistance and scientific input. His support and mentoring were invaluable for the circumstances, which have made me to the researcher I am today.

I would also especially like to thank Dr. Lissette Paratore-Hari and Iris Miescher, who were my supervisors in the early years of my PhD studies. They were patient mentors, who imparted a vast amount of practical and theoretical knowledge onto me. Their support was priceless for the completion of this thesis.

I am also obliged to Prof. Dr. Konrad Basler and Prof. Dr. Esther Stoeckli, for being my PhD co-examiners. They provided helpful discussions and input during our meetings and were always available for consultation.

I would also like to thank former and present members of the Sommer Lab, who have assisted me with either technical procedures or scientific discussions. Their friendship and support made the time I have spent in the lab unforgettable! Special thanks does to Annika, Jessica, Daniel Z., Martina, Kalina, Daniel S., Julien, Arianna, Luis, Mario, Simon, Sandra, Eylül, Gaea, Vadims, Yudong, Olga, Jaqueline, Swen, and any other members I might have forgotten.

I would also like to acknowledge the great collaboration with the Basler Lab. Our bi-annual Wnt meetings provided great input and feedback resulting from thorough discussions. In particular, I would like to thank Tomas, Patrik, Dario and Claudio for a great collaboration.

I'm also grateful for the support from technical and administrative staff, as well as, other colleagues from the Institute of Anatomy, especially the members of the Loffing Group.

Last but not least, it is inevitable to thank my family. My parents were always there for scientific and personal consolation. Most importantly I would like to thank my dear wife Fränzi for putting up with me in the hard times in which I was annoying and for always unconditionally supporting and pushing me in my thesis even though she didn't understand much of what I did.

Thank you all! I consider myself lucky to have worked with you and to know you.